THE DESIGN OF ENVIRONMENTAL TEST RIGS

Keith James Butler

Doctor of Philosophy

THE UNIVERSITY OF ASTON IN BIRMINGHAM

October 1986

THE UNIVERSITY OF ASTON IN BIRMINGHAM

Title : The Design of Environmental Test Rigs
Name : Keith James Butler
PhD 1986

SYNOPSIS

Product reliability and its environmental performance have become critical elements within a product's specification and design. To obtain a high level of confidence in the reliability of the design it is customary to test the design under realistic conditions in a laboratory. The objective of the work is to examine the feasibility of designing mechanical test rigs which exhibit prescribed dynamical characteristics. The design is then attached to the rig and excitation is applied to the rig, which then transmits representative vibration levels into the product.

The philosophical considerations made at the outset of the project are discussed as they form the basis for the resulting design methodologies. It is attempted to directly identify the parameters of a test rig from the spatial model derived during the system identification process. It is shown to be impossible to identify a feasible test rig design using this technique. A finite dimensional optimal design methodology is developed which identifies the parameters of a discrete spring/mass system which is dynamically similar to a point coordinate on a continuous structure. This design methodology is incorporated within another procedure which derives a structure comprising a continuous element and a discrete system. This methodology is used to obtain point coordinate similarity for two planes of motion, which is validated by experimental tests. A limitation of this approach is that it is impossible to achieve multi-coordinate similarity due to an interaction of the discrete system and the continuous element at points away from the coordinate of interest. During the work the importance of the continuous element is highlighted and a design methodology is developed for continuous structures. The design methodology is based upon distributed parameter optimal design techniques and allows an initial poor design estimate to be moved in a feasible direction towards an acceptable design solution. Cumulative damage theory is used to provide a quantitative method of assessing the quality of dynamic similarity. It is shown that the combination of modal analysis techniques and cumulative damage theory provide a feasible design synthesis methodology for representative test rigs.

Key Words : system identification; environmental tests; optimal designs; dynamic similarity; design methodologies.

ACKNOWLEDGEMENTS

I wish to thank my supervisors, Dr J. E. T. Penny and Mr T. H. Richards for their technical guidance and support during the duration of the project.

During the early stages of the project there was a collaborative phase with Cape Engineering; Warwick (Environmental Testing Engineers) and I would like to particularly thank Mr. J. Homfray for many informative discussions.

The author is indebted to the University of Aston in Birmingham and the Procurement Executive Ministry of Defence for the financial assistance they provided in the form of a research grant.

CONTENTS

LIST OF FIGURES

LIST OF TABLES

Note :-

The figures and tables are wherever possible inserted into the text close to where they referenced. Full page figures and tables are always inserted at the end of each chapter.

NOMENCLATURE

$\mathcal{E}_i$	Problem input space
$\mathcal{E}_o$	Problem ouput space
S	System transformation
$[m]$	Mass matrix
m_j	Mass element, number j
$[K]$	Stiffness matrix
k_j	Stiffness element, number j
$[\Phi]$	Normalised modal matrix
${}_r\phi$	Normalised characteristic vector of the r´th mode
$[I]$	Unity matrix
$[\lambda]$	Eigenvalue matrix
λ_r	Complex eigenvalue for the r´th mode
ω_r	Resonant frequency for the r´th mode
E	Young´s modulus
I	Second moment of area
ρ	Material density
A	Sectional area
ℓ	Length of beam or element
β_r	End constraint function
i, j, k	Coordinate position
Ω	Sweeping frequency
Y_{ii}	Point mobility for coordinate i
Y_{ij}	Transfer mobility between coordinates i and j
n, N	Degrees of freedom
k_{res}	Residual stiffness element
$\{z\}$	State varible vector (n-elements)

$\mathcal{R}$	Design space of real numbers
$\{b\}$	Design variable vector (k-elements)
$\Psi(z,b)$	Cost function
$h(z,b)$	State equations or constraints
ϕ	Zero
$\{\ell^i\}$	Sensitivity vector for the i´th variable
$[\ell]$	Sensitivity matrix
$\{Q\}$	Input force vector
$\{q\}$	Response vector
α_{ii}	Point receptance for coordinate i
α_{ij}	Transfer receptance between coordinates i and j
$M_{tot_{jj}}$	Equivalent total mass for discrete system at coordinate j
θ	Scalar
$\{x_k'\}$	Optimum solution vector
$\{\delta_{error}\}$	Design error
R_{jj}	Residual flexibility
$\in$	Term for a variable contained within a set

The following terminology has been adopted within the report for the design of environmentally representative test rigs.

Original structure or Carrier Body	The original structure is an existing structure from which physical measurements can be taken. The measurements obtained can represent the complete structure or a localized area of a

	very large structure.
Coordinates of interest	The direct dispacements at points on the original structure (where the measurements are taken) correspond to the coordinates of interest.
Continuous element	A continuous element connecting the coordinates is one for which the distributed nature of the mechanical properties are explicitly taken into account.
Discrete system	A discrete system is one for which the mechanical properties are "lumped".
Substitute structure or Test Rig	The test rig comprising the continuous element and a discrete system is called a substitute structure.
Dynamic similarity	If two structures exhibit the same dynamical characteristics over a prescribed frequency range then the two structures are said to be dynamically similar.

1. INTRODUCTION

1.1 TERMS OF REFERENCE

Product reliability and its environmental performance have become critical elements within a product specification, such that they are at least as important as the cost, weight and aesthetic attributes. This is particularly true for modern electro-mechanical designs that experience harsh vibrational environments, either during transportation or as part of their everyday functioning.

Modern numerical analysis techniques, although very sophisticated and accurate, are of little use when analysing such systems. Modelling techniques, where the behavioural characteristics are represented by well established laws of physics, are heavily reliant upon the modeller´s skill and extensive knowledge of the characteristics of the equipment. If inadequate information is known then lumped parameters and linearised characteristics are assumed, with the associated reduction in the realism of the model.

Since analytical techniques are incapable of providing a high level of confidence in the reliability of the equipment it is customary to test the design under realistic conditions in the laboratory. Various strategies have been proposed for realistic testing procedures, such as the presently used 3 axis testing sequence.

This technique and other testing procedures have been examined and it was considered that an alternative approach to realistic environmental testing of transported equipment or equipment exposed to vibrational loading was required. A study was performed, external to the present work, where the frequency range of typical transported equipment was identified and partitioned into three ranges. It was considered that the low frequency range (0 to 100 Hz) could be recreated by the use of a mechanical test rig having prescribed dynamical characteristics. These characteristics can be measured from the original carrier body in the form of frequency response curves.

If a mechanical test rig which exhibits the prescribed dynamical characteristics can be built then it can be used to test a range of transported equipment. This is because the dynamical characteristics of the test rig will change in the same fashion as the carrier body when the same equipment is attached to each structure.

This project, commissioned by the Ministry of Defence, is a collaborative effort between Cape Engineering; Warwick (Environmental Test Engineers) and Aston University; Birmingham. It has two distinct areas of interest;

i) A feasibility study performed by Cape Engineering to examine the operational parameters and functional constraints on such an approach.

ii) A feasibility study performed by Aston University to

examine the analytical implications of such test rigs and to establish a design methodology.

This work addresses the problems of designing mechanical test rigs which are capable of reproducing defined dynamical characteristics.

1.2 OBJECTIVES

The primary objective of the work is to examine the feasibility of designing a mechanical test rig that has prescribed dynamical characteristics. The test rig must be capable of supporting complete pieces of equipment.

It is possible to define intermediate objectives for the work;

1) Examine the possibility of using an approach based upon system identification techniques to derive the design parameters of a test rig. This approach uses the frequency response data from the original carrier body.
2) Examine the implications of using truncated, incomplete frequency response data.
3) Derive a design methodology to identify a system that is dynamically similar to a point coordinate on another system.
4) Examine the implications of two point coordinate similarity.
5) Derive a design methodology for a distributed

parameter system which has prescribed dynamical characteristics.

1.3 PROJECT STRUCTURE

The project has been structured into five main areas of work as shown in Figure 1. Effort has been directed to make a contribution in all five areas rather than pursue an exhaustive examination of all aspects within any one. A section on the philosophical considerations, made at the outset of the project, has been included to give a background on the reasoning applied throughout the work. It outlines what information was available and what expectations were assumed to be gained from applying the selected approach. To reflect the structure of the project, the relevant literature is reviewed in each area, rather than having a single literature review.

The first area relates to Chapter 3 and examines the implications of using system identification algorithms within a design synthesis process. Whilst considering system identification techniques it is important to allow for truncation effects of the frequency response data. The final aim of the system identification process is to derive mass, stiffness and damping matrices which represent a spatial model of the original structure. The truncation effects cause these matrices to be fully populated. It is not possible to derive a methodology which directly identifies the parameters of a suitable test rig by using

populated matrices. However, the ground rules for obtaining dynamic similarity between two structures are established. The effects of handling incomplete frequency response data is also examined.

At the outset of the project it was considered that a solution capable of achieving prescribed dynamical characteristics for a structure would be obtained from a test rig comprising an assembly of continuous and discrete elements in a system. The term 'substitute structure' was adopted to describe this system within the thesis. The discrete system was used to 'tune' the rig to the desired dynamical characteristics. Before it was possible to examine substitute structures it was considered necessary to examine simple systems to establish the fundamental concepts when designing dynamically similar structures.

A design methodology is derived (Chapter 4) which identifies the parameters of a discrete system which is dynamically similar to a point coordinate on another system. It is important to note that this similarity is only for one plane of motion. During the identification process a finite dimensional optimal design algorithm is developed.

A proposed design methodology for the substitute structure is discussed in Chapter 5. The methodology is used to identify a similar structure to a simple tapered cantilever. Experimental validation of the analytical

study (Chapter 6) shows that good point coordinate similarity is obtained between the two structures.

The next phase of the work was to apply the design methodology to two coordinates of interest on a single plane structure. The methodology was also applied to a two dimensional structure to examine out of plane similarity (Chapter 7). The coupling of the discrete system to the continuous element provides an acceptable level of dynamic similarity at the coupling coordinate. However, at coordinates away from the discrete system intermediate frequencies are noticable, resulting from the stationary characteristics of the discrete system. These intermediate frequencies have significant mode shapes and render the proposed design methodology untenable.

This highlights that only continuous elements can be used to design the mechanical test rig. An approach to designing a structure that exhibits prescribed dynamical characteristics is discussed in Chapters 8 and 9. A distributed parameter optimal design algorithm is proposed that can (under the right conditions) systematically direct an initial design estimate to one which has the defined dynamical characteristics. If the initial design estimate is incapable of moving in a feasible direction then the designer is informed and a new design estimate has to be instigated. Methods of quantatively assessing the quality of dynamic similarity are discussed.

PROJECT STRUCTURE

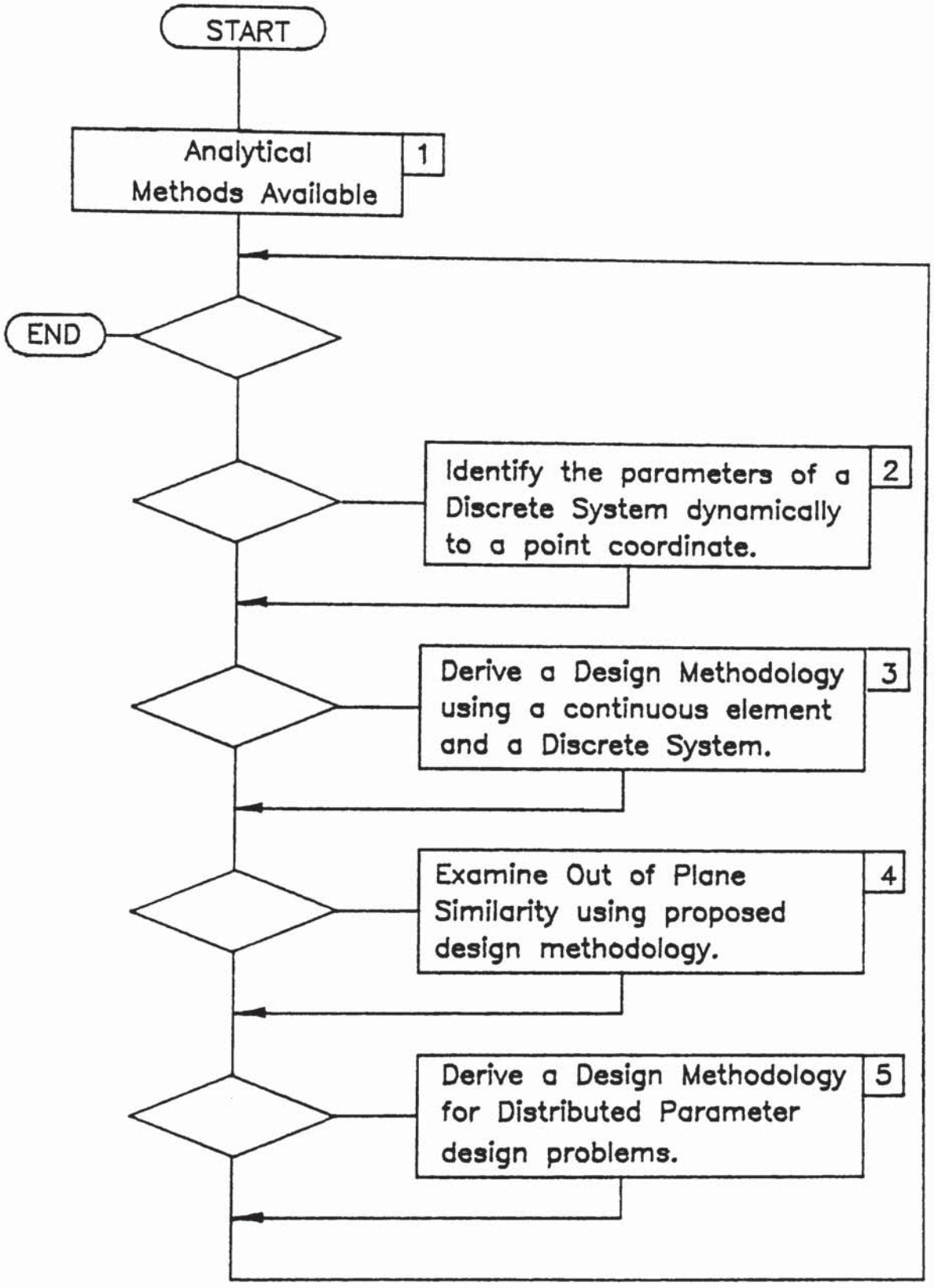

Figure 1

2. DESIGN PHILOSOPHY CONSIDERATIONS

2.1 PROBLEM DEFINITION

As the complexity and sensitivity of modern engineering designs increase, so does the expectations of the design's performance, reliability and availability. Coupled with these expectations are market forces which requires that the equipment is of minimum cost, made from the minimum of components, minimum material, light as possible etc. The first group of conditions represent the performance or behaviour of the equipment to external or environmental forces. They are generally classed as the state variables of the equipment. The other group of conditions, specifying the physical properties, such as size, weight, material etc. are classed as the design variables, since they specify the design of the equipment and are at the discretion of the designer. The design variables and state variables are related by well established laws of physics. The state variables cannot be measured directly and are usually established by either analytical modelling techniques or controlled experimental measurements of the physical system.

A typical complex modern design of a piece of equipment is likely to contain a mixture of electrical and mechanical sub-systems. It is the functioning of these sub-systems which affect the reliability of the whole of the equipment.

A general cause of failure within these sub-systems is due to the environment within which the equipment functions, or is transported through, imposing cyclic loading conditions onto the equipment.

If the development and evaluation of the performance of the equipment is achieved by a series of field tests, the cost and time scale would be prohibitive. The normal engineering approach to designing and evaluating equipment is to firstly model the equipment using numerical analysis techniques. If the equipment is a mixture of electrical and mechanical sub-sysems, then analytical techniques such as finite element analysis are of limited use. Also some of the sub-systems might be highly non-linear or discontinuous which makes realistic analog/digital simulation techniques difficult to apply. It is, therefore, always a desirable step to manufacture prototype equipment and test it under strict laboratory conditions. One testing procedure currently in use is to test a piece of equipment in three axes. The equipment is constrained in two axes to minimise sub-system movement in these axes and then excited in the third axis. After a specified period, the axis of excitation is moved to one of the previously constrained axes (the other two are then constrained) and the test is repeated. This test has the disadvantages of not being realistic, taking a long time to perform and has the possibility of over testing the equipment, thus incurring extra design penalties. This philosophy of testing is quite typical within experimental

testing procedures and often leads to testing for conditions that don't actually exist. This then results in a feedback to the designer who might incorporate the incorrect or over tested data within the design formulation. Hence the design can be over conservative, costly, heavy and still possibly fail in service due to inadequate or incorrect consideration being given to the actual operational environment of the equipment. For experimental tests to be meaningful it is necessary that the laboratory conditions are representative of the actual environments the equipment will experience during its working life.

The objective of this work is to enable the designer of the equipment to be able to specify the parameters of environmentally representative test rigs. Before this problem is addressed, it is worthwhile to examine the philosophy of the selected design approach.

2.2 SYSTEM ENGINEERING DEFINITION OF PROBLEM

The basic philosophy that has been adopted, within the work, is to consider the problem within the concepts of system theory. This approach has many advantages, which will be discussed later, the main one is it provides a mechanism for the systematic reduction of the problem into sub-systems with well defined input and output specifications. Since the problem is handled by a top-down analysis approach the reltionships of the sub-systems are

also well defined.

At this stage, system theory is briefly reviewed so that a set of working definitions can be established. A system can be defined as a set of resources, or elements, such as computer hardware, computer software, files, mannuals, machinery and personnel assembled with the aim of solving a class of problem. To design such a system it is necessary to define its boundary, its behaviour and its operational constraints.

Early research work establishing system theory considered the ultimate system to be the universe. Checkland (1) attempted to draw a systems map of the universe. Every system exists within the universe and it is a systems engineer´s first task to establish the hierarchy of the system under examination, within this overall universal structure. In other words, the first task of the systems engineer is to establish the boundary of the system. This must be achieved in context with the original problem to ensure that sufficient knowledge is available so that a solution may be obtained. The first task is, therefore, possibly the most difficult to achieve. For example, Ashby [2] maintains that "every material object contains no less than an infinity of variables." He illustrates his point by the following example: "The real pendulum has not only length and position, it has also mass, temperature, electric conductivity, crystalline structure, chemical impurities, some radio-activity, velocity, reflecting

power, tensile strength, a surface film of moisture, bacterial contamination, an optical absorption, elasticity, shape, specific gravity and so on. Any suggestion that we should study "all" of the facts is unrealistic and actually the attempt is never made".

The inference from this statement is that an abstract incomplete model of the system and system environment must be established, which contains sufficient attributes such that adequate solutions can be found for the class of problem under consideration.

It is possible to represent this by the following abstract system (Figure 2).

Problem representation

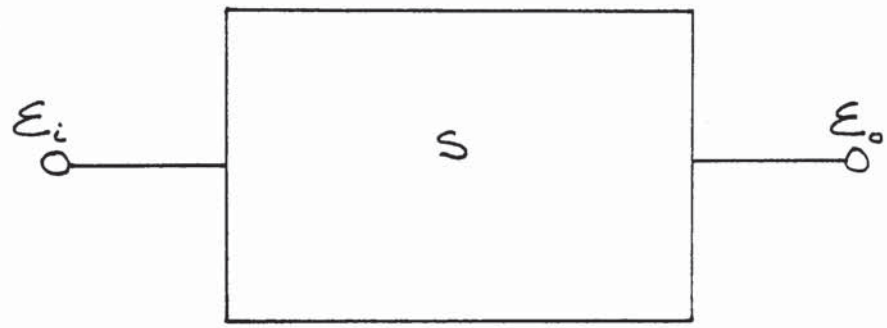

Figure 2

where $\mathcal{E}_i$ represents the incomplete input space to the system within the system environment

$\mathcal{E}_o$ represents the output space and will contain

solutions to problems set within the incomplete input space.

S represents the system which is capable of transforming problems within the input space ($\mathcal{E}_i$) into solutions contained within the output space ($\mathcal{E}_o$).

Once the boundary of the system has been established, the system is partitioned into modules so that the steps within the transition of the problem into a solution are identified. This partitioning process is repeated until all of the modules are fully defined.

Before it is possible to establish the boundary of the system it is necessary to examine further the class of the problem. In particular, the behaviour and operational constraints of the problem must be specified as they effect the choice of the modelling medium. Establishing the boundary is, therefore, an iterative design process where the total problem must be viewed in the context of possible solution processes.

2.3 MODELLING MEDIA

The basic objective of the design study is to be able to systhesise a model (the test rig) which has the same characteristics as the real system (the carrier body)

This type of model is called a homomorphic model where behavioural characteristics from the original system are used by many-to-one transformations to identify a simplified model. The number of design variables are less than the original system but the model is capable of reproducing similar behaviour for a restricted performance range.

This introduces a new concept, called the level of resolution, of the model. In effect this denotes the accuracy of the model and its ability to recreate similar behavioural characteristics as the original structure. The operational constraint that is imposed is that the more accurate the model, the higher the level of resolution that is required. This means that the greater the amount of data describing the original structure, both quantative and qualitative data, are required.

There are two possible modelling media that can be used to generate the simplified model

(a) Analogue representation

(b) Iconic representation

The discussion to date concerning a systems approach to solving the problem has been very generalised. It is worthwhile to consider some of the characteristics of this particular problem as they reduce the number of variables within the selection of a suitable modelling medium. The problem is concerned with recreating a dynamical environment which is similar to the original system. The

original system is a structure used to carry or support complex pieces of equipment. This equipment can fail due to prolonged exposure of cyclic vibratory forces.

A study made prior to this work identified that the dynamical range of these forces are limited from 5 to 100 Hz. The equipment can range from a few kilograms to several thousand kilograms. The size of equipment can range from a few centimetres to several metres in all axis. The equipment can be attached to the carrier body at one or more points.

A model (the test rig) is therefore required which can handle equipment having a large envelope of size and weight, have several attachment points and be capable of being used to perform fatigue studies.

(a) Analogue Representation

If the model is to be generated as an analogue representation then it is first necessary to specify the state variable equations of the carrier body.
The carrier structures used at present are very complex themselves and, therefore, it is proposed to collect data from the actual carrier body. This data will be in the form of frequency response plots. A technique would be required to identify the state variable equations from the frequency response plots. These equations are then used to generate an analogue model, where electric voltages

represent corresponding properties of the original structure. A typical analogue model configuration can be seen in Figure 3.

Analog model configuration

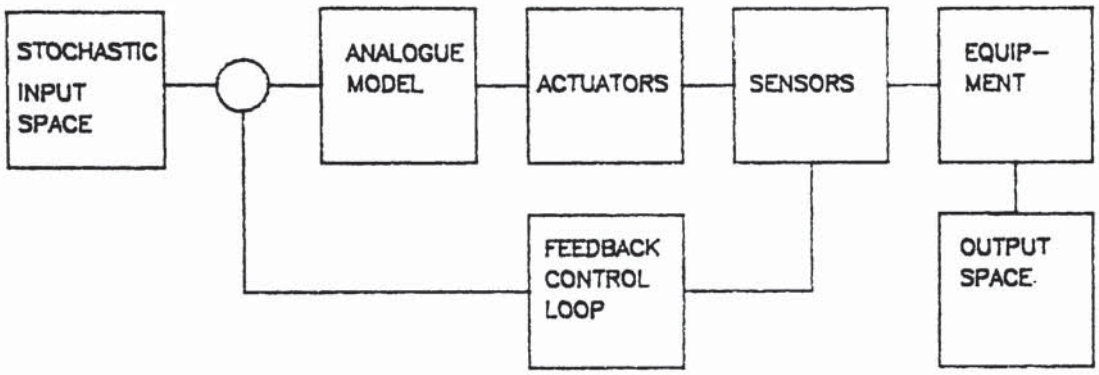

Figure 3.

In the analogue model a feedback from the interface of the actuators and the test equipment would be required to allow changes in the frequency response data due to the coupling effects of the specimen under test. The analogue model would require to have multiple outlets so that the actuators, one per attachment point, could apply realistic vibration levels to the equipment under test.

(b) Iconic Representation

When an iconic mcdel is generated, the model incorporates properties of the original system. For example, lengths or masses of elements within the original system are represented as scaled parameters within the model. These models are, therefore, physical or mechanical in nature. An obvious property that has to be retained is the distances between the attachment points. A continuous element connecting the points of interest is, therefore, required. This means that the geneation or design of the model is a design synthesis exercise where the distributed nature of the mechanical propeties of the connecting structure are explicitly taken into account.

A concept within the application of a system approach to problem solving is the principle of minimum commitment.

During any design process the designer is faced with a wide range of possible routes to a solution and the initial reaction is one of reducing the number of options as soon as is possible. This often leads to missing design solutions or artificially constraining the number of feasible solutions. These decisions to reject certain lines of possible solution are often made under a high level of uncertainty due to a lack of adequate information or reasoning.

The class of design problem and the system objective has been established and it is now necessary to establish the boundary. To finalise the boundary it is necessary to select a modelling medium, since the time scale and manpower resources within the project does not permit the examination of both modelling techniques. It is perhaps appropriate at this point to list the advantages and disadvantages of each modelling medium.

Analogue

The analogue model is an elegant solution

Given the state variable equation it is relatively easy to model

It is difficult to derive the state variable equations

It is difficult to control the phase between the attachment points

If digital simulation techniques used then there will be a real time modelling problem

If an analogue computer is used the repeatability of the tests are not certain. It would also be difficult to establish the level of dynamic similarity if the model changes with time.

When structures are coupled the frequency response characteristics at the attachment points change. A feedback loop is required between the equipment and the model so that the model represents changes with respect to the attached equipment.

Iconic

When coupling equipment to the rig the dynamic characteristics will change in the same manner as the original structure and the equipment. There is no requirement for any external modification system.

The model, once established, will be dynamically stationary with respect to time.

The model is easy to validate using well tested experimental measuring techniques.

If acceptable dynamic similarity has been achieved then a single point input forcing function will generate correct frequency response levels and phase at each attachment point.

The test rig will possibly have fatigue problems.

It is difficult to establish the parameters of the continuous element connecting the points of interest.

After considering the available knowledge about the two modelling media and the author´s background experience, it was decided to examine the possibility of using an iconic modelling representation.

2.4 MECHANICAL TEST RIG

A design methodology is required that will systematically derive the design variables for a mechanical test rig that exhibits prescribed dynamical characteristics. If this methodology is to be systematic, then a design synthesis sequence must be employed, rather than an intuitive reasoning process. If the design is to be achieved by synthesis then an orderly and formalised progression of a system model by transformation through three modelling domains must be achieved. These domains can be categorised by the following definitions;

Operational Domain

The operational domain or behavioural model is concerned with the abstract mechanism of performance of the system without regard to a particular realisation of its structure.

Structural Domain

The structural domain or "glass-box" model embeds operational models of the system elements and specifies the interconnections or relationships between the system elements. It is possible to deduce a program of system behaviour from the structural model.

Physical Domain

The physical domain entertains representations of the mechanical construction of the system. The physical model is the ultimate outcome of a synthesis excercise prior, of course, to fabrication. If this process is reversed, such that the designer moves through the physical and structural model to the operation model, then the process is known as analysis.

An important feature within the structural domain is the effect of coupling structures. When mechanical structures are coupled the frequency response characteristics of the coupled structure are different to the individual components. If the test rig is dynamically equivalent to the "clean" carrier body, then the change in the dynamical characteristics of the test rig will be the same as the carrier body when the equipment is attached. It is this feature that is the major reason for selecting an iconic modelling representation.

Another advantage of the mechanical test rig is the usage of the actual fixing mechanisms or linkages. These linkages are highly non-linear and have discontinuities. The linkages are usually very stiff in certain planes but allow large movements in others. By exciting the test rig and not the equipment directly, it will be possible to regenerate these conditions accurately. This emphasises the importance of the structural domain by establishing that the relationships between coordinates of interest (the transfer frequency response plots) are correct.

Within the physical domain it is envisaged that the test rig will comprise two distinct components, a continuous element and a discrete system. The continuous element is to connect the points or coordinates of interest. The distributed nature of the mechanical properties of the continuous element are explicitly taken into account. The difference between these properties and the dynamical characteristics of the carrier body are used to identify a discrete system. This discrete system is coupled to the continuous element so that the resultant structure, called the substitute structure is dynamically similar to the original carrier body.

The major disadvantage of a mechanical test rig is fatigue of the continuous element. If the test rig is to be used for a range of equipment then it will be necesary after the dynamical propeties have been established correctly, to examine the rig for possible fatigue failures.

2.5 CHOSEN APPROACH

Having selected the modelling medium that is to be used throughout the work the next step is to establish intermediate objectives. This is essentially the partitioning of the global system S , Figure 2, into sub-systems. Each sub-system should address a specific problem and each act as a step towards providing the ability of transforming problem specifications in the input space ($\mathcal{E}_i$) into solutions within the output space ($\mathcal{E}_o$).

One of the most significant steps within modern modal analysis techniques is possibly the development of system identification procedures. Its origins lie in the design of aerospace structures, but the technique is sufficiently general to be applied to any engineering structure where the dynamical characteristics are to be examined. Real data, in the form of frequency response plots, are recorded from physical structures. These data are then analysed to identify the resonance frequencies of the structure and the mode shapes of vibration. From this modal data it is then possible to derive mass and stiffness matrices representing a spatial model of the original body. This spatial model is within the class of homomorphic models and is in the operational domain. It is possible, therefore, to specify the first sub-system that should be examined. Given that the system identification process yields a homomorphic model in the operational domain it is necessary to examine

techniques which can synthesise a realisable structure within the physical domain.

Although the general design case is for multi-attachment point equipment it was considered that it would be worthwhile to examine the requirements for single point dynamic similarity. This is a special case of the multi-attachment point condition and will allow the examination of continuous structures as well as discrete systems.

One of the problems with the design of the test rig is already apparent since the specification for its operational domain has set a frequency range of interest. Now, the original carrier body and the equipment are continuous systems and therefore have an infinite set of modal characteristics. By specifying a frequency range the data that will be available to the designer will be truncated and incomplete. The implications of using this data and how it effects the iconic model will have to be examined.

The final two sub-systems that can be identified are;

a) the derivation of a systematic design methodology for a distributed parameter system which has prescribed dynamical characteristics (the continuous element within the substitute structure).

b) examining the iconic model during the structural domain phase when the discrete systems are coupled

to the continuous element. It is important to establish that the change in the frequency response characteristics of the substitute structure when the discrete system is coupled is deterministic and therefore suitable for inclussion within the design synthesis algorithm.

This means that the system S, Figure 2, has been partitioned into five major sub-systems or modules. It was proposed at the outset of the project to direct effort to all five areas rather than pursue an exhaustive examination of aspects within any one. The connecting link between all the areas of work is the primary objective of deriving a design methodology for environmentally representative test rigs. This is analgous to attempting to locate a river's source when starting from its estuary. As the traveller moves up the river confluences will be encountered and each route will be examined to establish which is likely to be the tributary. Short trips up the tributaries will be made but the main effort is always directed to taking the most likely route which will result in the river's source. Each confluence is essentailly a point within the project where a decision based upon the principle of minimum committment has to be exercised.

2.6 ASSESSMENT OF THE DESIGN METHODOLOGY

The design methodology will be ultimately assessed by its ability to derive acceptable, functional designs. These

designs will have to be realisable so that they can be built and validated before being used for environmental testing. It is not envisaged that a unique solution will be achieved for a given set of design conditions. In fact, it may well be that no solution can be achieved by the design methodology, in which case the designer must either accept the 'best case' or reformulate the problem. If the methodology does result in a solution it will be achieved by design optimisation techniques. Current design optimisation techniques for distributed parameter design problems utilize the theory of feasible directions to derive a solution. This means that the resultant solution will provide the required characteristics but it does not necessarily mean that the actual design represents the best or ultimate solution. Within any design optimisation technique the basis for selecting a feasible direction is made by deriving the set of conditions that give a minimum value to the cost equations. The quality of the final design is therefore a function of the completeness of the cost equations as well as the ability to optimise them.

THe traditional and obvious design basis used when optimising structures to have prescribed dynamical characteristics is to use modal or frequency response data. The problem is formulated as the eigenvalue problem and the sensitivity of its constituent elements is then examined to select a feasible direction. It was considered at the outset of the project that the likelyhood of achieving identical dynamical characteristics between the carrier

body and the test rig was slight. However, it was considered possible to design dynamically similar structures, the question was; what degree of similarity was acceptable ? This introduces a new state varible which describes the degree of similarity in the form of an error in the cumulative fatigue damage to the equipment. This error can be quantified and, therefore, can be incorporated within a design synthesis technique and used to terminate the optimisation procedure.

An alternative design basis would be to examine the design of a test rig where the aim would be to optimise on the cumulative damage criteria rather than frequency response data.

The philosophy of the design approach is to be able to derive a test rig which is dynamically representative of a carrier body for a specified frequency range. During the process of designing the test rig the fundamental elements that control specific dynamical characteristics will have been identified. It should then be possible to alter these characteristics, by simple element changes, to derive the dynamical characteristics of another carrier body. In this way the rig will act as a generalised carrier body platform upon which a whole range of different equipment may be examined.

3. BASIC CONCEPTS

3.1 INTRODUCTION

When an operational or prototype carrier body exists it is possible to obtain a set of frequency response plots of the body at defined co-ordinates of interest. These frequency response plots can be analysed by a computational technique to identify the resonant frequencies and mass normalised mode shape values at the co-ordinates where the response plots were obtained. Once the resonant frequencies and mass normalised mode shapes have been established it is then a simple procedure to create a spatial model of the original carrier body. This model comprises a set of matrices which represent the mass, stiffness and damping distribution of the carrier body for the co-ordinates of interest. The first objective of the work is to examine the possibility of using these experimentally derived matrices to identify the parameters of a mechanical test rig.

It is also necessary to establish the basic concepts of dynamic similarity. This is so that a library of design rules and guidelines can be established to assist the designer when attempting to achieve dynamic similarity between different physical structures.

3.2 LITERATURE REVIEW

3.2.1 SYSTEM IDENTIFICATION

The process of reducing a physical system to a mathemetical representation is a prevalent task amongst design and test engineers. This reduction procedure is typically a blend of skill, insight, experience and good judgment. Any mathemetical representation (or analogue model) of a proposed design is therefore, heavily dependent upon the skill of the modeller. When a design actually exists it is possible to perform controlled tests on it and subsequently derive a model from the experimentally derived data. This procedure of establishing a spatial model of the design from experimentally derived data is commonly known as system identification.

The derived spatial model can be classed as a homomorphic model with it´s status within the operational domain. This means that the model is capable of reproducing the physical system´s performance attributes but the model itself does not have any physical meaning. It is worthwhile to examine the development of the system identification technique from its origins within the design of aerospace structures to its present day usage. In particular it is necessary to establish whether researchers within this field have been capable of synthesising a physical representation from the

experimentally derived spatial model.

One of the first authoritive papers on the subject was by Young and On [3]. They reviewed in 1969 the state of the art of modelling from experimental data and concluded that no one methodology was the analysist´s panacea for model generation. They identified three broad classes of situations for each of which certain techniques are more appropriate.

These situations are

(i) Damping is present but the modes are only lightly coupled.

(ii) Damping is heavy and modes are strongly coupled.

(iii) Damping is so light that accurate measurement of response near resonance is not practicable.

In 1972 Flannelly and Berman [3] again reviewed the field of system identification and concluded that analysis techniques can be grouped into two broad classes.

(i) Modal techniques.

(ii) Non-modal techniques.

(a) Modal Techniques

A set of modal analysis techniques has been developed which uses frequency response measurements, such as mobility curves and concentrates on analysing the data on or near system resonance points. Then by the use of either direct or curve fitting analytical methods the mass, stiffness and damping matrices are identified. Of the direct methods the work by Raney [5], Potter and Richardson [6] and Thoren [7] serve as adequate examples. For instance, Thoren develops an approach where the orthonormal modal vectors are obtained by sweeping each significant resonance of the system. This approach assumes that the resonances are well spaced, well defined, lightly damped and uncoupled. Having derived the mode vectors it is then possible to obtain the mass, stiffness and damping matrices. Thoren uses the technique to model complex subsystems within a much larger structure. The derived matrices are then incorporated within a model of the larger structure which has been derived by conventional analytical modelling techniques. Thoren's approach provides an alternative to modelling complex subsystems as either lumped parameters or highly defined models which carry an associated cost penalty in computational time and model stability.

An alternative direct method has been developed by Ewins and Gleeson [8] for lightly damped structures where the accurate measurement of resonant amplitudes is not

practicable. The values of the frequency at the points of anti-resonance are used to compute the mode vectors and hence derive the mass and stiffness matrices.

The advantages of the direct method are that it is computationally efficient and very reliable.

In the curve fitting approach, numerical and graphical means have been developed to yield response curves which provide a best fit to the experimentally obtained data. The graphical method involves fitting a circle to near resonance data, dominated by damping effects, usually plotted on the Argand diagram. Klosterman [9] has suggested four procedures for deterining the modal vectors, but they are not in common use due to the techniques not being suitable for implementation on a computer.

It is possible to use numerical curve fitting procedures such as linearised least square and implement a graphical analysis technique on a computer.

The method developed by Gaukroger et al [10] is widely applicable since it may be used for curve fitting a large number of close resonances. A disadvantage of the method is that all unknowns are determined simultaneously and if the procedure fails at one stage, it is not possible to determine which mode is at fault. Goyder [11] proposes a technique, again based on a linearised least squares curve fitting process, where the parameters of each mode are

obtained sequentially. The basic assumption made is that over a small frequency band near each resonant frequency, the contributions to the total response from all modes except the local one is very nearly constant. Subsequent experimental work has shown this assumption to be quite valid for the typical well defined frequency response plot.

(b) Non-modal Techniques

Here the abstract parameters of mass and stiffness matrices are identified directly without recourse to the modal properties. Collins et al [12] presents a statistically based iteration procedure and Chan and Garga [13] and Grossman [14] introduce perturbation methods to improve the efficiency of the iteration. These methods are best suited to models of a relatively small number of degrees of freedom. Dale and Cohen [15] describe a method which is based on the conversion of a boundary value problem to an initial value problem. This method is suitable for identification of continuous structures such as beams and plates. The process is not reversible and therefore is not suitable for the identication of a test rig if the mass and stiffness matrices are known.

3.2.2 INCOMPLETE MODELS

Parallel with the development of system identification techniques, researchers were examining the use of

incomplete models to predict the dynamical behaviour of specified structures. This was an attempt to utilise the derived mass and stiffness matrices effectively by improving the analytical model. the first incomplete model, proposed by Berman and Flannelly [16], was based on measured normal modes fewer in number than spatial co-ordinates. The mass matrix was derived by intuitive means and improved by conditioning with the measured normal modes. Considerable care has to be exercised when applying this technique as the derived matrices are singular. Nevertheless, it is possible to compute the first N degrees of freedom of a measured P degree of freedom structure (N<P).

Ross [17] proposes three possible ways of handling the problem of incomplete models. The first, and easiest, is to reduce the number of spatial co-ordinates to the number of eigenvalues required. The second technique is to make the modal matrix non-singular by adding (P-N) arbitary linearly independent vectors and setting their associated eigenvectors sufficiently large to be outside the range of interest. The final approach is to synthesise the flexibility matrix which will only be of rank N, this results in the highest eigenvectors (P-N) being infinite. The measured modal matrix will be of order P and rank N and therefore cannot be inverted. The mass matrix is derived from a finite element model of the structure.

Berman and Wei [18] formalised the usage of incomplete

models to provide a technique known as analytical model improvement. A model of the structure is constructed, usually by finite element analysis and the incomplete modal data from the tested structure is used to improve the model's accuracy. The Guyan reduction relationship [19] or Kidder approximation routine [20] is used to generate the unknown elements of the incomplete modal data. The trend in incomplete modelling has gone from intuitively deriving the mass matrix and then computing the incomplete stiffness matrix to deriving the mass and stiffness matrix by finite element analysis and then computing the incomplete measured normal modes. These modes and the experimentally obtained mass and stiffness matrices are then used to improve the analytically derived model.

3.2.3 IMPROVED MASS AND STIFFNESS MATRICES

Generally, the mass and stiffness matrices obtained from a system identification procedure are fully populated and the mass matrix has negative elements when only translational responses are recorded. This means that the matrices do not have an obvious physical meaning. Depending upon the intented use of the derived matrices these attributes may be unimportant (if generation of other points of interest on the same structure are required) or critical (if predictions based on changes in mass or stiffness are made).

In 1978 Baruch and Bar-Itzhack [21] examined the problem of orthogonality of measured modes. They proposed a technique, based upon the minimisation of an Euclidean norm, where the errors between measured modes and required orthogonal modes were minimised. The corrected mode shapes were then used to compute a corrected stiffness matrix. The techique was limited since it assumed knowledge of an accurate mass matrix. Baruch [22] published another paper later in the year, showing an insufficient constraint had been applied in the original paper. A new improved procedure was offered, based on the original mathemetics but incorporating the correct constraint, i.e. the stiffness matrix should be symmetric. Wei [23] proposes a further modification to the procedure where the assumptions made to obtain the Lagrange multiplier can be by-passed. The technique provides an elegant methodology to derive an improved stiffness matrix. Ibrahim [24] presents a technique to identify a set of normal orthogonal modes from measured complex modes. This technique is useful when dealing with complex structures possessing, not necessarily high levels of damping, but a high degree of non-proportionality in damping distribution. Again the conditioned mode shapes and identified mass, stiffness and damping matrices are used to improve an analytically derived mathematical model of the structure. Goyder [11] attempted to use the orthogonality relationships to improve the stiffness matrix but the technique failed to provide meaningful results due to the sensitivity of the algorithm to truncation effects.

In 1981 Baruch [25] presented a general discussion of system identification procedures based on three reference basis. These were mass, mode shape or stiffness; the choice being made by what the analysist considered to be most important or most accurately recorded.

The assumption that the mass matrix is correct especially for a dynamic model which is often an approximate reduced version of a much larger model was questioned by Berman [26]. A mass matrix improvement algorithm was proposed where the analytical mass matrix was corrected to make it consistent with the measured modes. The recent trend in model improvement, typified by Berman and Nagy [27], is to develop an analytical model (usually by finite element analysis) and a model from experimental data. Then, by using a combination of the mathemetical concepts of [22], [23], and [26] new improved mass and stiffness matrices are generated. Within this methodology the matrices obtained from the system identification process are manipulated to have the same degrees of freedom as the analytical model. They are then used to provide small improvements to the analytical model, particularly to the damping distribution and to providing flexural stiffness at rigid joints.

3.3 DIRECT TEST RIG IDENTIFICATION

The review of existing system identification algorithms highlighted that the goal of each technique is to identify the modal parameters of the structure under test. These modal parameters are then used to derive a spatial model of the structure. The Goyder algorithm [11] was considered suitable for this work as the structures under consideration usually have well defined lightly coupled modes with a low level of damping (generally less than 5%) for the frequency range of interest. A limitation of the Goyder algorithm is the number of degrees of freedom must be equal to the co-ordinates of interest. This is to avoid matrix singularity problems during the analysis. This limitation introduces two sources of error into the analysis.

(i) The finite spatial representation of the body

(ii) The finite number of resonant frequencies.

Error correcting terms are introduced into the analysis to allow for the effects of resonance frequencies above and below the range of interest.

Once the finite modal parameters have been established the basic orthogonality relationships can be used to derive the

spatial model.

$$[\Phi]^T[M][\Phi] = [I]$$

$$[M] = [\Phi]^{-T}[\Phi]^{-1} \qquad (31)$$

$$[\Phi]^T[K][\Phi] = [\lambda]$$

$$[K] = [\Phi]^{-T}[\lambda][\Phi]^{-1} \qquad (32)$$

where $[M]$ and $[K]$ are the mass and complex stiffness matrices respectively and the columns of $[\Phi]$ are the complex mode shapes.

A simple cantilever (Figure 4) was examined to obtain a set of mass, stiffness and clamping matrices. In its simplist form the structure can be considered as a two dimensional problem in one plane of motion. At the two coordinate points selected, the translational and rotational frequency response plots were generated.

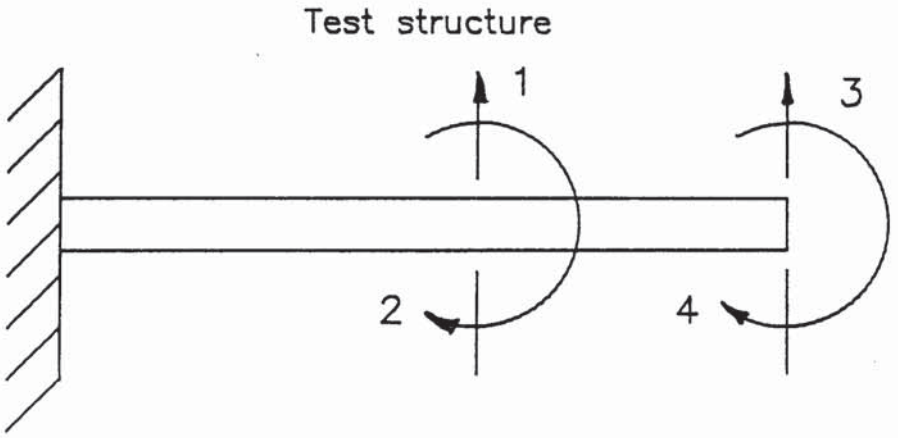

Figure 4

The forcing function was applied to each position

(translational and rotational) in sequence and a set of 4x4 mobility plots were obtained and hence a set of 4 mass, stiffness and damping matrices were derived (Table 1). An examination of this set of matrices shows that

(i) They are all different

(ii) They are all fully populated.

If the eigenvalue problem is solved for each set then the first four resonant frequencies and mode shape vectors for the simple beam are obtained. This demonstrates that depending upon the choice of the reference coordinate (generally the coordinate where the forcing function is applied) it is possible to obtain as many different sets of mass, stiffness and damping matrices as coordinates of interest. Since we are considering continuous systems, there is an infinite set of possible reference coordinates and response coordinates. This is a design class called homomorphic models where there are many to one transformations to the model. This feature is invaluable for design analysis procedures but unfortunately the transformations are not reversible.

There is, therefore, no unique set of mass, stiffness and damping matrices for any given continuous system.

A practical continuous structure also has an infinite number of resonance frequencies. The terms of reference of the project is to examine the possibility of deriving a test rig which is dynamically similar to a carrier body for

up to the first four modes of vibration. Since a restricted range of frequency is to be examined (which is always the case with continuous systems) then truncation effects will be experienced. These manifest as fully populated matrices within the spatial model.

As a result of the two observed conditions, it is not possible to identify the parameters of a continuous structure directly from the spatial model. However, an implication of (31) is that structures that exhibit the same mode shape vectors at the same coordinates of interest will have the same mass distribution. If the resonant frequencies of the structures are the same then the stiffness distribution will be the same. Therefore, it is theoretically possible for different physical structures to have identical dynamic characteristics at selected coordinates over a limited frequency range.

3.4 DYNAMIC SIMILARITY

A study was made to examine which parameters were critical if dynamic similarity was to be achieved between two structures. Simple continuous beam structures were used as it was possible to define the dynamical characteristics by simple mathematical expressions [28].

In the first instance, the work examined the conditions that had to be achieved if identical dynamical

characteristics were to be obtained. These conditions will represent the ideal case and it is then a matter of establishing a variance to these conditions which still yields an acceptable level of similarity.

The generalised expression for the resonance frequencies of a simple beam element is

$$\omega = (\beta_r^2)\sqrt{\frac{EI}{\rho A \ell^4}} \qquad (33)$$

where (β_r^2) is a function of the end constraints.

An immediate observation can be made; if two structures are to be dynamically equivalent then the end constraints must be the same for each structure.

The ratio E/ρ is approximately constant for a wide range of materials from steel to aluminium or even woods such as spruce. It is, therefore, only possible to manipulate the geometry to obtain a physically different structure.

Consider a simple cantilever, shown in Figure 4. If this cantilever was assumed to be the original structure, then two conditions for different beams were examined.

Case 1 Changing the depth and length.

Case 2 Changing the breadth and depth.

For each case, the change in one dimension was reflected in a change to the other dimension such that no resultant change should occur in the resonant frequencies

(Appendix 1). Once the parameters of each equivalent cantilever was established they were analysed using finite element analysis.

The resonant frequencies for both conditons were the same as the original structure. However, when the breadth was retained and the length altered, Case 1, the eigenvectors differed. The elements representing translational movement are the same but the values representing rotation are greater. This is a result of altering the rotational inertia of the beam by reducing the length. This characteristic is highlighted in Figure 5 where the tip of each beam has the same amplitude in translation, but different rotational values.

At this stage point coordinate similarity in one plane of motion (vertical translation) has been achieved between the two structures (Figure 5a and 5b) at their tips (position x). The amplitude of the mode shape is 0.78 $1/\sqrt{k_g}$ for all three conditions. The slope of the mode shape (the value in brackets below the mode shape amplitude) varies according to the length of the beam. If the equipment that is to be tested have two or more attachment points, then a minimum requirement for the rig is dynamic similarity at the corresponding number of points. The whole equipment and fixing mechanism is to be used within the test and, therefore, a fixed dimension between the attachment points provides a design constraint. If this fixed dimension is overlayed on Figures (6a) and (6b) then it is obvious that

the equipment does not receive the same dynamical input characteristics.

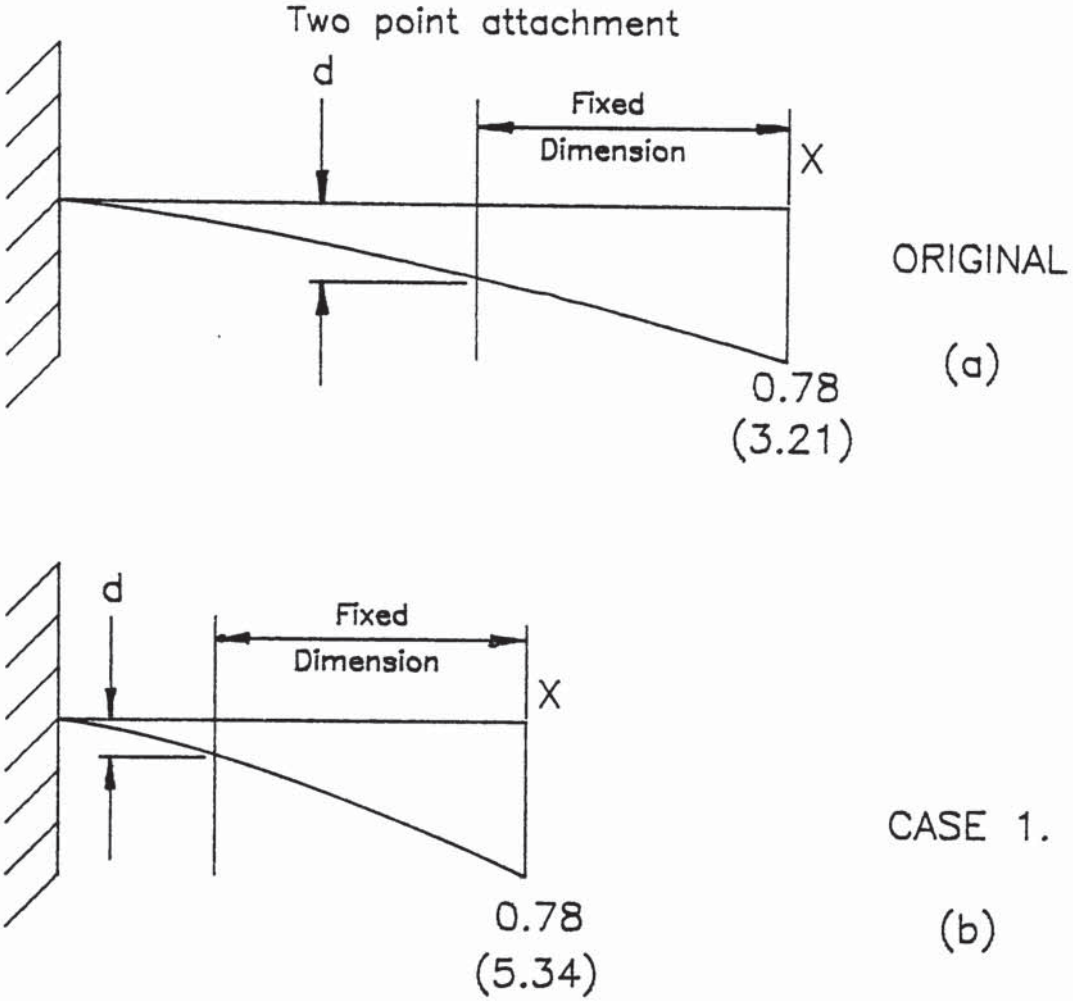

Figure 6.

The amplitude of the translational mode shape value at position (d) in Figure 6a is greater than the amplitude at (d) in Figure 6b. This results in a discrepancy in the dymamical input characteristics.

Complete correlation of dynamic characteristics are obtained for Case 2 where the length is retained and the sectional area altered.

From these observations it is possible to deduce two further design rules for dynamic similarity

(i) The mass and stiffness distributed of the two structures must be the same

(ii) The distances between coordinate points of interest should be the same.

The final test performed on these single beam elements was to examine the effect of applying a simple spring/mass system to the tip of each beam (Figure 7)

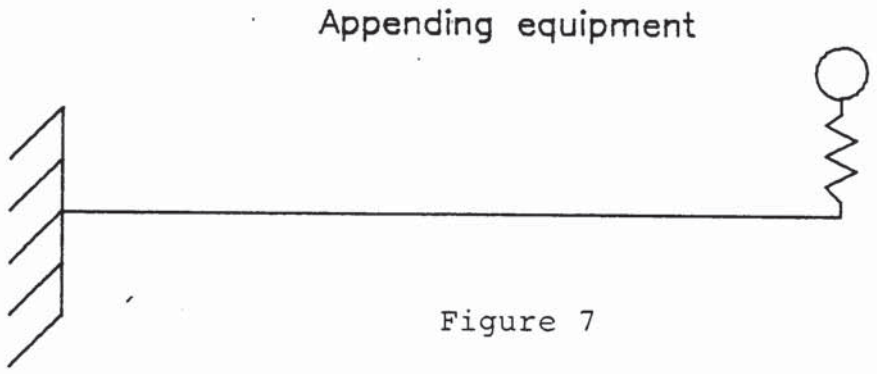

Figure 7

The spring/mass system represents a piece of equipment being attached to the carrier body. This simple test is to demonstrate the premise that when the same equipment is attached to dynamically similar structures the changes in the modal characteristics is the same for each structure. This was found to be correct for both cases. Case 1 exhibited the same characteristics as before, correct resonance frequencies and correct translational mode shape vector values. Case 2 exhibited the identical changes that the original structures showed.

3.5 TRUNCATED DATA

A limitation of the system identification technique used is that the number of coordinates of interest must equal the number of degrees of freedom. This means that a finite number of resonance frequencies is used within the analysis. It has already been shown that this causes the matrices within the spatial model to be fully populated. Another aspect that has to be examined is whether the number of degrees of freedom or the number of planes of motion considered have any effect upon the accuracy of the identified modal parameters. An alternative way of considering this is as whether the completeness of the experimental data affects the accuracy of the modal parameters.

Two studies were made using truncated incomplete mobility plots.

(a) A simple continuous system

(b) A multiple degree of freedom discrete system.

It is possible to express the dynamic characteristics of the two types of system with well defined mathematical equations and hence obtain the resonant frequencies and eigenvectors (mode shapes).

(a) Continuous System

A uniform section cantilever 0.3m long was used to represent a simple continuous system (Figure 4).

When generating the mobility plots, for the beam, the loading was retained at the tip (translation only) and the response station positions and planes were varied. The nomenclature for the mobility is

Y_{ij} where i =forcing station

j =response station

the mobility can be expressed as

$$Y_{ij} = \Omega \sum_{r=1}^{n} \frac{{}_r\phi_i \, {}_r\phi_j}{(\omega_r^2 - \Omega^2)} \qquad (34)$$

where Ω is the excitation frequency and has values within the swept frequency range.

${}_r\phi$ is the mass normalised mode shape for the r^{th} mode

The first analysis was for a point load at the tip and responses taken at the tip for translation and rotation, thus providing the first two resonances for analysis. The contributions from the first eight modes were accounted for when generating the mobility plots. A system identification of the mobility plots yielded the correct natural frequencies for the first two modes. The elements of the eigenvectors represent the vertical motion and slope of the mode shape at the tip. It is important to note that

these eigenvectors are mass normalised and it is, therefore, tenable to compare eigenvector values providing the structure and loading conditon are retained constant. The value of the mode shape in the vertical plane of the tip is 7.1754 (the units are $1/\sqrt{kg}$) for the first mode and 7.193 for the second (Figure 8).

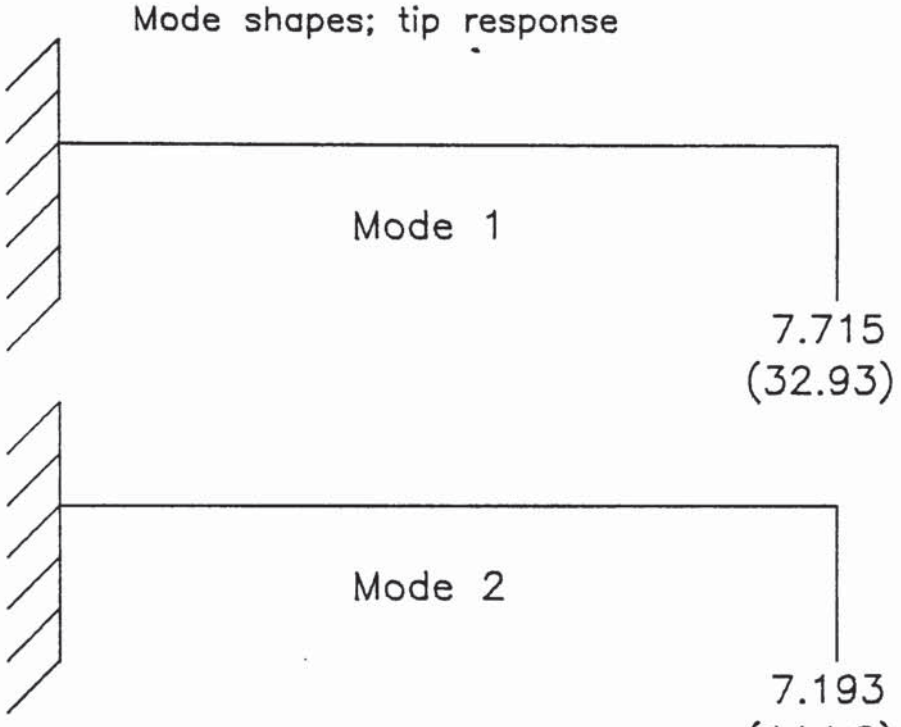

Figure 8.

Having just the values of the tip for vertical motion and rotation is insufficient data to plot the mode shape.

The next stage considered translational responses at a point .181 metres from the beam root and at the tip. A system identification of the mobility plots produced correct values for the first two modes. This time the eigenvectors contained values defining the mode shape in the vertical plane at .181m and the tip. The values for the first mode are shown in Figure 9.

Mode shapes; vertical response

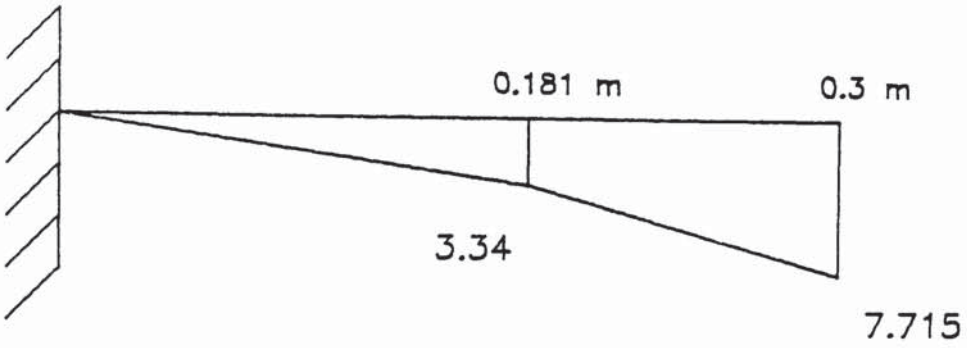

and the second mode

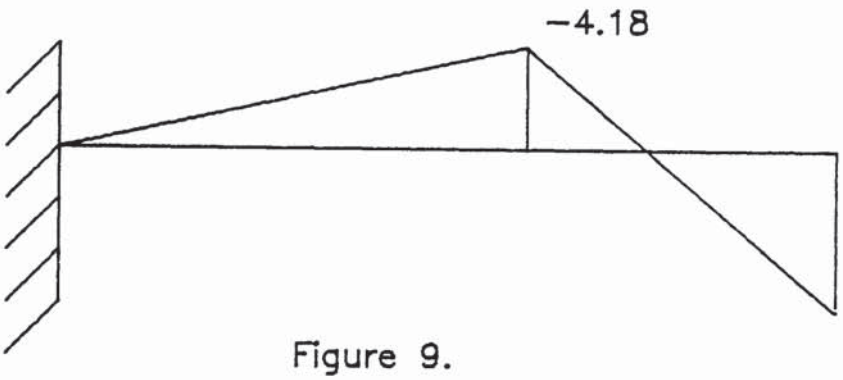

Figure 9.

The value at the tip in the vertical plane corresponds to the values obtained from the first analysis. This time though the mode shape is more completely defined since two coordinates on the beam have been used.

Using the same position on the beam (.181m and tip) four mobility plots were generated which accounted for translational and rotational effects. Considering the first two modes from the system identification (Figure 10).

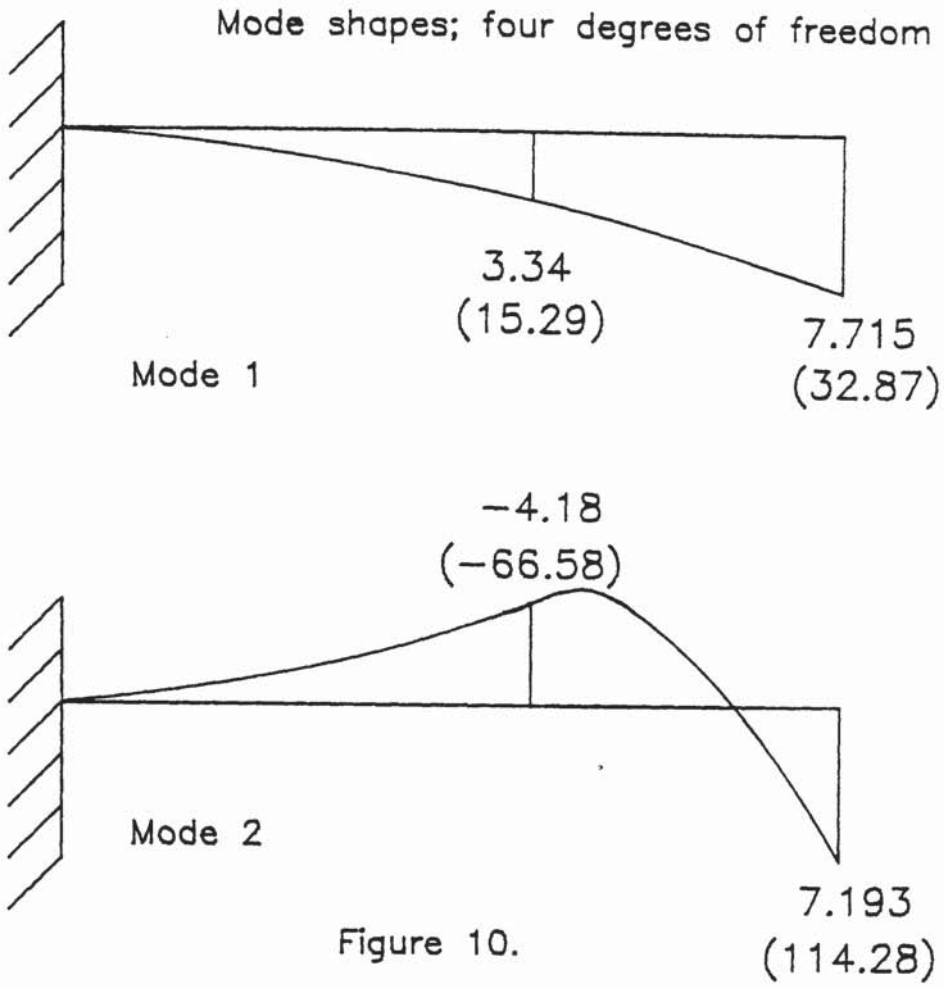

Figure 10.

The values for the mode shape in the vertical plane are the same as those obtained from the two degree of freedom analysis. The rotational values, where available, also correspond to the two degrees of freedom analysis.

Translational responses only were examined for four positions along the beam (0.085, 0.081, 0.239 and 0.3 metres). Contributions from the first eight modes were taken into account when generating the four mobility plots. The system identification yielded the correct values for the first four resonances and the following mode shapes (Figure 11).

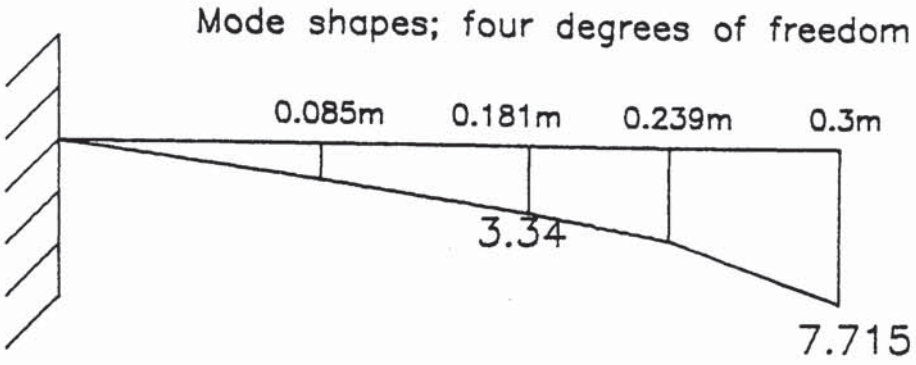

Mode 1

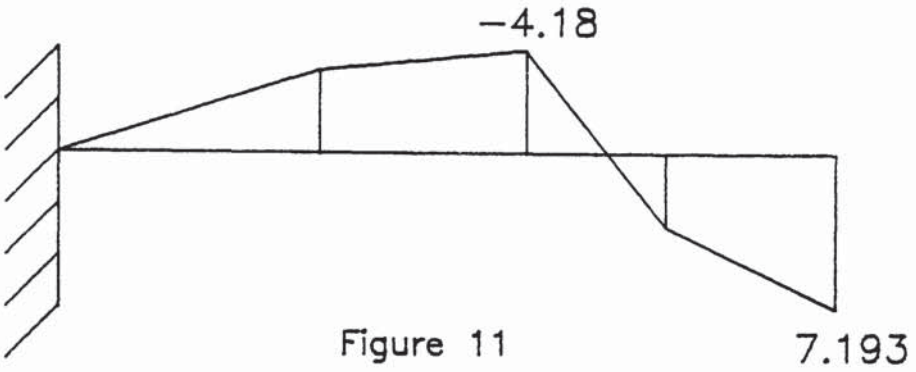

Figure 11

Mode 2

Having four values for translational displacement along the beam allows better definition of the actual mode shape. The values of mode shape at .181 m and the tip are the same as the values obtained from the two degree of freedom analysis.

Although this simple prcedure has only been performed for two and four degrees of freedom it demonstrates that eigenvector values are a function of the structure geometry. The absolute values of the eigenvector elements

fully define the beam motion irrespective of the degree of freedom considered (i.e. the same absolute value of tip motion in the vertical plane for a two degree of freedom model as a multidegree of freedom model).

As an alternative to the classical equations for the dynamic behaviour of beams it is possible to analyse their behaviour by the use of finite element analysis. This technique discretises the beam into a finite set of elements.

Typically, the mass matrix, which is symmetrical, for one element of length ℓ and end sectional areas A_1, A_2 comprises

$$\rho\ell\begin{bmatrix} \left(\frac{2}{7}A_1+\frac{3}{35}A_2\right) & \left(\frac{1}{28}A_1\ell+\frac{1}{60}A_2\ell\right) & \left(\frac{9}{140}(A_1+A_2)\right) & \left(\frac{1}{60}A_1\ell-\frac{1}{70}A_2\ell\right) \\ & \left(\frac{1}{168}A_1\ell^2+\frac{1}{280}A_2\ell^2\right) & \left(\frac{1}{60}A_2\ell+\frac{1}{70}A_1\ell\right) & \left(-\ell^2\times\frac{2}{280}(A_1+A_2)\right) \\ & & \left(\frac{2}{7}A_2+\frac{3}{35}A_1\right) & \left(-\frac{1}{60}A_1\ell-\frac{1}{28}A_2\ell\right) \\ & & & \left(\frac{1}{280}A_1\ell^2+\frac{1}{160}A_2\ell^2\right) \end{bmatrix}$$

where suffix 1 is left end of element

2 is right end of element

a similar expression is obtained for the stiffness matrix, where the translational and rotational effects are distributed throughout the matrix.

The same geometric values for the cantilever were used (as

the previous analysis) and a two element representation was made of the beam.

The results from the finite element analysis shows the limitations that can occur when discretising a continuous system. The use of only two elements to represent a beam is very coarse and not likely to provide high accuracy for the third and fourth natural frequencies.

The first frequency was computed very accurately at 589.35 rad/s (an error of .005%),Figure 12

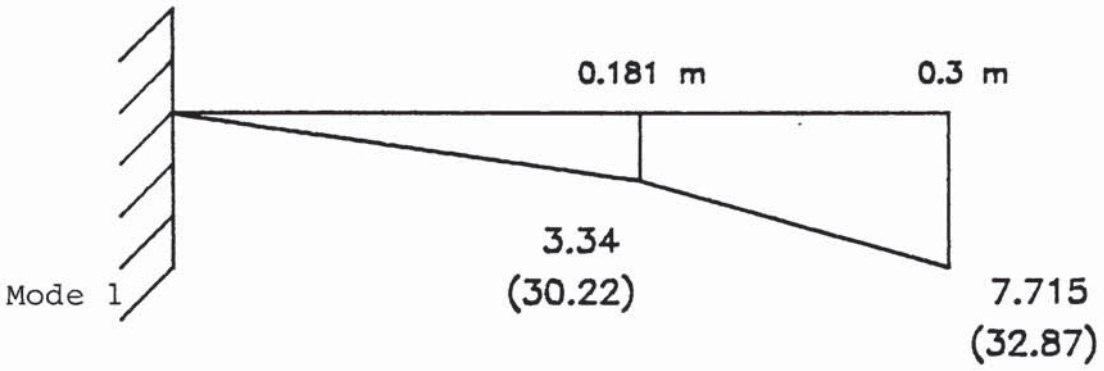

The second frequency had an error of 2.56% and a mode shape

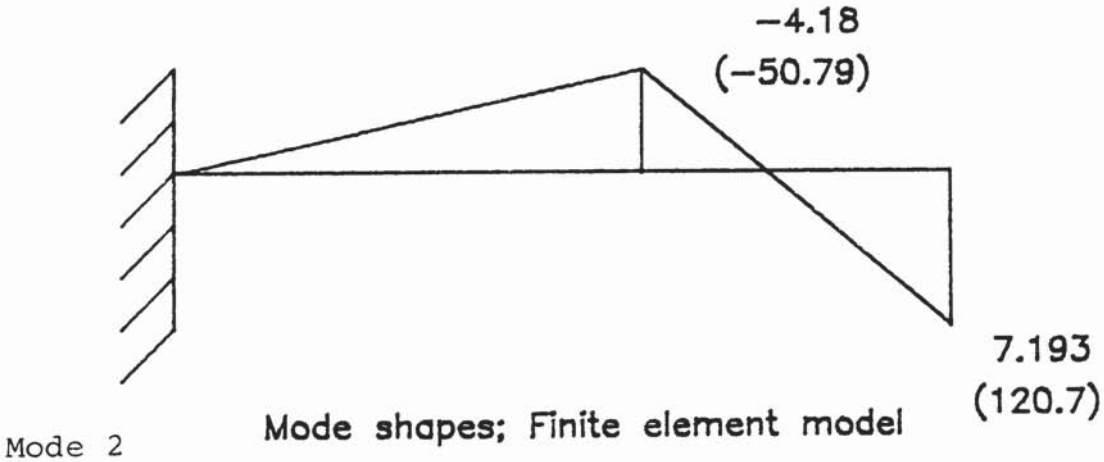

Mode shapes; Finite element model

Figure 12.

The mode shape values for vertical displacement correlate very well with the results from the classical equations.

A six element (12 degree of freedom) finite element model was generated for the same cantilever dimensions as before and the first four modes were computed. The natural frequencies were very accurate and full correlation of mode shapes (including absolute values) were obtained with the classically derived mode shapes.

This emphasises that the same absolute values for mass normalised eigenvectors are obtained irrespective of the number of degrees of freedom examined for a continuous system.

This is for either classical analysis using single expressions defining the dynamic characteristics or discrete models representing the continuous structure.

(b) Discrete System

If the eigenvalue problem is examined for a discrete system then it is possible to write

$$([K] - \omega_r^2 [M]) \{_r\phi\} = \phi \qquad (35)$$

or

$$[M]^{-1}[K] \{_r\phi\} = \omega_r^2 \{_r\phi\} \qquad (36)$$

Discrete system

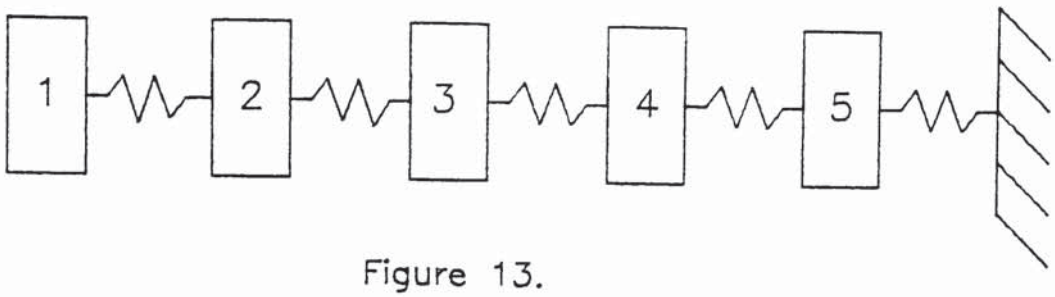

Figure 13.

If [K] is taken as representing linear discrete springs then it is possible to observe that the natural frequencies and mode shapes are independent of system geometry.

A five degree of freedom system (Figure 13) was used to generate a set of five mobility plots. The forcing function was taken to be applied at mass m_5 and the responses measured at masses 1 to 5. When a system identification was performed using this complete set of mobility data it was possible to identify all the natural frequencies and the complete mass normalised mode shapes. Hence it was possible to regenerate the mass and stiffness matrices very accurately.

The set of mobility plots were truncated by removing the last plot Y_{15} . A system identification was performed on this incomplete set, considering only the first four modes. The natural frequencies of the first four modes were identified accurately.

The first and second mode shapes compares reasonably well with the first four values of the complete system mode shape (Table 2).

As the higher modes are examined the correlation between the modes deteriorates until mode four bears no resemblence to the first four elements of the fourth mode of the complete system.

If the four response stations are retained and the total degree of freedom of the complete system are examined, then interesting results are obtained.

The first four values of each mode shape are identified correctly for all five degrees of freedom of the system. These values correlate exactly with the corresponding values in each mode shape. However, they are not complete as the fifth element is missing. It is not possible, therefore, to generate the mass and stiffness matrices using the orthogonality relationship of equation (31) since the $\{_r\phi\}$ vectors are incomplete.

The full mode shape matrix would be

$$\begin{bmatrix} {}_1\phi_1 & {}_2\phi_1 & {}_3\phi_1 & {}_4\phi_1 & {}_5\phi_1 \\ {}_1\phi_2 & {}_2\phi_2 & {}_3\phi_2 & {}_4\phi_2 & {}_5\phi_2 \\ {}_1\phi_3 & {}_2\phi_3 & {}_3\phi_3 & {}_4\phi_3 & {}_5\phi_3 \\ {}_1\phi_4 & {}_2\phi_4 & {}_3\phi_4 & {}_4\phi_4 & {}_5\phi_4 \\ ? & ? & ? & ? & ? \end{bmatrix}$$

and the handling of such a matrix would produce singularity problems.

A system identification analysis was performed for three response stations and the first three modes of vibration. Exactly the same trend as for the four response stations was obtained i.e. the mode shape correlation for the first three elements of the complete mode shape is initially reasonable but deteriorates to no correlation for the last mode examined.

Although system identification analysis was performed for two response stations and a single response station the resultant mode shape values had little meaning in reality.

This analysis has shown that for discrete spring/mass systems it is necessary to have a one to one mapping for the complete system, of the degrees of freedoms and the response stations. Otherwise, techniques must be devised to complete the truncated mode shapes prior to them being useful for subsequent analysis.

3.6 SUMMARY OF BASIC CONCEPTS

It is possible to summarise the findings relating to the

basic concepts of dynamic similarity as:

1. It is impossible to identify the parameters of a dynamically similar test rig directly from the mass, stiffness and damping matrices. This is due to truncation effects of the frequency response data from the original structure and that an infinite set of mass, stiffness and damping matrices exist, depending upon the coordinates of interest, for each continuous system.

2. If two structures exist that have the same eigenvector values at specified coordinates, and the same resonant frequencies within a defined frequency range, then they are dynamically similar for that frequency range.

3. If two structures are to exhibit an identical set of modal characteristics, they must have the following features:
   (i) the same end constraints
   (ii) the same mass and striffness distribution
   (iii) the same dimensions between the coordinates of interest.

4. When truncated incomplete data is used, measured from physical structures, the values of the mode shape vectors do not depend upon the number of degrees of freedom measured. It is also possible to model the

characteristics of the complete body by considering the eigenvector values for only one plane of motion.

Equivalent beams

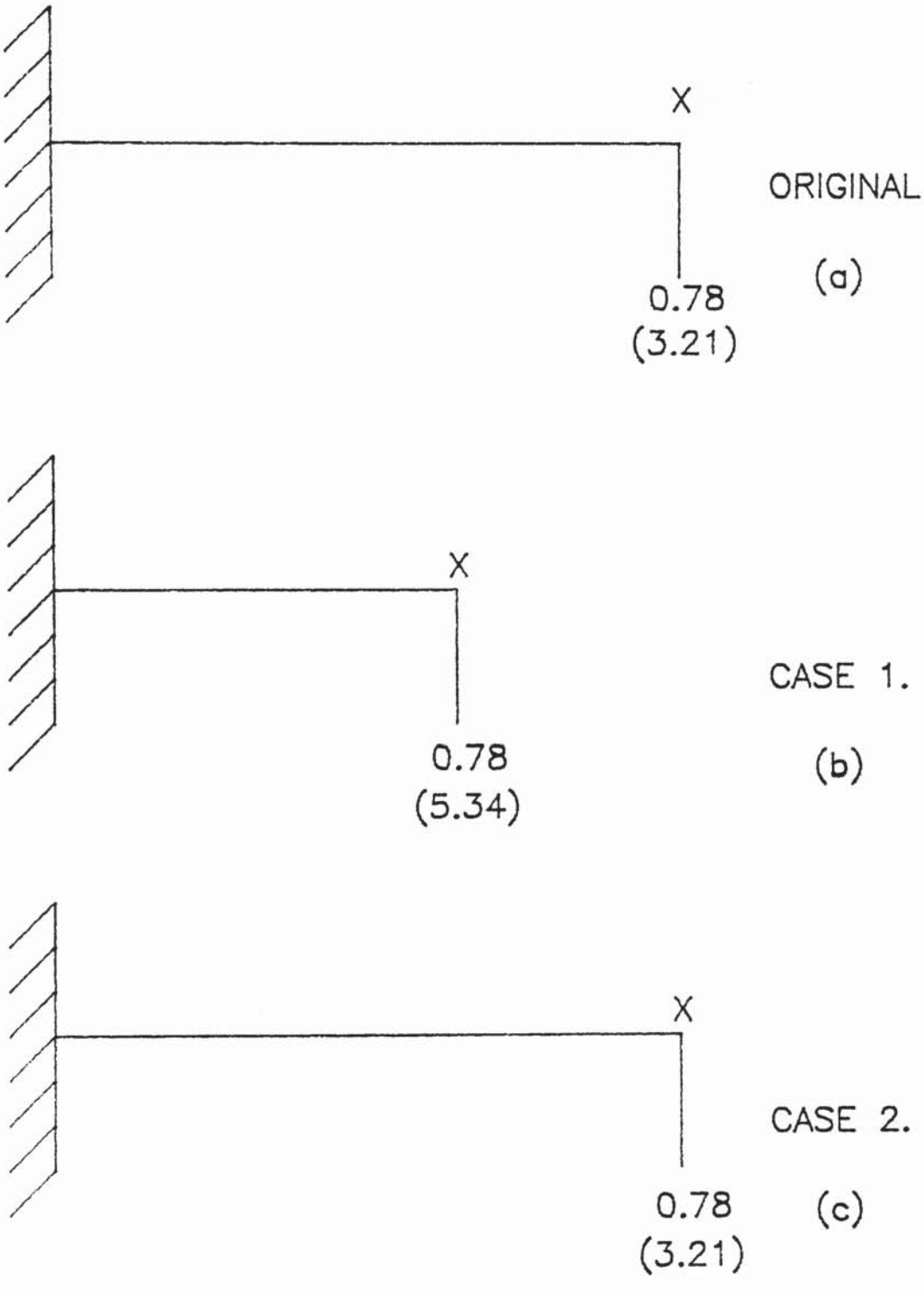

Figure 5

TABLE 1

A set of mobility curves were obtained from the stucture shown in Figure 4 for two coordinates and two planes of motion (vertical translation and rotation). Using the resultant 4x4 mobility matrix it was possible to obtain the following sets of mass, stiffness and damping matrices. These matrices represent spatial models of the structure viewed from different forcing coordinates.

Forcing station 1

Mass matrix

$$\begin{bmatrix} 2.6779E\text{-}2 & -1.5123E\text{-}5 & 3.6838E\text{-}3 & 1.3000E\text{-}4 \\ -1.5123E\text{-}5 & 4.7839E\text{-}5 & 1.7134E\text{-}4 & -8.8280E\text{-}6 \\ 3.6838E\text{-}3 & 1.7134E\text{-}4 & 6.5947E\text{-}3 & 3.0090E\text{-}5 \\ 1.3000E\text{-}4 & -8.8280E\text{-}6 & 3.0090E\text{-}5 & 5.4770E\text{-}6 \end{bmatrix}$$

Stiffness matrix

$$\begin{bmatrix} 4.2730E5 & 2.0723E3 & -9.2486E4 & -1.1991E4 \\ 2.0723E3 & 3.9948E3 & -1.7816E4 & 1.1911E1 \\ -9.2486E4 & -1.7816E4 & 1.3005E5 & -9.2650E2 \\ -1.1991E4 & 1.1911E1 & -9.2650E2 & 7.1647E2 \end{bmatrix}$$

Forcing station 2

Mass matrix

2.8939E-2	7.2460E-4	-5.4640E-5	4.3826E-4
7.2460E-4	1.0202E-4	3.2803E-4	5.0364E-5
-5.4640E-5	3.2803E-4	7.1314E-3	1.7807E-4
4.3826E-4	5.0364E-5	1.7807E-4	3.3681E-5

Stiffness matrix

2.1229E6	-8.3933E4	-1.2654E6	2.9544E3
-8.3933E4	4.8773E3	4.4933E4	-8.3414E2
-1.2654E6	4.4933E4	8.0622E5	-1.4466E3
2.9544E3	-8.3414E2	-1.4466E3	6.8034E2

Forcing station 3

Mass matrix

2.0160E-1	-9.6074E-3	-6.6394E-2	2.9045E-3
-9.6074E-3	5.1641E-4	3.5491E-3	-1.5074E-4
-6.6394E-2	3.5491E-3	4.4184E-2	-1.7536E-3
2.9045E-3	-1.5074E-4	-1.7536E-3	7.8795E-5

Stiffness matrix

8.5986E6	-5.9400E5	-3.3562E6	1.3746E5
-5.9400E5	4.6992E4	1.9976E5	-5.2023E3
-3.3562E6	1.9976E5	1.5205E6	-8.2908E4
1.3746E5	-5.2023E3	-8.2908E4	6.5198E3

Forcing Station 4

Mass matrix

$$\begin{bmatrix} 2.2680E\text{-}1 & -2.0575E\text{-}3 & -2.3290E\text{-}1 & 9.8992E\text{-}3 \\ -2.0575E\text{-}3 & 2.1036E\text{-}4 & -4.9530E\text{-}4 & 9.1474E\text{-}5 \\ -2.3290E\text{-}1 & -4.9530E\text{-}4 & 2.9445E\text{-}1 & -1.3348E\text{-}2 \\ 9.8992E\text{-}3 & 9.1474E\text{-}5 & -1.3348E\text{-}2 & 6.3788E\text{-}4 \end{bmatrix}$$

Stiffness matrix

$$\begin{bmatrix} 4.1124E7 & -5.9986E5 & -4.4056E7 & 1.9147E6 \\ -5.9986E5 & 1.3336E4 & 6.1867E5 & -2.6996E4 \\ -4.4056E7 & 6.1867E5 & 4.7360E7 & -2.0623E6 \\ 1.9147E6 & -2.6996E4 & -2.0623E6 & 9.0569E4 \end{bmatrix}$$

TABLE 2

Mode 1

Complete System	Truncated System
0.10185	0.10506
0.40208	0.3906
0.72619	0.708
1.0218	0.9918
1.2121	-

Mode 2

Complete System	Truncated System
0.25745	0.2716
0.95915	0.9127
0.43240	0.4181
0.18334	0.1757
1.0375	-

Mode 3

Complete System	Truncated System
0.09479	0.209
0.3293	0.14246
0.3575	0.14589
0.9034	0.415
1.5661	-

Mode 4

Complete System	Truncated System
0.16834	0.8421
0.1864	0.0827
3.0219	0.59949
0.3255	0.06365
0.0424	-

4. POINT COORDINATE SIMILARITY

4.1 INTRODUCTION

It is possible, sometimes, to examine the performance of a structure by exciting it at a single point. This type of environmental test is usually representative of a piece of equipment being attached at a single point to a much larger carrier structure. There are two ways that this test can be performed:-

(a) Directly — A force is applied directly to the structure and the frequency response functions are measured.

(b) Indirectly — a mechanical test rig is designed having identical dyanamical characteriscs to the large structure at a point coordinate and then exciting the rig with a simple swept frequency.

If the second approach is considered then it is necessary to obtain point coordinate dynamic similarity of the carrier structure by using either a distributed parameter test rig or a finite dimensional test rig.

It is usual when specifying a test procedure to state the frequency range of interest. If this is the case and the

structure under examination exhibits well defined resonances, which are lightly coupled, then it is possible to identify a finite number of resonances. Since the problem is for a single coordinate and a defined frequency range with a finite number of resonances a system with a restricted set of characteristics is suitable for such an application.

Discrete systems exhibit these characteristics where the motion of a selected mass may be taken as the single coordinate position and the degrees of freedom of the discrete system being equal to the finite number of resonances of interest.

A design methodology is required which is capable of identifying the parameters of a discrete spring/mass system which is capable of reproducing an acceptable level of dynamic similarity to a point coordinate on a carrier structure.

Work performed by Salter [29] showed that it was possible to use a highly tuned continuous system to reproduce the characteristics of a discrete system over a restricted frequency range. No attempt was made to match the tuned system to the characteristics of a particular body, but an adoption of half-octave spacing for the resonant frequencies was made. An arbitrary value of the weight of the system (called by Salter a foster-parent) was employed

so that an upper limit could be placed upon the dead weight of the test specimen. A configuration for a discrete sping/mass system was proposed and a practical implementation of such a system was developed and tested. The configuration can be seen in Figure 14.

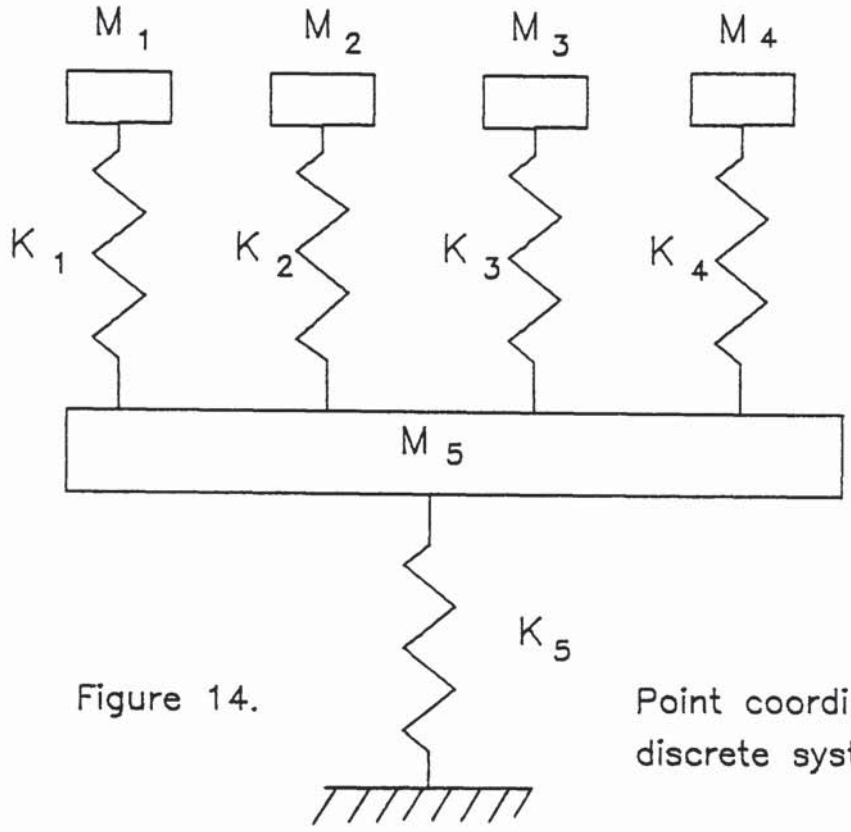

Figure 14. Point coordinate discrete system.

Having established the objective of the work it is now necessary to derive the design methodology. This should be capable of performing the translation of the dynamic characteristics of a point coordinate on the carrier structure into a discrete spring/mass system. The class of problem can be categorised as a finite dimensional optimal design problem.

In most problems of engineering design of mechanical structures the structure being designed is required to behave according to some law of physics. This behaviour is

described analytically by a set of variables called state variables. There is a second set of variables that describe the structure, rather than its behaviour. These variables are called design variables since they are to be chosen by the designer. The equations that determine the state variables of mechanical or structural systems generally depend upon the design variables, so that the two sets of variables are related. The concept of the state and design variable vectors is central to the derivation of the finite dimensional optimal design algorithm.

The finite dimensional optimal design problem is first developed in a generalised form and then a solution applicable to identifying the parameters of the discrete system is developed. Finally, an algorithm is proposed and a computer implementation of the design methodology is discussed.

4.2 OPTIMAL DESIGN PROBLEM

The fundamental mathematical concepts used within the design optimisation procedure are outlined in Appendix 2.

Let the state variable $\{z\}$ be a n- element vector such that it is within the design space R^n,

$$\{z\} \in R^n \tag{401}$$

The design variable $\{b\}$ is a k- element vector such that

$$\{b\} \in R^k \tag{402}$$

It is possible to define the finite dimensional optimal design problem as a problem of determining $\{b\}.R^k$ to

minimise $$\Psi_o(z, b) \tag{403}$$

subject to constraints

$$h(z, b) = \phi \tag{404}$$

$$\Psi(z, b) \leqslant \phi \tag{405}$$

where

$$h(z, b) = \begin{Bmatrix} h_1(z, b) \\ \cdot \\ \cdot \\ h_n(z, b) \end{Bmatrix} \qquad \Psi(z, b) = \begin{Bmatrix} \Psi_1(z, b) \\ \cdot \\ \cdot \\ \Psi_m(z, b) \end{Bmatrix}$$

all of the functions of the problem are required to have first-order derivatives.

Further it is required that the (n+k) dimensional composite vectors

$$\left\{ \frac{\partial \Psi_i}{\partial z}, \frac{\partial \Psi_i}{\partial b} \right\}^T \tag{406}$$

are linearly independent for all i with $\Psi_i(z, b) = \phi$ and that the n * n matrix $[\partial h / \partial z]$ is non-singular. The assumption that the matrix $[\partial h / \partial z]$ is non-singular guarantees that there is a basis solution of equation (404) for $\{z\}$ as a function of $\{b\}$. This will become apparent later when the sensitivity coefficients are manipulated to yield an optimum solution. The final assumption is that the state variable $\{z\}$ is differentiable with respect to $\{b\}$.

The equation (404) is non-linear and, therefore, cannot be solved in closed form. Thus one cannot practically reduce the optimal design problem to an explicit non-linear programming problem in terms of only the design variable vector. However, the natural form of the equations of structural and rigid body mechanics can be used to develop practical numerical methods for design analysis.

4.2.1 DESIGN SENSITIVITY ANALYSIS

The problem is specifically a structural dynamics problem and so it is worthwhile to examine the finite dimensional optimal design technique when applied to the solution of the eigenvalue problem [30]

Given that

$$\{b\} \in R^k$$
$$\{z\} \in R^n$$
$$\{\phi\} \in R^n$$
$$\{\lambda\} \in R^1$$

the task is to minimise

$$\Psi(z, \lambda, b) \tag{407}$$

subject to the state equations

$$h(z, b) = \phi \tag{408}$$

$$[K(b)]\{\phi\} = \lambda[M(b)]\{\phi\} \tag{409}$$

and constraints

$$\Psi(z, \lambda, b) \leq \phi \tag{410}$$

where

$$h(z, b) = \begin{Bmatrix} h_1(z, b) \\ \cdot \\ \cdot \\ h_n(z, b) \end{Bmatrix}$$

$$[K(b)] = [k_{ij}\{b\}]_{n \times n}$$

$$[m(b)] = [m_{ij}\{b\}]_{n \times n}$$

$$\Psi(z, \lambda, b) = \begin{Bmatrix} \Psi_1(z, \lambda, b) \\ \cdot \\ \cdot \\ \Psi_m(z, \lambda, b) \end{Bmatrix}$$

The symmetric matrices $[M(b)]$ and $[K(b)]$ represent mass and stiffness values within the system. The scalar λ is the eigenvalues.

A full treatment of the analysis is discussed in Appendix 3 where the derivation of the sensitivity coefficients of with respect to the corresponding design variables is developed. Once the sensivity coefficients have been established it is possible to then manipulate the design parameters to provide the characteristics that are required. If equation (A317) is considered then

$$\{\ell^i\} = \frac{\partial \Psi_i}{\partial b}^T - \frac{\partial h}{\partial b}^T \xi^i + \frac{\partial \Psi}{\partial h} \ell^\lambda \tag{411}$$

The vectors $\{\ell^i\}$ yield the explicit derivatives of the cost and constraint functions with respect to the design variables. During the optimisation process it is usual to select the derivatives with the greatest magnitude since they have the most significant effect on the design. This approach is called the steepest descent where the vectors which direct the design to an optimum at the fastest rate are selected.

4.2.2 DISCRETE SYSTEM IDENTIFICATION

It is not possible to employ steepest descent selection criterion for this particular problem due to two functional constraints on the cost equation.

Consider two systems (A) and (B)

If a force $Q_k(\omega)$ is applied at coordinate k on system (A) then it is possible to measure a response $q_i(\omega)$ at coordinate i resulting from the input force. If the damping is considered to be negligible then the frequency response of the system can be expressed as a receptance.

$$\alpha_{ik}(\omega) = \frac{q_i(\omega)}{Q_k(\omega)} = \sum_{r=1}^{n} \frac{{}_r\phi_i \, {}_r\phi_k}{(\omega_r^2 - \omega^2)} \qquad (412)$$

for point receptance the response coordinates i and the

forcing coordinate k are the same and the receptance expression is

$$\alpha_{ii}(\omega) = \sum_{r=1}^{n} \frac{{}_r\phi_{ii}^2}{(\omega_r^2 - \omega^2)} \qquad (413)$$

It is possible to specify the point coordinate receptance for each system

System (A)

$$\alpha_{A_{ii}}(\omega) = \sum_{r=1}^{n} \frac{{}_r\phi_{ii}^2}{(\omega_{A_r}^2 - \omega^2)}$$

System (B)

$$\alpha_{B_{jj}}(\omega) = \sum_{r=1}^{n} \frac{{}_r\phi_{jj}^2}{(\omega_{B_r}^2 - \omega^2)}$$

Consider the condition when ω tends to zero ie $\omega \rightarrow \phi$

$$\alpha_{A_{ii}}(\phi) = \sum_{r=1}^{n} \frac{{}_r\phi_{ii}^2}{\omega_{A_r}^2} \qquad \alpha_{B_{jj}}(\phi) = \sum_{r=1}^{n} \frac{{}_r\phi_{jj}^2}{\omega_{B_r}^2} \qquad (414)$$

Now, the mode shape values are mass normalised such that

$$[\Phi]^T [M][\Phi] = [I] \qquad (31)$$

The objective of comparing the two systems (A) and (B) is to obtain the same dynamical characteristics at the respective coordinates i and j on each system. In otherwords the resonance frequencies and mode shape values are equal. Equation (31) implies that if the mode shape vectors are the same then the mass distribution of each system must be the same. However, we are only considering point coordinate excitation and response measurements. It is, therefore, necessary to obtain a single mass term for each point coordinate, which represents the effective "dynamical" mass of the system at that coordinate. This means that the mass distribution in equation (31) is now represented by a diagonal mass matrix $[\tilde{M}]$.

$$[\Phi]_A^T [\bar{M}_A] [\Phi]_A = [I] \qquad [\Phi]_B^T [\bar{M}_B] [\Phi]_B = [I]$$

or for coordinate i or for coordinate j

$$\{\phi_{A_{ii}}\}^T [\bar{M}_A] \{\phi_{A_{ii}}\} = 1 \qquad \{\phi_{B_{jj}}\}^T [\bar{M}_B] \{\phi_{B_{jj}}\} = 1$$

$$\sum_{r=1}^{n} m_{A_{ii}} {}_r\phi_{ii}^2 = 1 \qquad \sum_{r=1}^{n} M_{B_{jj}} {}_r\phi_{jj}^2 = 1 \qquad (415)$$

for the two systems to have the same dynamical characteristics at coordinates i and j the mass terms $m_{A_{ii}}$ and $M_{B_{jj}}$ must be the same. The term M_{Tot} has been used to represent this value.

If equation (415) is substituted into (414) then

$$M_{Tot_{ii}} = \frac{1}{\alpha_{ii}(\phi)} \sum_{r=1}^{n} \frac{1}{\omega_{A_r}^2} \qquad M_{Tot_{jj}} = \frac{1}{\alpha_{jj}(\phi)} \sum_{r=1}^{n} \frac{1}{\omega_{B_r}^2} \qquad (416)$$

It is possible to use this observation within the design process when identifying the parameters of a discrete system which is dynamically similar to a point coordinate on a continuous structure.

Since equation (416) states that the total mass of the discrete system is a fixed quantity it implies

$$\sum_{i=1}^{n+1} \delta m_i = \phi \qquad (417)$$

This is a functional constraint on the cost equation as it is implicit that one or more of the terms (δm_i) must be negative.

The second functional constraint is that the anti-resonances of the discrete system are fixed at the outset to be the same as the frequency response curve from the carrier structure.

By definition anti-resonances occur where

$$\alpha_{jj}(\omega) = \sum_{r=1}^{n} \frac{r\phi_{jj}^2}{(\omega_r^2 - \omega^2)} = \phi \qquad (418)$$

Throughout the optimisation analysis these values are to remain stationary. Therefore, any changes (δm_i) to the mass matrix [M] must be reflected to the corresponding elements of the stiffness matrix [K] before the sensitivity equation (A312) is computed.

This means that the derivative of the state equation (318) will always be zero and therefore the second term of equation (411)

$$-\frac{\partial h^T}{\partial b}\, \xi^i$$

can be eliminated.

Finally, since the discrete system does not have physical dimensions it is not possible to establish a relationship between the parameters of the discrete system and cost equations. The first term of equation (411)

$$\frac{\partial \psi_i^T}{\partial b}$$

can be eliminated.

Note that the mass and stiffness matrices [M] and [K] are related to the cost equation via the eigenvalue sensitivity analysis of the third term of equation (411).

Equation (411) therefore reduces to

$$\{\ell^i\} = \frac{\partial \psi}{\partial \lambda}\, e^{\lambda} \qquad (419)$$

The problem that is now posed is how to optimise the mass

and stiffness matrices of the discrete system so that they reproduce a similar frequency response to the point co-ordinate on the carrier body.

The sensitivity matrix $[\ell]$ has a greater number of independent variables (k) than the number of degrees of freedom of interest (n). One particular numerical method used to analyse this type of problem is called Linear Programing [31].

The problem can be expressed in a generalised form as

$$[\ell]\{\delta m\} = \{\delta\omega\} \qquad (420)$$

where

$[\ell]$ is the sensitivity matrix $(n \times k)$ $k > n$

$\{\delta m\}$ is the vector of mass changes $(k \times 1)$

$\{\delta\omega\}$ is a vector of freq difference $(n \times 1)$

The equation of constraint is (417)

The usual Linear Programing technique is to select linear independent columns from $[\ell]$ to form a square matrix (called the basis matrix).

$$\sum_{i=1}^{n} \{x_{B_i}\} = [B]^{-1}\{b\} \quad x_B = \{x_{B_1}, x_{B_2}, \ldots x_{B_n}\} \qquad (421)$$

The solution of equation (421) will produce a feasible solution for the n-component vector $\{x_{B_i}\}$. It is implicit within this statement that the $(k-n)$ variables not associated with the columns of $[\ell]$ appearing in $[B]$ are zero.

If the configuration of the discrete spring/mass system of Figure 14 is examined it will be noted that there are $(n+1)$ design variables. Since it is not possible for one of the masses to equal zero it means that an unbounded solution will exist for the linear programming problem.

If a column $\{\ell_j\}$ not used within the formulation of $[B]$ is scaled by an arbitrary scalar ϑ and the effects of the product removed from the $\{\delta\omega\}$ vector, then a new unbounded feasible solution for $(n+1)$ variables can be formulated.

$$\sum_{i=1}^{n} \{x_{B_i}'\} = [B]^{-1}\{b - \vartheta\ell_i\} \qquad (422)$$

There are two possible ways to improve the feasible solution

(a) Check the remaining columns of $[\ell]$ to see if an improvement to the cost equation can be achieved. This approach is only applicable when $(k>n+1)$

(b) Change the sign of one or more columns within the basis matrix $[B]$ to see if an improvement to the cost equation is achieved. An observation made of the mechanics of matrix inversion (Appendix 4) allows this procedure to be performed without re-computing the matrix inversion for $[B]$.

The second approach is used within the design optimisation algorithm to select the most suitable design changes. The

equation (422) is solved for each column (j) within the matrix $[\ell]$.

This yields a set of linear independent column vectors each representing a feasible solution to the unbounded problem. Taking advantage of the mechanics of matrix inversion a sorting algorithm is used to find the optimum combination of each solution vector $\{x'_{B_i}\}$.

$$\sum_{i=1}^{n+1} x'_{B_i} = \delta e \qquad (423)$$

The cost equation (417) states that $\delta e = \phi$ is the only solution that is acceptable.

The error δe for the optimum solution vector $\{x'_{B_i}\}$ is, therefore, back substituted into the corresponding vector so that the sum of the elements is zero. The vector is then multiplied by an arbitrary scalar so that the final weighted vector indicates a feasible direction in which a solution may be sought.

4.3 DESIGN ALGORITHM

The methodology will be outlined first to show the overall strategy used and the relationships of the individual elements. A detailed discussion of each element and its implementation will then be presented.

i) Obtain data from a point coordinate receptance curve for the N degrees of freedom of interest. The data required is,

a) Resonant frequencies.

b) Anti-resonant frequencies.

c) The Receptance when $\omega = \phi$.

ii) Establish total mass of system and derive a tentative mass and stiffness distribution $\{b\}$.

iii) Solve the eigenvalue problem, equation (409).

iv) Compare the solution against the required parameters. If it is acceptable print the mass and stiffness matrices (final design vector $\{b_o'\}$) and then terminate the program.

v) Perform a sensitivity analysis by solving equation (A312) to obtain matrix of sensitivity coefficients $[\ell]$

vi) Perform optimisation analysis using equation (422) and cost equation (417).

vii) Weight optimum design change vector (423) so that a feasible direction is obtained

viii) Calculate a new stiffness matrix

ix) Solve the eigenvalue problem.

x) Compare the resultant anti-resonance values against the specified anti-resonance values to ensure

equation (418) is fulfilled.

xi) If the comparison is acceptable then the procedure is repeated from step (iv).
Otherwise an iterative technique is performed to calculate a new stiffness matrix and the procedure is repeated from step (viii).

i) Obtain Data

The methodology can be used only for lightly damped one dimensional problems. It is, therefore, necessary to use point coordinate frequency response curves as the basic data medium. These curves typically have alternate resonant and anti-resonant frequencies. Once the number of degrees of freedom have been decided then the corresponding resonsnt and anti-resonant frequencies should be reorded.

The data will normally be captured by the use of accelerometers attached to the carrier body (Inertance). The design algorithm requires the value of the recptance plot as the forcing frequency tends to zero, therfore, the effects of has to be removed from the inertance plot.

ii) Initail Mass and Stiffness Matrices

The equation (416) is used to establish the total mass of the discrete system. Since the total mass is a function of the values of the mode shapes at the coordinate of interest

the value will vary depending upon the geometry of the carrier body and the coordinate selected for point similarity.

The generation of the initial mass matrix is performed by distributing the total mass $M_{tot_{jj}}$ evenly between the discrete elements. The stiffness values are determined by the following procedures;

1) The earthing stiffness K_s, Figure 14 is set by the reciprical of the receptance when the frequency is zero

ie $$K_s = \frac{1}{\alpha_{jj}(\phi)} \qquad (424)$$

2) The stiffness values K_1 to K_4, Figure 14 are established by

$$\sum_{j=1}^{n-1} K_j = A_j^2 m_j \qquad (425)$$

where A_j is the anti-resonance frequency for mode j

m_j is the discrete mass element number j

Various weighting functions were examined when establisinging the initial mass matrix. It was found that no improvement in the identification reliability or convergence rate was achieved by using sophisticated weighting functions. The simple mass distribution of allocating the total mass between the elements was used in the final software.

iii) Solve Eigenvalue Problem

The mass and stiffness matrices are used to solve the eigenvalue problem. The algorithm used has to be efficient as it is repeatedly called within the methodology.

iv) Check for acceptable Spatial Model

This activity is included to ensure that the design methodology has only one exit. The decision as to whether an acceptable level of similarity has been achieved can be made by the designer (running the software interactively). An alternative method of terminating the algorithm is by specifying an acceptable level of error of the resonant frequencies and iterating until this condition is achieved.

v) Sensitivity Analysis

If the solution of the eigenvalue problem does not yield the correct frequencies then it will be necessary to change the mass and stiffness matrices. In order to know the level of change required it is necessary to perform a sensitivity analysis of the mass matrix with respect to frequency (finite dimensional optimal design problem) to obtain the sensitivity matrix (Equation 419).

Consider the eigenvalue problem for a discrete system

$$[K]\,[\Phi] = [\lambda]\,[M]\,[\Phi] \qquad (426)$$

Now $$[\lambda_{new}] = [\lambda_{old}] + [\delta\lambda] \quad (427)$$

Substituting equation (426) into (427)

$$([K]+[\delta K])([\Phi]+[\delta\Phi]) = ([\lambda]+[\delta\lambda])([M]+[\delta M])([\Phi]+[\delta\Phi]) \quad (428)$$

for the rth mode

$$([K]+[\delta K])(\{{}_r\phi\}+\{\delta_r\phi\}) = (\lambda_r+\delta\lambda_r)([M]+[\delta M])(\{{}_r\phi\}+\{\delta_r\phi\}) \quad (429)$$

solving the expression for $\delta\lambda_r$ and ignoring second order derivatives yields

$$\delta\lambda_r = (\{{}_r\phi\}^T[\delta K]\{{}_r\phi\} - \lambda_r\{{}_r\phi\}^T[\delta M]\{{}_r\phi\}) \quad (430)$$

The expression is then solved for small changes in the mass matrix (and the corresponding change in the stiffness matrix, equation 425) to obtain the sensitivity matrix $[\mathcal{L}]$.

For this particular application the number of independent variables is always greater than the number of degrees of freedom. It is, therefore, a problem that does not have a unique solution, but can be classified as a linear programming problem with an unbounded solution [31], equation (421).

Before the manipulation of the sensitivity matrix is examined it is worthwhile to consider the effects of

truncated data upon the discrete system. The identification of a discrete system is based upon a knowledge of the receptance as $\omega \rightarrow \phi$ and will always encompass the first N modes. There will be no resonant frequencies lower than the range of interest. However, higher resonant frequencies exist, which have to be accounted for by means of a residual term within the conceptual model.

For the higher modes

let

$$R_{jj} = \sum_{r=n+1}^{\infty} \frac{{}_r\phi_{jj}^2}{\omega_r^2} \qquad (431)$$

which is known as the residual flexibility.

The receptance can now be written as

$$\alpha_{jj}(\omega) = \sum_{r=1}^{n} \frac{{}_r\phi_{jj}^2}{\omega_r^2 - \omega^2} + R_{jj} \qquad (432)$$

The treatment of high frequency residuals by Ewins and Gleeson [8] show that for a point receptance the term $1/R_{jj}$ can be expressed as a single spring (K_{res}). This spring will act on mass m_5 and the excitation to the system should be applied through the spring (Figure 15).

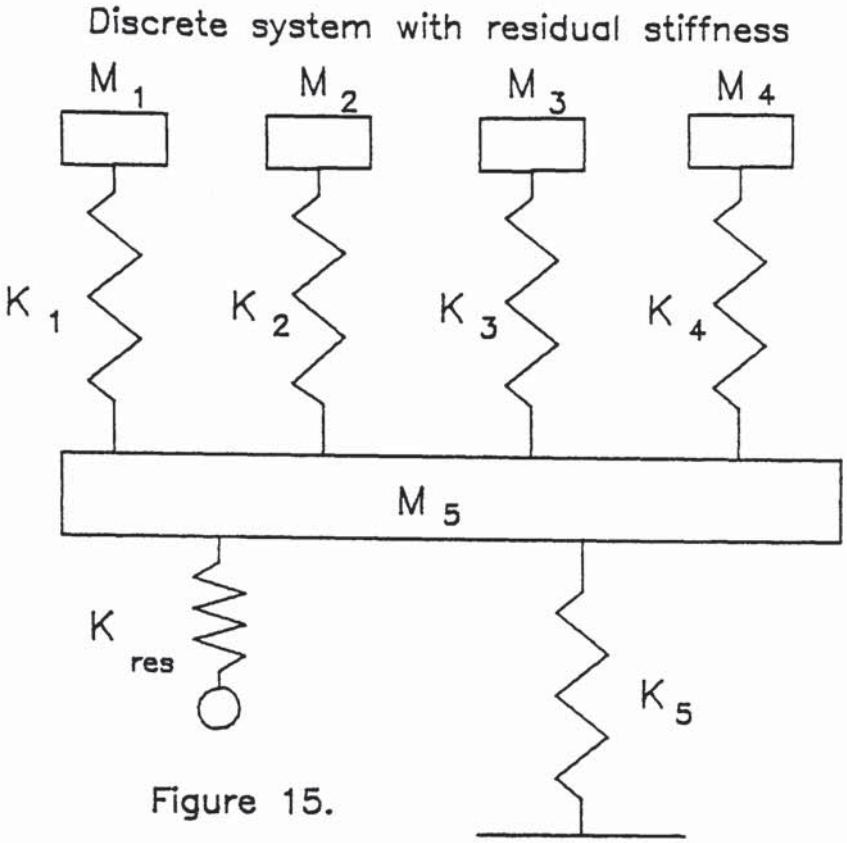

Figure 15.

The value of K_{res} is established after the first iteration. The difference between the first resonant frequency of the original data and the first resonant frequency derived from the eigenvalue solution is used to calculate the value of K_{res}.

$$K_{res} = (\omega_{1_{orig}} - \omega_{1_{sol}}) / \delta\lambda_{15} \qquad (433)$$

where $\delta\lambda_{15}$ is the change in the eigenvalue for the first mode when the stiffness matrix $[\delta K_s]$ is used.

vi) Perform optimisation analysis

The sensitivity matrix has a greater number of independent variables (masses) then the number of degrees of freedom of interest. The equation (422) and Appendix 4 are used to

solve the sensitivity matrix.

vii) Weight optimum design change vector

The unbounded feasible solutions (422) are examined to find the vector nearest to satisfying the cost equation (417). This vector is then scaled to satisfy equation (417). This step ensures that the total mass of the discrete system remains constant.

viii) New Stiffness Matrix

Once the mass matrix has been established then the stiffness matrix can be formed using equation (425). This is to ensure that the anti-resonance values remain stationary whenever changes to the mass matrix are made.

ix) Solve Eigenvalve Problem

The mass and stiffness matrices are used to solve the eigenvalue problem.

x) Compare Anti-resonant values

Throughout the analysis it is important to retain the anti-resonant frequency values for the the discrete system stationary. If the mass distribution is determined by the sensitivity analysis and linear programming technique then the stiffness matrix has to be manipulated to yield the

correct resonant and anti-resonant frequencies.

Point coordinate receptance can be written as

$$\alpha_{jj}(\omega) = \sum_{r=1}^{n} \frac{{}_r\phi_{jj}^2}{(\omega_r^2 - \omega^2)} \qquad (434)$$

this can be represented graphically by Figure 16.

The anti-resonant frequencies are the points when the curves sum to zero.

or

$$\sum_{r=1}^{n} \frac{{}_r\phi_{jj}^2}{(\omega_r^2 - A_r^2)} = \phi \qquad (434)$$

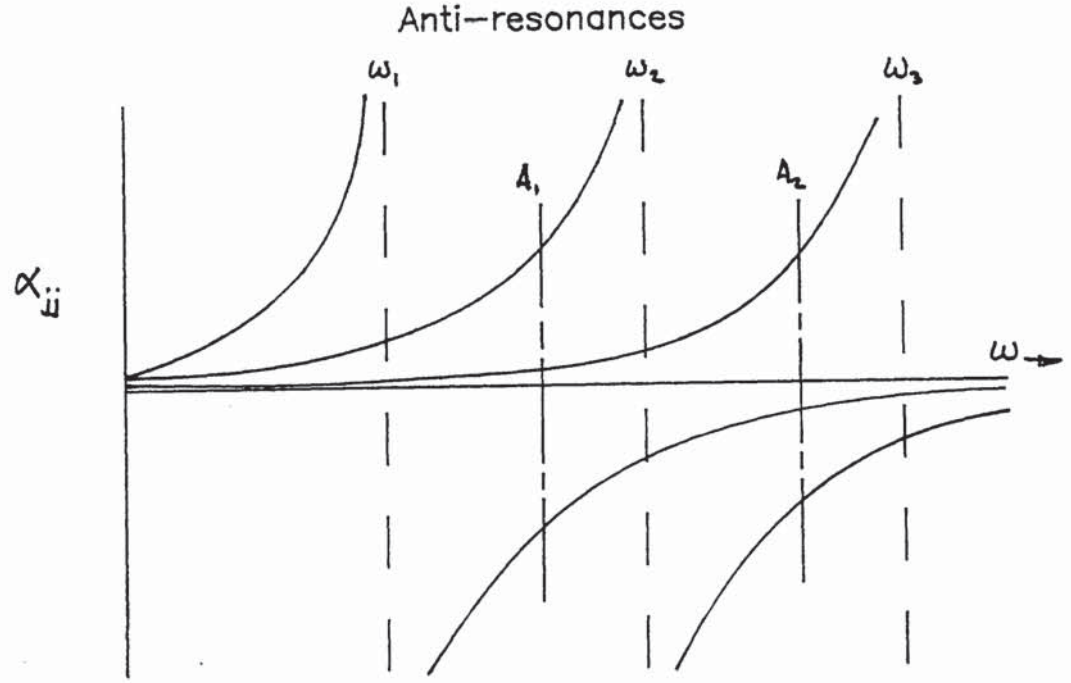

Figure 16.

The solution of the eigenvalue problem, step (ix) yields a set of eigenvectors $[{}^{1}\bar{\Phi}]$ which can be used to compute the anti-resonance error.

$$\delta_{error}(\bar{I}) = \sum_{r=1}^{n} \frac{{}_{r}{}^{1}\phi_{ij}^{2}}{(\omega_r^2 - A_r^2(\bar{I}))} \quad \bar{I} = 1 \text{ to } n \qquad (436)$$

where ${}_{r}{}^{1}\phi_{ij}^{2}$ is the computed new value.

xi) Check for acceptable errors

If the vector $\{\delta_{error}\}$ is unacceptable then the error can be used to modify the stiffness matrix. The corrections to the mass and stiffness matrices are based on linearity assumptions, which are not totally correct. Therefore, changes to the matrices are scaled so that during any one iteration a direction is established that will result in a convergent solution.

4.4 EXAMPLE OF POINT COORDINATE SIMILARITY

Consider a simple pinned-pinned beam, Figure 17a. This structure can be thought of as the carrier body which is capable of having different equipment attached at position (1). If the frequency range is defined it is possible to

count the number of resonant frequencies of interest, or alternatively, the first "n" resonant frequencies can be specified. It is always good practice to record to at least twice the highest frequency so that the effects of the high frequency values can be accounted for by a residual term in the subsequent system identification analysis.

Figure 17 shows in pictorial form the three main phases of the point coordinate similarity identification.

(a) Phase 1 Specify the carrier structure and the dynamic range of interest.

(b) Phase 2 Obtain the point coordinate receptance curve. There must be one pair of resonance and anti-resonace values for each degree of freedom of interest.

(c) Phase 3 Identify the parameters of the finite dimensional test rig.

A point receptance curve, Figure 18, was generated for the coordinate (1) in Figure 17a. The first eight modes of vibration were considered, although the number of degrees of freedom of interest was four.

The values for the first four resonances and anti-resonances were recorded, as was the value of the

receptance when $\omega=\phi$. These values were then used within the computer program to identify the parameters of a dynamically similar discrete system. The modal values of the original beam structure and the identical discrete system are shown in Table 3.

The identification procedure was terminated after the fourth iteration as the greatest error was 2.4% for the second resonance.

A comparison of the receptance of the original pinned-pinned beam and the identified discrete system is shown in Figure 19. The two plots are sufficiently close as to consider that the two structures are dynamically similar over the frequency range of interest.

4.5 THE EFFECTS OF APPENDING EQUIPMENT

The pinned-pinned beam had a concentrated mass applied at the position (1) as shown in Figure 20. This mass represents a piece of equipment.

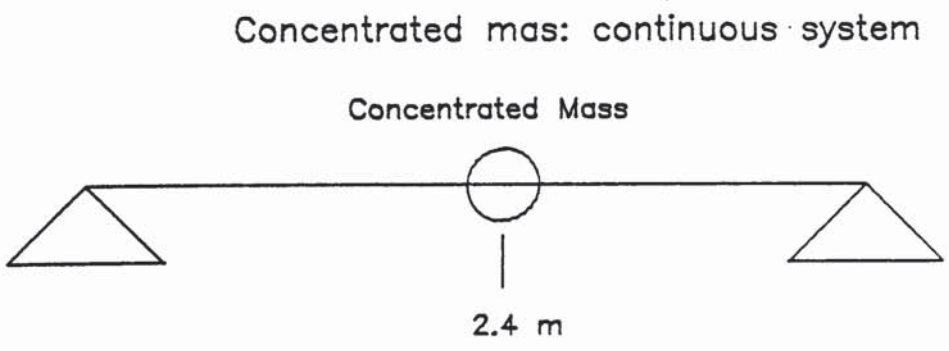

Figure 20.

If the equivalent mass is to be applied to the discrete system then it must be appended to the mass m_s , Figure 21.

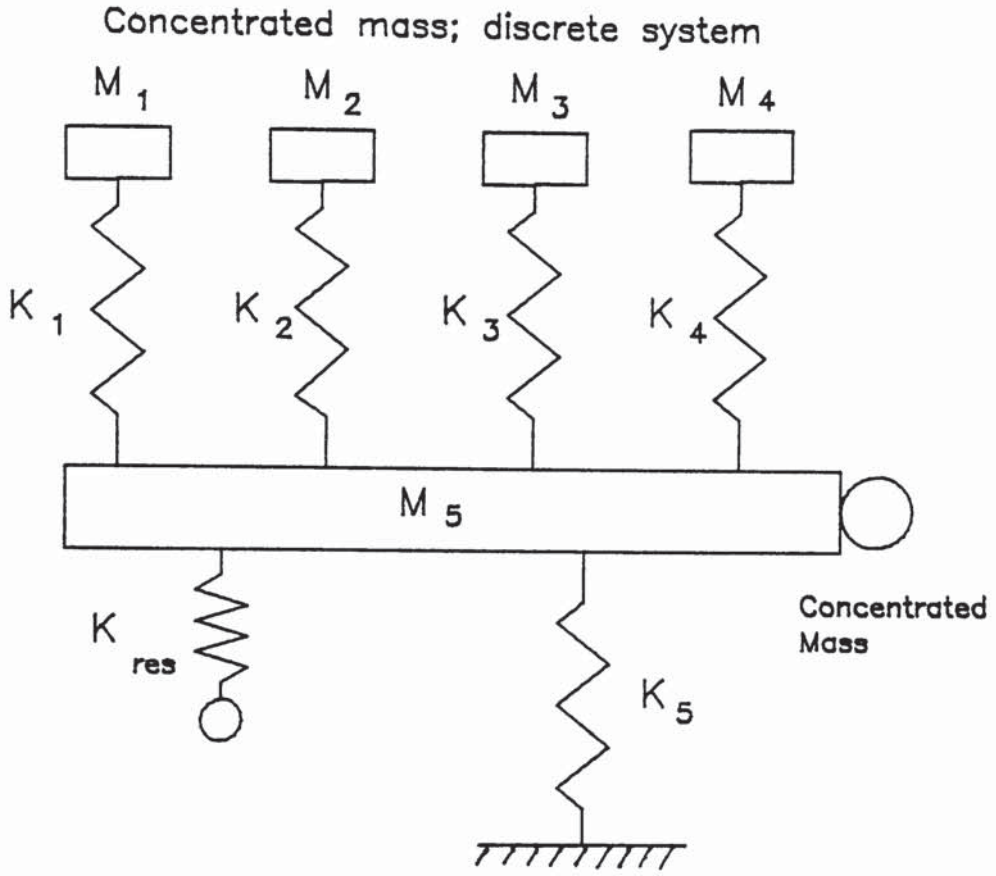

Figure 21.

Now, the addition of the concentrated mass to each system should cause them to have the same change in dynamical characteristics.

The eigenvalue problem was solved for the discrete system, Figure 21. But, the solution of the pinned-pinned beam is not so straightforward. The structure is one dimensional but has two planes of motion. Therefore, the concentrated mass will have a rotary inertia value. Two finite element

analysis runs were performed; one modelling the system correctly and the other setting the rotary inertia to zero. The results of all three runs (discrete system and pinned-pinned beam) are shown in Table 4. When the rotary inertia is set to zero the change in the dynamical characteristics of the discrete system and the pinned-pinned beam are identical. This demonstrates that dynamic similarity has been achieved for one plane of motion. However, since the concentrated mass has rotary inertia the dynamic similarity is actually lost when the physical condition is considered. This is particularly evident at the higher frequencies. This emphasises that great care must be used so that the structures are compared under a consistant set of conditions.

4.6 SUMMARY OF POINT COORDINATE SIMILARITY

1. It is possible to obtain point coordinate similarity of a continuous structure in one plane of motion by a discrete system.

2. A system identification algorithm for finite dimensional structures has been implemented. It is very easy to use as it only requires the receptance value as $\omega \rightarrow \emptyset$ and a set of resonant and anti-resonant values equal to the number of degrees of freedom.

3. A residual spring term has been incorporated within the finite dimensional model to allow for high frequency terms.

4. The optimisation algorithm uses a modified linear programming technique which provides an unbounded set of basic solutions.

5. The quality of the similarity over the frequency range of interest is very good. It is possible to obtain resonant frequencies within 3% error using only four iterations of the identification technique.

6. The similarity is only for one plane of motion and therefore, is lost when the same equipment (concentrated mass) is applied to both the original structure and the finite dimensional model.

7. This condition would not be important for one dimensional vibration problems such as torsional transmission systems.

8. The finite dimensional model is very difficult to realise as a physical structure. This problem is addressed in Chapter 6.

POINT SIMILARITY

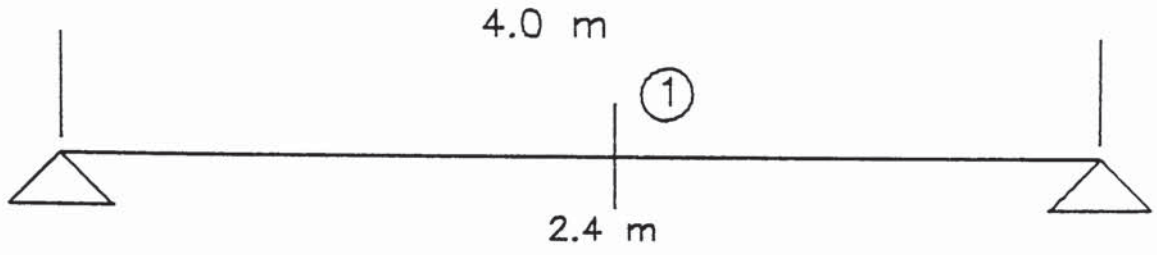

(a)

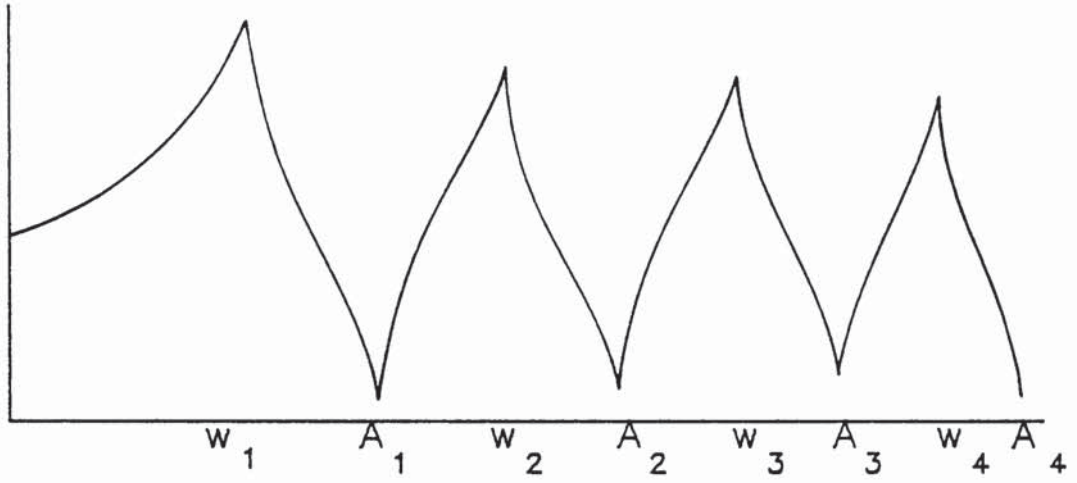

(b)

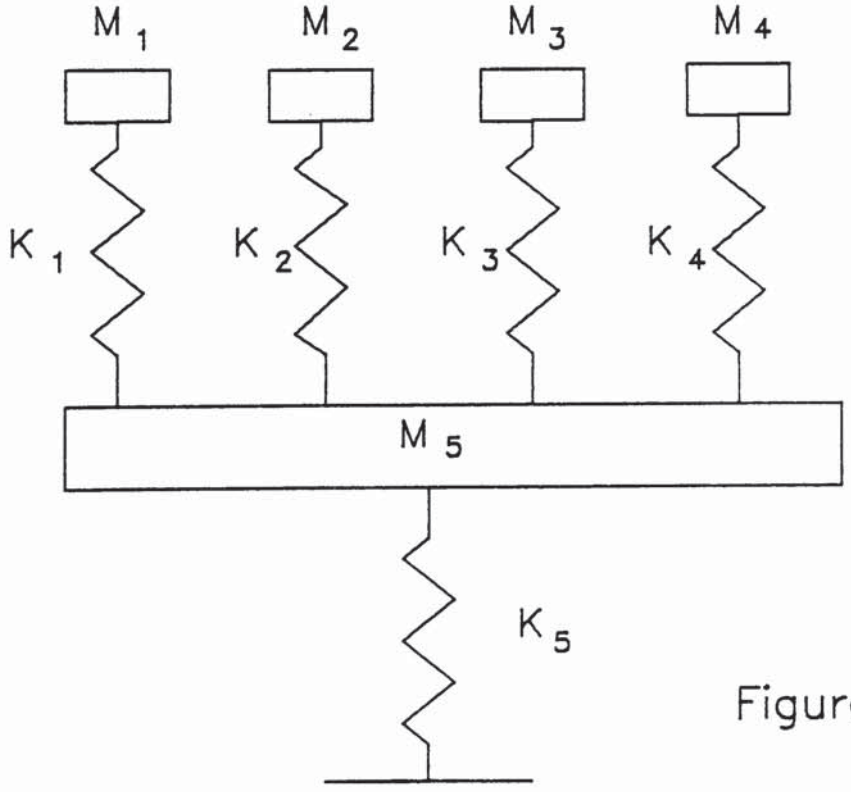

(c)

Figure 17

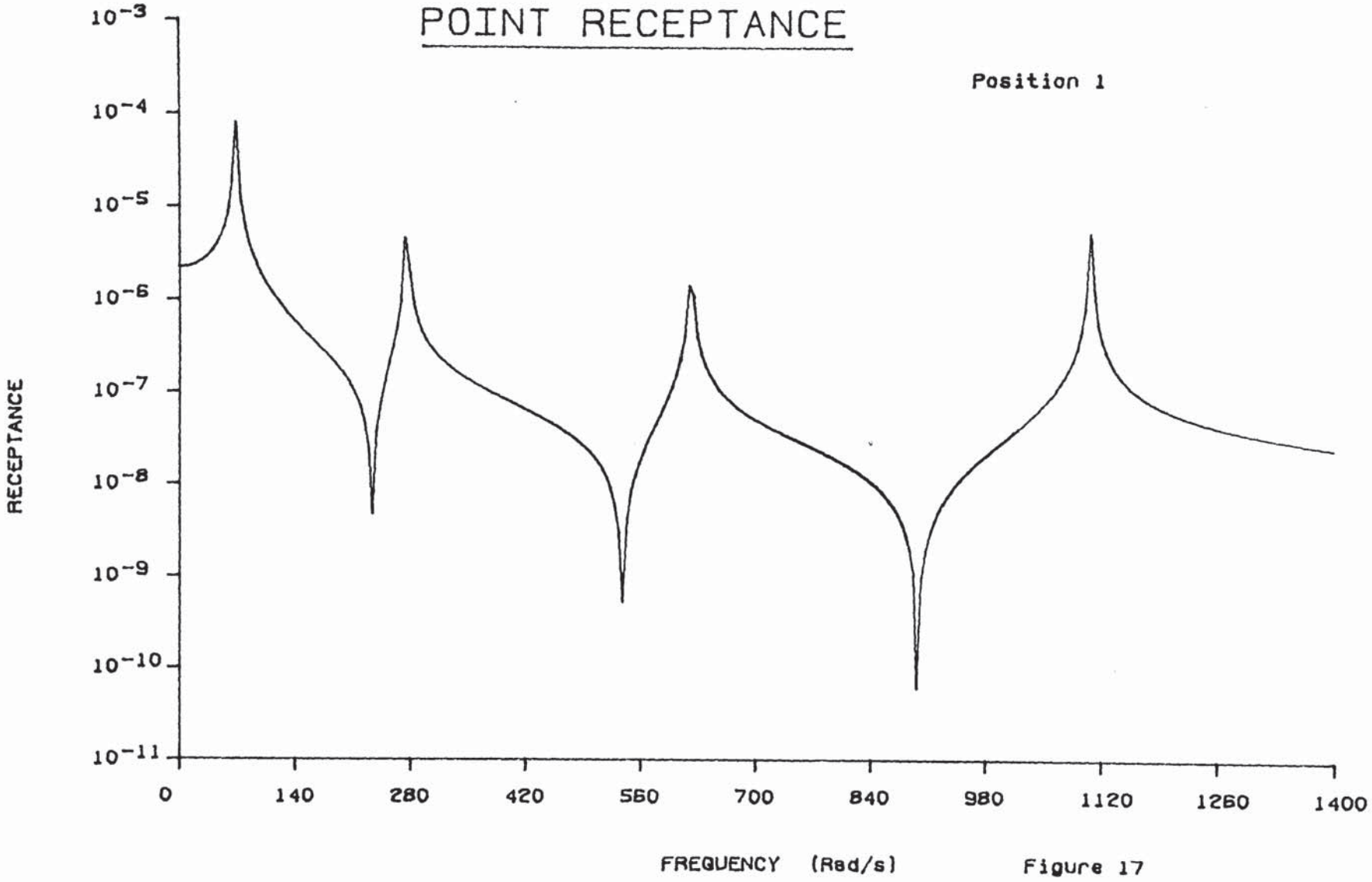
POINT RECEPTANCE
Position 1
RECEPTANCE
10-3
10-4
10-5
10-6
10-7
10-8
10-9
10-10
10-11
0
140
280
420
560
700
840
980
1120
1260
1400
FREQUENCY (Rad/s)

Figure 17

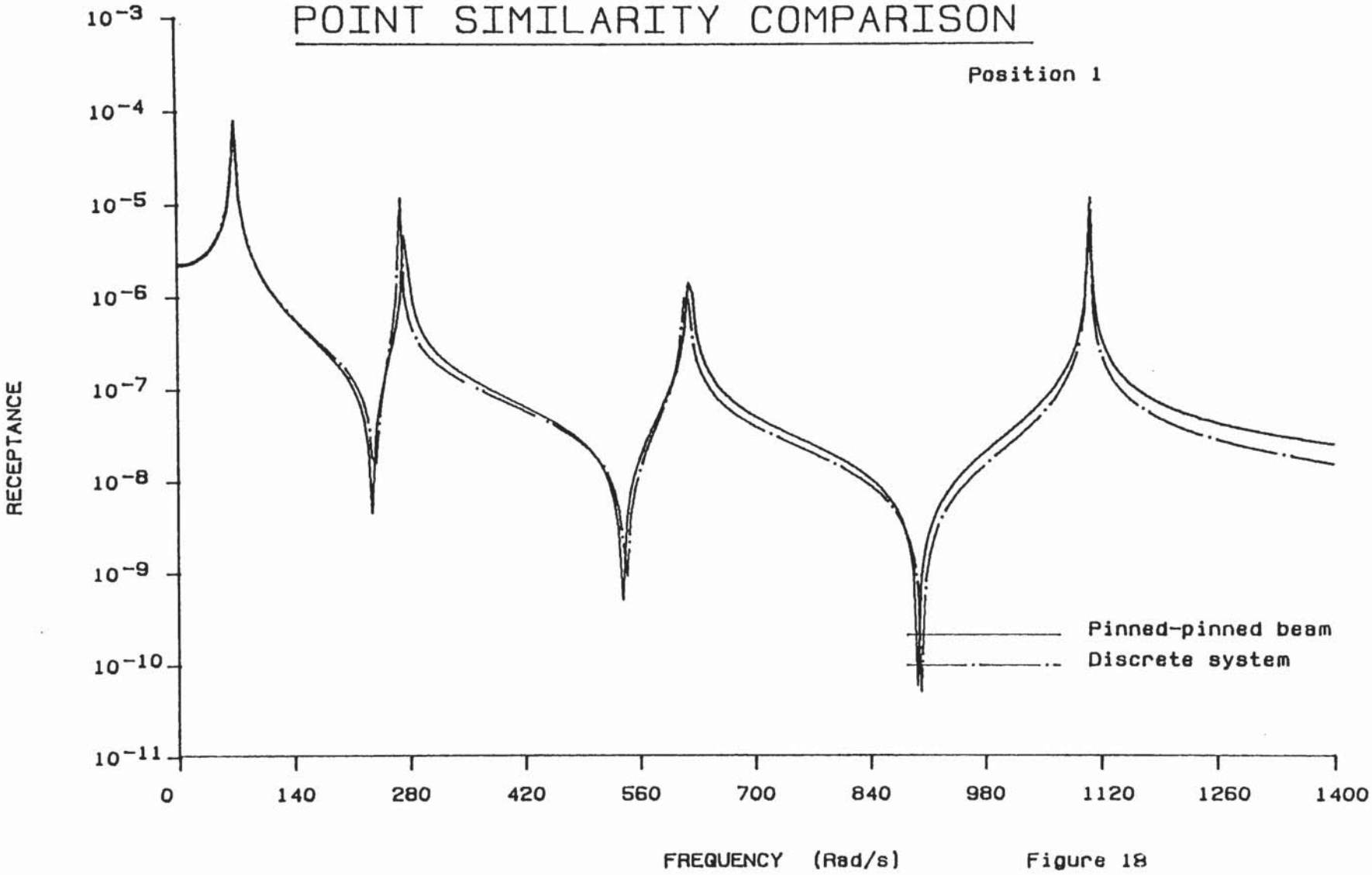
POINT SIMILARITY COMPARISON
Position 1
RECEPTANCE
10^{-3}
10^{-4}
10^{-5}
10^{-6}
10^{-7}
10^{-8}
10^{-9}
10^{-10}
10^{-11}
0
140
280
420
560
700
840
980
1120
1260
1400
FREQUENCY (Rad/s)
Pinned-pinned beam
Discrete system

Figure 18

TABLE 3

Point Coordinate Dynamic Similarity

Original Structure		Discrete System	
Resonance Freq	Mode Shape	Resonance Freq	Mode Shape
69.13	0.1015	68.97	0.103
276.95	0.0629	270.31	0.0553
625.03	0.0637	617.39	0.0574
1131.01	0.1070	1104.72	0.095

The above values are for the Position 1 on the pinned-pinned beam and the dynamically similar discrete system.

TABLE 4

Point Coordinate Dynamic Similarity

The effects of appending a piece of eqipment at the position 1 on the pinned-pinned beam and mass (Figure 21) of the discrete system are shown below.

Resonance Frequencies

Original Structure		Discrete System
With Inertia	Without Inertia	
65.77	65.81	66.08
268.09	272.05	277.33
593.28	614.28	622.79
1015.65	1059.89	1079.85

It is particularly noticable that the original structure with rotary inertia losses dynamical similarity at the higher modes.

5. PROPOSED DESIGN METHODOLOGY

5.1 INTRODUCTION

At the outset of the project it was considered that a solution capable of achieving prescribed dynamical characteristics for a given structure would be obtained from a mechanical test rig comprising an assembly of continuous and discrete elements in a system. This system has been called the substitute structure.

The function of the continuous elements is to connect the coordinates of interest and to provide a framework onto which the test specimen can be attached. The coordinates of interest are the points on the original structure where the frequency response data are collected. Since the continuous elements will have physical dimensions they will provide a set of dynamical characteristics. If this set is not the prescribed characteristics then the discrete elements are used to 'tune' the substitute structure.

This design philosophy introduces three main problems;

a) How to identify the parameters of the continuous elements and a suitable connection matrix (the structure's topology).

b) How to identify the parameters of the discrete elements.

c) The coupling effects when the discrete elements are attached to the continuous elements.

Although it was impossible to use the spatial model derived by system identification techniques directly to identify a test rig it was possible to use the spatial model within the proposed design methodology. The system identification procedure used experimentally recorded data and derived a spatial model which was representative of the original structure for the coordinates where the data were recorded. This spatial model was a homomorphic model and was representative of the original structure for a limited range of degrees of freedom.

If a continuous element is derived (Chapter 8) which has the same coordinates of interest as the original structure then a spatial model for the continuous element can be derived which is consistant with the original structure's spatial model. This attribute is the basis of the proposed methodology. Since each spatial model is consistant then the difference between them represents the dynamical characteristics that have to be applied to the continuous element to achieve dynamic similarity. The difference between the two spatial models is in the form of residual mass, stiffness and damping matrices which have to be used to identify the parameters of the discrete elements.

5.2 MODEL SYNTHESIS

The first design methodology was formulated using modal synthesis techniques in an attempt to achieve a physically realisable test rig. The methodology can be partitioned into the following activities.

(a) Perform a system identification on a set of truncated experimental frequency response data for 'n' coordinates and 'n' degrees of freedom, recorded from the original carrier body. The system identification process yields mass, stiffness and damping matrices that are fully populated.

(b) Derive a structure which connects the coordinates of interest (from the original body) and comprises continuous elements.

(c) Generate a finite element model of the continuous elements. Each coordinate (or node of the finite element model) will have at least two, degrees of freedom. This will probably not be consistant with the experimental data which is usually only measured for translational responses at each coordinate. The work on handling truncated frequency response data has shown that it is valid to use selected eigenvector values to represent the mode shapes of a structure. It is, then, possible to identify the eigenvector values which correspond to the translational motion of the coordinate of the carrier body.

(d) Use the identified mode shape values and the

resonant frequencies from the finite element model to generate a set of frequency response plots which are consistant with the experimental frequency response data. A system identification of these frequency response plots produces a set of mass, stiffness and damping matrices for the continuous elements.

(e) Take the two spatial models; one representing the carrier body and the other the continuous elements. Remove the spatial model of the continuous elements from the spatial model of the carrier body, leaving a set of residual mass, stiffness and damping matrices. These residual matrices represent the degree of "dis-similarity" between the two structures.

(f) Identify a suitable discrete system capable of 'tuning' the continuous element.

This proposed design methodology was examined by attempting to achieve dynamic similarity, for the first four modes, between a tapered cantilever and a uniform section cantilever and a discrete spring/mass system. Initially, a finite element model of the tapered cantilever, Figure 22a, was generated and the first four modes of vibration were recorded. Four coordinates of interest were specified and the translational mode shape values for these coordinates were extracted. These values, plus the resonant frequencies, were used to generate a set of four mobility plots which were taken to represent the experimentally

obtained mobility data. It was assumed that the forcing function to the beam was applied at the free end in the vertical plane. These mobility plots were then analysed by a system identification algorithm to obtain the mass and stiffness matrices. (Note: when the mobility plots were generated a small level of hyteretic damping, 3%, was introduced for stability but was not considered within the subsequent analysis).

An uniform section cantilever of arbitary section, Figure 22b, but the same length as the tapered cantilever was chosen as the continuous element. It was possible within the system identification package to generate the mobility plots of simple beam elements. This feature was used to generate a set of mobility plots where the forcing function was applied to the free tip of the uniform section cantilever. A system identification analysis of these plots yielded the second spatial model.

Step (e) within the design methodology algorithm was performed to obtain the residual mass and stiffness matrices. The final step within the design algorithm was to identify the characteristics of the discrete system, used to dynamically 'tune' the continuous element. Two conditions were considered for the treatment of the discrete elements.

(1) The discrete elements were distributed about the continuous element.

(2) The discrete elements act a single point coordinate.

5.3 DISTRIBUTED DISCRETE ELEMENTS

An examination of the residual mass matrix showed that the off diagonal terms included negative values. All of the off diagonal terms represent transfer mass elements that have to be either added or removed between the coordinates of interest. Although it is relatively easy to model this condition it is very difficult to achieve a physical representation of it. Therefore, for the initial study, all of the off diagonal terms were set to zero. Essentially this means that four concentrated masses, equal to the diagonal terms, were located at the relevant coordinates of the uniform section cantilever, Figure 23.

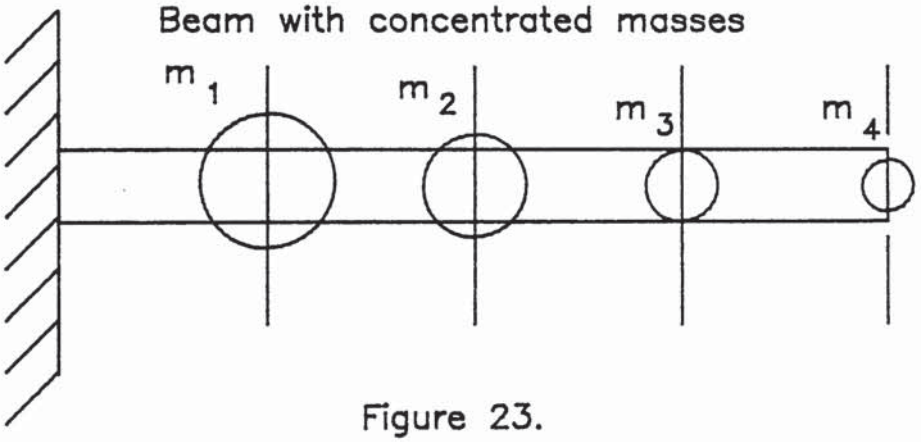

Figure 23.

The residual stiffness matrix when normalised with respect to one value is shown if Figure 24.

$$\begin{bmatrix} 58.6 & -28.0 & 7.4 & -0.8 \\ -28.0 & 24.3 & -11.2 & 2.0 \\ 7.4 & -11.2 & 8.4 & -2.4 \\ -0.8 & 2.0 & -2.4 & 1.0 \end{bmatrix}$$

Figure 24.

An immediate observation that can be made of Figure 24 is that the sums of the modulus of the off diagonal terms for rows 2 and 4 are greater then the diagonal element. This infers that an active system would be required which is capable of generating this condition. The design or consideration of active systems was outside of the specification for this particular work, therefore, the effects of various passive spring configurations were examined.

The simplest distributed discrete spring/mass configuration is shown in Figure 25 where the values of the diagonal terms of the residual stiffness matrix are used.

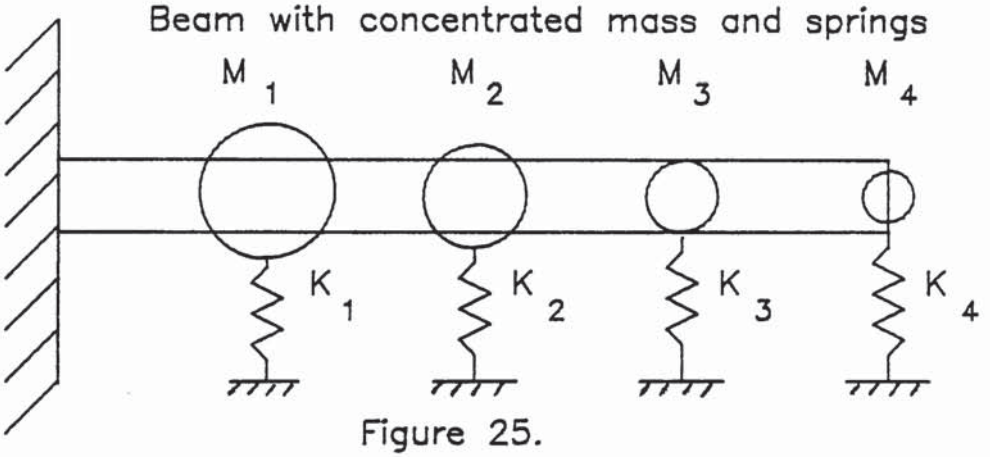

Figure 25.

The resultant resonant frequencies and mode shapes for the first four modes bore little resemblance to the tapered cantilever. A sensitivity analysis, examining effects on resonant frequencies due to changes in mass and stiffness values was performed. The results of this study indicated that it would not be possible to achieve an acceptable

degree of dynamic similarity using this configuration. Nine other configurations of discrete spring/mass systems attached to the uniform section cantilever were examined. It was impossible to identify any configuration that gave an acceptable level of dynamic similarity. In each of the configurations examined the level of resolution of the model (the discrete system) was very low, actually utilizing only a few elements within the residual matrices. It was this primary reason why it was impossible to achieve dynamic similarity and an alternative method where a much higher level of resolution, of the model, was required.

5.4 DYNAMICAL DIFFERENCE TECHNIQUES

5.4.1 BACKGROUND THEORY

The point coordinate discrete system identification algorithm discussed in Chapter 4 utilised values taken from a point receptance curve. These values, the resonance and anti-resonance frequencies, were used to directly identify the parameters of a discrete system.

It is possible to generate a point receptance curve by using the residual mass and stiffness matrices obtained at step (e) within the proposed design methodology. Once a point receptance curve has been generated then it is possible to identify a discrete system (Chapter 4). If this approach is adopted to identify the discrete system from the residual matrices via a point receptance curve

then the resultant discrete system has a very high level of resolution since all the elements within the residual mass and stiffness matrices are used to generate the receptance curve. This approach, therefore, appears to provide a methodology where the resultant discrete system will provide the required dynamical characteristics.

If the residual matrices are used to identify a multi-degree of freedom discrete system which acts at a point coordinate then it is necessary to firstly examine the implications of impedance coupling. This work has been extensively discussed by Ewins and Gleeson [8], Ewins and Sainsbury [32] and Klosterman [33]. The procedure is to obtain frequency responses for two structure at the points at which the connections are to be made and then to calculate the responses of the combined structure using impedance coupling techniques (Appendix 5). It is proposed to examine the inverse of this process where the dynamical differences between the two structures are obtained when they are separated into their component forms.

Dynamic data are usually analysed or manipulated using one or more of three possible states (Figure 26). It is possible to compute any one state from another since the relationships between the various states are well defined.

STATE	DESCRIPTION
$[Z]$	Frequency response plots
$[\omega]$ $[\Phi]$	Resonant frequencies and mode shapes.
$[M]$ $[K]$ $[C]$	Mass, stiffness and damping matrices.

Figure 26.

Given that three possible states exist for dynamic data the implications of using each state to derive a residual point receptance plot was examined. The three possible approaches can be catagorised as

i) Direct use of frequency response curves.

ii) Eigenvector difference.

iii) System identification difference.

Throughout the study of the different approaches the same beam elements were used for the original structure (Figure 22a) and the continuous element (Figure 22b).

5.4.2 DIRECT APPROACH

Under normal experimental measuring conditions inertance or mobility plots are obtained from the original structure. These plots are normally for translational movements only, as the measurements of rotational movements and the application of couples to structures is very difficult.

The continuous element (prismatic beam) was modelled using

finite element analysis and a set of frequency response curves were generated which were consistant with the coordinates of interest on the original structure. It was then possible to use directly the frequency response data to derive the residual point receptance curve.

Both the original structure and the continuous element within the substitute structure were cantilevers. At any coordinate there were six planes of motion, but generally only two were considered; vertical translation and rotation normal to the horizontal in the vertical plane.

If the process of coupling two structures is examined [Appendix 5] then equation (A504) defines the receptance for the point of connection. This receptance has the form of equation (501) ie. two planes of motion.

$$\alpha_x = \begin{bmatrix} \alpha_{vv} & \alpha_{v\theta} \\ \alpha_{\theta v} & \alpha_{\theta\theta} \end{bmatrix} \qquad (501)$$

Previous work (Chapter 3) has examined the effects of achieving dynamic similarity between two beam structures. It was found that when the distances between the coordinate points of interest, the mass and stiffness distribution and the end constraints were the same, for each structure, then by achieving point similarity in one plane of motion it automatically gave the correct similarity for the other plane of motion. Based on this observation only the dynamic stiffness plots (inverse receptance plots) for vertical translation were used during the study.

Consider two systems A and B

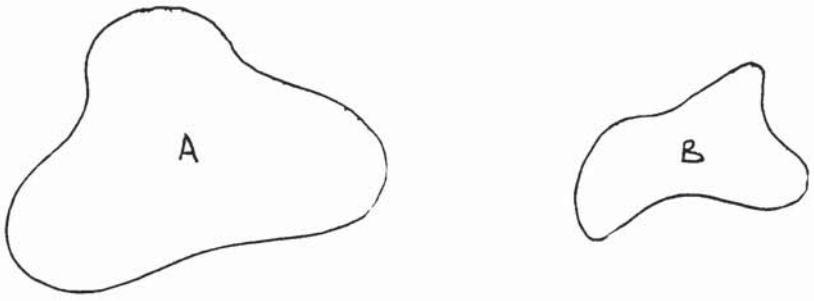

If it is assumed that system B is a sub-system of A such that

$$A \supseteq B \tag{502}$$

then a system C can represent the changes that have to be made to B such that

$$A = (B + C) \tag{503}$$

System A can therefore be considered as the resultant of coupling systems B and C

using (A504)

$$[\alpha_A] = ([\alpha_B]^{-1} + [\alpha_C]^{-1})^{-1}$$

or rearranging

$$[\alpha_C] = ([\alpha_A]^{-1} - [\alpha_B]^{-1})^{-1} \tag{504}$$

this expression can be used to obtain the dynamic

difference between two structures.

Dynamic stiffness plots were generated for the original structure [Figure 27] and the continuous element within the substitute structure [Figure 28]. When the two plots are compared directly [Figure 29] the differences in resonance and anti-resonance values between the two structures is readily observed. For the purposes of clarity, particularly at the anti-resonance positions, the difference between the two structures is shown in Figure 30.

The following observations can be made from Figures 29 & 30;

1) Within the general region of each anti-resonance two peaks exist.

2) These peaks correspond to the anti-resonances of the individual structures.

3) Prior to each anti-resonance region a resonant frequency occurs.

4) The plots presented are modulus values of dynamic stiffness and these resonant frequencies correspond to cross over points of the two plots.

5) The de-coupled system has the general level of the

continuous element when going from a resonance to an anti-resonance value and the general level of the original structure when going from an anti-resonance to a resonant value.

6) The resultant residual difference curve is not readily synthesised into an identifiable structure.

5.4.3 EIGENVECTOR DIFFERENCE APPROACH

The second approach utilizes the resonance frequencies and the mass normalised mode shapes (Eigenvectors).

Consider a set of mass normalised mode shapes for the original structure

$$[\bar{\Phi}_{orig}]^T [M_{orig}] [\bar{\Phi}_{orig}] = [1] \qquad (505)$$

and the continuous element

$$[\bar{\Phi}_{cont}]^T [M_{cont}] [\bar{\Phi}_{cont}] = [1] \qquad (506)$$

The work on dynamic similarity between continuous elements (Chapter 3) showed that to achieve dynamic similarity it was necessary to have the same mass and stiffness distribution for each element. If a difference exists between the original structure and the continuous element then an adjustment will have to be made to the continuous element.

ie $$[M_{orig}] = [M_{cont}] + [M_{res}] \qquad (507)$$

where $[M_{res}]$ is difference in mass distribution.

or $$[M_{res}] = [M_{orig}] - [M_{cont}] \quad (508)$$

providing the same spatial ,coordinates are retained and using (505) & (506)

$$[M_{res}] = [\Phi_{orig}]^{-T}[\Phi_{orig}]^{-1} - [\Phi_{cont}]^{-T}[\Phi_{cont}]^{-1} \quad (509)$$

It would be computational efficient to use

$$[M_{res}]^{-1} = [\Phi_{orig}][\Phi_{orig}]^{T} - [\Phi_{cont}][\Phi_{cont}]^{T} \quad (510)$$

and then invert $[M_{res}]^{-1}$.

If the stiffness matrices are considered then for the original structure

$$[\Phi_{orig}]^{T}[K_{orig}][\Phi_{orig}] = [\omega^{2}_{n_{orig}}] \quad (511)$$

and the continuous element

$$[\Phi_{cont}]^{T}[K_{cont}][\Phi_{cont}] = [\omega^{2}_{n_{cont}}]$$

applying the same philosophy as above yeilds the residual stiffness matrix

$$[K_{res}]^{-1} = [\Phi_{orig}][\omega^{2}_{n_{orig}}][\Phi_{orig}]^{T} - [\Phi_{cont}][\omega^{2}_{n_{cont}}][\Phi_{cont}]^{T} \quad (512)$$

and then invert $[K_{RS}]^{-1}$.

The total structure or system is always considered and the identified residual mass and stiffness matrices represent the changes that have to be made to the continuous element to achieve dynamic similarity.

The original structure and the continuous element were used to generate residual mass and stiffness matrices which were used to generate the point dynamic stiffness curve for the coordinate representing the tip of the beams (Figure 31). This was then coupled with the point dynamic stiffness curve for the tip of the continuous element. A comparison of the original structure against the coupled system is shown in Figure 32.

The following observations can be made from Figures 31 & 32;

1) Where the original structure has an anti-resonance the coupled system has two anti-resonances and one resonant value.

2) The anti-resonances are approximately symmetrical about the original structure's anti-resonances.

3) The first anti-resonance of each pair is a function of the continuous element's characteristics.

4) The eigenvalue problem was solved for the residual mass and stiffness matrices [Table 5]. The resonant frequencies are higher than the original structure's values so that when the continuous element and the residual system are coupled the resultant resonant frequencies are correct.

5) The dynamic stiffness curve for a point coordinate of the residual system has the correct form and is therefore capable of being synthesised to identify a discrete system.

5.4.4 SYSTEM IDENTIFICATION DIFFERENCE APPROACH

The third approach was based upon a System Identification process. The objective was to reduce a set of mobility curves, obtained from the original structure, to a set of mass, stiffness and damping matrices. A restriction of this approach was that the matrices had to be square, analysed from 'n' degrees of freedom and 'n' coordinates of interest. A corresponding set of mobility curves were obtained from an analysis of the continuous element and processed using the same System Identification algorithm. This provided two sets of consistant mass, stiffness and damping matrices. The differences between the matrices were the residual matrices which were used to regenerate the frequency response curves (Figures 33 & 34).

The following observations can be made from Figures 33 & 34;

1) Where the original structure has an anti-resonance the coupled system has two anti-resonances and one resonant value.

2) The anti-resonances are not symmetrical about the original structure´s anti-resonances.

3) The first anti-resonance of each pair is a function of the continuous element´s characteristics.

4) The second anti-resonance of each pair coincides with the original structure for the first two anti-resonances. The difference in the third anti-resonace can be attributed to truncation effects.

5) The resonant frequencies of the coupled system correlate exactly with the original structure.

6) The general level of the dynamic stiffness curve for the coupled system overlays the original stucture.

7) The dynamic stiffness curve for a point coordinate of the residual system has the correct form and is therefore capable of being synthesised to identify a discrete system.

5.4.5 APPRAISAL OF DYNAMICAL DIFFERENCE APPROACHES

Throughout all the different approaches to achieve a point coordinate receptance curve from the different modal data states the following features were consistant;

1) The anti-resonances of individual structures or systems were dominate during the coupling or dynamic difference procedure.

2) The positions of the anti-resonances were invariant during the coupling or dynamic difference process. In other words the anti-resonances of the individual structures or systems always appeared in the resultant system.

3) The position of the resonance frequencies varied according to the individual levels of each dynamic stiffness curve.

4) Point dynamic stiffness curves were used as the investigation was restricted to one dimensional, one plane of motion problems.

The objective of the investigation was to identify a suitable dynamic difference approach which resulted in a

realisable point receptance curve. Once this curve was established a technique ,discussed in Chapter 4, was capable of identifying the parameters of a discrete system which had the same dynamic characteristics as the receptance curve.

The first approach, the direct use of frequency response curves, resulted in a dynamic stiffness curve that was not suitable for subsequent analysis as it was not of a recognisable form.

The second approach, eigenvector difference, used a set of mode shapes from each structure to derive directly the residual mass and stiffness matrices. By using these matrices it was possible to generate the required point dynamic stiffness curve. The approach was very simple with the minimum of computational effort.

The third approach, System Identication difference, used frequency response plots to identify mass and stiffness matices for each structure. The difference between these matrices was the residual mass and stiffness matrices which were used to generate the required point dynamic stiffness curve. The technique requireed a high level of computional technique.

The second and third approach fulfilled the objective of identifying a suitable point receptance curve from a set of modal data. The choice of which technique to use will be

based upon whether the synthesis technique is using experimentally obtained data or finite element models.

The selection of the continuous element can not be arbitary as it's anti-resonance values must correspond with the original carrier structure.

5.5 SUMMARY

1) It has been proposed that a structure capable of achieving prescribed dynamical characteristics would be obtained from a mechanical test rig comprising an assembly of continuous and discrete elements in a system.
2) This system is called the substitute structure.
3) A design methodology based upon dynamical difference techniques has been proposed. The basic philosophy is to obtain a residual spatial model which represents the dynamical difference between the original structure and the continuous elements.
4) The derived residual spatial model can be represented by mass and stiffness matices which are fully populated.
5) It is impossible to directly identify a distributed discrete system, which is physical meaningful and can be attached to the continuous elements.
6) It is possible to identify a multi-degree of freedom discrete system which acts at a point coordinate by using the residual spatial model. This technique is

dependant upon the derivation of a point coordinate receptance plot.

7) It is impossible to derive a meaningful point coordinate receptance plot by directly manipulating the receptance plots of the original structure and the continuous elements.

8) It is possible to derive a point coordinate receptance plot for the residual spatial model by using eigenvector difference or system identification difference techniques.

PROPOSED STRUCTURES

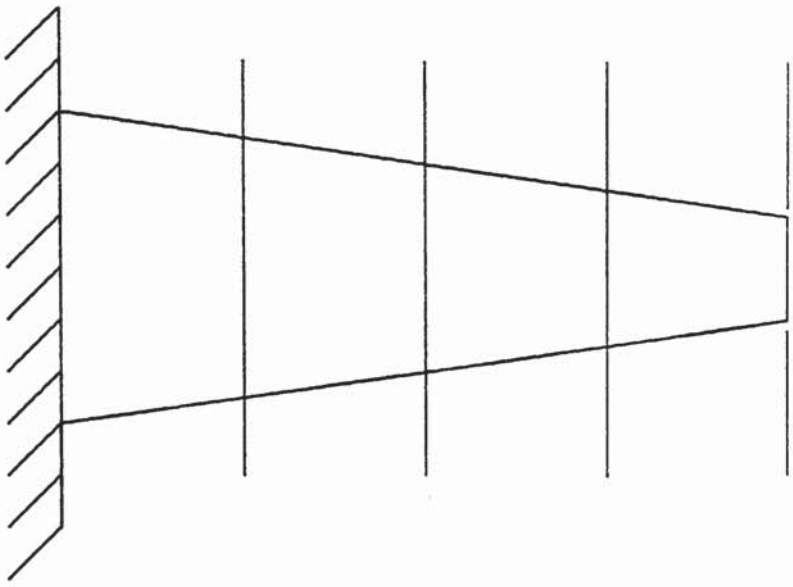

(a) Tapered Cantilever
(Original Structure)

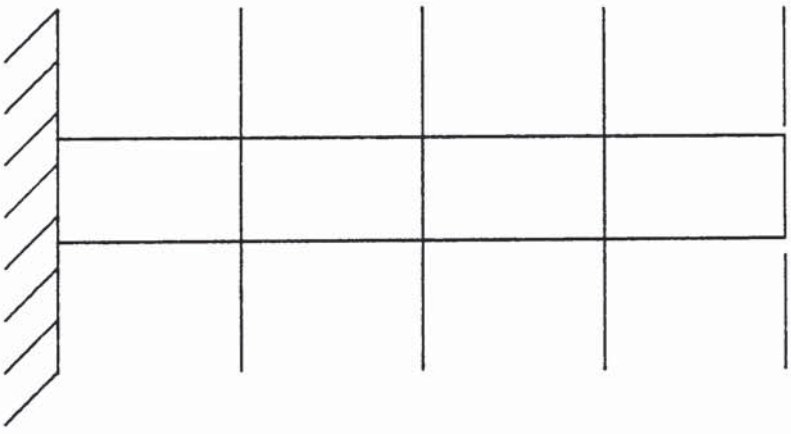

(b) Uniform section Cantilever
(Continuous Element)

Figure 22.

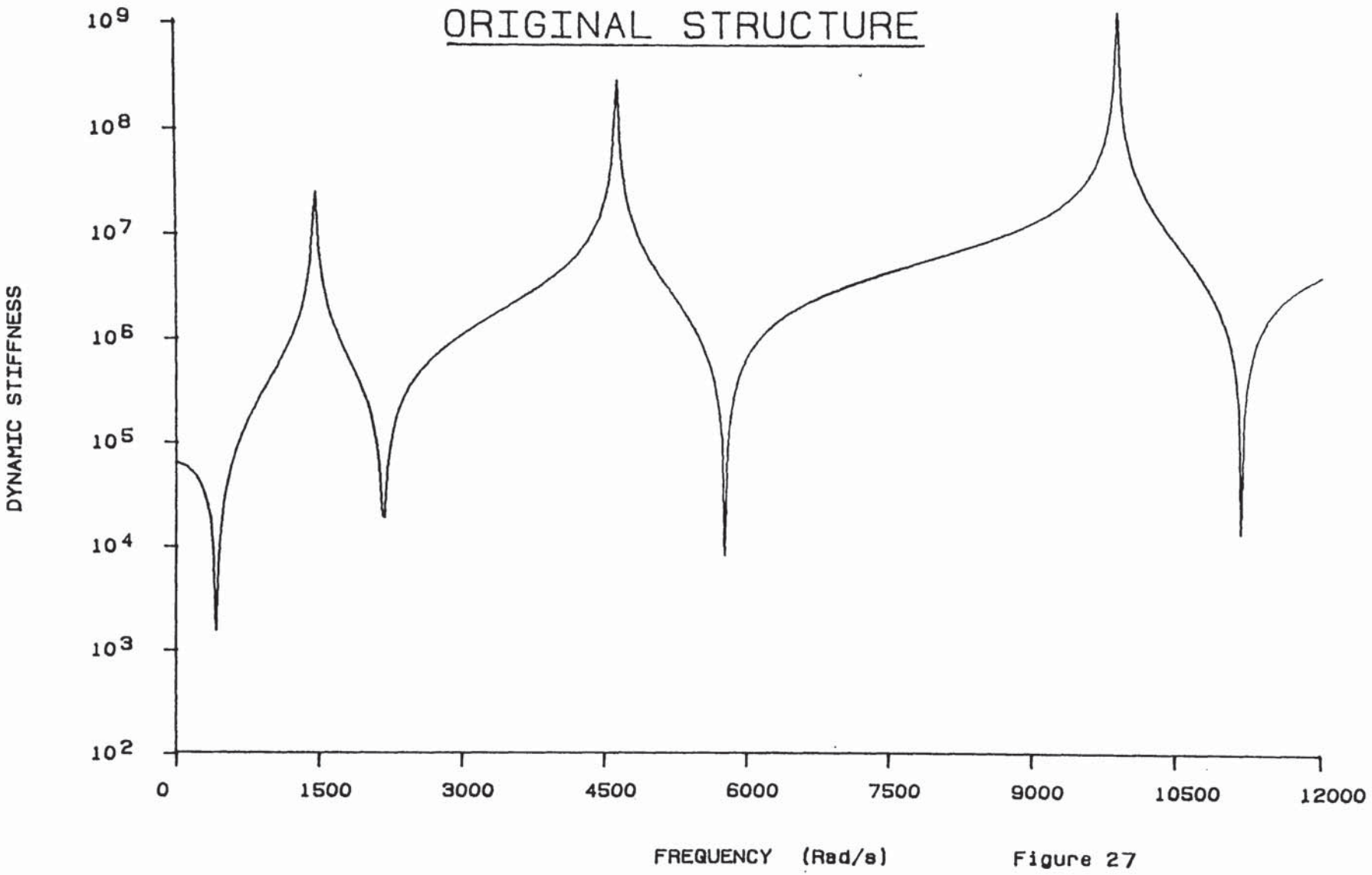
ORIGINAL STRUCTURE
DYNAMIC STIFFNESS
10^9
10^8
10^7
10^6
10^5
10^4
10^3
10^2
0
1500
3000
4500
6000
7500
9000
10500
12000
FREQUENCY (Rad/s)

Figure 27

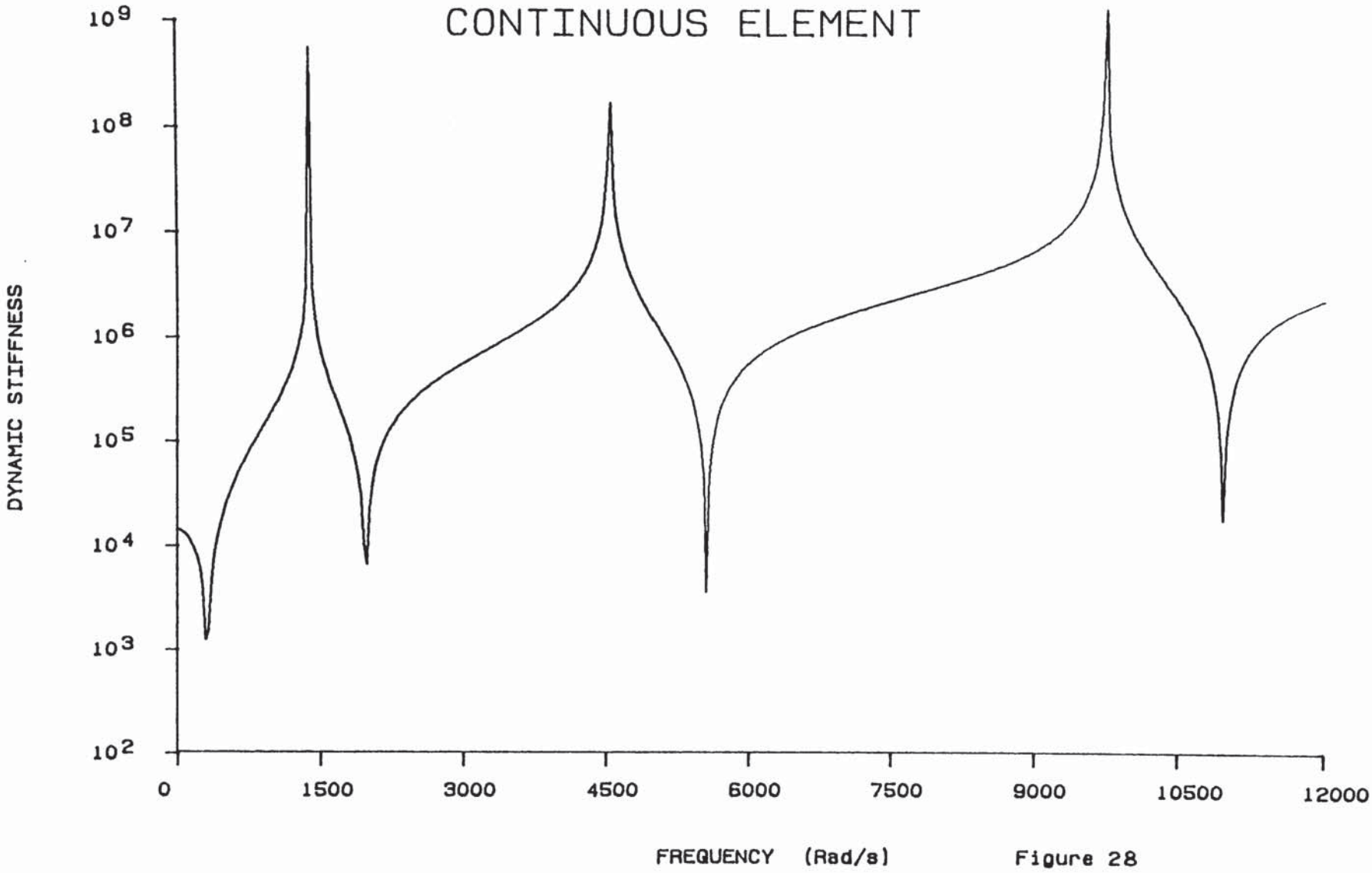
CONTINUOUS ELEMENT
DYNAMIC STIFFNESS
10^9
10^8
10^7
10^6
10^5
10^4
10^3
10^2
0
1500
3000
4500
6000
7500
9000
10500
12000
FREQUENCY (Rad/s)

Figure 28

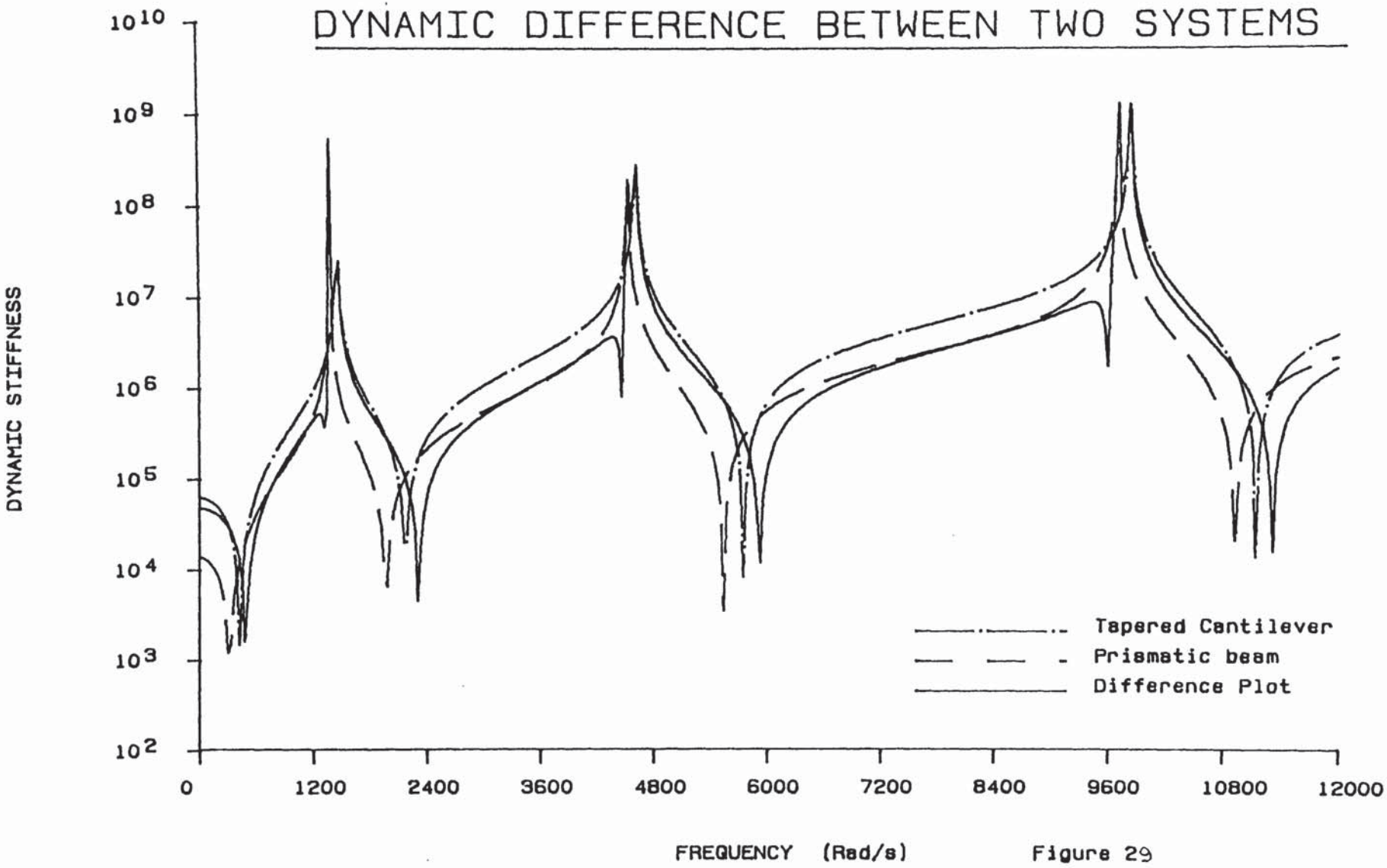
DYNAMIC DIFFERENCE BETWEEN TWO SYSTEMS
DYNAMIC STIFFNESS
10^{10}
10^{9}
10^{8}
10^{7}
10^{6}
10^{5}
10^{4}
10^{3}
10^{2}
0
1200
2400
3600
4800
6000
7200
8400
9600
10800
12000
FREQUENCY (Rad/s)
Tapered Cantilever
Prismatic beam
Difference Plot

Figure 29

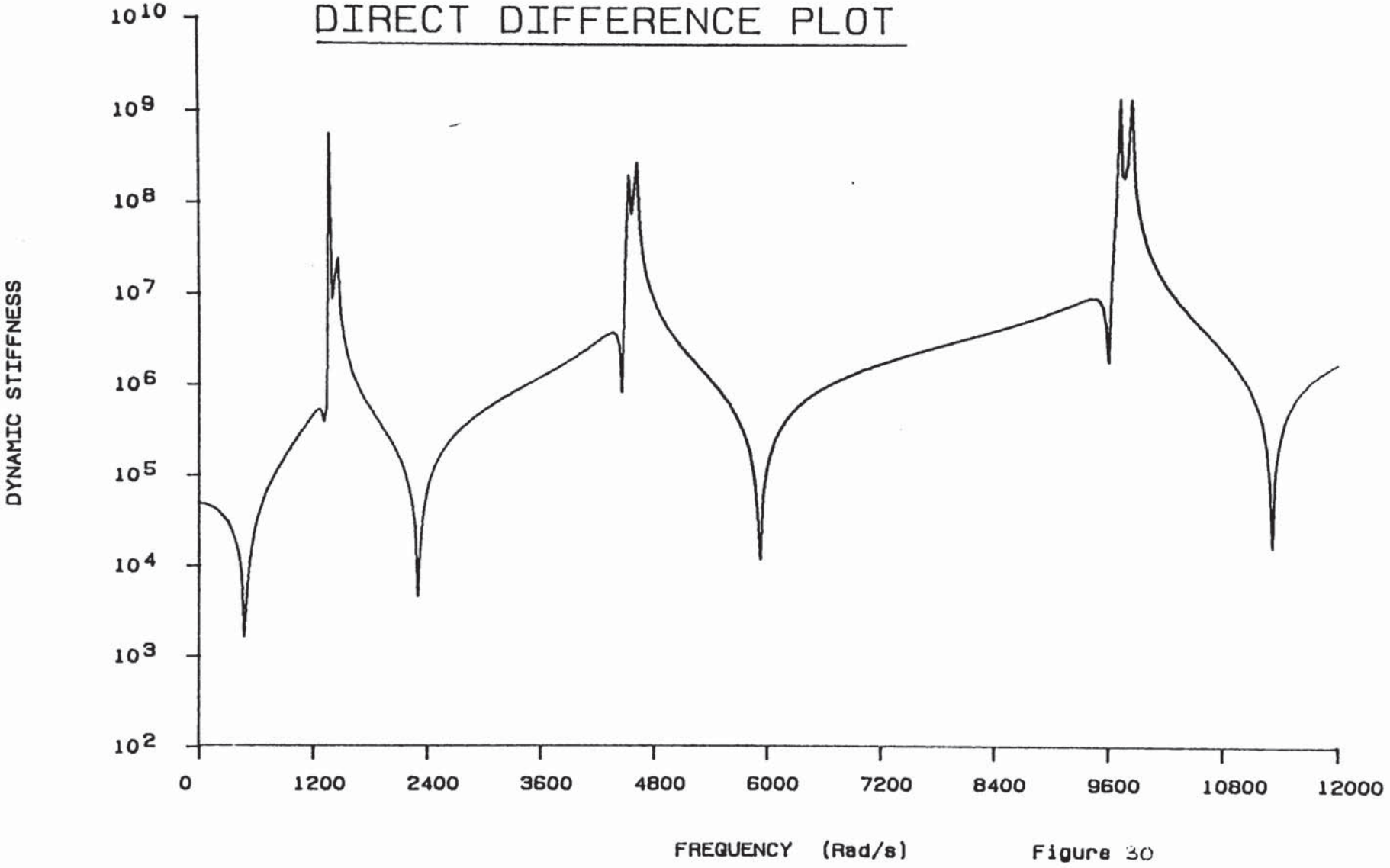
DIRECT DIFFERENCE PLOT
DYNAMIC STIFFNESS
10^{10}
10^{9}
10^{8}
10^{7}
10^{6}
10^{5}
10^{4}
10^{3}
10^{2}
0
1200
2400
3600
4800
6000
7200
8400
9600
10800
12000
FREQUENCY (Rad/s)

Figure 30

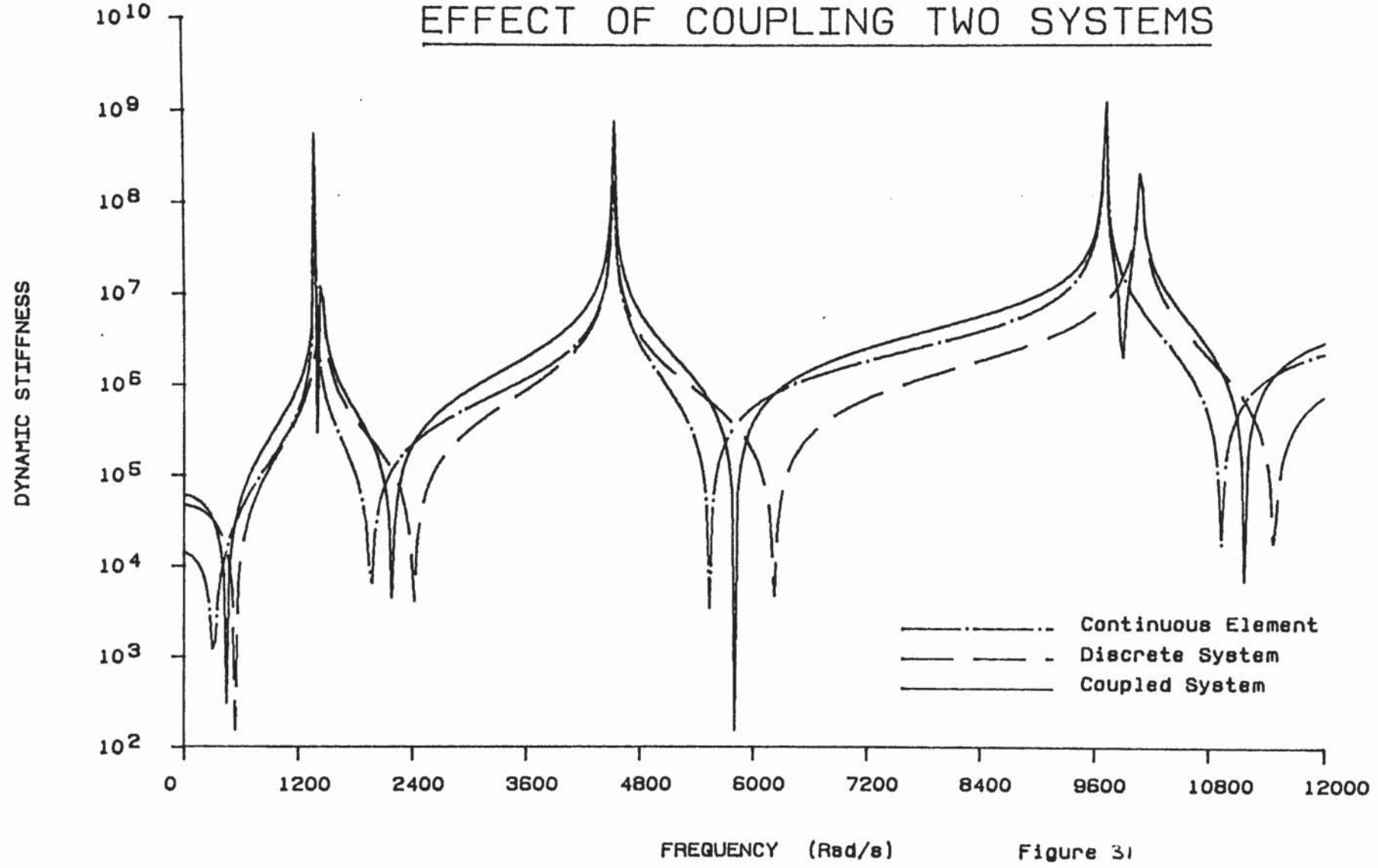
EFFECT OF COUPLING TWO SYSTEMS
DYNAMIC STIFFNESS
10^{10}
10^{9}
10^{8}
10^{7}
10^{6}
10^{5}
10^{4}
10^{3}
10^{2}
0
1200
2400
3600
4800
6000
7200
8400
9600
10800
12000
FREQUENCY (Rad/s)
Continuous Element
Discrete System
Coupled System

Figure 31

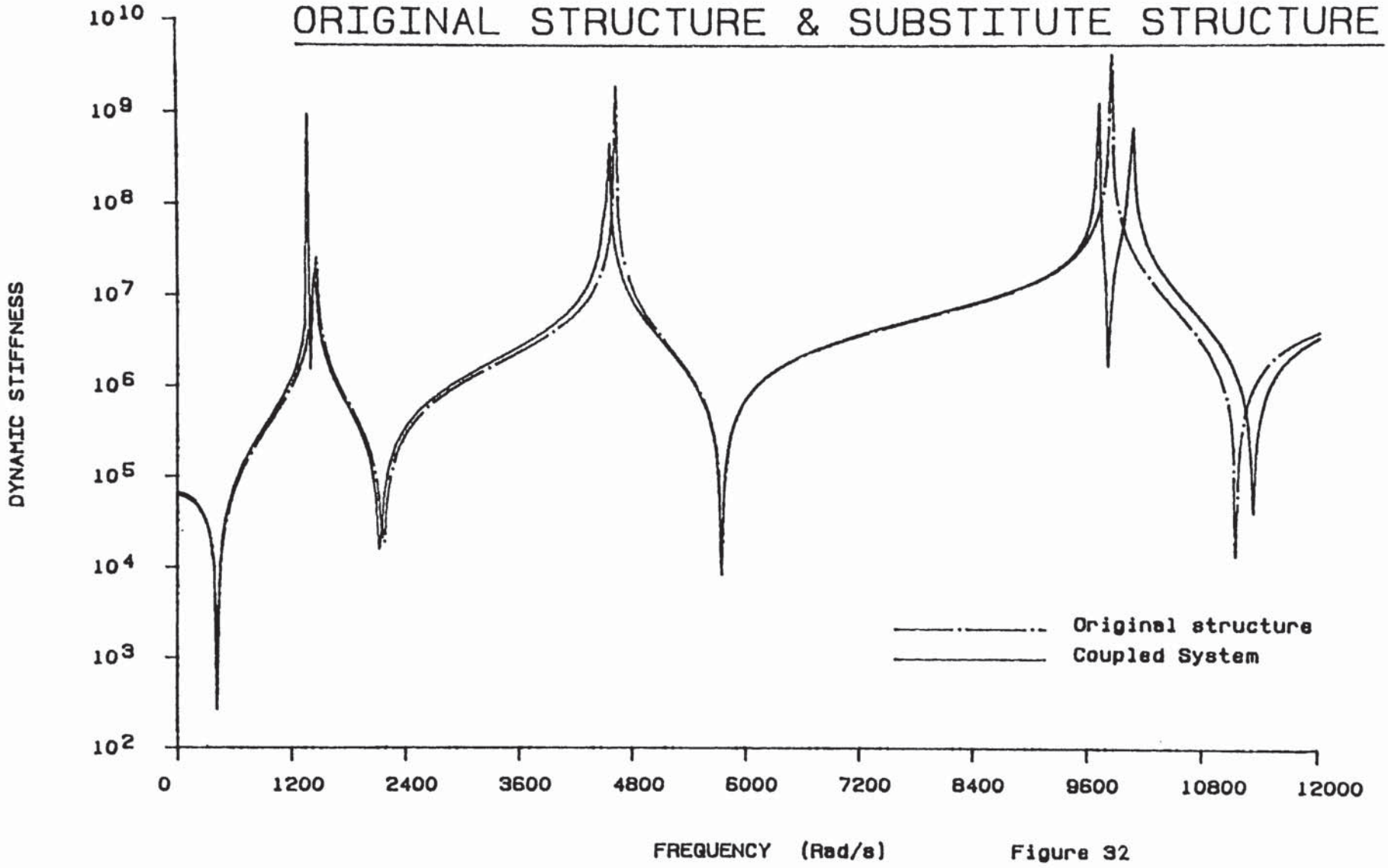
ORIGINAL STRUCTURE & SUBSTITUTE STRUCTURE
DYNAMIC STIFFNESS
10^{10}
10^{9}
10^{8}
10^{7}
10^{6}
10^{5}
10^{4}
10^{3}
10^{2}
0
1200
2400
3600
4800
6000
7200
8400
9600
10800
12000
FREQUENCY (Rad/s)
Original structure
Coupled System

Figure 32

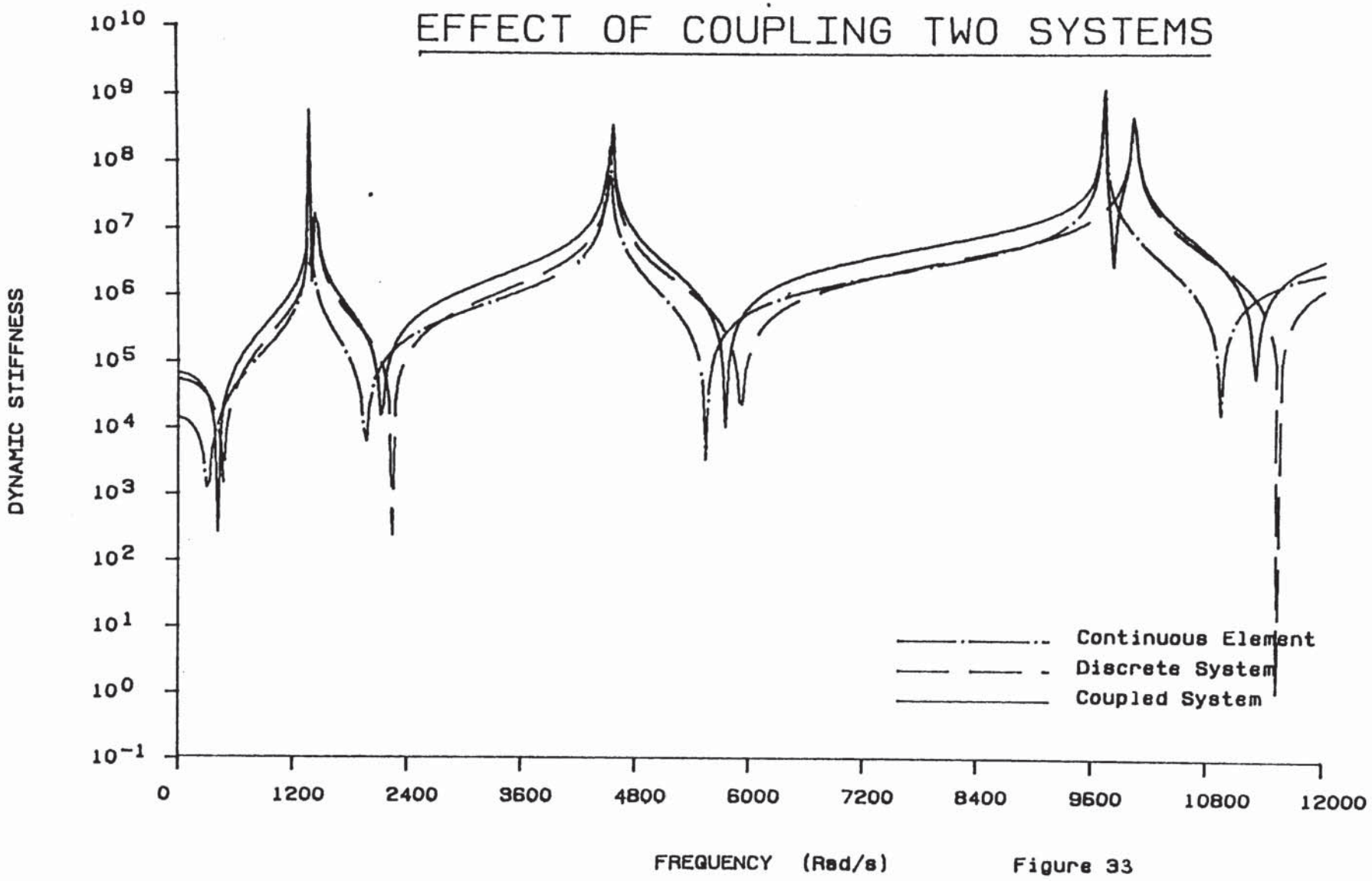
EFFECT OF COUPLING TWO SYSTEMS
DYNAMIC STIFFNESS
10^{10}
10^{9}
10^{8}
10^{7}
10^{6}
10^{5}
10^{4}
10^{3}
10^{2}
10^{1}
10^{0}
10^{-1}
0
1200
2400
3600
4800
6000
7200
8400
9600
10800
12000
FREQUENCY (Rad/s)
Continuous Element
Discrete System
Coupled System

Figure 33

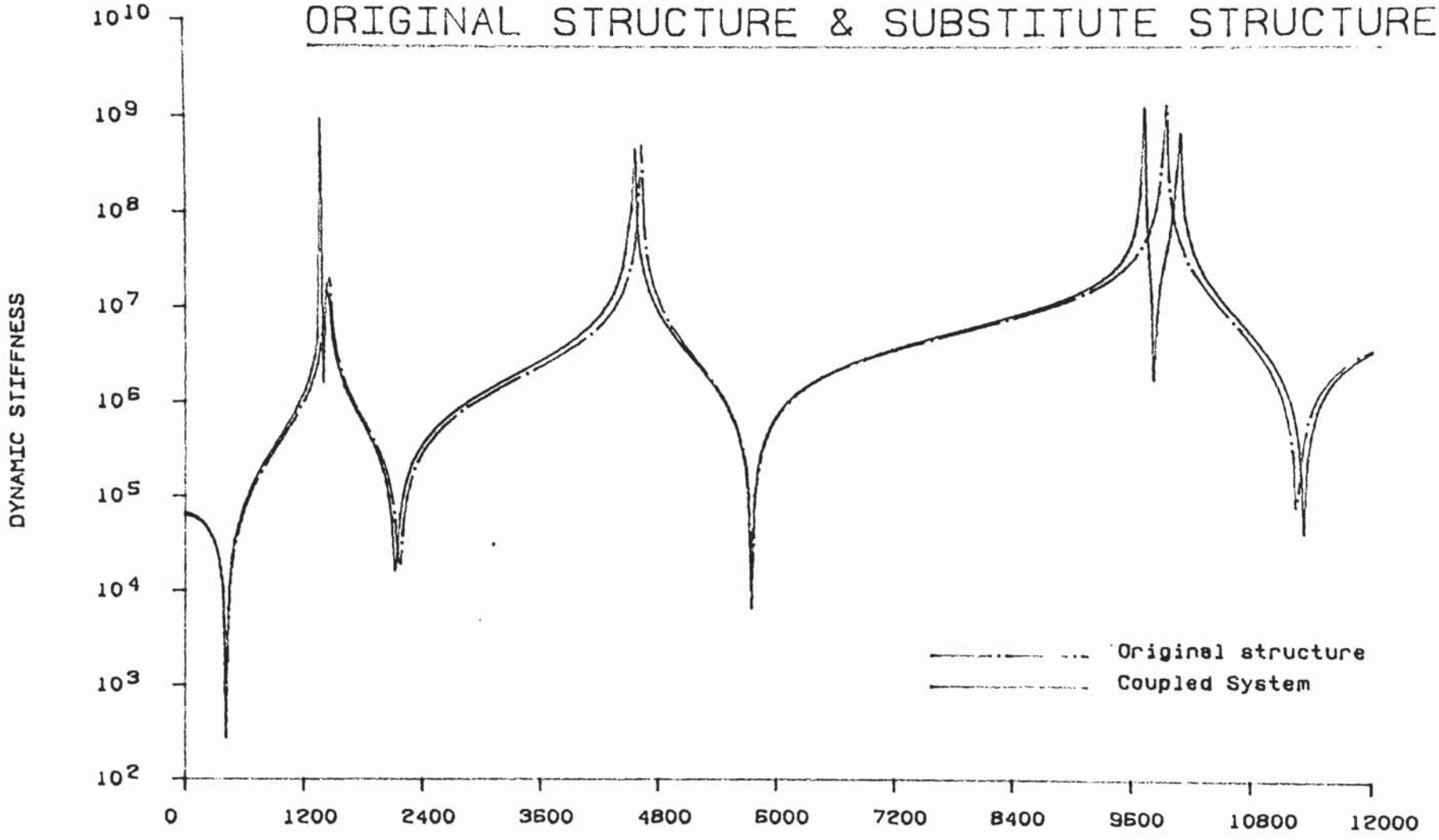
ORIGINAL STRUCTURE & SUBSTITUTE STRUCTURE
DYNAMIC STIFFNESS
10^{10}
10^{9}
10^{8}
10^{7}
10^{6}
10^{5}
10^{4}
10^{3}
10^{2}
0
1200
2400
3600
4800
6000
7200
8400
9600
10800
12000
FREQUENCY (Rad/s)
Original structure
Coupled System

Figure 34

EIGENVALUE ANALYSIS

[M]ARRAY:=

0.157	2E-2	-1.2E-2	9E-3
2E-2	0.181	1.4E-2	-1.7E-2
-1.2E-2	1.4E-2	0.216	4.1E-2
9E-3	-1.7E-2	4.1E-2	8E-2

[K]ARRAY:=

8037261	-5056942	1844882	-286079
-5056942	6682276	-4566320	1224279
1844882	-4566320	5117760	-1940753
-286079	1224279	-1940753	948420

EIGENVALUE RESULTS

EIGENVALUE NO.(1)= 611.6449

EIGENVECTOR NO.(1)

0.233	0.747	1.344	1.935

EIGENVALUE NO.(2)= 2300.08033

EIGENVECTOR NO.(2)

0.952	1.583	0.35	-1.918

EIGENVALUE NO.(3)= 5862.85526

EIGENVECTOR NO.(3)

1.709	9.4E-2	-1.264	1.879

EIGENVALUE NO.(4)= 11304.2732

EIGENVECTOR NO.(4)

-1.651	1.664	-1.322	1.888

Table 5.

6 DESIGN METHODOLOGY ASSESSMENT

6.1 INTRODUCTION

The proposed design methodology is based upon identifying the parameters of a mechanical test rig which is made up from an assembly of continuous and discrete elements in a system. It was shown in the previous chapter that it was possible to manipulate the dynamical difference between the original structure and the continuous element to obtain a point coordinate receptance curve. The work in Chapter 4 established a design methodology which identified, from a point coordinate receptance curve, the parameters and configuration of a discrete system. This discrete system was capable of reproducing the dynamical features of the original point coordinate receptance curve for the number of degrees of freedom of interest. The final section of work within Chapter 5 examined the implications of impedance coupling and dynamical difference techniques. This was to establish the ground rules for the proposed design methodology.

It was decided that an assessment of the proposed design methodology should be performed by using relatively simple one dimensional structures. This was so that the planes of freedom of the structure under examination were restricted. This ensured that the problem was totally perceivable and not overly complex so that the effectiveness of the design methodology was easily observed and not embedded within a complex design synthesis problem. A tapered cantilever

(Figure 22a) was selected as the original structure as it appeared to offer a reasonably complex structure which was easy to visualise, easy to model and ultimately manufacture.

The selection of the continuous element within the substitute structure was achieved by a blend of intuitive reasoning and an application of the design guide-lines established in Chapters 3 and 5. The prismatic beam element (Figure 22b) was selected as the continuous element within the substitute structure.

In Chapter 3 it was established that for identical dynamic similarity the following conditions had to be achieved;

1) The end constraints should be the same.
2) The distances between points of interest should be the same.
3) The mass and stiffness distribution should be the same.

The prismatic beam element was the same length as the tapered cantilever. Therefore, the first two conditions were fulfilled, but the third condition, the same mass and stiffness distribution was not achieved. Hence the requirement for a discrete system which was capable of dynamically tuning the continuous element to yield an acceptable level of dynamic similarity. It was noted that a disadvantage of selecting a prismatic beam as the continuous element was that it was physically similar to the tapered cantilever. Nevertheless, the resonant

frequencies of the two structures were significantly different so that the effects of the discrete system could be observed.

6.2 SINGLE POINT SIMILARITY : THEORETICAL STUDY

The first task, of the theoretical study, was to identify the discrete system parameters. The proposed design methodology was followed using the system identification difference technique to obtain the dynamical difference between the original carrier structure (the tapered cantilever) and the continuous element (the prismatic beam). This approach was selected as it is the most likely technique to be used by the designer when physical structures were available for measurement. The resultant residual mass and stiffness matrices were used to generate a point coordinate dynamic stiffness curve (Figure 35). This curve represents the dynamical difference between the two structures at the tips of each beam and was, therefore, the position where the discrete system had to be positioned. The resonance frequencies, anti-resonance frequencies and the value of the receptance curve when $\omega \rightarrow \phi$ were used within the discrete system identification methodology (Chapter 4). The identified discrete system was configured as Figure 15.

The discrete system was positioned at the tip of the prismatic beam and was assumed to be connected to the beam by a point connection at the mass m_4 (Figure 36). A

dynamic stiffness plot was generated for this coupled system (Figure 37) and plotted against the original structure for a direct comparison (Figure 38).

The resonant frequencies of the substitute structure correspond exactly with the original structure. However, an anomaly occurs at each anti-resonance position of the substitute structure. Instead of the substitute structure having only one anti-resonance between each resonant frequency of the original structure it has two anti-resonances, close together, separated by a resonant frequency. A careful examination of Figure 38 shows that the first anti-resonance of each pair results from the continuous element and the second from the discrete system. The small amplitude resonant frequency between the two anti-resonances is created when the two systems are coupled. A table showing the values of the resonance and anti-resonace values for the original structure and the substitute structure is shown in Table 6. The values for the continuous element are also shown so that the contribution of the discrete system is highlighted.

To avoid this double anti-resonance feature of the substitute structure it is necessary for the continuous element to have the same anti-resonant values as the original structure. This is highlighted in the previous chapter where the effects of coupling dynamically different structures are examined. It emphasises that the continuous element within the substitute structure cannot be derived

by intuitive reasoning and that a systematic design methodology is required.

Mode	Orig structure (Hz)	Cont element (Hz)	Subs structure (Hz)
Res 1	67	47	66
Anti-res 1	230	220	220 & 233
Res 2	346	310	341
Anti-res 2	725	715	718 & 726
Res 3	917	873	914
Anti-res 3	1542	1511	1510 & 1554

Table 6.

Although small discrepancies occurred at the anti-resonance positions of the substitute structure, it was decided that the overall dynamic similarity of the two structures were sufficiently close to warrant experimental validation. Before this was pursued however, a small study was undertaken to ensure that when the continuous element had the same anti-resonances as the original structure the twin anti-resonance feature did not exist.

A test was performed using two prismatic beams of different sectional area but the same resonance and anti-resonance values. The two beams did not have the same total mass so the receptance curves for the tips of each beam were the same shape execpt for the general level of the smaller section beam which was lower (Figure 39). The proposed design methodology was applied to this problem and a discrete system was identified which gave dynamic

similarity at the tips of each beam. The discrete system was coupled to the beam with the smaller sectional area. The resultant receptance curve for the substitute structure exactly overlays the receptance curve for the larger section beam (Figure 40). The continuous element within the substitute structure does not have to have the same resonance frequencies as the original structure since the coupling of the discrete system alters the resonance frequencies. It does though have to have the same anti-resonace values as these were dominate during the connection of different systems. This small example highlights the importance of the anti-resonances of the continuous element and that when they are correct exact dynamic similarity is achieved at the coordinate point of interest.

6.3 SINGLE POINT SIMILARITY : EXPERIMENTAL STUDY

6.3.1 DISCRETE ELEMENT DESIGN

Concurrent with this work on dynamic similarity, Cape Engineering Warwick Ltd, were studying the implications of designing structures that had the characteristics of a single spring/mass system.

The normal schematic representation of a discrete element is a simple helical spring with a mass attached to one end. This representation is not feasible as a physical structure for use in conjunction with the continuous element for the following reasons;

a) The mass has to be constrained to move within fixed guides.

b) The high levels of hysteretic damping within the spring.

c) The difficulty of fixing a mass to the spring and the spring to the continuous element.

It was therefore, necessary to design a continuous structure that exhibited the characteristics of a discrete element, whilst being capable of effective attachment to the continuous element. The definition of a discrete element was taken as a structure that had a factor of at least 20 between the fundamental and the second frequency.

A structure that exhibits this characteristic is shown in Figure 41a. Since the discrete system has to be attached to the continuous element the structure in Figure 41a can be treated as one quater of the physical discrete element (Figure 41b).

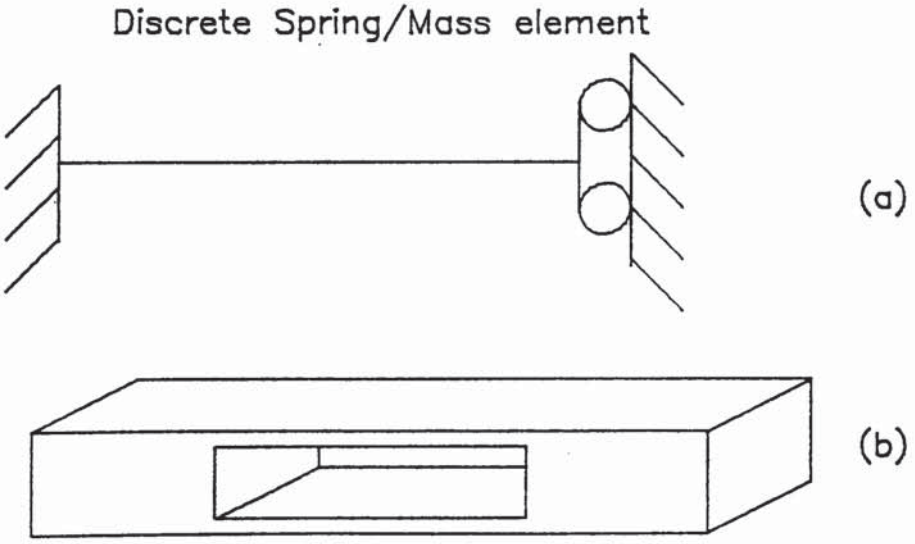

Figure 41

The stiffness and mass of each discrete element is known, from the discrete system identification methodology, and so it is a simple calculation to establish the length and breath of each element. The length is found by

$$\ell = \sqrt[3]{\frac{E\,b\,d}{K_n'}} \qquad (601)$$

where K_n' is one quarter of te discrete element stiffness.

The mass and stiffness values (m_1 and k_1) of the first discrete spring/mass element were used to derive the dimensions of a discrete element (Figure 41b). A finite element model was then generated for the element and the factor of difference between the first and second frequency was 22.6. This fulfilled the requirement for a minimum factor of 20 between the two frequencies. The Engineers at Cape Warwick performed a finite dimensional optimal design study on the elements dimensions. They established the optimum ratio between the length, breadth and depth of the element to maximise the factor between the first two modes.

6.3.2 EXPERIMENTAL TECHNIQUE

The results from the identification of the discrete system were restricted to the first three modes of the original structure. The well spaced resonances of the original structure meant that the first discrete element within the discrete system had it´s second resonance before the fourth resonance of the original structure. After the third mode

the experimental results for the substitute structure were not meaningful as they were coloured by the higher modes of the discrete elements. The three discrete elements were designed to the form of Figure 41b and attached to the continuous element in the order shown in Figure 42.

The third element was 20mm from the tip of the beam. The earthing spring, K_4 (Figure 36) within the discrete system configuration, was achieved by using a leaf spring between the tip of the beam and an earthing strap. The mass m_4 was achieved by fixing an appropriate accelerometer, of the correct mass, to the underneath of the beam at the tip.

The beams were clamped within rigid towers that were fixed to a steel base plate. The base plate (2 metres * 1 metre * 0.2 metres deep) was supported at its edges by a hard wood frame. This particular support system was well established and the fundamental frequency was well above the range of interest.

The substitute structure was excited by striking the tip of the beam with a calibrated force hammer. An average of 8 excitions were taken to produce each frequency response plot. The data capture and analysis equipment was a GENRAD 2502 system. When the tapered cantilever was excited with the force hammer it was found that the first anti-resonance was poorly defined and so a small electo-magnetic shaker was used.

6.4 COMPARISON OF THEORETICAL AND EXPERIMENTAL RESULTS

The first task of the study was to compare the results from the physical tapered cantilever (original structure) with the results from the finite element model of the original structure. The primary objective of this was to ensure that the clamping (ie the end restraints) of the tapered cantilever were correct. A comparison of the first four modes of the physical structure and the finite element model are shown below in Table 7.

Mode	Orig structure		F.E. Orig structure	
	Res	Anti-res	Res	Anti-res
1	64	216	67	230
2	324	670	346	725
3	890	1320	917	1542
4	1673	-	1776	-

Table 7.

A plot of the measurements made from the physical beam is shown in Figure 43. The values are mass corrected to allow for the effect of the accelerometer at the beam's tip. The values of the physical beam are consistantly lower, by approximately 5%, than the predicted values from the finite element model. This can be attributed to three main reasons;

a) The end restraints of the physical tapered cantilever are permitting very small rotational movements.

b) The finite element model does not include damping effects. It is typical for this type of structure

to have a hysteretic damping level between 2 and 4%.

c) The resolution of the data within the GENRAD system. The technique which was used to identify the values on the screen, by the use of 'cross hairs', had a step of 2 Hz for the frequency range under consideration.

The experimental data obtained from the substitute structure had the same form as the theoretical substitute structure. Where the original structure had just one anti-resonance between each resonant frequency the substitute structure had two anti-resonances and an associated resonant frequency (Figure 44). The first and second resonance frequency and the first anti-resonant frequency for the experimental original structure and substitute structure are within 5% (Figure 45 and Table 8). As the frequency increases the difference between the two structures increase. This is due to the difference in the rotary inertia between the two structures.

Mode No.	Orig. structure (Hz)	Subs. structure (Hz)
Res 1	64	67
Anti-res 1	216	190 & 219
Res 2	324	322
Anti-res 2	670	607 & 690
Res 3	890	855
Anti-res 3	1320	-

Table 8.

When the physical substitute structure is compared with the

theoretical substitute structure the physical values are consistantly lower, as is the comparison for the original structures. The same reasons as before apply plus the following new ones;

a) The discrete elements do not act at a concentrated point on the physical structure but are placed in a row at the tip of the continuous element. The third element is 20 mm from the tip.

b) Small variations in the length of the beams used for the discrete elements or the central positioning of the discrete elements and their method of attachment can cause frequency variations. For example in Figure 44 there is a small resonance at 420 Hz which must be created by a discrete element rotating about the axis of the continuous element.

Table 9 shows a comparison of the physical substitute structure against the theoretical substitute structure.

Mode No.	Subs. structure Physical (Hz)	Subs. structure Theoretical (Hz)
Res 1	67	66
Anti-res 1	190 & 219	220 & 233
Res 2	322	341
Anti-res 2	607 & 690	718 & 728
Res 3	855	914
Anti-res 3	-	1510 & 1554

Table 9.

Although small discrepancies do occur between the experimental data for the substitute structure and the

original structure the receptance levels, the general shape of the receptance curves and the values of the resonance frequencies are sufficiently close to consider that the two structures are dynamically similar.

The general level and shape of the receptance curves for the experimental work correlated well with the theoretical study such that it can be considered that the proposed design methodology has been validated for point coordinate similarity problems.

6.5 EFFECTS OF MEASURING RESPONSES AT A NODE

When data are being recorded from physical structures it is always a possibility that a selected response station is a node for one vibration mode within the frequency range of interest. If an analytical study has been performed prior to the measurements being taken then guidance can be given to the test engineers as to the optimum positions for the response stations. This is an ideal case and unfortunately is not always possible in practice. It is, therefore, necessary to examine the implications of using frequency response data which includes data captured from a response station at which a node occurs. It is important to establish that it is still possible to identify a discrete system which provides dynamic similarity when the discrete system is positioned at a node.

The tapered cantilever and the prismatic beam (Figures 22a & 22b) were used as the original structure and the continuous element respectively. Two case were considered, where a finite element analysis showed that nodes occurred for the second and third modes. Each beam considered had a length of 500mm.

Case 1 Responses were generated for the coordinate 375 mm from the root of the cantilever which is the node position for the second mode.

Case 2 Responses were generated for the coordinate 250 mm from the root of the cantilever which is the node for the third mode.

Case 1 : 375 Co-ordinate

The design methodology was applied to the two structures where four coordinates were considered, one of which was at 375 mm from the root of the cantilever. Care was taken to ensure that the other coordinates were not at a node for the frequency range of interest. The dynamical difference technique was applied so that the residual mass and stiffness matrices were obtained. The residual point coordinate receptance curve was generated for the 375 mm coordinate and a discrete system representing the first and third modes of the continuous element was identified.

The coupling of this discrete system to the continuous

element is shown in Figure 46. The resonance frequencies of the substitute structure correspond accurately to the original structure. There is a small resonance and anti-resonance at approximately 2000 Rad/s which is caused by the small positional difference of the node point between the original structure and the continuous element.

Since the discrete system is positioned at the node of the second mode it is impossible for the system to contribute anything to the dynamic similarity at this frequency. This is highlighted in Figures 47, 48 and 49, which show the first three modes of interest of the original structure and the substitute structure. An observation that can be made of this analysis is the creation of intermediate resonances between the original frequencies of interest. This feature is dealt with in detail in the next section as its major effects are exhibited when transfer similarity is considered. In Figure 47, the first mode, the original structure and the substitute structure have similar frequencies and the mass normalised mode shapes overlay each other. The mode shape for the continuous element is also plotted. This is of higher amplitude than the substitute structure because the element has less mass and is of greater flexibility than the substitute structure. The effect of the discrete system is easily observed as it reduces the amplitude of the mode shape for the whole of the continuous element. The third mode of the substitute structure and the second mode of the original structure, Figure 48, shows that the mode shape for the substitute

structure is the same as the continuous element. The resonant frequency is also similar to the continuous element.

When the fifth mode of the substitute structure and the third mode of the original structure is examined, Figure 49, the substitute structure has reverted back to being dynamically similar to the original structure. It is interesting to note that the mode shape amplitude of the substitute structure is the same as the original structure upto the coordinate where the discrete system is positioned. After this position the amplitude of the substitute structure is greater than the original structure and less than the continuous element.

Case 2 : 250 Co-ordinate

When the coordinate of interest is 250 mm from the root of the cantilever the third mode was not effective within the identification of the discrete system. The design methodology was applied to this case and the parameters of the discrete system were identified. As before, these parameters were directly inserted into the mass and stiffness matrices of a finite element model of the continuous element to obtain a spatial model of the substitute structure. The eigenvalue problem was solved for the spatial model and the mode shapes compared with the original structure.

The full implications of this analysis are discussed in the next section when two point coordinate simialarity is considered. The Figures 50, 51 and 52 show the first three modes of interest for this condition. In Figure 50 the amplitude of the mode shape for the first mode of the substitute structure and the original structure are very close. The resonant frequency for the original structure is 419 rad/s, compared to 430 rad/s for the substitute structure and 323 rad/s for the continuous element. This figure amply demonstrates the effect of the discrete system on the continuous element. The resonant frequency is increased by 107 rad/s, the amplitude of the mode shape reduced to similar levels of the original structure and the whole of the substitute structure is dynamically similar to the original structure. The second mode, Figure 51, shows that the mode shape of the substitute structure and the original structure overlay upto the 250 mm coordinate. After this position the two curves diverge with the substitute structure´s mode shape amplitude lying between the original structure and the continuous element.

The node is within the third mode and therefore no contribution to dynamic similarity is made from the discrete system at this frequency. This is clearly shown in Figure 52 where the amplitude of the substitute structure overlays the continuous element.

Although point coordinate similarity has been achieved at a node position it is impossible to obtain overall similarity

for the substitute structure using a discrete system derived from data recorded at a node on the original structure. If a theoretical study of the original structure has not been made to provide guidance to the test engineer then it is important that sufficient response stations are recorded to ensure that an adequate amount of data exists for the system identification and subsequent analysis so that node points , if at all possible, can be avoided.

6.6 TWO POINT SIMILARITY : THEORETICAL STUDY

The basic objective of the work is to derive a design methodology for mechanical test rigs such that the dynamical characteristics of the test rig are representative of any specified structure. This structure, the original structure, can be a complete structure in it's own right or part of a very large structure. Once the test rig (substitute structure) has been designed and manufactured it can be used to test a range of equipment in realistic environmental conditions. Up to the present stage, only single point attachment has been considered and it is, therefore, necessary to examine the implications of obtaining dynamic similarity for at least the same number of coordinates as attachment points.

Although multi-point attachment was to be considered, the initial study was restricted to one dimensional problems that have two planes of motion. In this way the basic

design rules were established without having to also resolve a difficult multi-dimensional problem. The tapered cantilever and prismatic beam used within the previous section were again employed.

If any point on a structure is considered it will have up to six planes of motion. It is sometimes possible due to structural constraints or symmetry to be able to reduce the number of freedoms of interest without reducing the level of resolution of the problem. For example, when dealing with simple beam elements it is normal to only consider two planes of motion; vertical translation and vertical rotation. The restricted receptance expression for any coordinate x on the beam can be defined as;

$$\alpha_x = \begin{bmatrix} \alpha_{vv} & \alpha_{v\theta} \\ \alpha_{\theta v} & \alpha_{\theta\theta} \end{bmatrix} \qquad (602)$$

where v is the vertical translation.

θ is the vertical rotation.

Consider a simple cantilever (Figure 53) with two coordinate points (a) and (b)

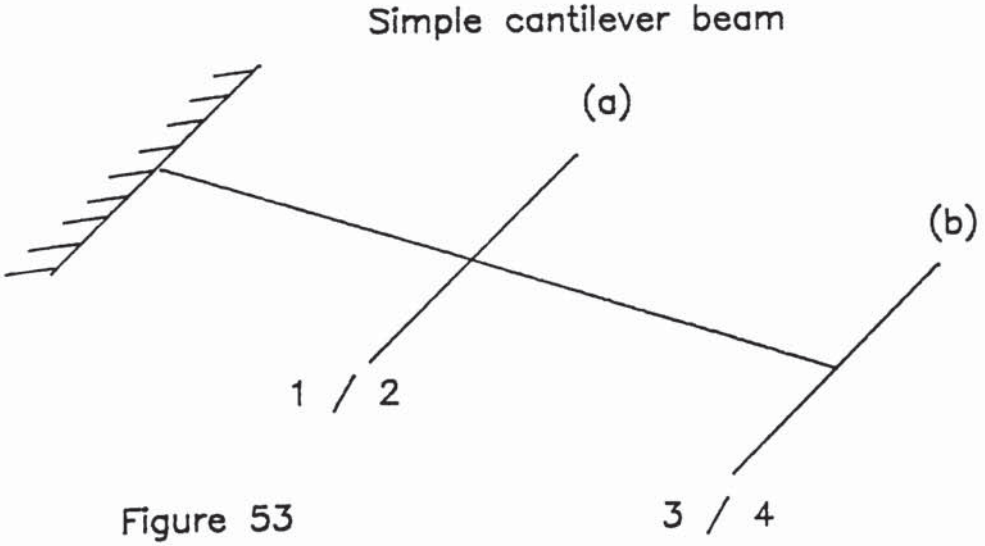

Figure 53

the receptance can be written as

$$\alpha_{ab} = \begin{bmatrix} \alpha_{11} & \alpha_{21} & \alpha_{31} & \alpha_{41} \\ \alpha_{21} & \alpha_{22} & \alpha_{32} & \alpha_{42} \\ \alpha_{31} & \alpha_{23} & \alpha_{33} & \alpha_{43} \\ \alpha_{41} & \alpha_{24} & \alpha_{34} & \alpha_{44} \end{bmatrix} \qquad (603)$$

Work on truncated and incomplete mode shapes (Chapter 3) showed that it was possible to isolate the receptance curves for one plane of motion without losing the integrity of the data and hence the spatial model. This observation allowed the complete receptance matrix to be reduced even futher so that only the vertical translational responses were considered, equation 604,

$$\alpha_{ab_{(vert)}} = \begin{bmatrix} \alpha_{11} & \alpha_{13} \\ \alpha_{31} & \alpha_{33} \end{bmatrix} \qquad (604)$$

This matrix is a partial description of the structure for vertical translation. Nevertheles, providing a consistant set of coordinates are retained throughout the reduction process, it is a full description of the motion at the coordinates (a) and (b) for the frequency range of interest.

In the previous chapter an expression was derived which

obtained the dynamic difference between two structures, equation (504)

$$[\alpha_c] = ([\alpha_A]^{-1} - [\alpha_B]^{-1})^{-1} \qquad (504)$$

where α_A is the receptance for the original structure

α_B is the receptance for the continuous element

The vertical receptance matrix (604) can be substituted, for each structure, into equation (504) when calculating the dynamic difference between two structures, providing a consistant set of coordinates is used. This process is in fact used during the identification procedure within the single point coordinate similarity design problem. The residual matrix $[\alpha_c]$ is for the difference between the whole of the original structure and the continuous element at the coordinates of interest. The complete residual receptance matrix is used within the identification of the single multi-degree of freedom discrete system. It is, therefore, implicit within this process that only one multi-degree of freedom discrete system is required to obtain dynamic similarity for the whole of the substitute structure.

To examine this hypothesis two design cases were considered;

Case 1 The discrete system identified in section 6.2

which was used to examine the single point coordinate similarity between the tapered cantilever and the substitute structure was used. The coordinate of interest was at the tip of the tapered cantilever which was 500 mm from the beam´s root.

Case 2 The coordinate of interest was moved to 300 mm from the root of the tapered cantilever.

Case 1 : 500 mm Co-ordinate

When the effects of placing the discrete system at a frequency node were examined (Section 6.5) intermediate frequencies to those of interest were obtained. If these frequencies have significant mode shape values then they will effect the quality of dynamic similarity for the whole structure. To examine this effect and to establish that only one discrete system was required to ´tune´ the whole of the structure the parameters of the discrete system identified in section 6.2 were included into the mass and stiffness matrices for the continuous element, which were obtained from the finite element model. The resultant matrices represent a spatial model for the substitute structure at the coordinates of interest. The eigenvalue problem was solved for these matrices and the mode shapes for the first five modes were compared with the original tapered cantilever.

For the first mode, Figure 54, the mode shape for the

substitute structure overlays the original structure. The mode shape for the continuous element is also shown so that the effects of coupling the discrete system to the continuous element are visable. Since the mode shapes for the substitute structure and the original structure overlay each other it emphasises that a single multi-degree of freedom discrete system is capable of 'tuning' the whole of the substitute structure. The discrete system has increased the first resonance frequency of the continuous element from 313 rad/s to 429 rad/s. The effects of the discrete system upon the continuous element are, therefore, quite substantial.

However, an undesirable effect manifests in the second mode of the substitute structure. This mode has a resonant frequency of 1407 rad/s which is not comparible to the original structure.

If the individual spring/mass elements of the discrete system are examined, then the first spring/mass element (m_1 and k_1) has a resonant frequency of 1475 rad/s. This is reflected in the mode shape vector by the corresponding value for mass m_1 being much higher than the other mode shape elements. The value of the mode shape at the coordinate where the discrete system is attached is very low and, therefore, the resonance does not appear when the point receptance plot for the substitute structure is examined (Figure 38).

If the mode shape for the second resonance of the substitute structure is plotted (Figure 55) then the resonance of the first element of the discrete system has significant effects. Obviously, these effects will be detrimental to the quality of dynamic similarity when multi-point attachment for the transported equipment is considered.

The plot for the third mode of the substitute structure corresponds to the second mode of the original structure (Figure 56). The mode shape curve for the substitute structure overlays the mode shape curve for the original structure. The mode shape for the continuous element is plotted so that the effects of the discrete system are easily observed.

The fourth mode of the substitute structure does not correspond to the original structure. An examination of the mode shape vector reveals that the second spring/mass element of the discrete system (k_2 and m_2) is resonating. The mode shape value at the coordinate where the discrete system is coupled is very small and hence the resonance does not appear in the point receptance plot. The fifth mode of the substitute structure correlates to the third mode of the original system.

If it is assumed that the two attachment coordinates for an item of equipment are at the 300 mm and 500 mm positions then the following observations can be made:

(a) The dynamic similarity at the 500 mm coordinate of the substitute structure and the original structure are acceptable. This means that the correct level and amplitude of vibrational response is transmitted to the equipment via this coordinate.

(b) At the 300 mm coordinate there is an intermediate frequency between each of the original frequencies of interest. The mode shape values of these frequencies are significant.

(c) Due to these extra frequencies, the level of dynamic similarity at the 300 mm coordinate is not acceptable.

If the transfer receptance between the 500 mm coordinate and the 300 mm coordinate is examined, Figure 57, then the significance of the intermediate frequencies are very clear. If the transfer receptance for the substitute structure is plotted against the transfer receptance for the original structure, then the intermediate frequencies resulting from the discrete system apparent, Figure 58.

Case 2 : 300 mm Co-ordinate

The design methodology was applied to the tapered cantilever and the continuous element where the coordinate of interest was at 300 mm from the root of the beams. The

300 mm coordinate was selected as no node points occur at this coordinate for the frequency range of interest. The total mass of the identified discrete system was greater than when the discrete system was placed at the tip of the continuous element beam. The total mass of the discrete system was a function of the coordinate position selected and was found by the simple expression established in Chapter 4, equations (414) and (416).

$$\frac{1}{\sum_{r=1}^{n} {}_r\phi_{jj}^2} = \frac{1}{\alpha_{jj}(\phi)} \sum_{r=1}^{n} \frac{1}{\omega_r^2} \qquad (414)$$

$$m_{tot_{jj}} = \frac{1}{\alpha_{jj}(\phi)} \sum_{r=1}^{n} \frac{1}{\omega_r^2} \qquad (416)$$

The eigenvector value ${}_r\phi_{jj}$ for the first mode was the major contributor to the total mass of the discrete system. As the coordinate selected nears a constrained coordinate on the structure the mode shape amplitude reduced, thus increasing the total mass of the discrete system. For example, the total mass of the discrete system for the 300 mm coordinate was 1.196 Kg compared to 0.228 Kg at the 500 mm coordinate.

When the identified discrete system was coupled to the continuous element at the 300 mm coordinate the point coordinate frequency response plot for the resultant substitute structure was dynamical similar to the original structure (Figure 59).

The first mode (Figure 60) of the substitute structure overlays the original structure which indicates a high level of similarity. The mode shape for the continuous element is plotted so that the contribution of the discrete system to dynamic similarity can be observed.

The second mode of the substitute structure does not correspond to a resonance of the original structure. The same characteristics that were exhibited when the discrete system was at the 500 mm coordinate were obtained for the discrete system at 300 mm. The first spring/mass element (k_1 and m_1) was resonating but the mode shape value at the coupling coordinate was insignificant. This explains why the point receptance plot for the substitute structure at the 300 mm coordinate was dynamically similar to the original structure, since it was a node point when the individual spring/mass elements of the discrete system resonated.

A plot of the second mode of the substitute structure (Figure 61) showed a very large amplitude at the tip of the beam. If the equipment was attached at the 300 mm and 500 mm coordinate then by positioning the discrete system at 300 mm the level of dynamic similarity was worse than using the continuous element on its own.

A plot of the third mode (Figure 62) showed that the mode shape of the substitute structure followed closely the original structure upto the connection point of the

discrete system. Between the 300 mm and 500 mm coordinates the mode shape for the substitute structure fell progressively away from the original structure. This showed that the discrete system was effecting dynamic similarity from the position of maximum constraint upto the coupling point but then over restrained the continuous element's motion.

The effects of distributing the discrete system between the two coordinates of interest was examined. The general level of each of the respective residual receptance curves were halved to proportion half of the dynamic similarity contibution to each position. This had the effect of halving the total mass of each discrete system. The discrete systems were identified separately and then coupled to the spatial model of the continuous element. An eigenvalue analysis of the resultant mass and stiffness matrices was performed and can be seen in Table 10.

When two discrete systems are coupled to the continous element, then two intermediate resonant frequencies are obtained. These resonant frequencies, again correspond to the individual spring/mass elements of the discrete systems. A point receptance curve for the 500 mm coordinate is shown in Figure 63. It shows that distributed discrete systems are incapable of achieving an acceptable level of dynamic similarity, even at the coordinate of coupling of one of the systems.

6.7 TWO POINT SIMILARITY; EXPERIMENTAL STUDY

The experimental validation of the theoretical study of two point coordinate similarity was performed by considering the transfer frequency response function between the 500 mm and 300 mm coordinates. An accelerometer was attached at the 300 mm coordinate and the input function was applied at the 500 mm coordinate of each structure.
The transfer inertance plot for the original structure (Figure 64) shows well defined resonances and just one anti-resonance between the third and fourth mode. This plot corresponds to the theoretical study, as shown in Table 11.

The results follow the same trend as discussed in Section 6.4 with the experimental values slightly lower than the theoretical values.

When the transfer inertance plot for the substitute structure is examined (Figure 65) then the intermediate resonaces, predicted in the theoretical study, are exhibited. A comparison of the theoretical study and the experimental test is shown in Table 12.

6.8 SUMMARY OF DESIGN METHODOLOGY ASSESSMENT

1. The design methodology is viable for single point coordinate similarity.

2. If the anti-resonance frequencies of the continuous element are different to the original structure then spurious frequencies are created. The experimental work, used to validate the theoretical study, confirmed this phenomenon.

3. If the discrete system is positioned at a frequency node point then it is ineffective for that frequency and hence an acceptable degree of dynamic similarity is not achieved.

4. The most effective position to couple the discrete system is at the least constrained coordinate of the continuous element. This also has the advantage of the total mass of the discrete system is at a minimum and, therefore, the least constrained position represents a design optimum.

5. If the whole structure is considered then a single discrete system will dynamically 'tune' the whole of the structure. Unfortunately, intermediate frequencies are generated which can be directly attributed to the individual spring/mass elements.

These intermediate frequencies have significant effect upon the quality of the dynamic similarity.

6. When two point coordinate similarity is considered, then it is impossible to achieve an acceptable level of dynamic similarity due to the transfer frequency response function of the intermediate frequencies.

7. From these observations it is possible to deduce that the mass and stiffness distribution of the continuous element must be as close as possible to that of the original structure. A discrete system should then be used to provide a small 'tuning' effect placed at the position of least constraint on the continuous element. If the total mass of the discrete system is very small then the intermediate resonances caused by the individual spring/mass elements should be minimal.

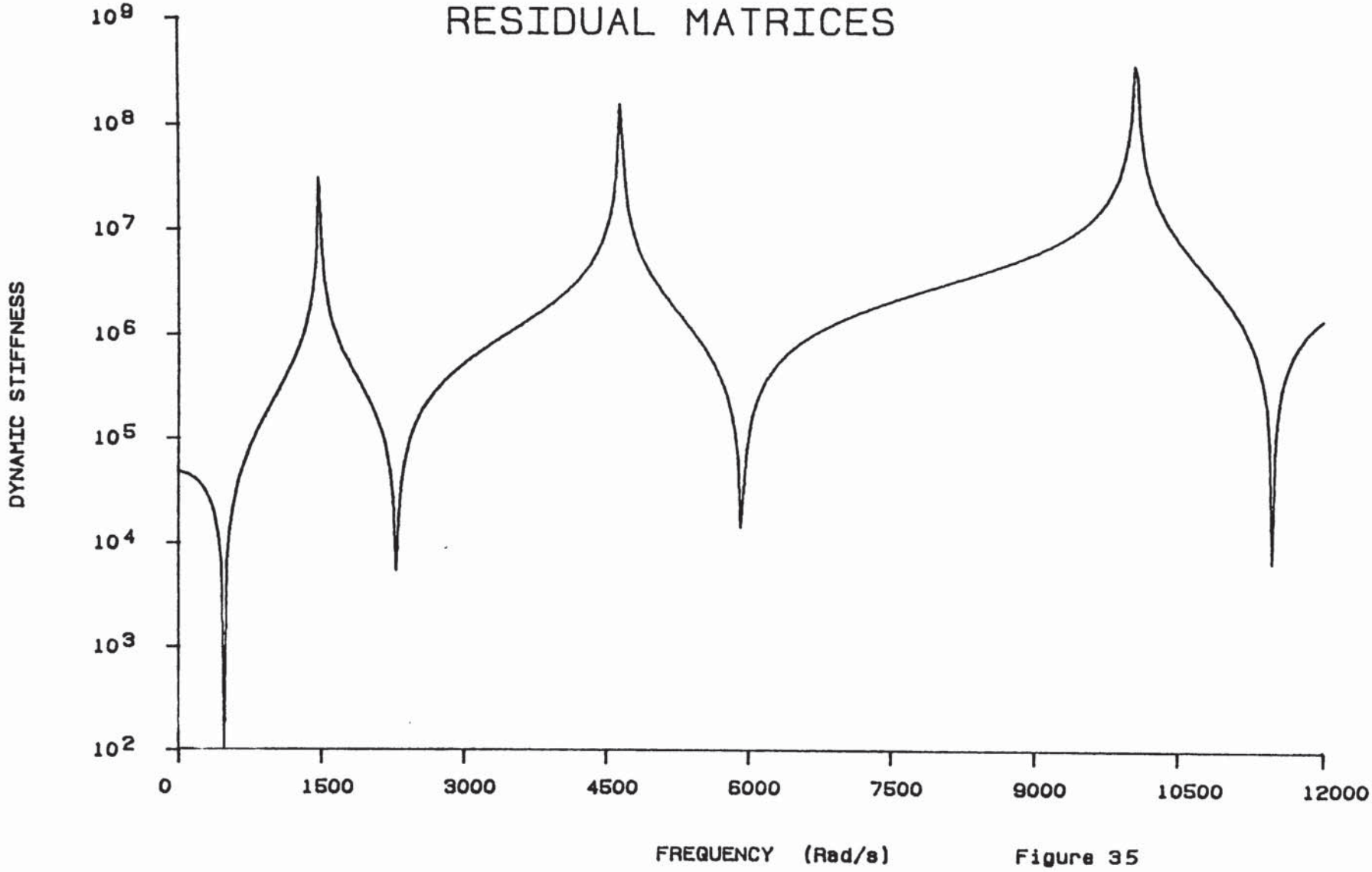
RESIDUAL MATRICES
DYNAMIC STIFFNESS
10^9
10^8
10^7
10^6
10^5
10^4
10^3
10^2
0
1500
3000
4500
6000
7500
9000
10500
12000
FREQUENCY (Rad/s)

Figure 35

SUBSTITUTE STRUCTURE

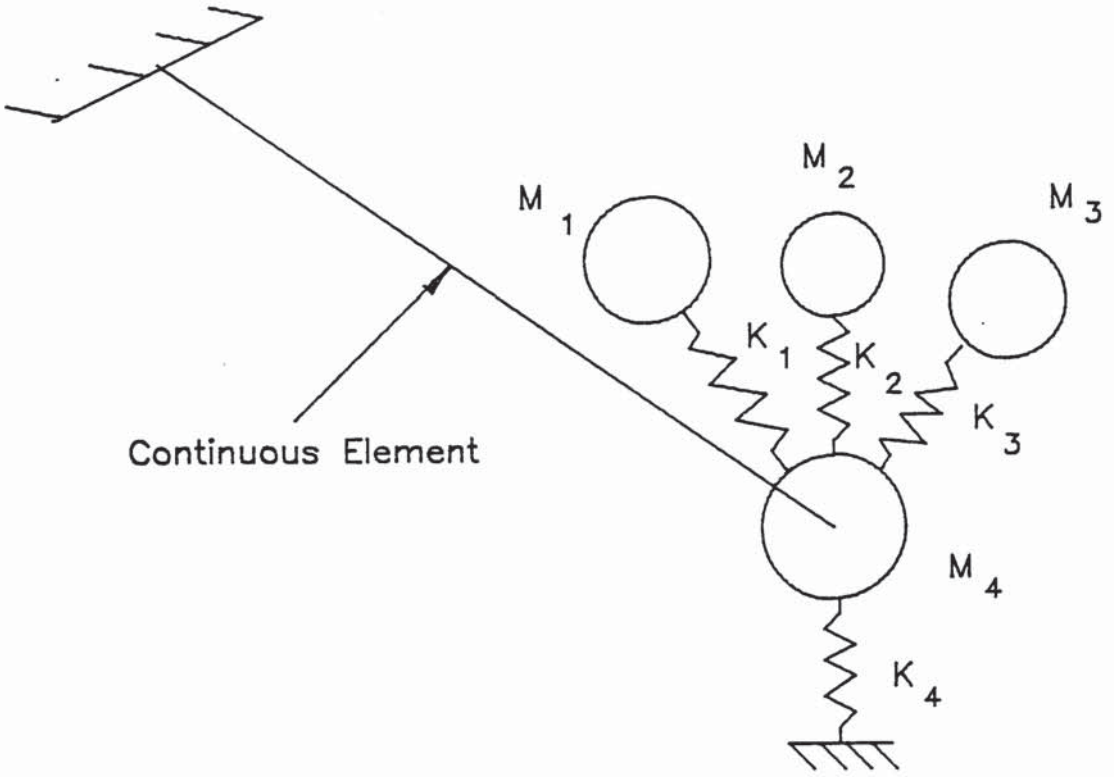

Figure 36

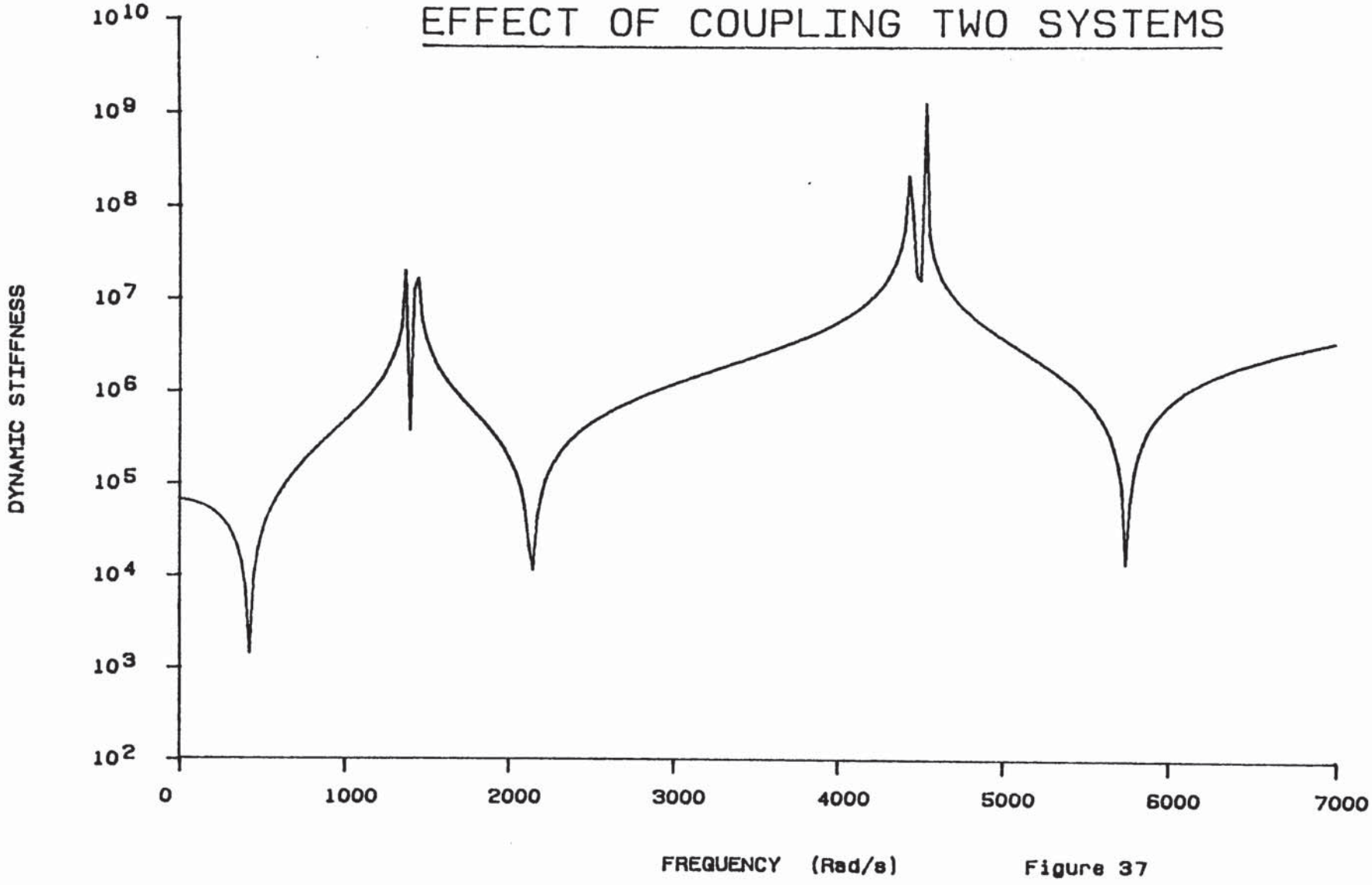
EFFECT OF COUPLING TWO SYSTEMS
DYNAMIC STIFFNESS
10^{10}
10^{9}
10^{8}
10^{7}
10^{6}
10^{5}
10^{4}
10^{3}
10^{2}
0
1000
2000
3000
4000
5000
6000
7000
FREQUENCY (Rad/s)

Figure 37

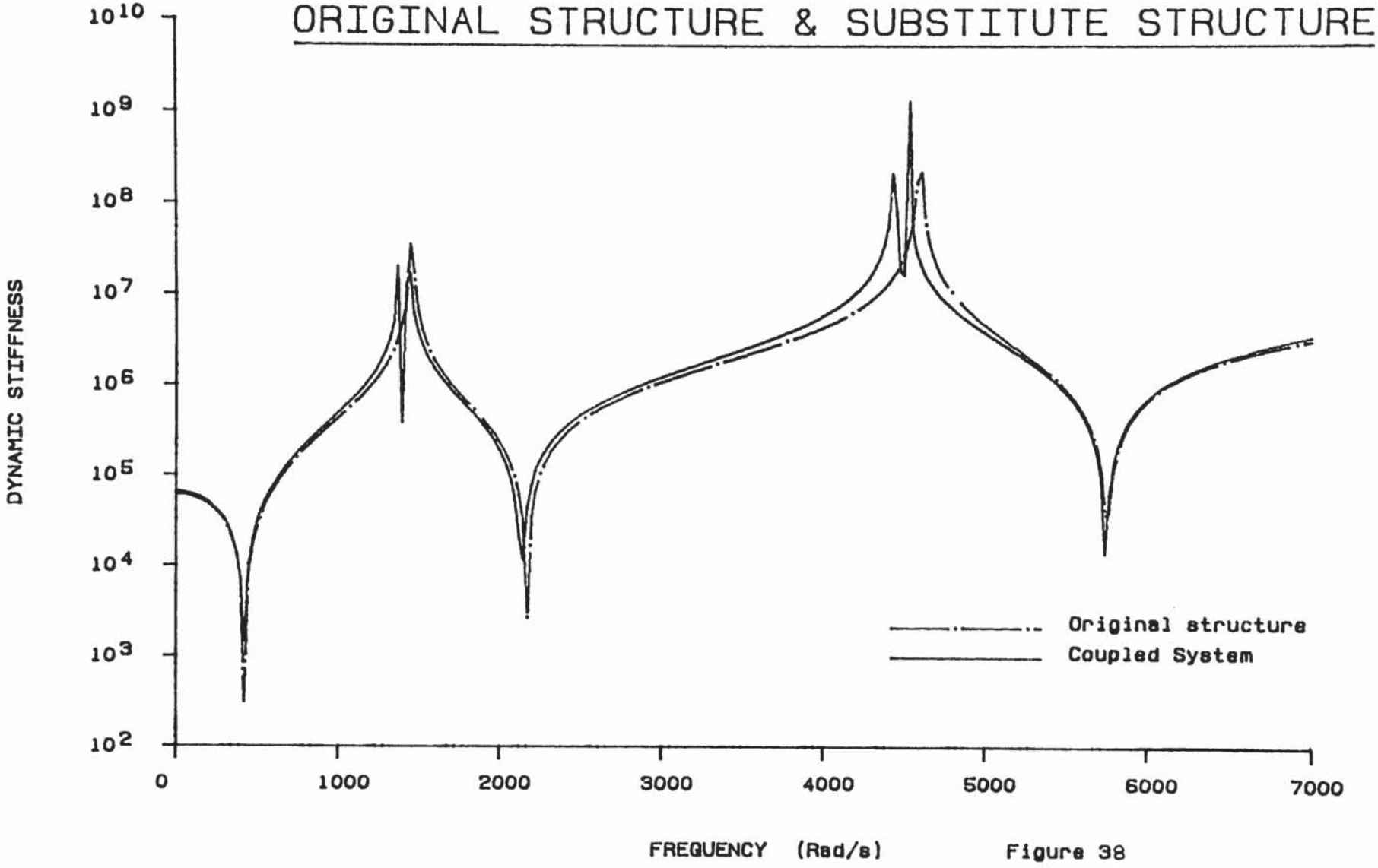
ORIGINAL STRUCTURE & SUBSTITUTE STRUCTURE
DYNAMIC STIFFNESS
10^{10}
10^{9}
10^{8}
10^{7}
10^{6}
10^{5}
10^{4}
10^{3}
10^{2}
0
1000
2000
3000
4000
5000
6000
7000
FREQUENCY (Rad/s)
Original structure
Coupled System

Figure 38

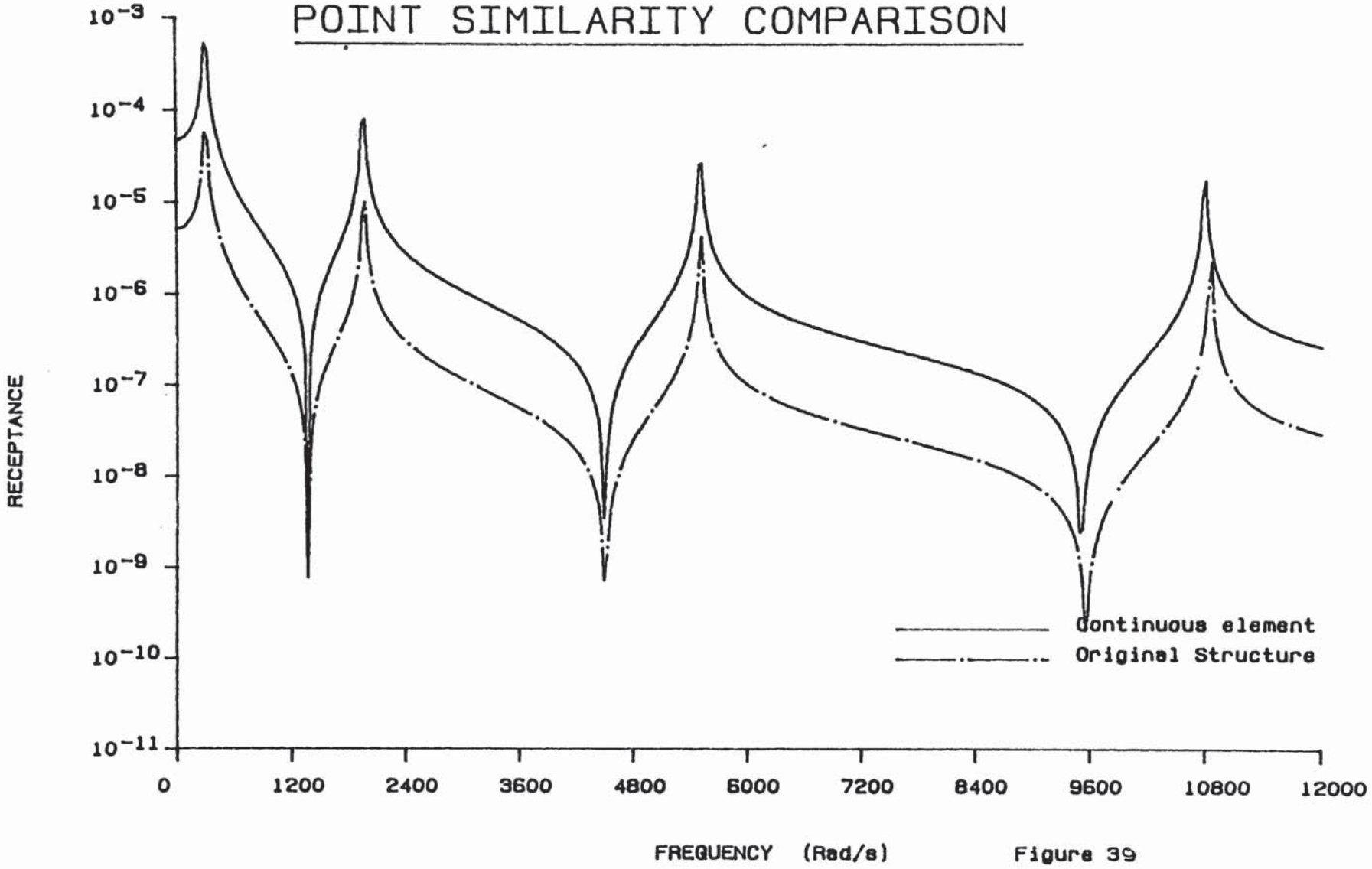
POINT SIMILARITY COMPARISON
RECEPTANCE
10-3
10-4
10-5
10-6
10-7
10-8
10-9
10-10
10-11
0
1200
2400
3600
4800
6000
7200
8400
9600
10800
12000
FREQUENCY (Rad/s)
Continuous element
Original Structure

Figure 39

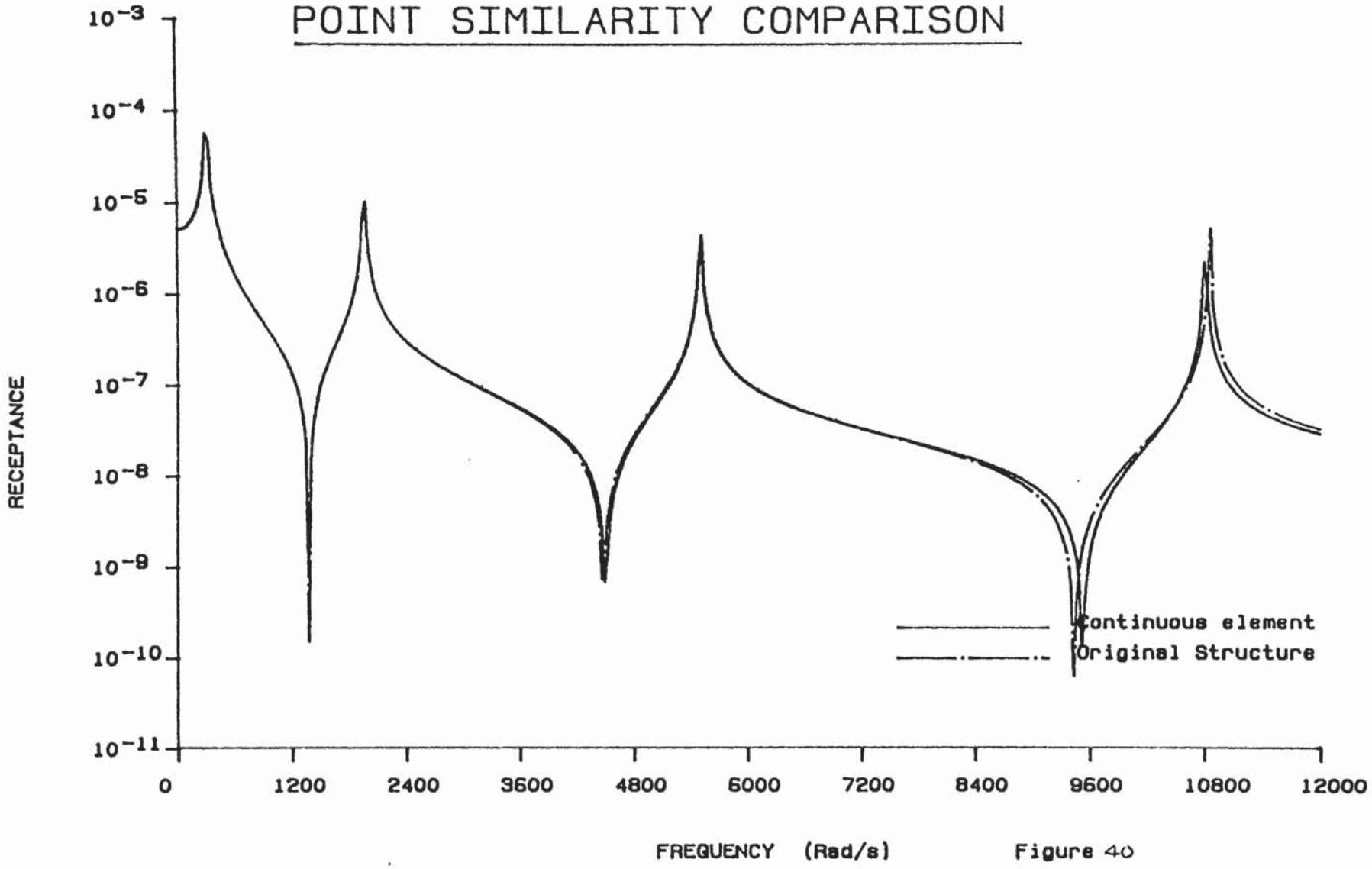
POINT SIMILARITY COMPARISON
RECEPTANCE
10-3
10-4
10-5
10-6
10-7
10-8
10-9
10-10
10-11
0
1200
2400
3600
4800
6000
7200
8400
9600
10800
12000
FREQUENCY (Rad/s)
Continuous element
Original Structure

Figure 40

Physical substitute structure

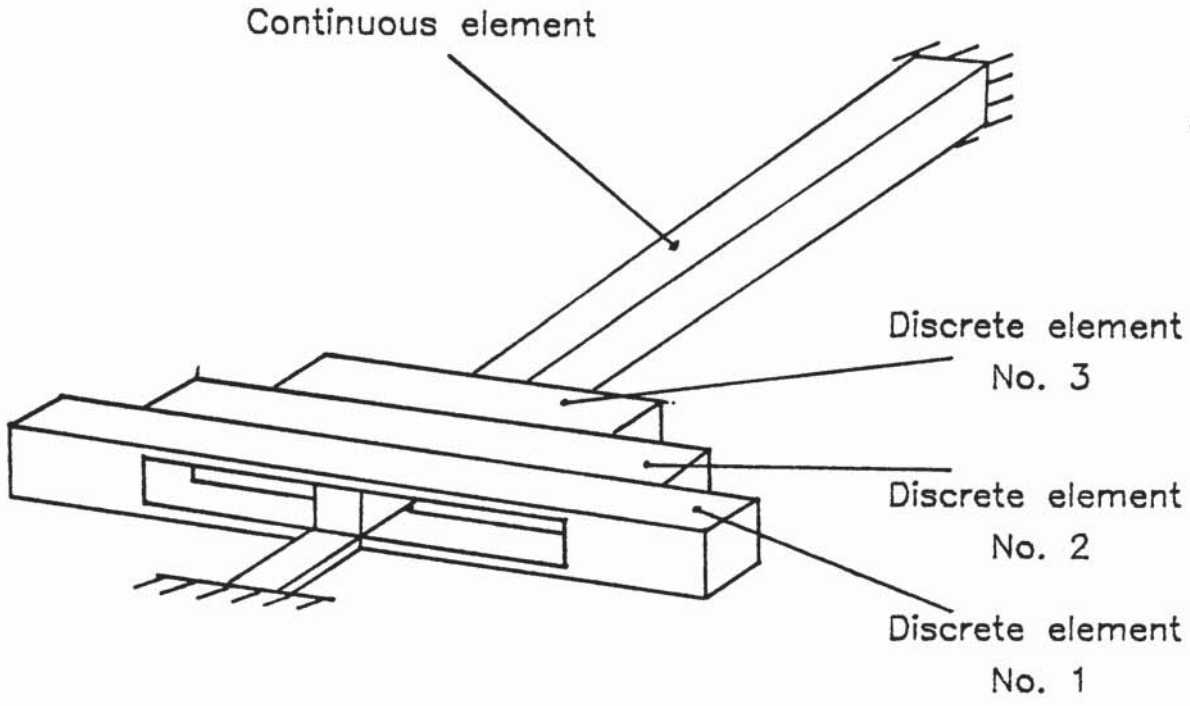

Figure 42

Original structure; Experimental data

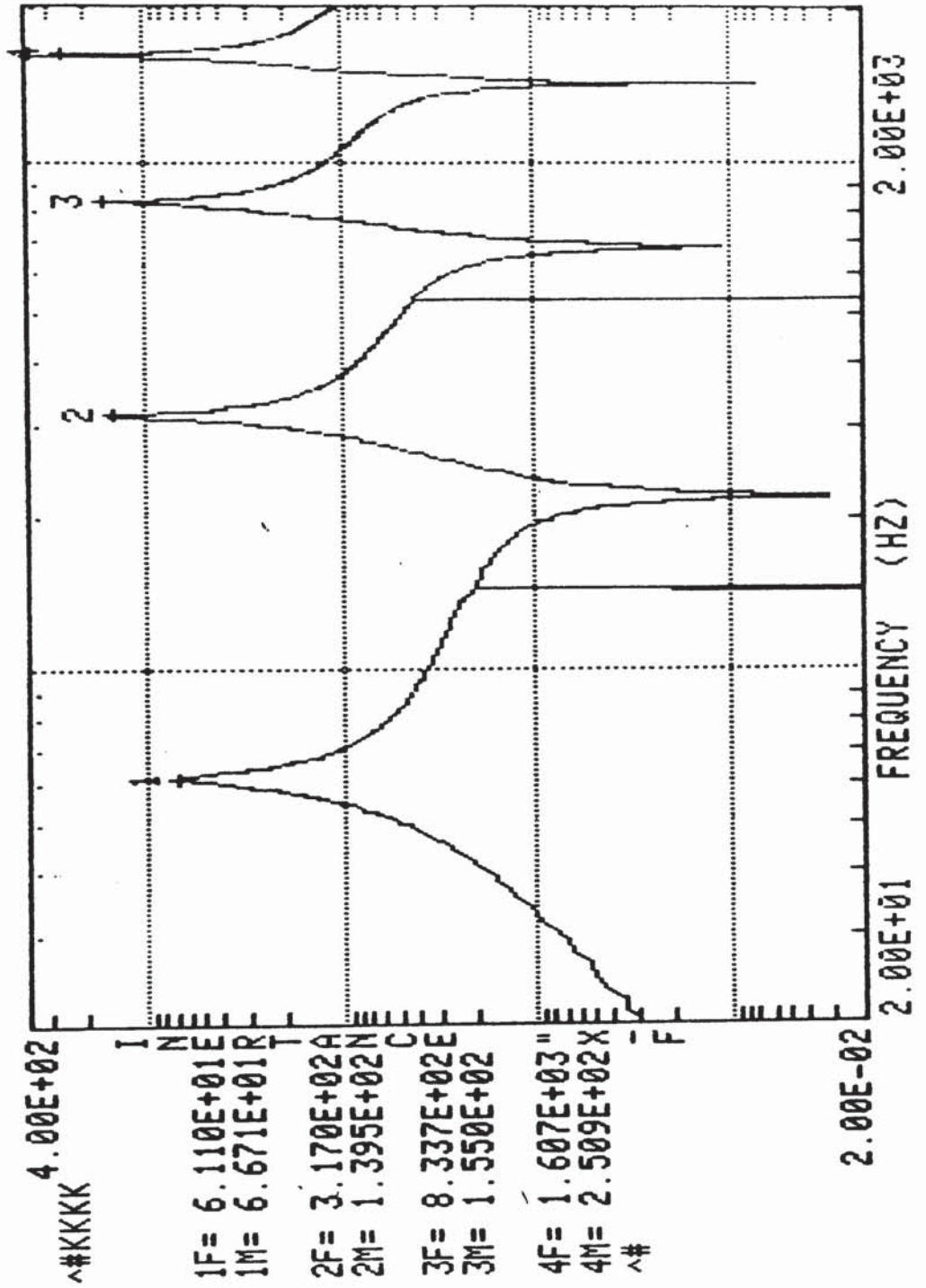

Figure 43

Substitute structure; Experimental data

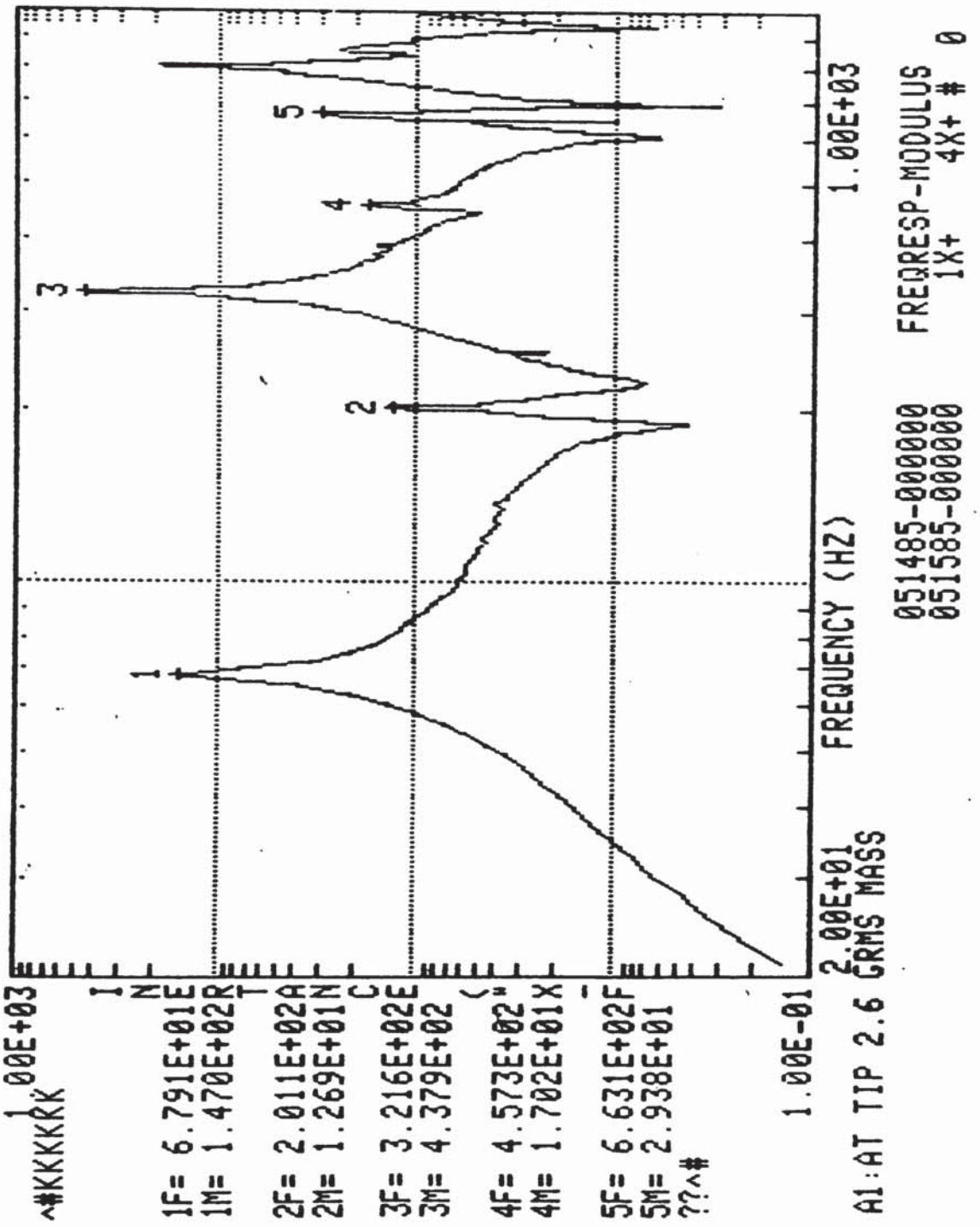

Figure 44

Comparison of Physical structures

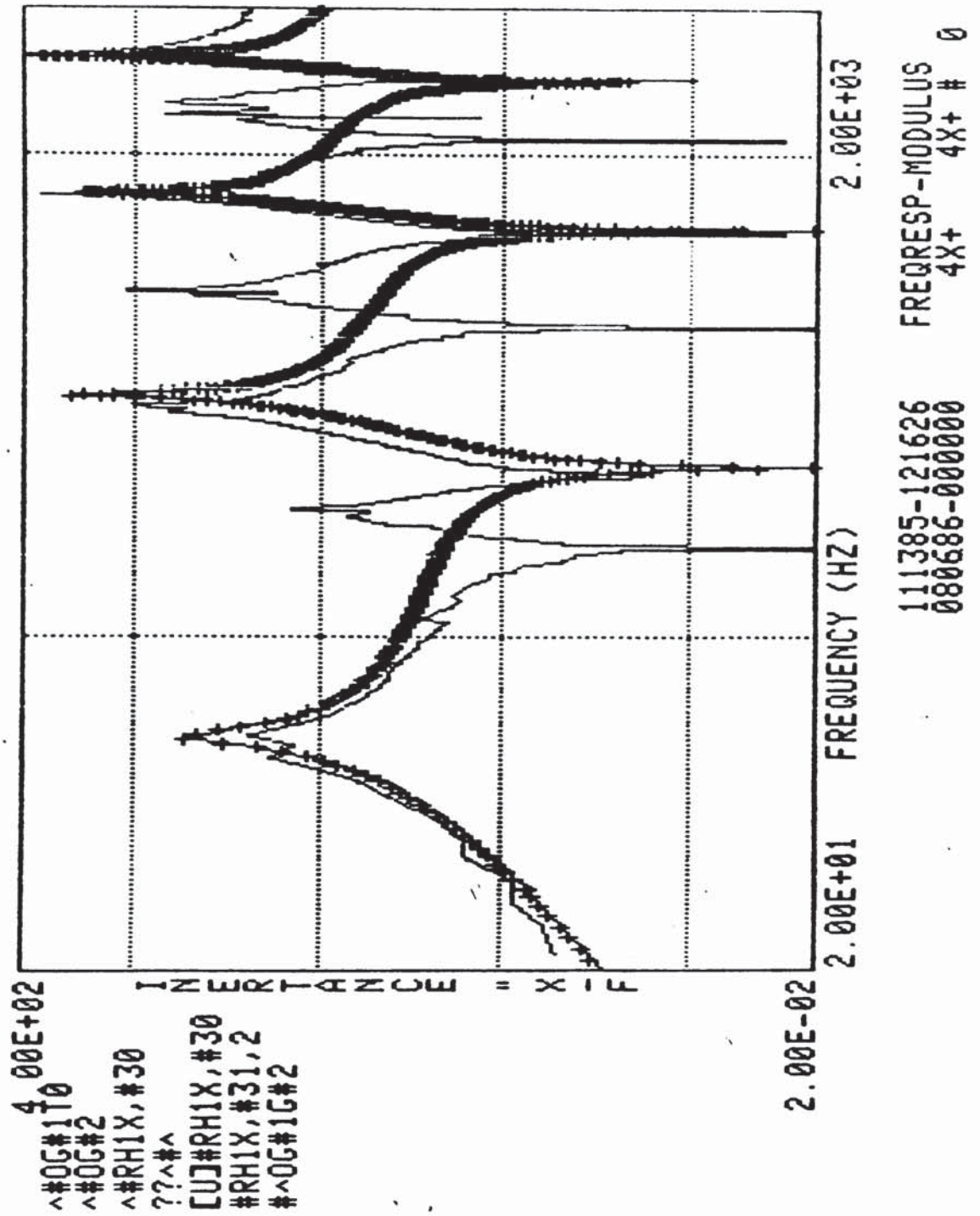

+ + + Tapered cantilever

——— Substitute structure

Figure 45

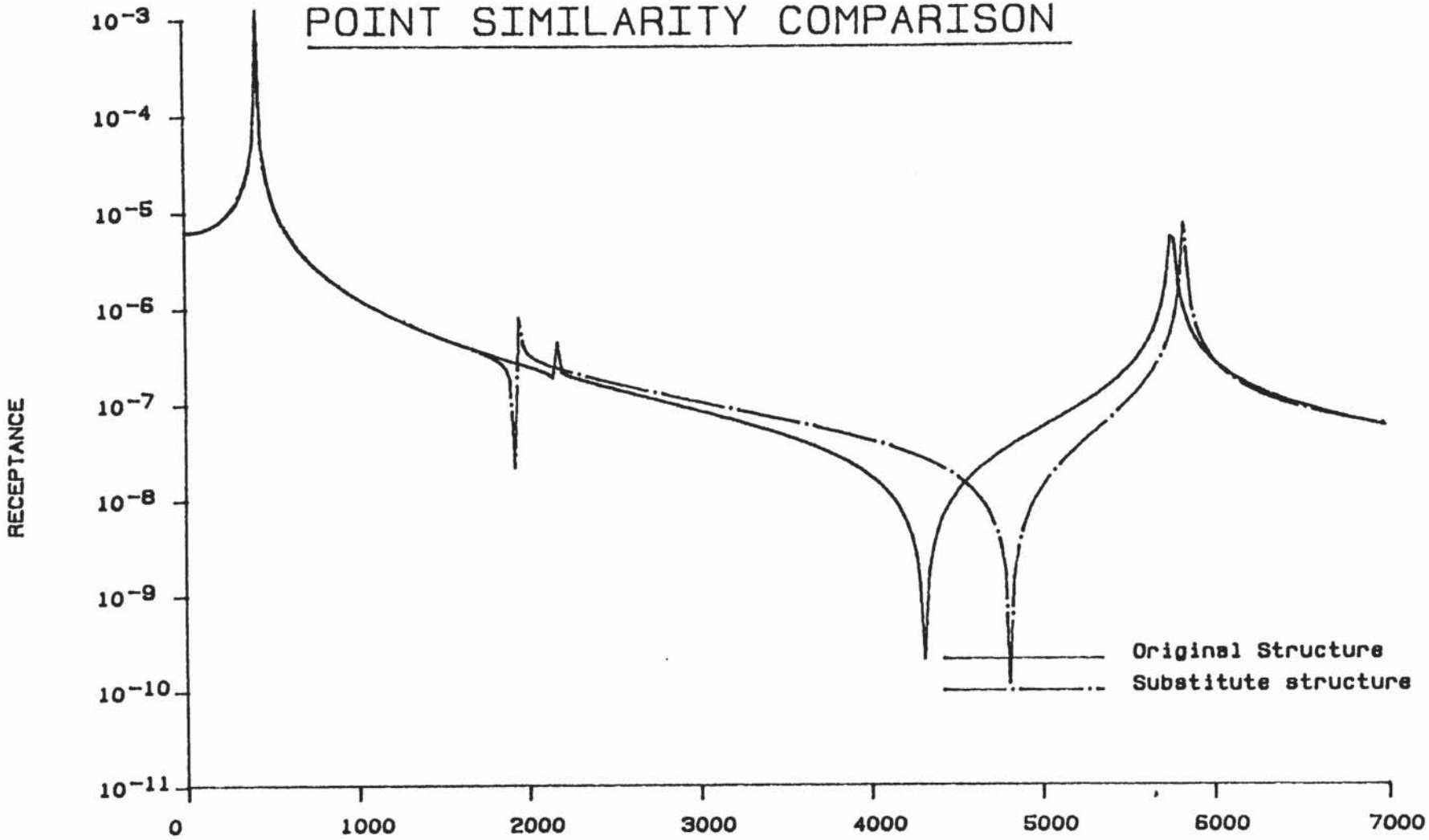
POINT SIMILARITY COMPARISON
RECEPTANCE
10^-3
10^-4
10^-5
10^-6
10^-7
10^-8
10^-9
10^-10
10^-11
0
1000
2000
3000
4000
5000
6000
7000
FREQUENCY (Rad/s)
Original Structure
Substitute structure

Figure 46

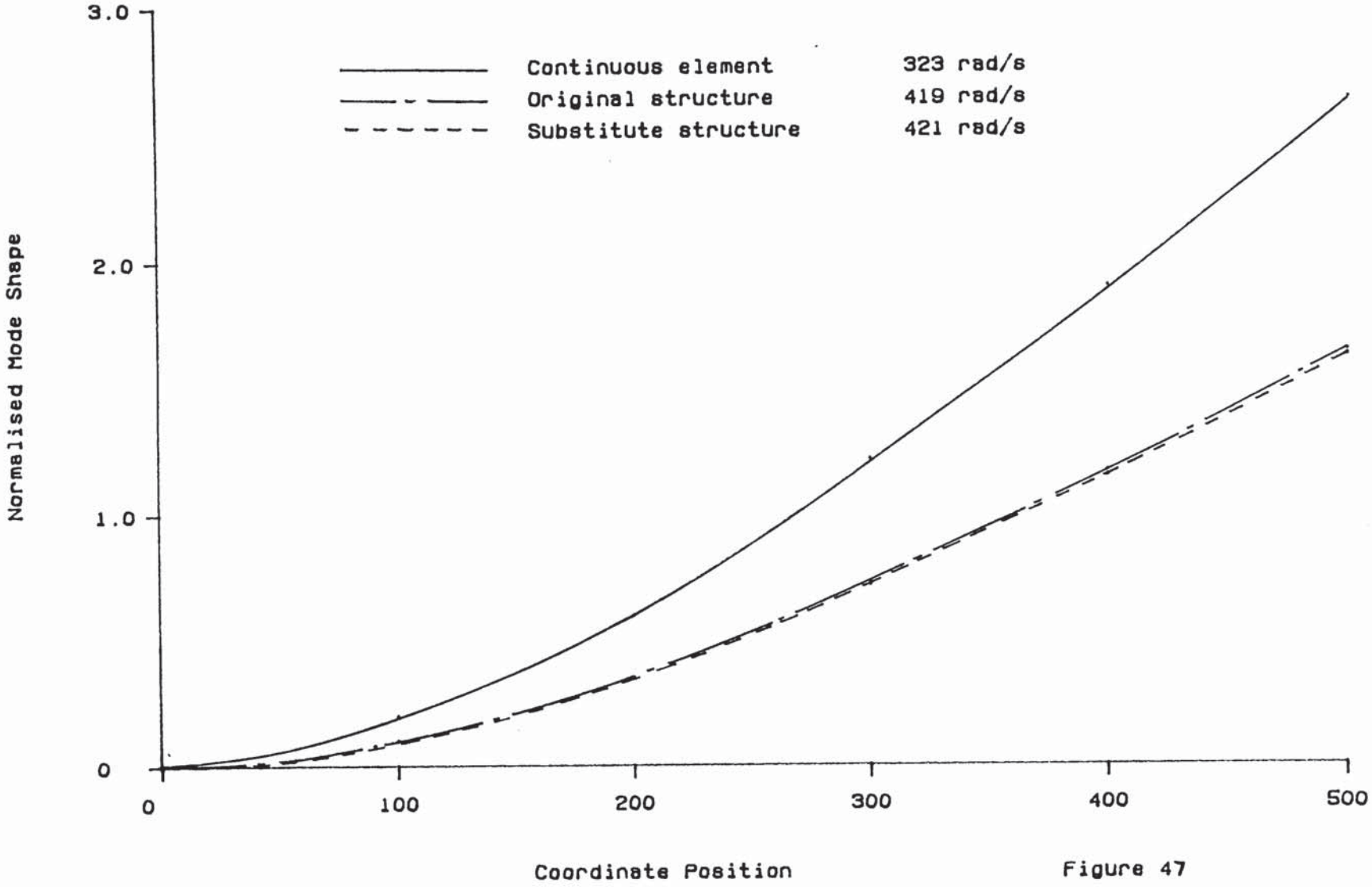

Discrete System at 375 mm

Figure 47

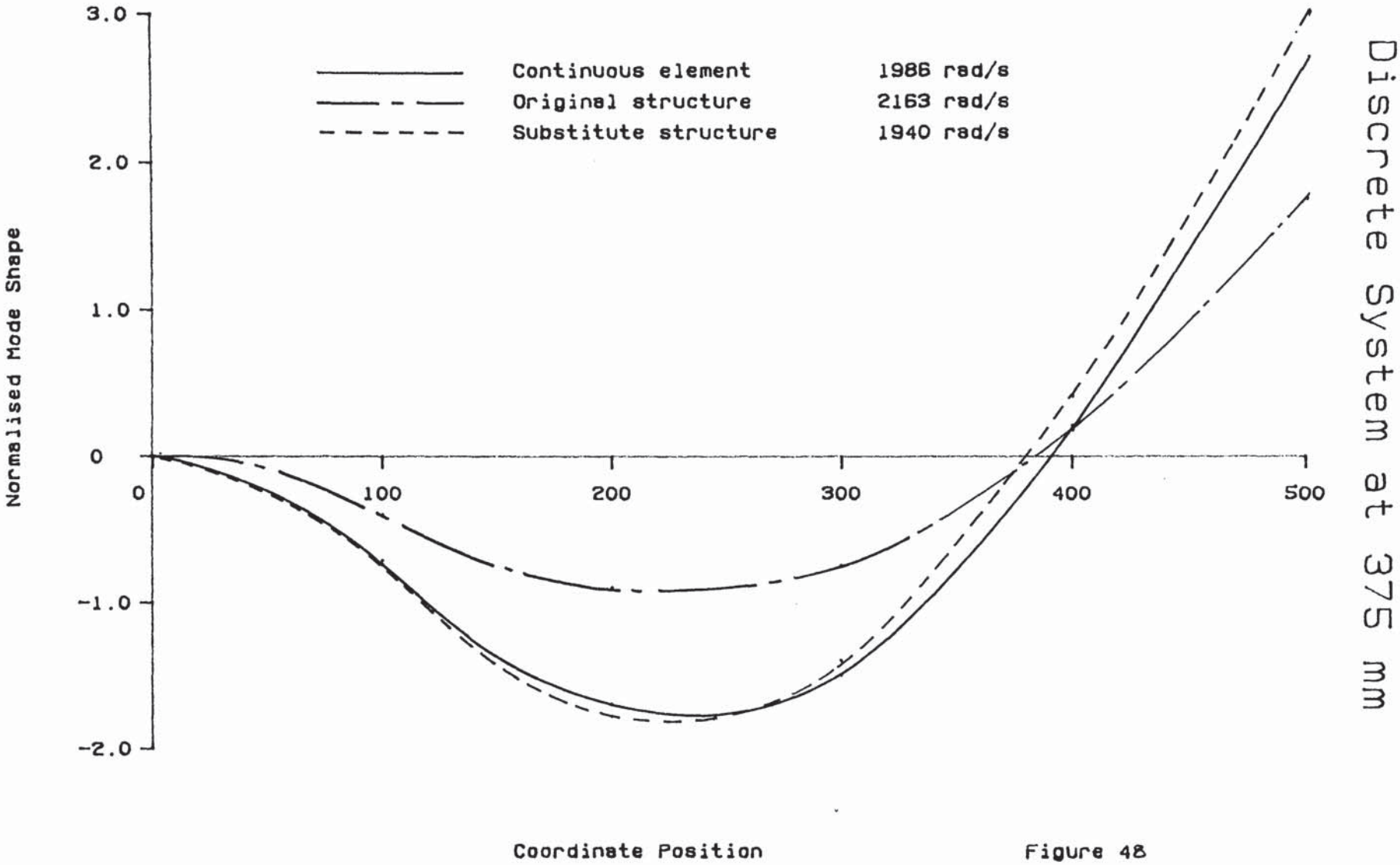
Discrete System at 375 mm
Continuous element 1986 rad/s
Original structure 2163 rad/s
Substitute structure 1940 rad/s
Normalised Mode Shape
3.0
2.0
1.0
0
-1.0
-2.0
0
100
200
300
400
500
Coordinate Position

Figure 48

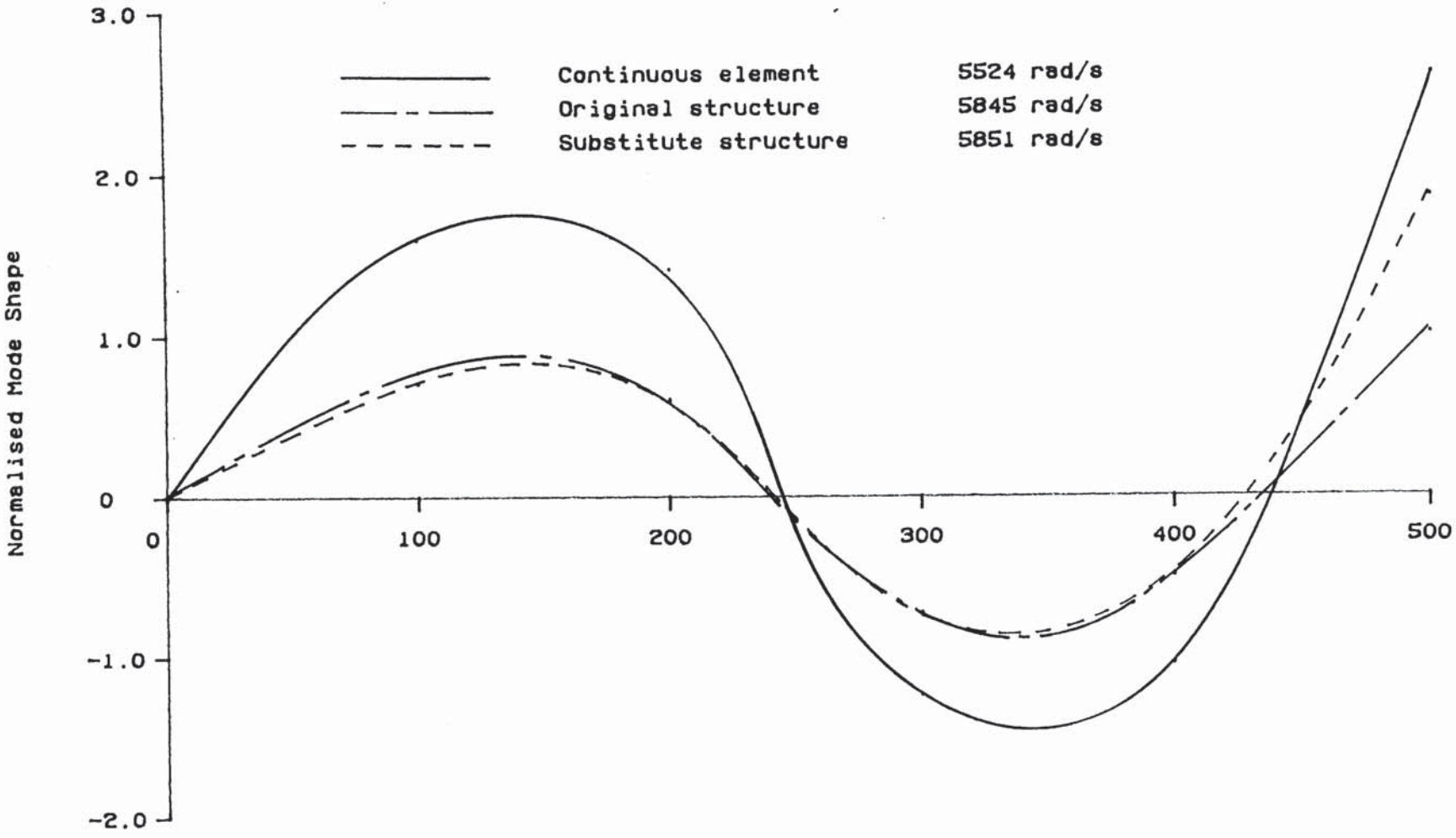
Discrete System at 375 mm
Continuous element 5524 rad/s
Original structure 5845 rad/s
Substitute structure 5851 rad/s
Normalised Mode Shape
3.0
2.0
1.0
0
-1.0
-2.0
0
100
200
300
400
500
Coordinate Position

Figure 49

Discrete System at 250 mm
Continuous element 323 rad/s
Original structure 419 rad/s
Substitute structure 430 rad/s
Normalised Mode Shape
Coordinate Position
0
1.0
2.0
3.0
0
100
200
300
400
500

Figure 50

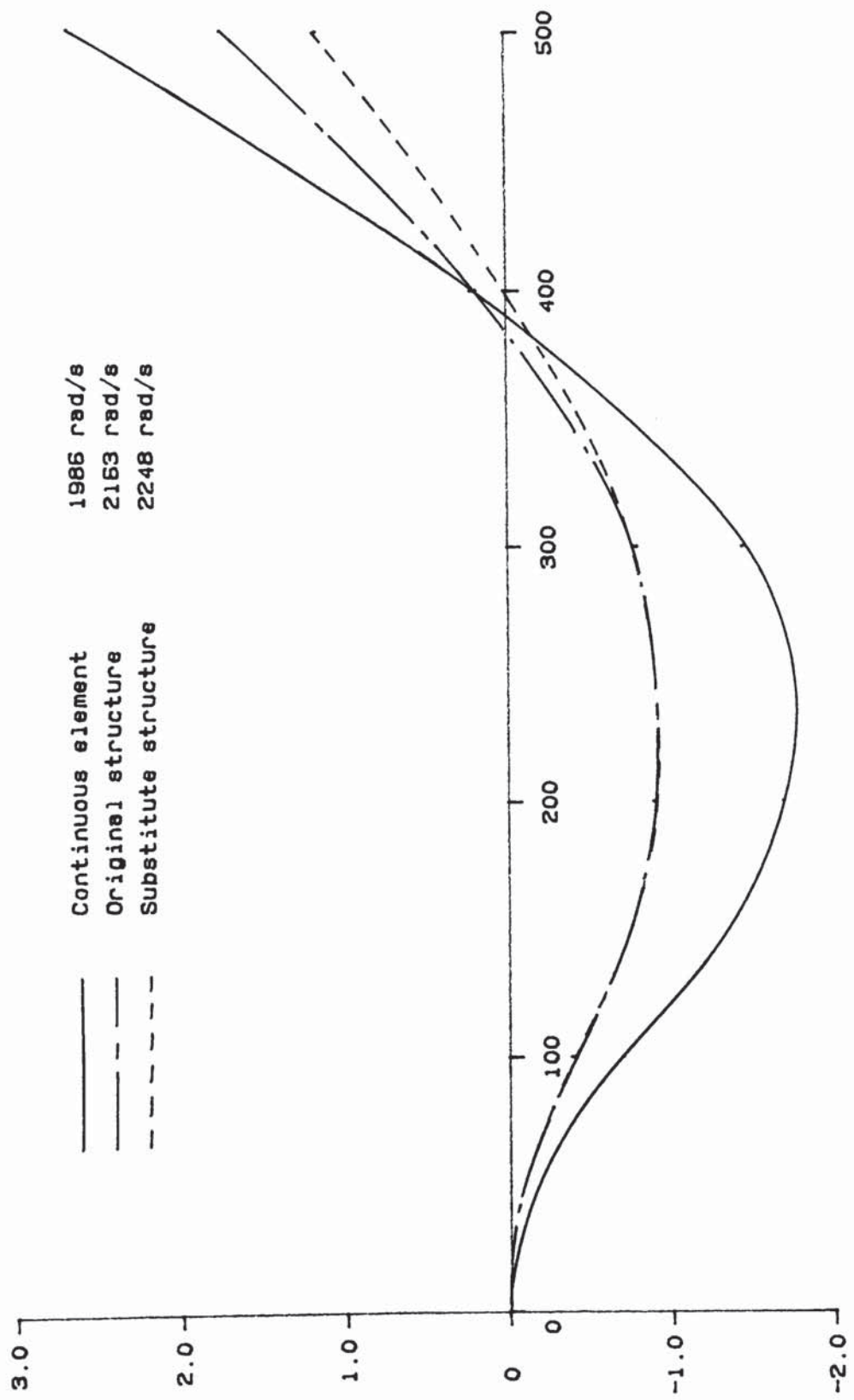
Discrete System at 250 mm
Continuous element 1986 rad/s
Original structure 2163 rad/s
Substitute structure 2248 rad/s
Normalised Mode Shape
Coordinate Position
3.0
2.0
1.0
0
-1.0
-2.0
0
100
200
300
400
500

Figure 51

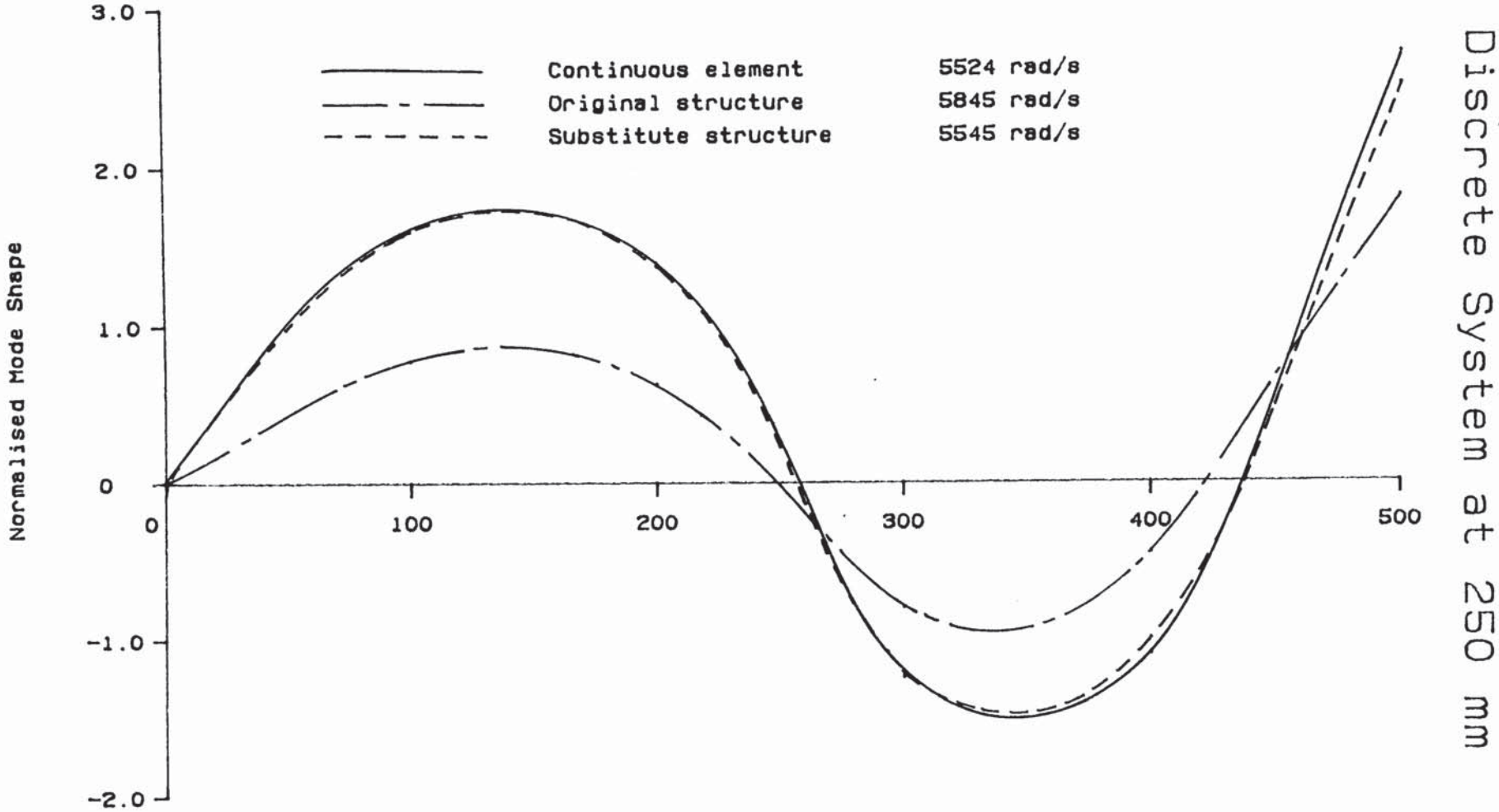
Discrete System at 250 mm
Continuous element 5524 rad/s
Original structure 5845 rad/s
Substitute structure 5545 rad/s
Normalised Mode Shape
Coordinate Position
3.0
2.0
1.0
0
-1.0
-2.0
0
100
200
300
400
500

Figure 52

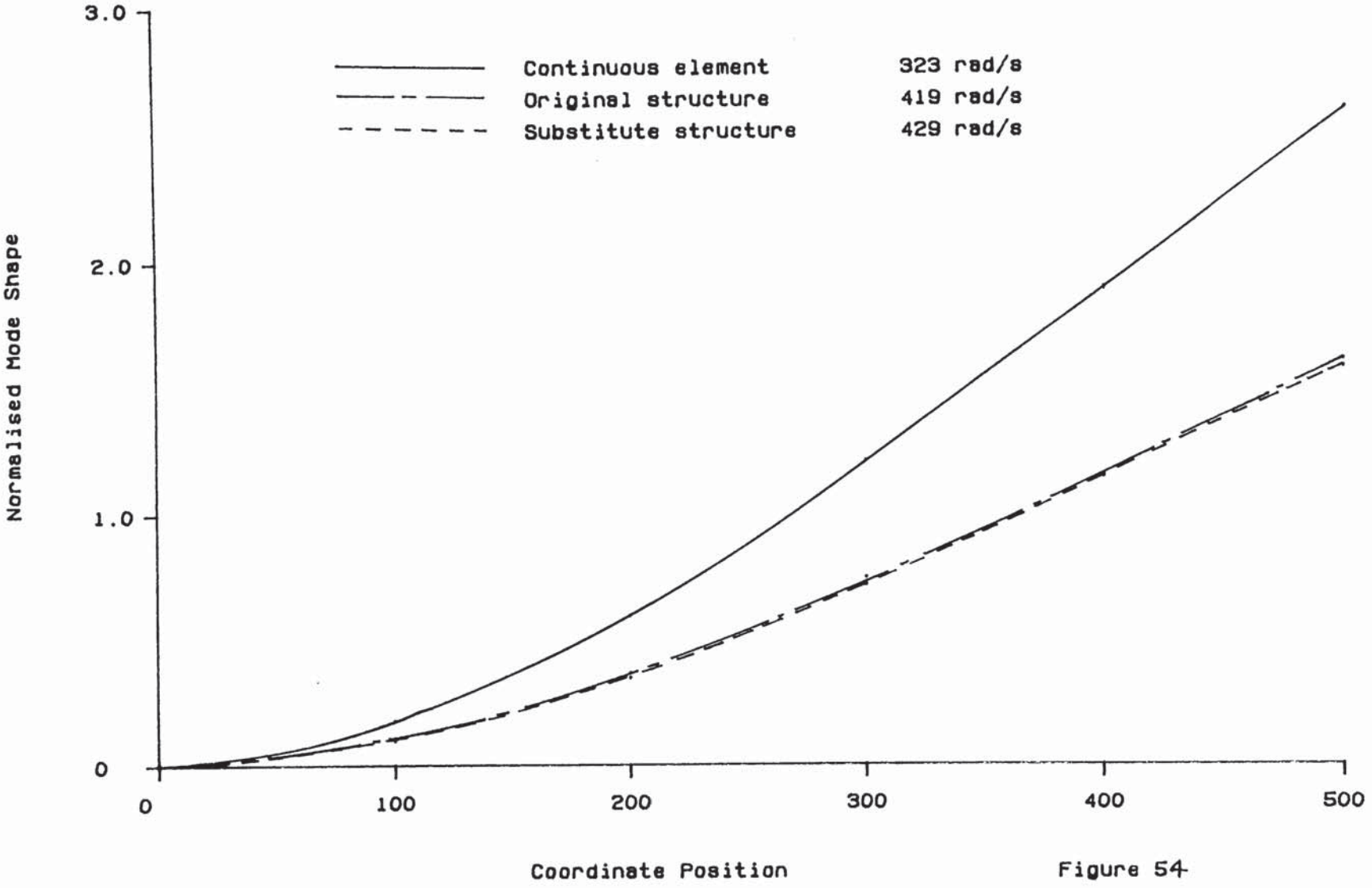
Discrete System at 500 mm
Continuous element 323 rad/s
Original structure 419 rad/s
Substitute structure 429 rad/s
Normalised Mode Shape
3.0
2.0
1.0
0
0
100
200
300
400
500
Coordinate Position

Figure 54

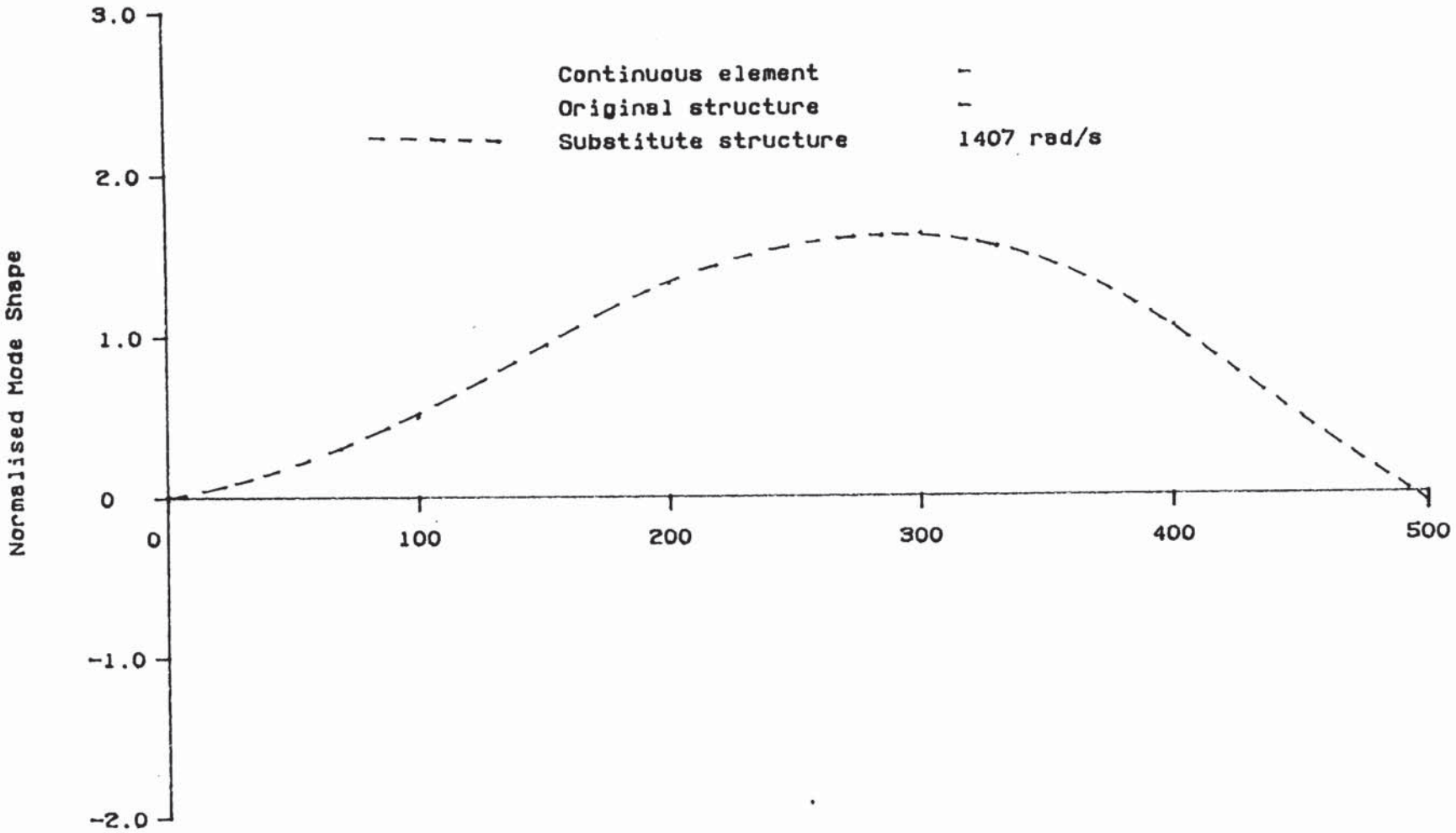

Discrete System at 500 mm

Figure 55

Discrete System at 500 mm
Continuous element 1986 rad/s
Original structure 2163 rad/s
Substitute structure 2137 rad/s
Normalised Mode Shape
Coordinate Position
3.0
2.0
1.0
0
-1.0
-2.0
0
100
200
300
400
500

Figure 56

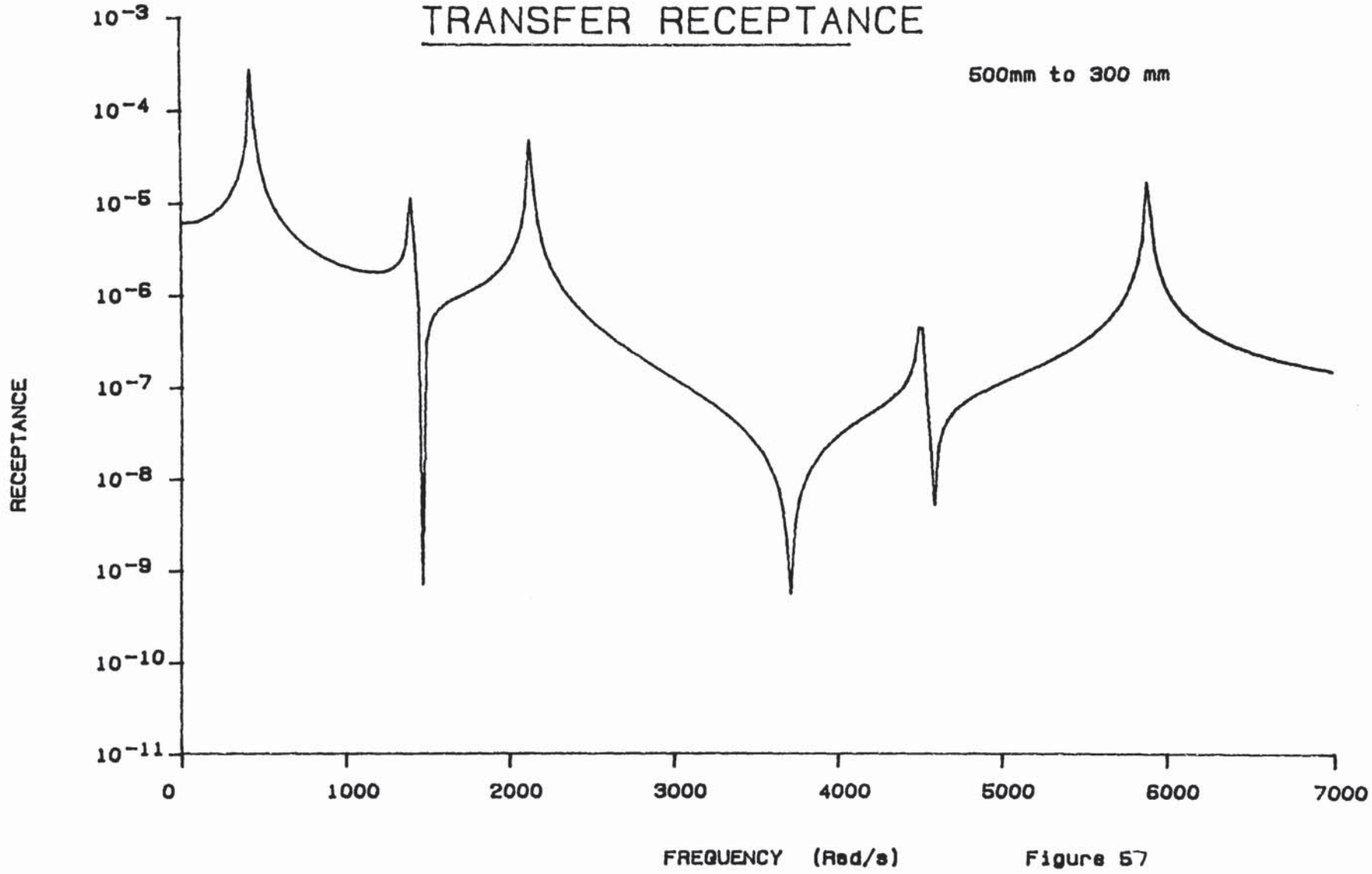
TRANSFER RECEPTANCE
500mm to 300 mm
RECEPTANCE
10-3
10-4
10-5
10-6
10-7
10-8
10-9
10-10
10-11
0
1000
2000
3000
4000
5000
6000
7000
FREQUENCY (Rad/s)

Figure 57

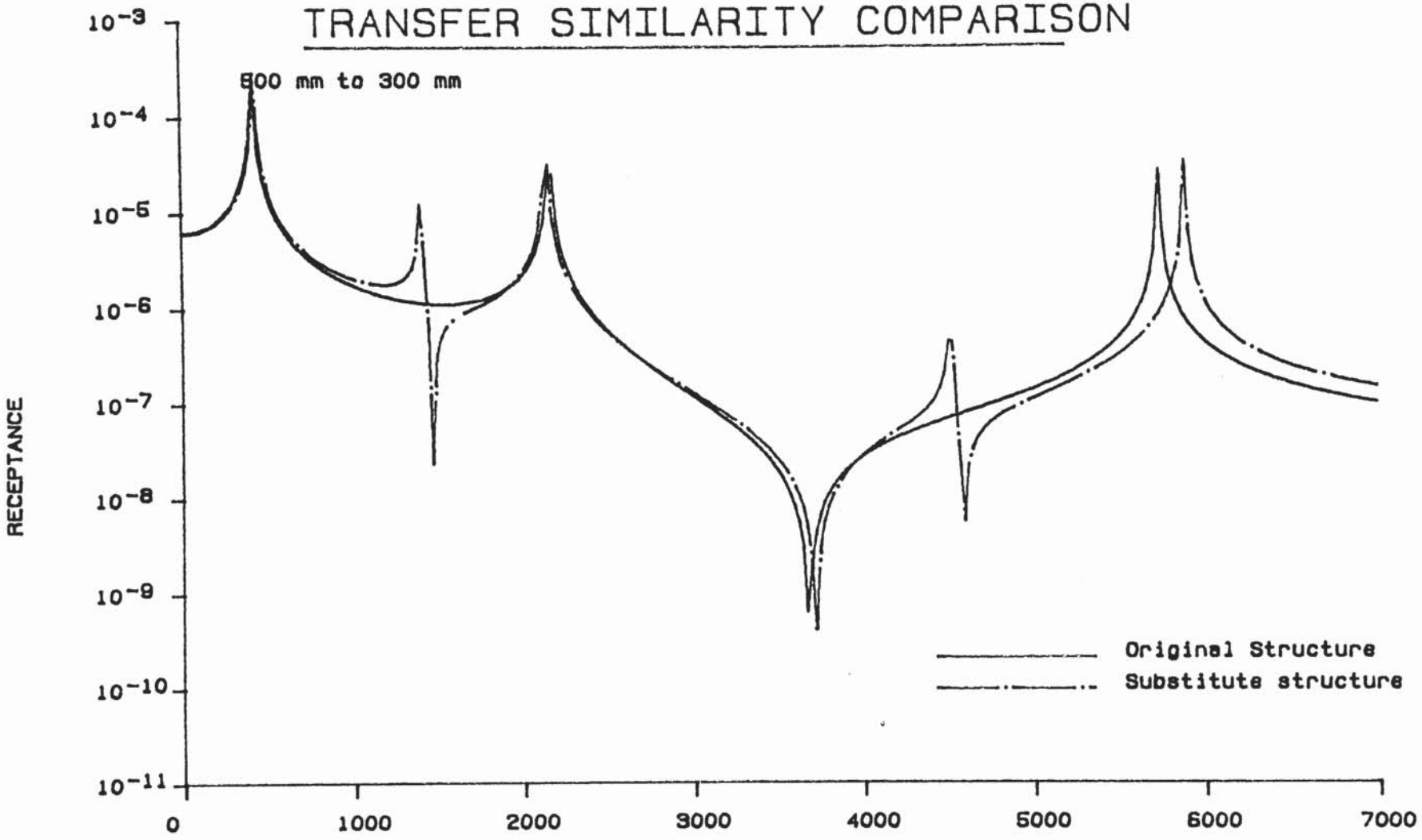
TRANSFER SIMILARITY COMPARISON
600 mm to 300 mm
RECEPTANCE
10-3
10-4
10-5
10-6
10-7
10-8
10-9
10-10
10-11
0
1000
2000
3000
4000
5000
6000
7000
FREQUENCY (Rad/s)
Original Structure
Substitute structure

Figure 58

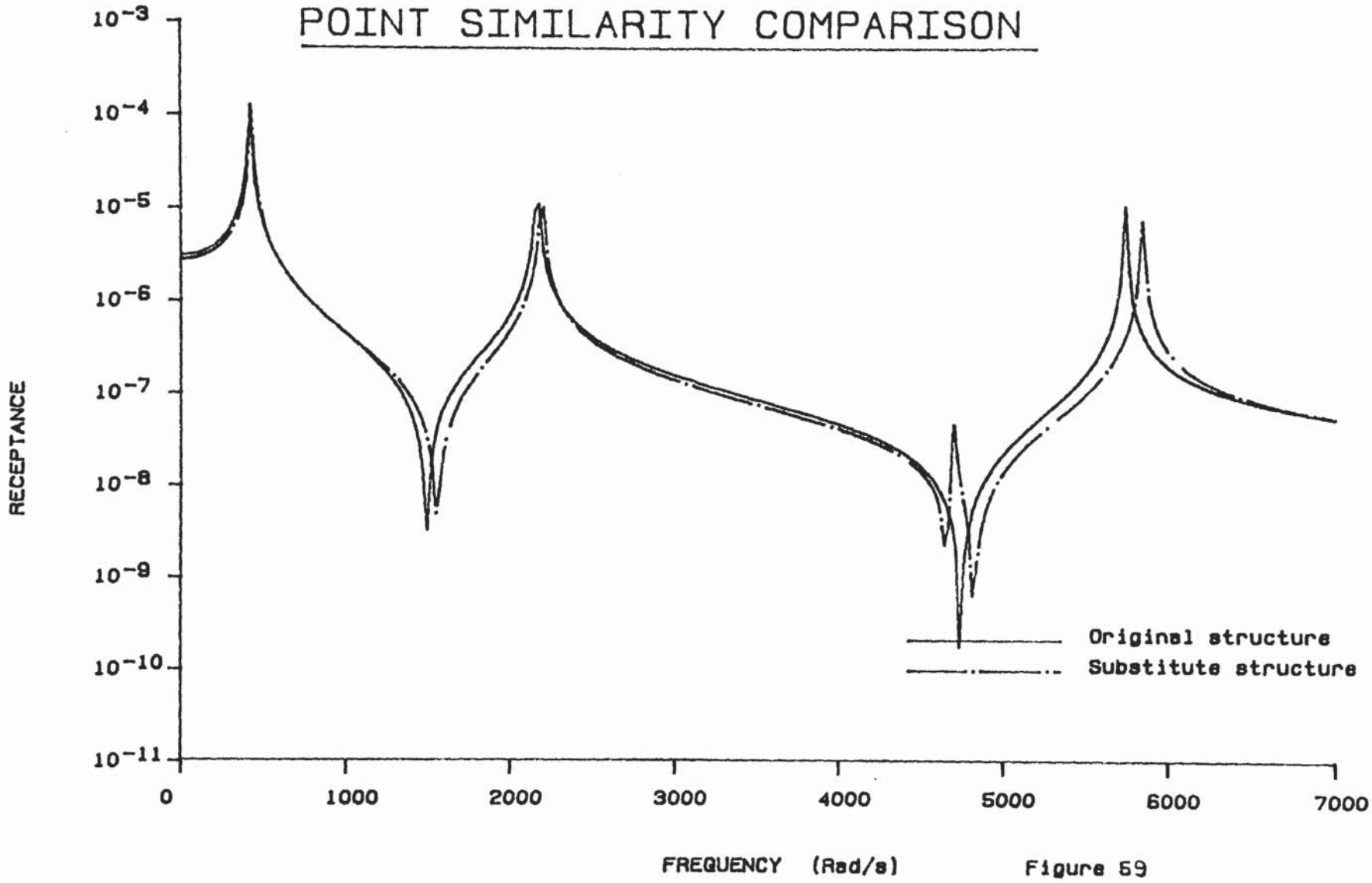
POINT SIMILARITY COMPARISON
RECEPTANCE
10-3
10-4
10-5
10-6
10-7
10-8
10-9
10-10
10-11
0
1000
2000
3000
4000
5000
6000
7000
FREQUENCY (Rad/s)
Original structure
Substitute structure

Figure 59

Discrete System at 300 mm
Continuous element 323 rad/s
Original structure 419 rad/s
Substitute structure 429 rad/s
Normalised Mode Shape
3.0
2.0
1.0
0
0
100
200
300
400
500
Coordinate Position

Figure 60

Discrete System at 300 mm
Continuous element
Original structure
Substitute structure
1312 rad/s
Normalised Mode Shape
3.0
2.0
1.0
0
-1.0
-2.0
0
100
200
300
400
500
Coordinate Position

Figure 61

Discrete System at 300 mm
Continuous element 1986 rad/s
Original structure 2163 rad/s
Substitute structure 2190 rad/s
Normalised Mode Shape
Coordinate Position
3.0
2.0
1.0
0
-1.0
-2.0
100
200
300
400
500

Figure 62

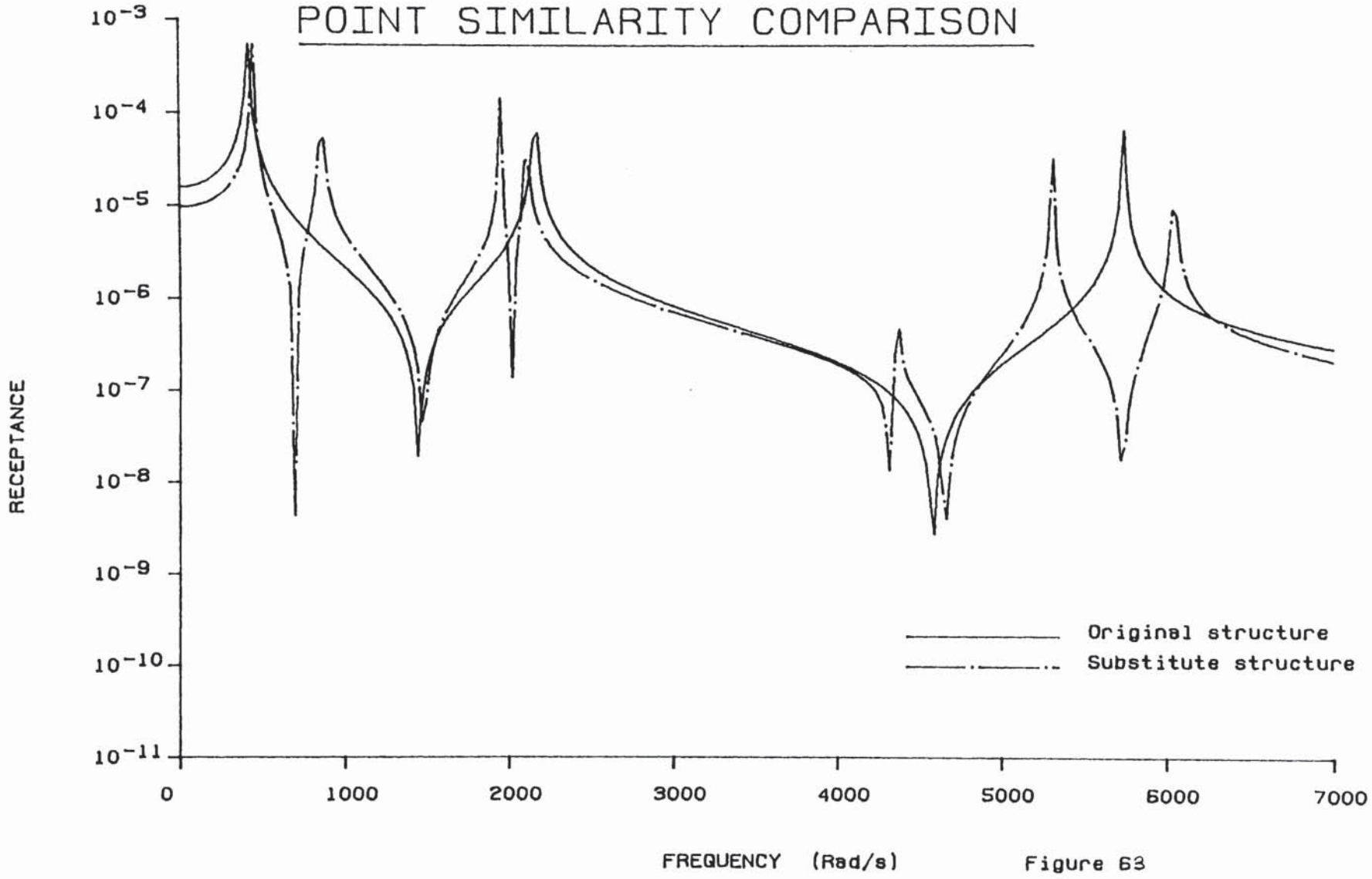
POINT SIMILARITY COMPARISON
RECEPTANCE
10-3
10-4
10-5
10-6
10-7
10-8
10-9
10-10
10-11
0
1000
2000
3000
4000
5000
6000
7000
FREQUENCY (Rad/s)
Original structure
Substitute structure

Figure 63

Original structure; Experimental data

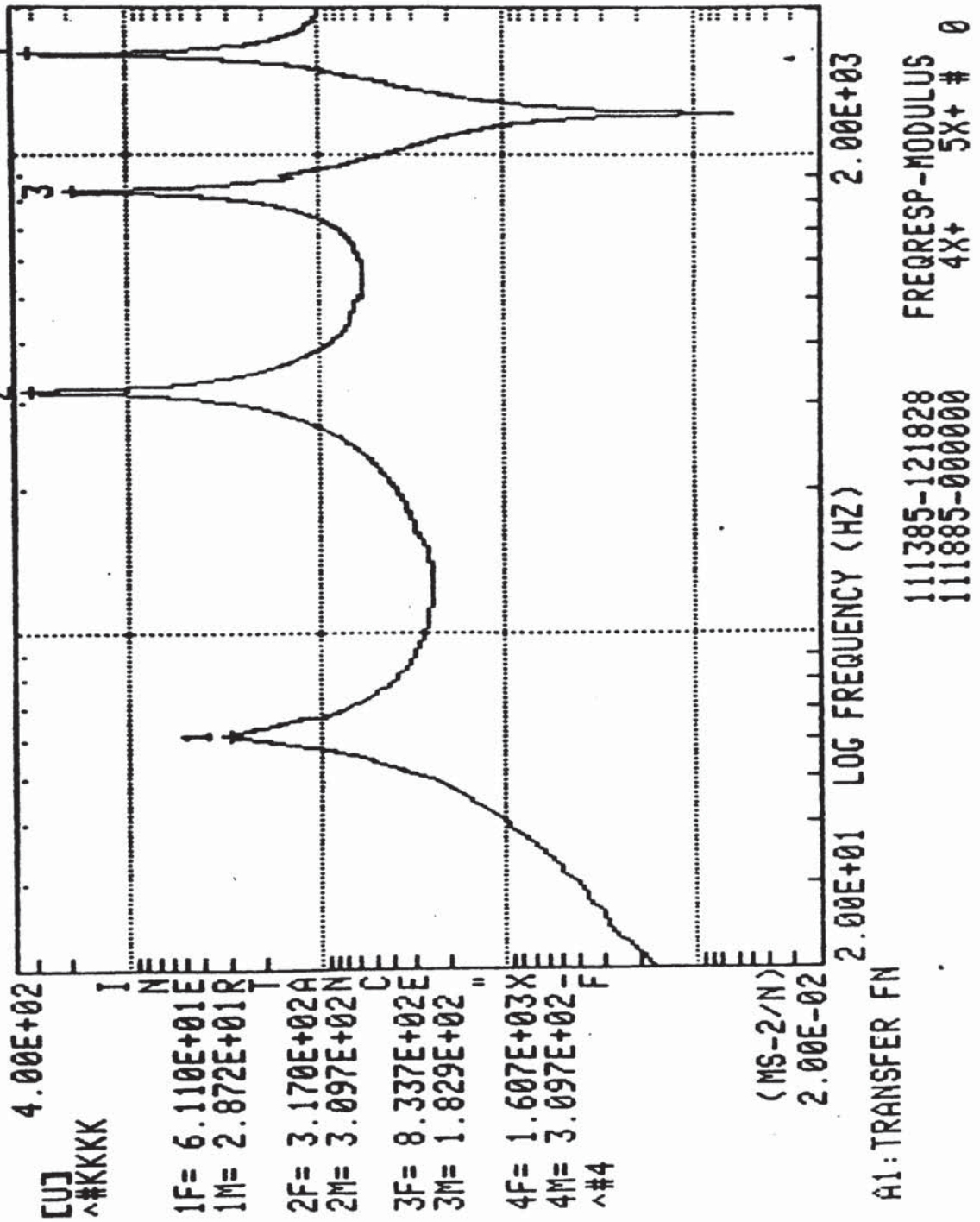

Figure 64

Substitute structure; Experimental data

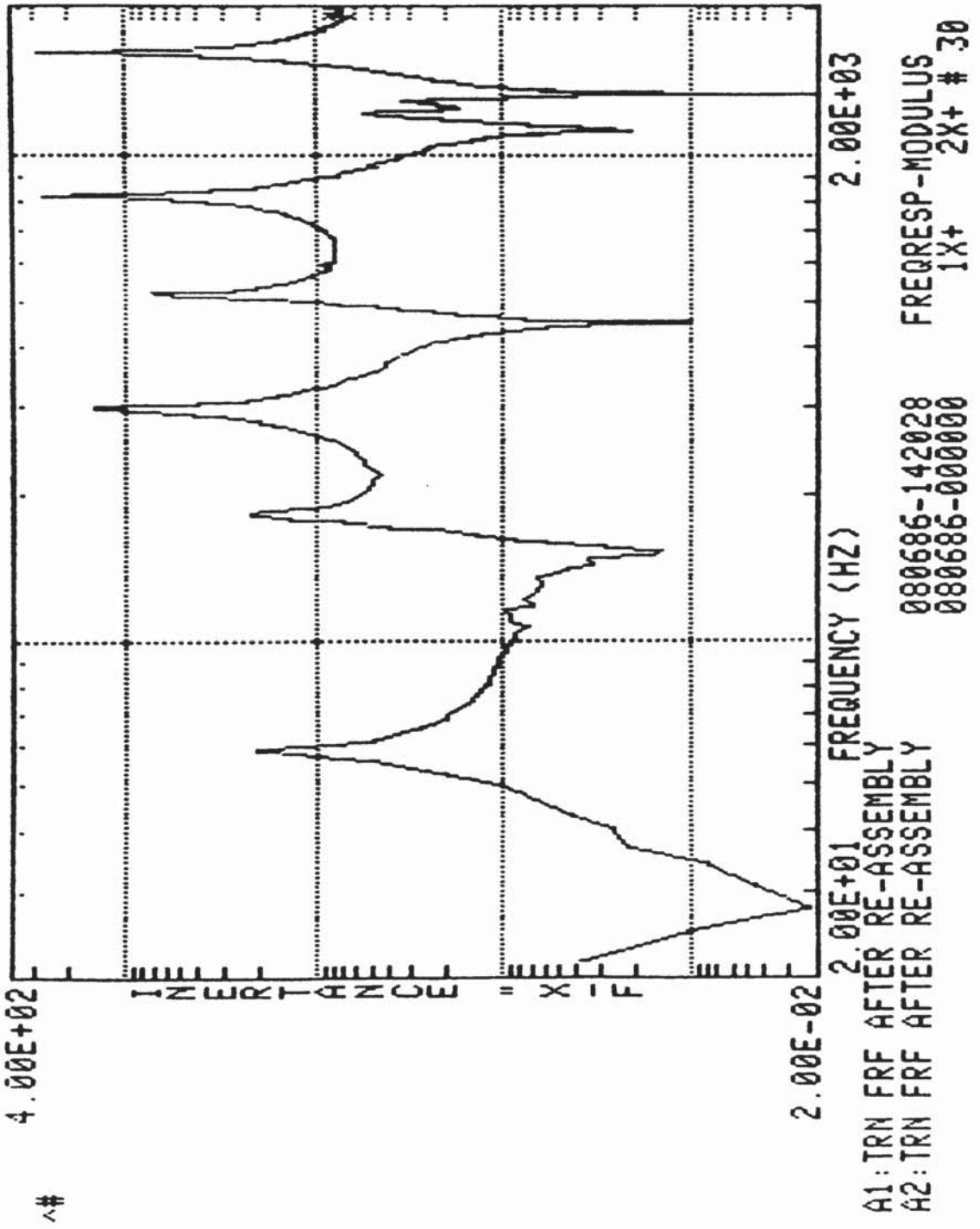

Figure 65

TABLE 10

Distributed discrete system.

Mode No.	Original Structure		Substitute structure	
	Res Freq	Mode Shape	Res Freq	Mode Shape
1	67.63	0.1654	71.6	0.122
	-	-	136.9	-1.05
	-	-	315.4	1.396
2	346.1	1.81	348.8	0.853
	-	-	695.0	-0.201
	-	-	839.7	-0.964
3	914.0	1.879	959.0	1.21

TABLE 11

Transfer frequency response - Original structures.

Mode No.	Orig Structure Res Freq	F.E. Orig structure Res Freq
1	61.1	67.0
2	317.0	346.0
3	833.7	917.0
4	1607.0	1776.0

TABLE 12

Transfer frequency response - Substitute structures.

Mode No.	Orig Structure Res Freq	F.E. Orig structure Res Freq
1	59.02	71.6
2	-	136.9
3	180.2	315.4
4	299.2	348.8
5	520.0	695.0
6	814.8	839.7

7 OUT OF PLANE SIMILARITY

7.1 INTRODUCTION

In the previous chapters two main problem areas have been addressed;

a) developing an identification technique for discrete systems which are dynamically similar to any point coordinate on a continuous structure.

b) examining a proposed design methodology which utilizes a continuous element and a discrete system to achieve dynamically representative structures. The comparisons have so far been for original structures that are one dimensional, such as simple beam elements.

In the majority of real world problems the original structure will be a two or three dimensional body. This introduces the problem of out of plane similarity and whether a single multi-degree of freedom discrete system acting at a single point is capable of achieving complete dynamic similarity for the whole of the substitute structure.

During the philosophical considerations which were made at the outset of the project (Chapter 2), it was considered that a possible solution might exist where the physical appearance of the substitute structure was different to that of the original structure. The work in Chapter 3

esblished three conditions for dynamical equivalence between structures;

i) The same mass and stiffness distribution.

ii) The same dimensions between coordinates of interest.

iii) The same end constraints.

Whilst the design methodology was being established and verified using one dimensional problems it was expedient to use a continuous element which was physically simialar to the original carrier body. By adopting this approach the conditions (ii) and (iii) were easily satisified for dynamical equivalence, leaving only condition (i) to be examined. this approach was again used for the initial work on out of plane similarity so that the number of design variables were kept to a minimum.

A simple portal frame was used as the original carrier body, Figure 66. One of the cantilevered beams was of a greater section than the others so that the motion at the free end of the structure was a combination of vertical translation, vertical rotation and an out of plane twisting motion. The coordinates of interest were taken as 2, 3, 5 and 7 (Figure 66d). In particular the nodes 3 and 7 were observed as it was assumed, arbitarily, that these were the attachment points for any supported or carried equipment.

7.2 SELECTION OF THE CONTINUOUS ELEMENT

7.2.1 LIGHT CONTINUOUS ELEMENT

The portal frame, Figure 66a, was modelled using the finite element analysis package (Pafec 75) to obtain the first four modes of vibration. The first stage of the eigenvalue difference technique (Chapter 5) was used to obtain a spatial model of the portal frame for the coordinates of interest.

When the design methodology is applied to physical carrier bodies it is unlikely that the designer will know all of the sectional areas and topology of the carrier body. He has therefore, to apply a generalised design synthesis algorithm to obtain an acceptable continuous element (discussed in Chapter 8). However, at this stage, since the dimensions of the original structure are known, it is sensible to use this knowledge in the derivation of the continuous element.

In the previous work using one dimensional structures the continuous element always had mass and stiffness values which were less than the original structure's. This ensured that it was possible to identify a positive definite residual mass matrix, from which the parameters of the discrete system were identified. It therefore followed that the initial choice for the continuous element, for the

portal frame exercise, should be another portal frame with reduced sectional areas for the elements. The 'continuous element' portal frame had the same end restraints and spatial coordinates as the original structure.

The reduced sections assumed for the continuous element were

Section of beam 1

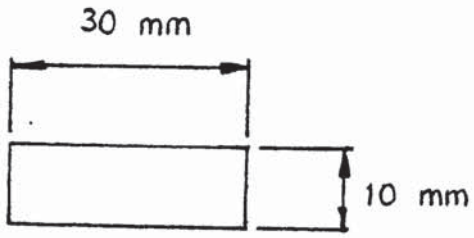

Section of beam 2 and 3

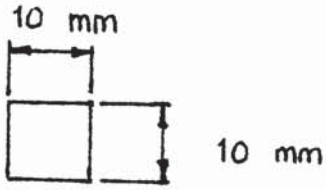

A finite element analysis of this structure was performed and the modal data for the first four modes were recorded. An examination of the receptance plot for node 7, Figure 67, (which was initially chosen for the coupling coordinate of the discrete system) showed that it would not be possible to gain an acceptable level of similarity. The position of the first anti-resonance of the continuous element, at node 7, was less than the first resonance frequency of the original structure. Now, the work on coupling structures has shown that during the coupling process the positions of the individual structure's anti-resonances do not alter. If it was attempted to identify a discrete system using this very light continuous element there would always be a resonance and anti-resonance of the substitute structure before the first resonance of the original structure. The dynamic

similarity would therefore not be acceptable.

7.2.2 RESIDUAL MASS MATRIX

The sectional areas of beams 1, 2 and 3 were increased so that an acceptable distribution of resonances and anti-resonances of the continuous element were obtained when compared to the original structure. It was then possible to apply the design methodology to the two sets of resonance frequencies and mode shapes. The dynamic difference technique using eigenvalues and eigenvectors (Chapter 5) was used to obtain the residual mass and stiffness matrices. The resultant mass and stiffness matrices for this analysis can be seen in Table 13. If the eigenvalue problem is solved for these matrices the algorithm will fail since the mass matrix is not positive definite.

To determine the reason for this failure the mode shape values of each structure must be examined. The continuous element was selected to be lighter than the original structure so that the mass distribution would be less than the original structure´s. Since the mode shape values are mass normalised they should be greater in amplitude than the corresponding values for the original structure. The design methodology incorporates this feature implicitly within the algorithm used to derive the residual mass and stiffness matrices.

The mode shape values for the first and third mode conform to this explanation. However, in the second and fourth modes the values for node 5 of the continuous element were less than the corresponding values for the original structure. This results into one of two conditions;

a) A negative value on the leading diagonal of the mass matrix.

b) A very small value on the leading diagonal of the mass matrix.

In an attempt to avoid this undesirable feature the coordinates of interest were changed. The modal values for node 6 were substituted for node 5, but the same feature was observed for the fourth mode at node 6. The approach of intuitively deriving the continuous element was not totally robust and it was concluded that design evaluations and assessments must be performed by the design engineer when deriving the continuous element. It must be borne in mind that it had been possible to satisfy the second and third conditions for dynamic similarity by using the same spatial coordinates and end restraints for the continuous element as the original structure. Even when the problem was restricted to just the one design variable (ie the same mass and stiffness distribution), it proved to be very difficult to obtain a satisfactory continuous element. This emphasised the importance of a systematic design synthesis algorithm for the design of the continuous

element when the designer was faced with all three design variables to be established.

Resulting from this work it is possible to define another design rule to assist with the derivation of the continuous element. When the continuous element is being designed it is necessary to compare the mode shape values for the coordinates of interest against the original structure. The mass normalised mode shape values should always be greater than the original structure's so that the residual mass matrix is positive definite. This will normally be achieved by reducing the sectional areas of the individual beam elements, however, care should be exercised to ensure that the resonant frequency distribution is correct.

7.2.3 SUITABLE CONTINUOUS ELEMENT

The sectional areas of the beam elements 1,2 and 3 were increased until it was possible to derive a residual mass matrix which was positive definite. The work in the previous chapter had shown that it was important to ensure that the coordinates of interest selected do not correspond to a node point within the frequency range of interest. A check was made for this condition and it was established that all the coordinates selected were acceptable.

One of the design rules that was established in Chapter 6 was the optimum position for the discrete system. It was found that the optimum position for the discrete system

upon the continuous element was at the least constrained coordinate. This had the advantage of the discrete system being of minimum mass for any given continuous element configuration.

Within the finite element model, Figure 66d, node 7 was the least constrained coordinate on the continuous element. The design methodology was used to identify the parameters of the discrete system which was to be coupled at node 7. A comparison plot for the substitute structure and the original structure at node 7 (Figure 68) had the characteristic double anti-resonance feature caused by the difference in anti-resonances between the continuous element and the original structure. The figure does not, however, show the dynamical effects away from the point of connection. To examine the quality of similarity of the whole of the substitute structure with the original structure it was necessary to model the whole substitute structure using a finite element modelling technique.

7.3. DISCRETE SYSTEM POSITION

A finite element model was generated for the substitute structure. The same characteristics that were obtained for the one dimensional structures used in Chapter 6 were obtained . A new intermediate resonant frequency was obtained between each of the original resonance frequencies. The frequency was caused by one of the discrete spring/mass elements resonating. The resonance

caused mode shape values that had a significant effect on the quality of the dynamic similarity of the substitute structure, as was the case for the single plane structure. Where the original structure had three resonance frequencies within the first 650 rad/s the substitute structure had five resonances. The mode shape values for the intermediate frequencies within the range of interest were negligible at node 7. A comparison plot of the substitute structure and the original structure, using the modal data from the finite element analysis (Figure 69) was the same as the plot obtained from the coupling analysis (Figure 68). If this plot was taken in isolation then it could be mistakenly assumed that the two structures were dynamically similar.

If the coordinate, node 3, of the finite element model is examined, then the intermediate frequencies are easily observed. A casual examination of Figure 70 would suggest that the two structures are significantly different and that little similarity exists between them. However, if the intermediate frequencies are removed from the plot (Figure 71) then the level of similarity is greatly improved with only a discrepancy at the second resonance and the first anti-resonance. This quite dramatic change in the level of dynamic similarity demonstrates that when out of plane similarity is considered it is impossible to achieve an acceptable level of similarity using only one discrete system.

The reason for this can be attributed to a fundamental difference between continuous structures and discrete systems. Within the design methodology the parameters of the discrete system are identified by using the values of the anti-resonances of the original structure at the coordinate where the discrete system is positioned. The resonance frequency of each spring/mass element is matched to each anti-resonance frequency, equatiuon (425). This explains why the intermediate resonance frequencies are not apparent at the attachment coordinate when a frequency response curve is generated for the coordinate. On a continuous structure the same resonant frequency is experienced over the whole of the structure. The anti-resonances though are a function of the mode shape amplitudes and, therfore, varies over the whole of the structure. A discrete system has stationary resonance and anti-resonance frequencies which means that when a discrete system is coupled to a continuous system at one point then coordinates away from the connection will interact with the discrete system. It is this interaction which results in the resonances and anti-resonances that are observed in Figure 70.

In an attempt to minimise the undesirable interaction between the discrete system and the continuous element, the coordinate of interest was altered to node 5. This node was at the free end of the frame and between the two nodes (3 & 7) which were assumed to be the attachment points for the transported equipment.

The corresponding discrete system for node 5 was identified and coupled to the continuous element, Figure 72. The characteristics double anti-resonance was obtained. The intermediate frequencies at this coordinate had negligible mode shape values and, therefore, did not appear on the curve for the substitute structure. The plot for node 3 with the discrete system at node 5 showed an unacceptable level of similarity (Figure 73). Likewise, the plot for node 7 (Figure 74) showed an unacceptable level of similarity. Even when the discrete system was in close proximity to the attachment coordinates it was impossible to obtain an acceptable level of dynamic similarity for two dimensional strucutres using a single discrete system.

7.4. DISTRIBUTED DISCRETE SYSTEMS

The effects of using distributed discrete systems was examined by identifying two discrete systems, one at node 2 and the other at node 3. The total mass of each discrete system was half that of a single discrete system acting at the corresponding coordinate. The substitute structure was modelled with the two discrete systems attached. The resultant analysis showed two intermediate frequencies were generated between each original frequency of the original structure. A point coordinate receptance plot for node 3 showed poor dynamic similarity when compared to the original structure (Figure 75). Although the intermediate frequencies associated with the discrete system at node 3

had negligible mode shape values, the intermediate frequencies caused by the discrete system at node 2 had considerable effects.

A comparison plot between the substitute structure and the original structure (Figure 76) at node 7, shows very little dynamic similarity. The substitute structure clearly displays the multiple resonances and anti-resonances caused by the interactions of the stationary characteristics of the discrete systems with the continuous element.

The very poor level of dynamic similarity exhibited by distributed discrete systems show that this approach is not tenable.

7.5 ASSESSMENT OF THE QUALITY OF DYNAMIC SIMILARITY

An assessment of the quality of dynamic similarity between two structures should examine the following features;

a) The resonance frequencies.

b) The anti-resonance frequencies.

c) The general level of the frequency response plots.

In the introduction to the chapter a review of previous work highlighted the ideal conditions for dynamic similarity. By careful design and selection of the same end constraints the work was restricted to examining a procedure to obtain the same mass and stiffness distribution. It was found to be possible to achieve acceptable point dynamic similarity using the proposed

design methodology. This similarity was at the coordinate where the discrete system was attached to the continuous element. However, at other coordinates on the substitute structure the dynamic similarity was lost. It would therefore not be possible to representatively test multi-point attachment equipment on such a substitute structure. The substitute structure at coordinates away from the discrete system exhibit the resonance frequencies of the original structure as well as intermediate frequencies caused by the stationary dynamical characteristics of the discrete system.

If anti-resonances are considered then they are a function of mode shape values and resonances. Now, a resonant frequency is the same at any point on the structure, but the mode shape vector varies. Therefore, the anti-resonance value will vary from point to point on the structure. The discrete system only acts at one point and has fixed anti-resonance values. The combination of these fixed discrete system characteristics and the varying anti-resonances of the continuous element create the generation the the new intermediate resonance and anti-resonance frequencies. These resonance frequencies destroy the dynamic similarity between the substitute structure and the original carrier body. This feature is also present in one dimensional structures. Since the discrete system acts at one point the mass and stiffness distribution for the substitute structure cannot be the same as the original structure.

The discrete system was capable of altering the general level of the whole of the continuous element.

7.6 SUMMARY OF ADDITIONAL DESIGN CONSTRAINTS

These additional design constraints can be employed during the application of the proposed design methodology;

1. The first anti-resonance of the continuous element should be equal to the first anti-resonance of the original structure or at least greater than the first resonant frequency of the original structure. This ensures that it is possible to identify the first resonance of the substitute structure correctly.

2. There should be only one resonant frequency of the continuous element between adjacent frequencies of the original structure.

3. The mode shape values for the coordinate of interest of the continuous element should be greater than the corresponding coordinates on the original structure.

4. The use of distributed discrete systems is not tenable.

5. The stationary dynamical characteristics and point

application of a discrete system means that it cannot be used to effectively alter the overall mass and stiffness distribution.

6. The dynamical characteristics of the continuous element should be sufficiently similar to the original structure so that a single discrete system can be used to provide a small ´tuning´ effect.

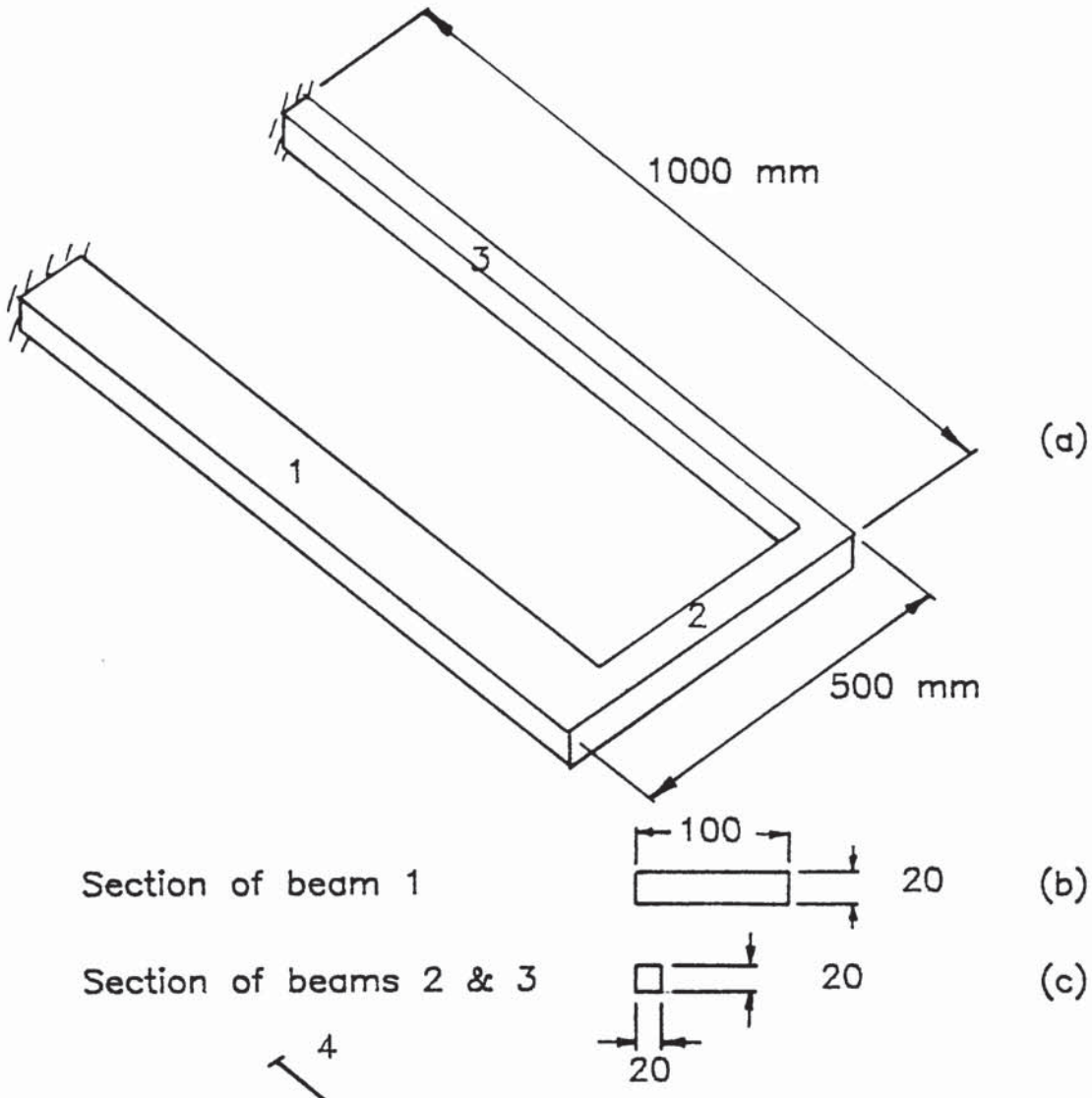
Portal Frame
1000 mm
3
1
2
500 mm
(a)
100
Section of beam 1
20
(b)
Section of beams 2 & 3
20
(c)
20

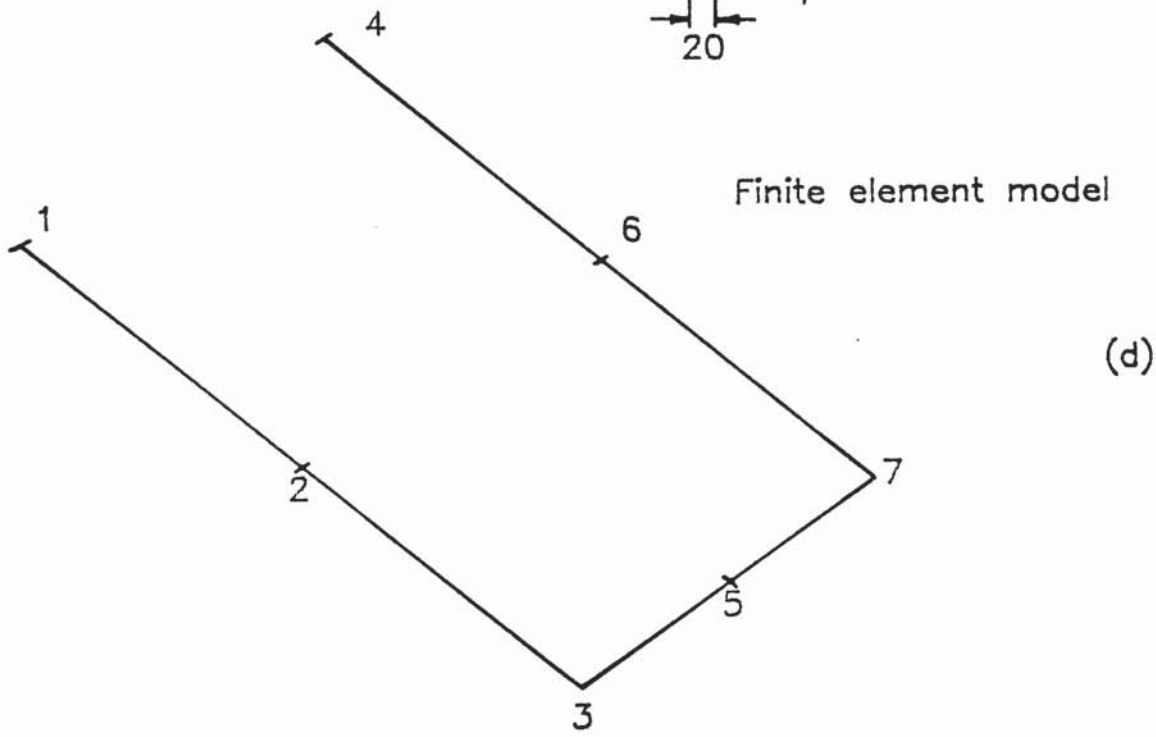
4
Finite element model
1
6
(d)
7
2
5
3

Figure 66

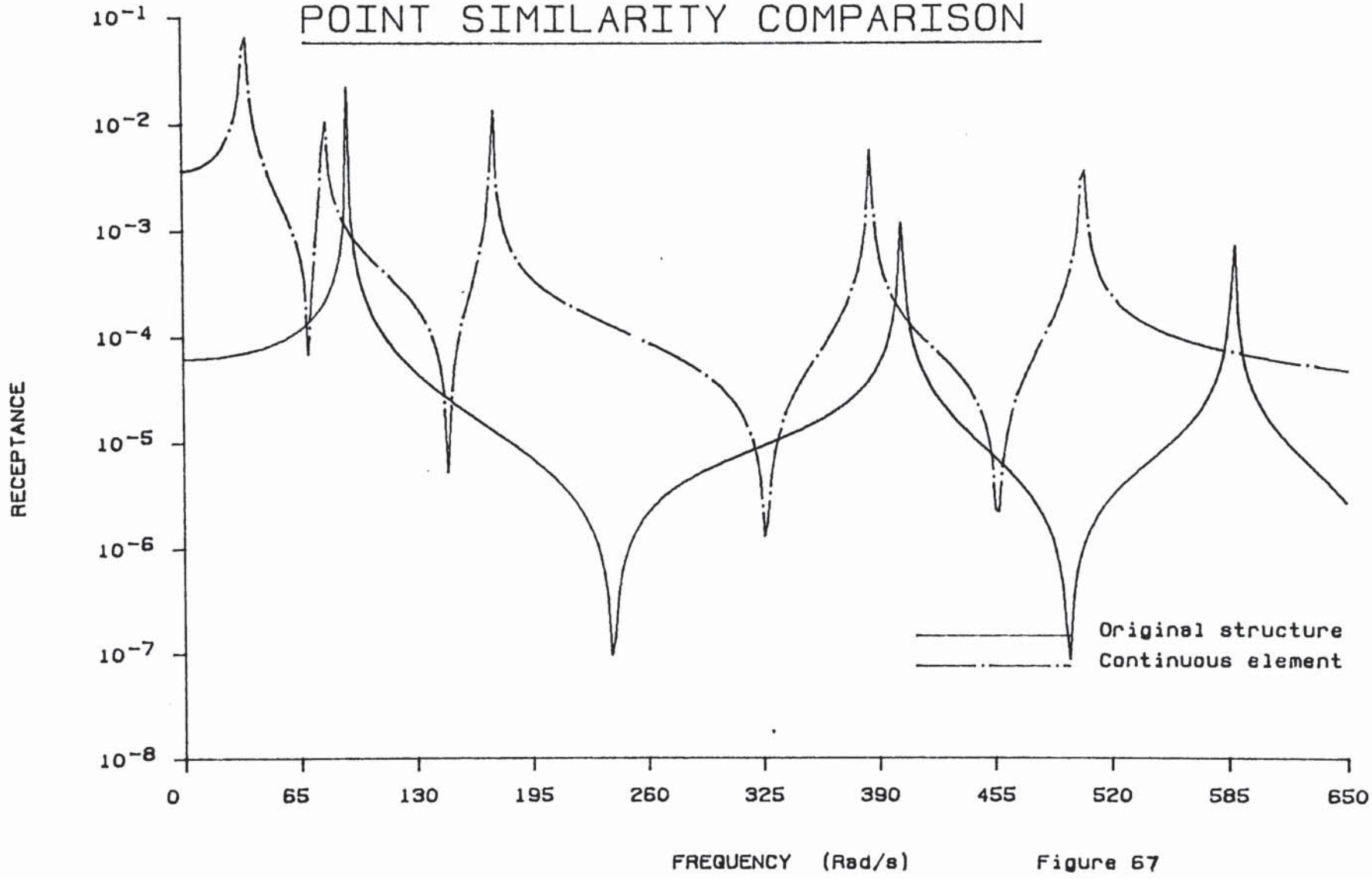
POINT SIMILARITY COMPARISON
RECEPTANCE
10^{-1}
10^{-2}
10^{-3}
10^{-4}
10^{-5}
10^{-6}
10^{-7}
10^{-8}
0
65
130
195
260
325
390
455
520
585
650
FREQUENCY (Rad/s)
Original structure
Continuous element

Figure 67

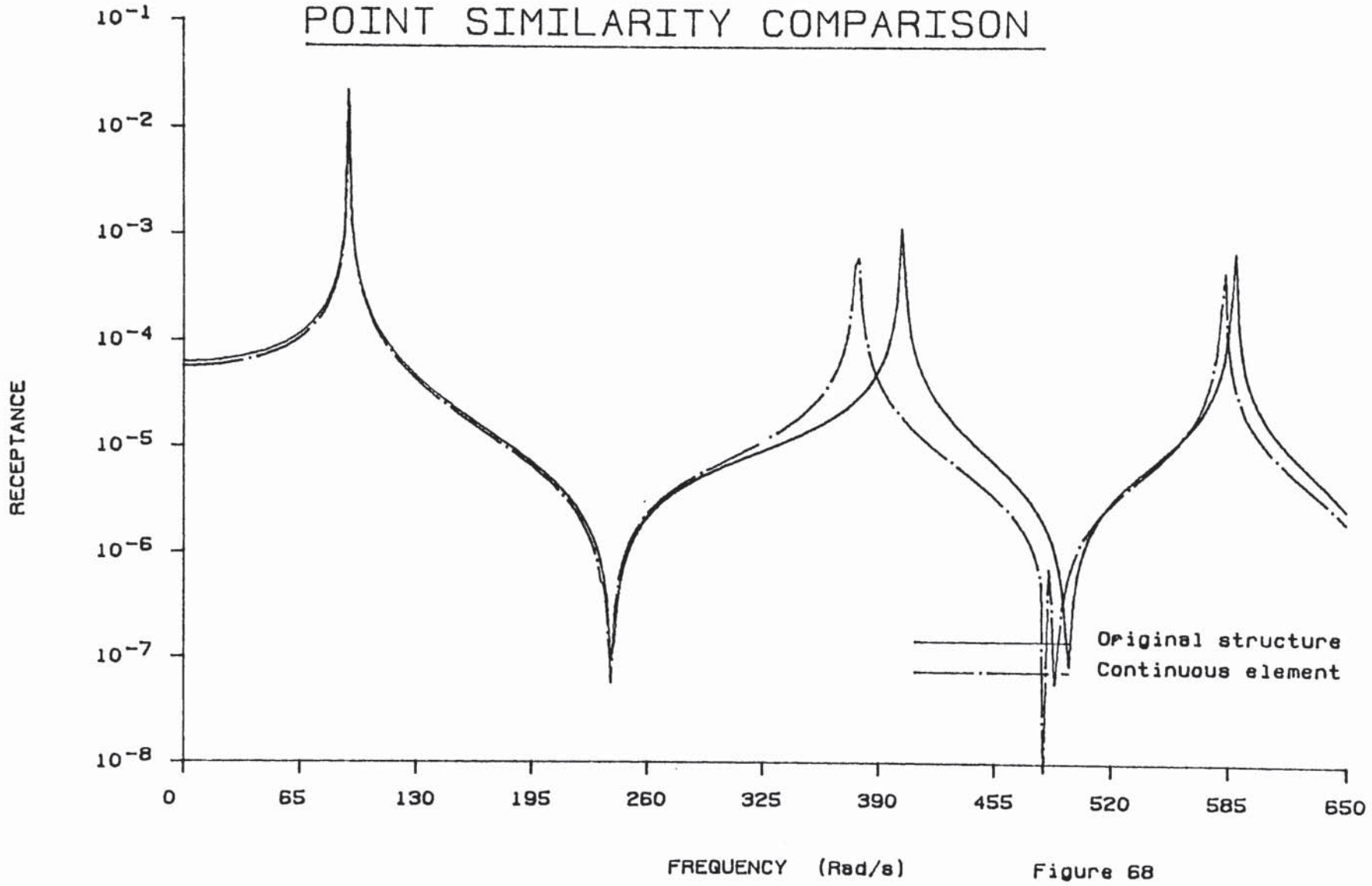
POINT SIMILARITY COMPARISON
RECEPTANCE
10^{-1}
10^{-2}
10^{-3}
10^{-4}
10^{-5}
10^{-6}
10^{-7}
10^{-8}
0
65
130
195
260
325
390
455
520
585
650
FREQUENCY (Rad/s)
Original structure
Continuous element

Figure 68

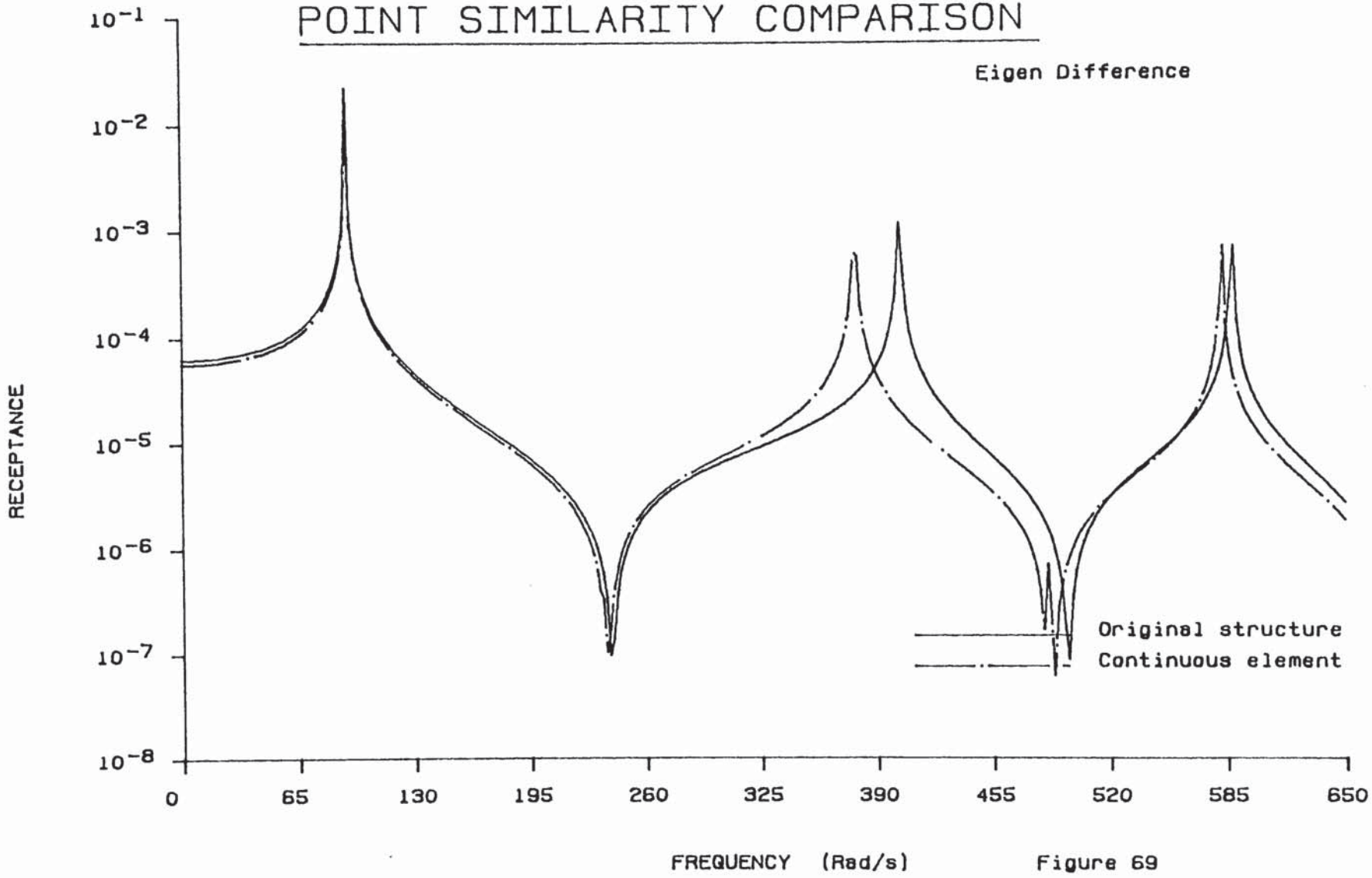
POINT SIMILARITY COMPARISON
Eigen Difference
RECEPTANCE
10^{-1}
10^{-2}
10^{-3}
10^{-4}
10^{-5}
10^{-6}
10^{-7}
10^{-8}
0
65
130
195
260
325
390
455
520
585
650
FREQUENCY (Rad/s)
Original structure
Continuous element

Figure 69

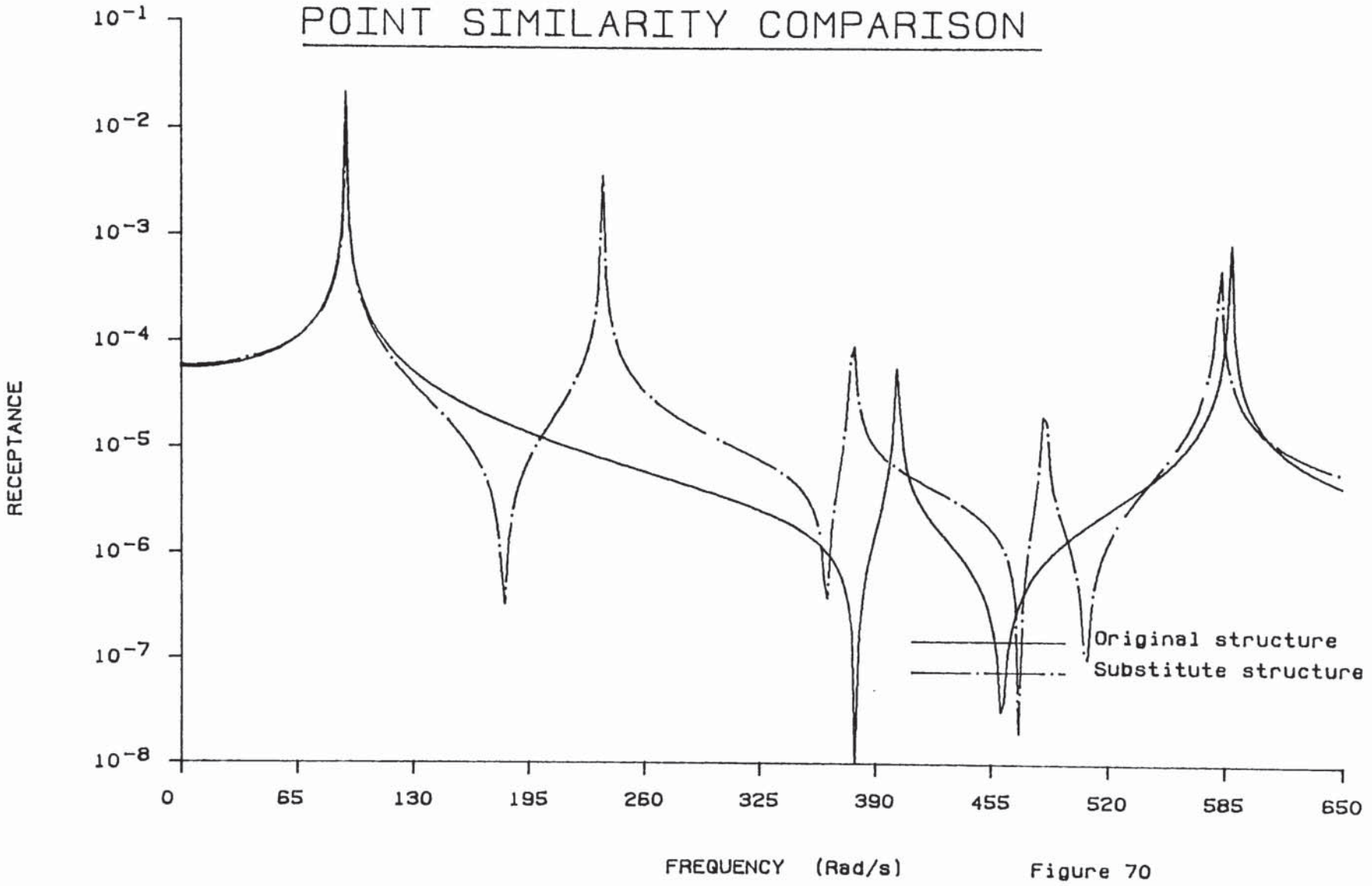
POINT SIMILARITY COMPARISON
RECEPTANCE
10^{-1}
10^{-2}
10^{-3}
10^{-4}
10^{-5}
10^{-6}
10^{-7}
10^{-8}
0
65
130
195
260
325
390
455
520
585
650
FREQUENCY (Rad/s)
Original structure
Substitute structure

Figure 70

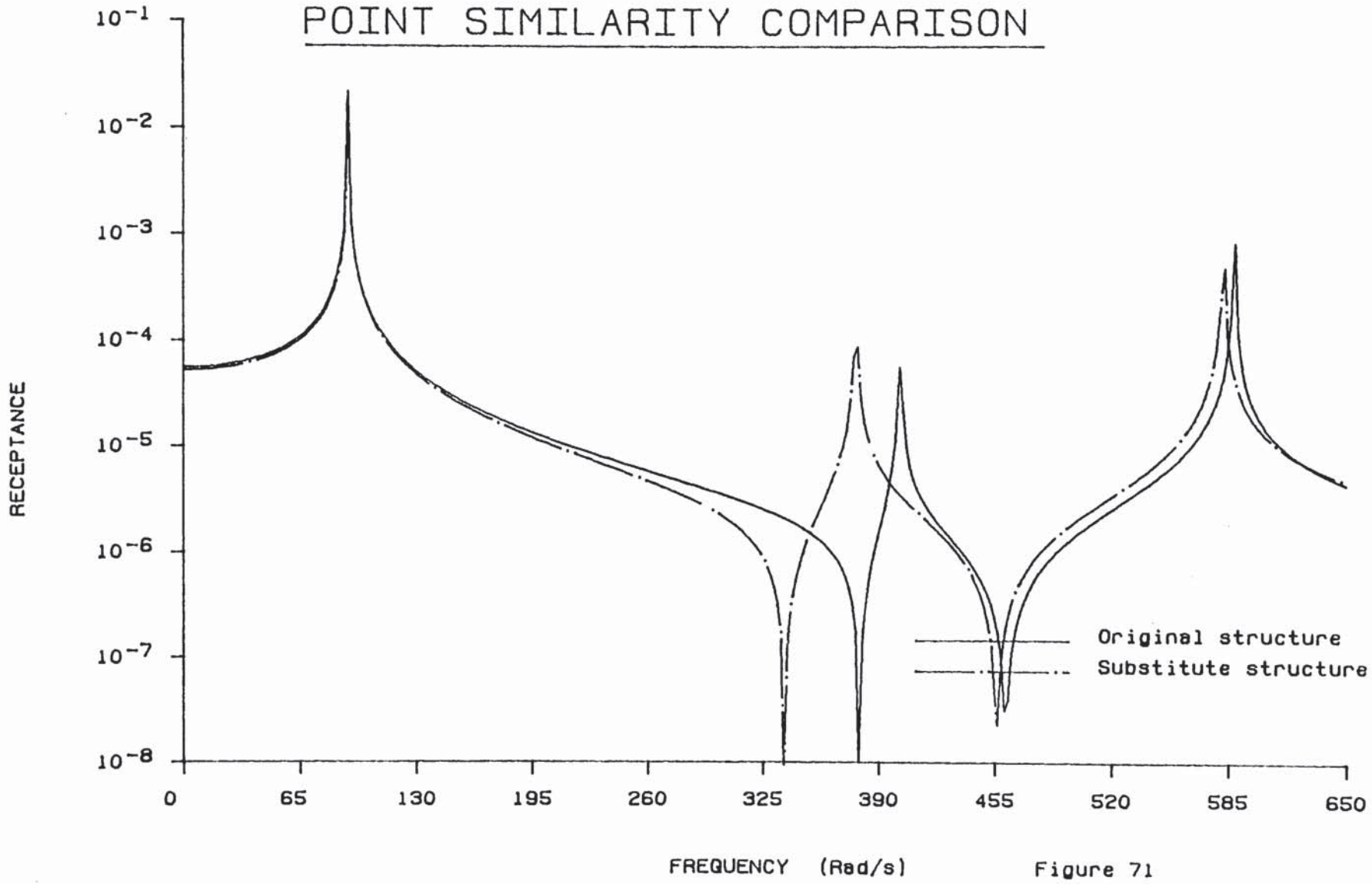
POINT SIMILARITY COMPARISON
RECEPTANCE
10^{-1}
10^{-2}
10^{-3}
10^{-4}
10^{-5}
10^{-6}
10^{-7}
10^{-8}
0
65
130
195
260
325
390
455
520
585
650
FREQUENCY (Rad/s)
Original structure
Substitute structure

Figure 71

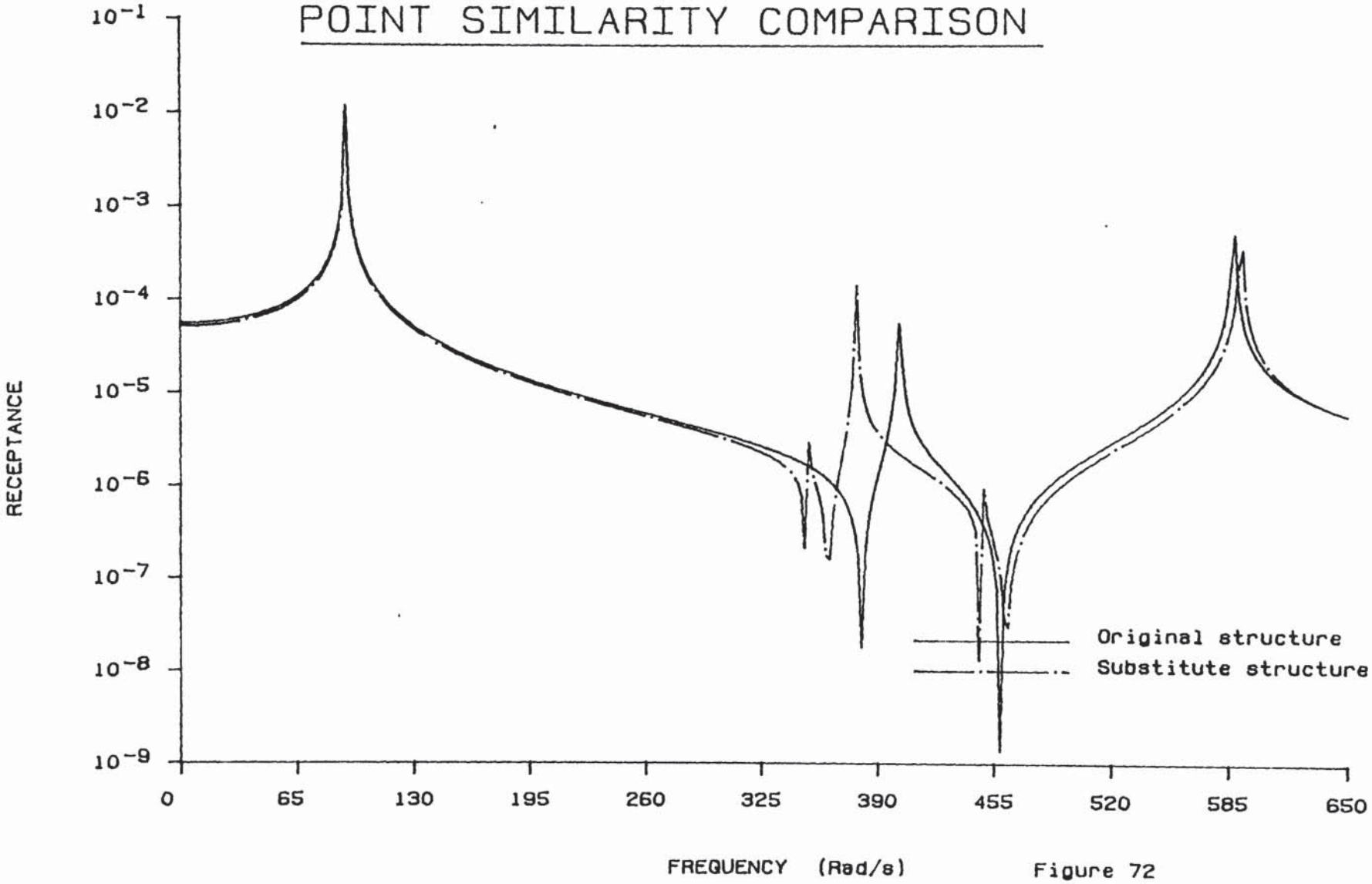
POINT SIMILARITY COMPARISON
RECEPTANCE
10^{-1}
10^{-2}
10^{-3}
10^{-4}
10^{-5}
10^{-6}
10^{-7}
10^{-8}
10^{-9}
0
65
130
195
260
325
390
455
520
585
650
FREQUENCY (Rad/s)
Original structure
Substitute structure

Figure 72

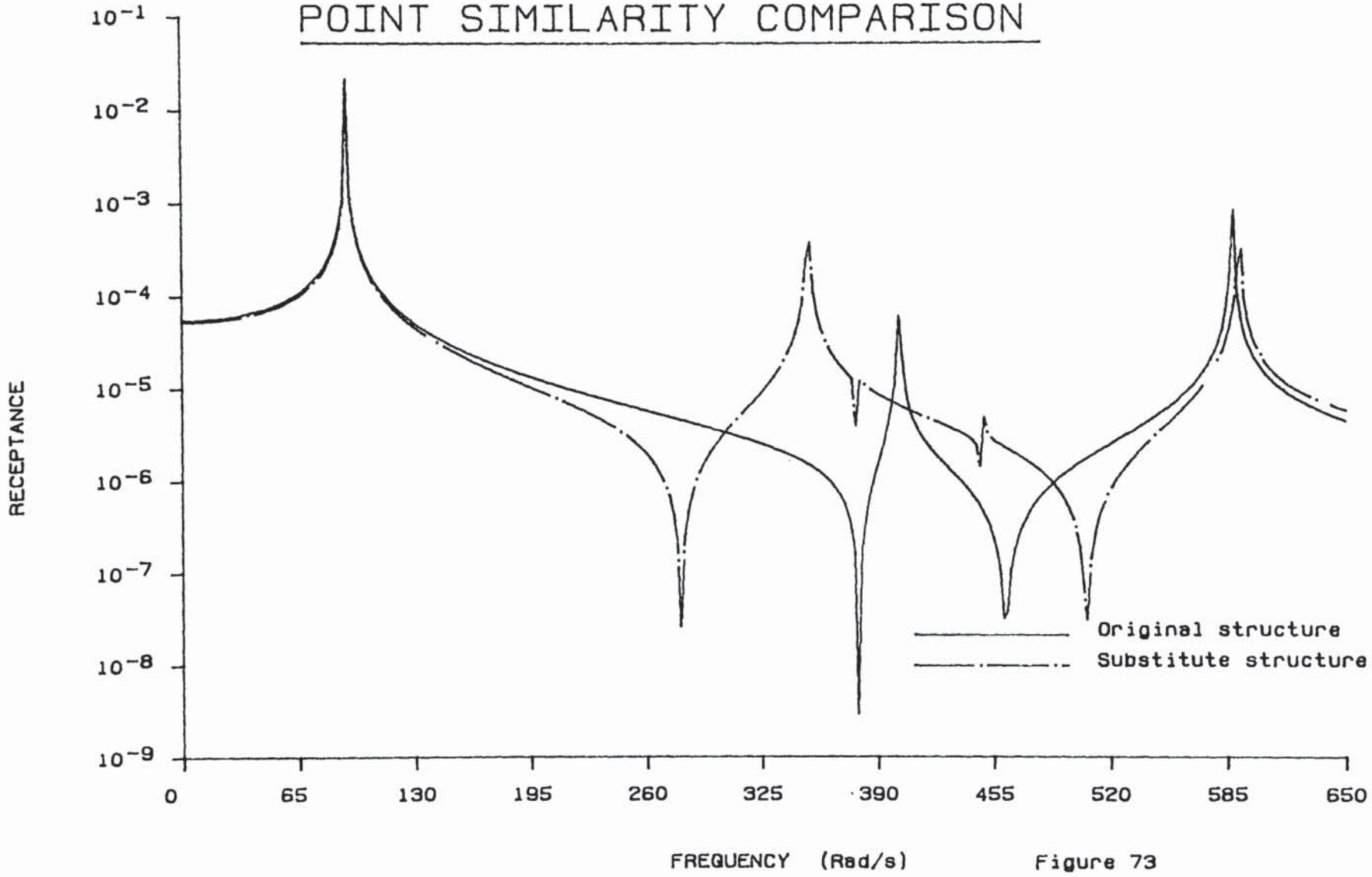
POINT SIMILARITY COMPARISON
RECEPTANCE
10^{-1}
10^{-2}
10^{-3}
10^{-4}
10^{-5}
10^{-6}
10^{-7}
10^{-8}
10^{-9}
0
65
130
195
260
325
390
455
520
585
650
FREQUENCY (Rad/s)
Original structure
Substitute structure

Figure 73

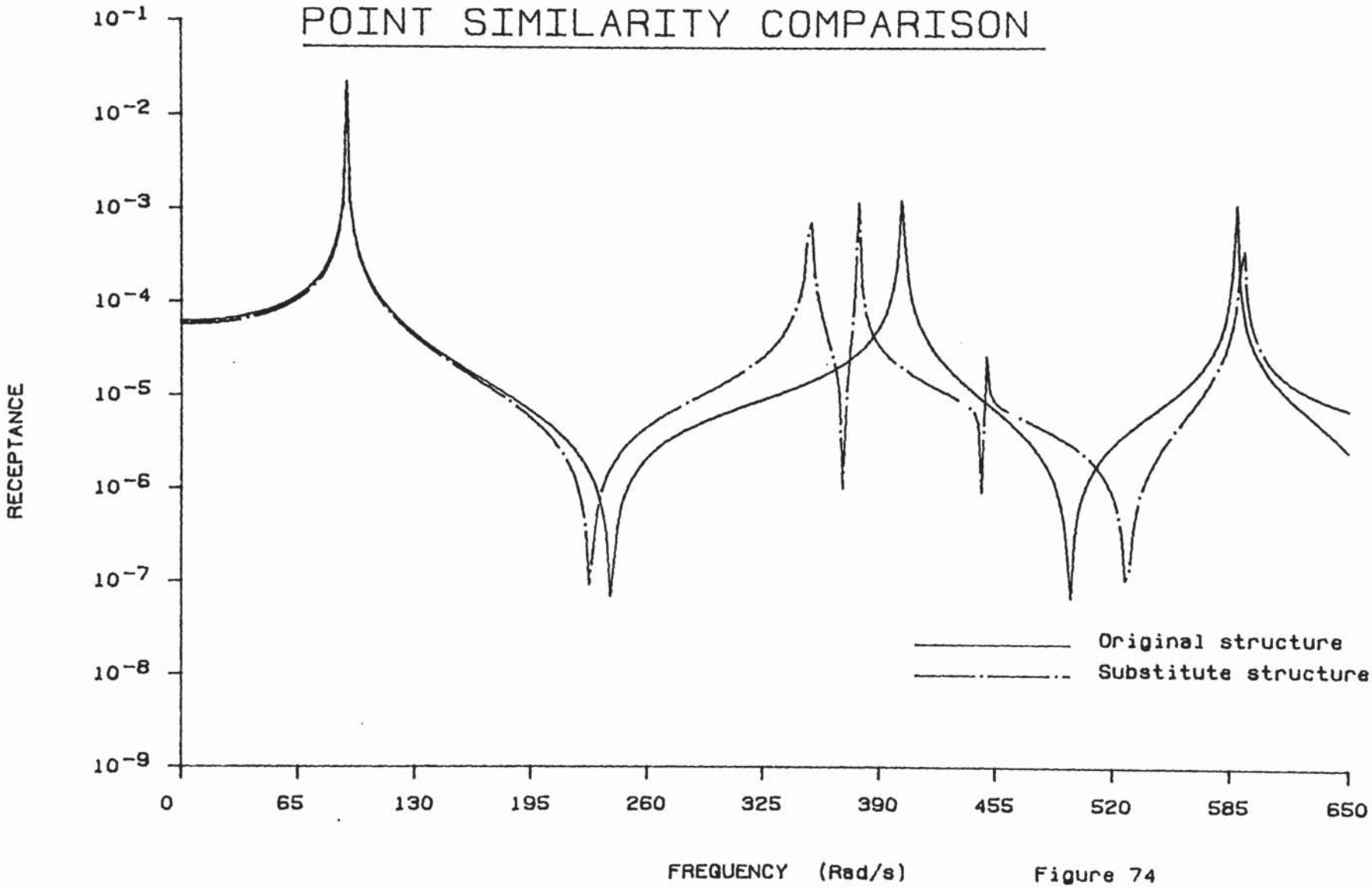
POINT SIMILARITY COMPARISON
RECEPTANCE
10^{-1}
10^{-2}
10^{-3}
10^{-4}
10^{-5}
10^{-6}
10^{-7}
10^{-8}
10^{-9}
0
65
130
195
260
325
390
455
520
585
650
FREQUENCY (Rad/s)
Original structure
Substitute structure

Figure 74

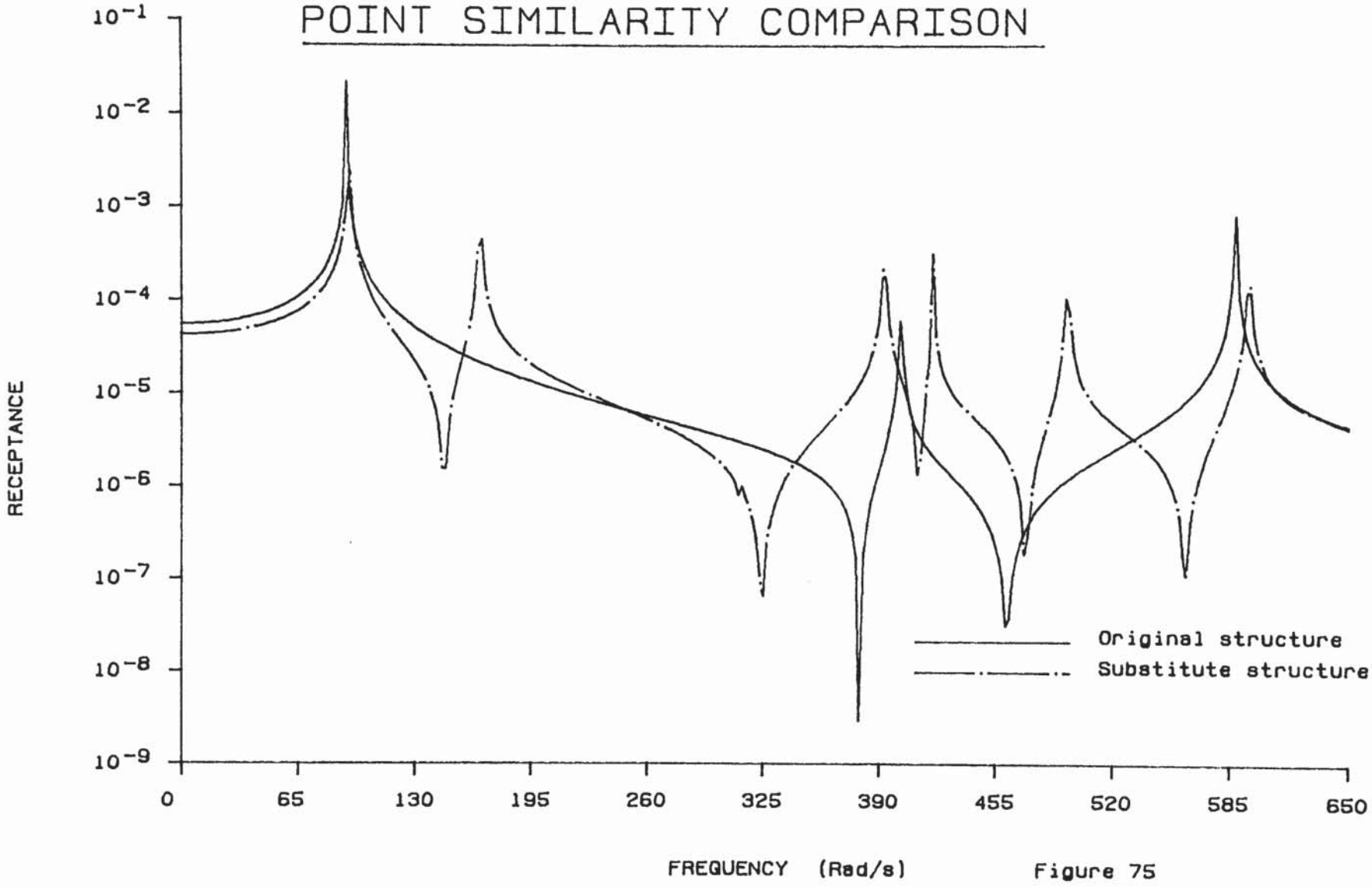
POINT SIMILARITY COMPARISON
RECEPTANCE
10^{-1}
10^{-2}
10^{-3}
10^{-4}
10^{-5}
10^{-6}
10^{-7}
10^{-8}
10^{-9}
0
65
130
195
260
325
390
455
520
585
650
FREQUENCY (Rad/s)
Original structure
Substitute structure

Figure 75

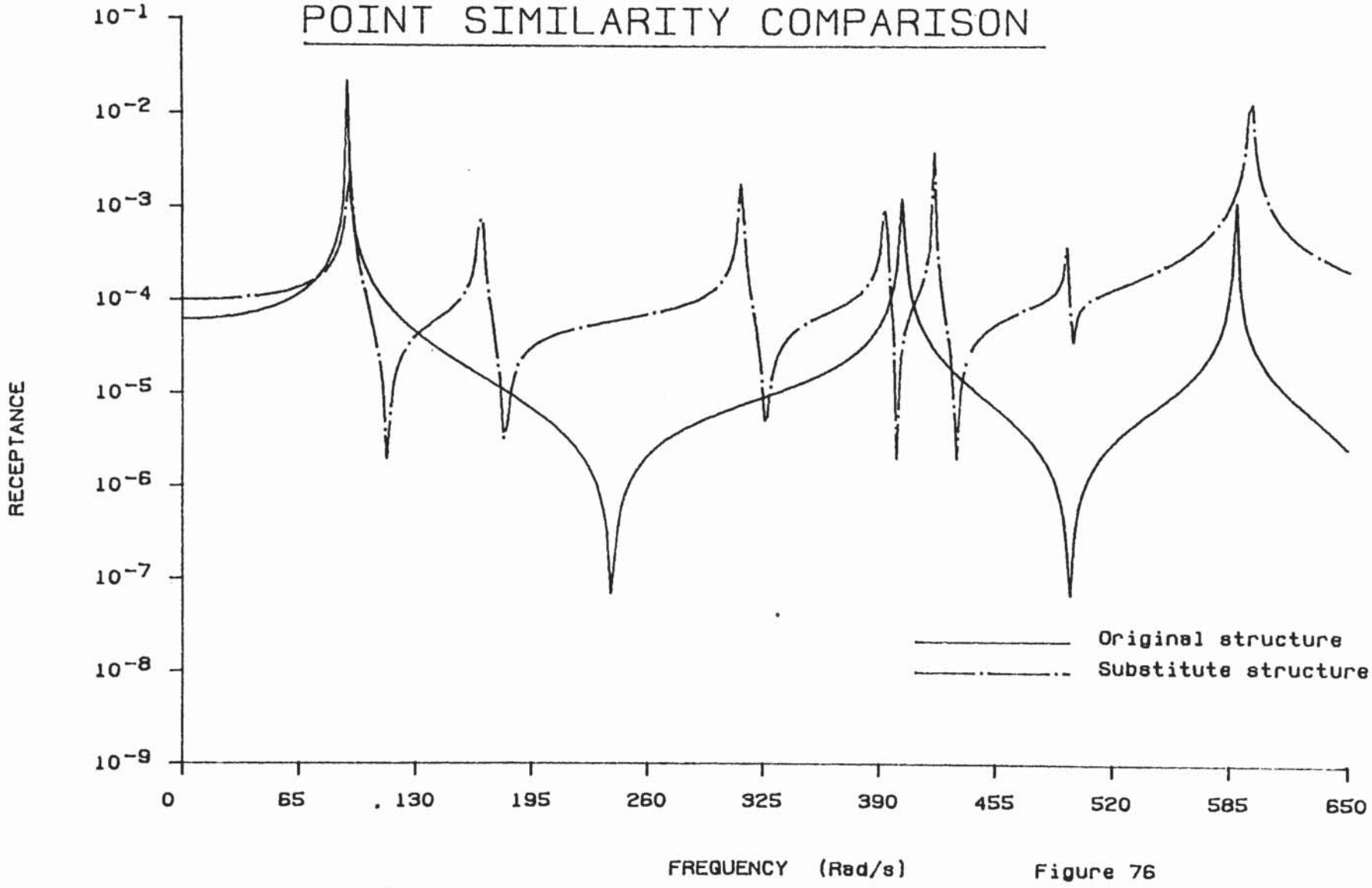
POINT SIMILARITY COMPARISON
RECEPTANCE
10^{-1}
10^{-2}
10^{-3}
10^{-4}
10^{-5}
10^{-6}
10^{-7}
10^{-8}
10^{-9}
0
65
130
195
260
325
390
455
520
585
650
FREQUENCY (Rad/s)
Original structure
Substitute structure

Figure 76

TABLE 13

RESIDUAL MATRICES

[M]ARRAY:=

5.482	-1.797	0.533	0.617
-1.797	0.896	-0.184	-0.216
0.533	-0.184	4E-3	3E-3
0.617	-0.216	3E-3	8E-3

[K]ARRAY:=

31138339	-10749477	-65436	393365
-10749477	3916103	25227	-146957
-65436	25227	1382	-16
393365	-146957	-16	17411

8 DESIGN OF THE CONTINUOUS ELEMENT

8.1 INTRODUCTION

For a long time it has been common engineering practice to test sophisticated equipment under controlled laboratory conditions. The alternative is to develop and evaluate the performance of the equipment by a series of field tests, but often the costs and time scale are prohibitive. The normal engineering approach to designing and evaluating equipment is to first model the equipment using numerical analysis techniques. Once an acceptable design has been achieved prototype systems are manufactured and evaluated by testing under strict laboratory conditions. If the results of the laboratory testing are acceptable experimental validation is then sought under operational conditions.

It is possible by the use of modern numerical analytical techniques to develop a design to fruition without actually manufacturing prototypes. However, it is not desirable to instigate full production of the design without first manufacturing at least one prototype for experimental validation. If this validation is to be useful it is necessary that the prototype is tested under realistic operational conditions.

If the test rig is to be representative of a carrier body or a localised region of the carrier body, it is necessary to know the dynamical characteristics of that body or

structure. This will usually be a set of frequency response curves measured at the coordinates where the equipment is fixed and its immediate surrounding area. The data which are available to the designer of the test rig will be

(a) A set of frequency response curves for the frequency range of interest.

(b) The spatial dimensions of the coordinates where the frequency response curves were recorded.

The designer of the test rig has to derive a design which is capable of reproducing these dynamical characteristics. This is potentially possible by two techniques.

(i) Using electro-magnetic shakers to reproduce the dynamical characteristics of the attachment points.

(ii) Using a mechanical test rig where the distributed nature of the mechanical properties are capable of generating the defined frequency response characteristics.

A proposed design methodology for the mechanical test rig has been examined in the previous chapters. The properties of the continuous element were always derived by intuitive reasoning so that effort was directed to the identification of the discrete system and the effects of coupling

structures. It was found that the addition of the discrete system, used to dynamically tune the continuous element, caused undesirable effects at the out of plane coordinates for the two dimensional models. It was concluded that the use of a discrete system to effect large scale dynamical changes to the characteristics of the continuous element was not feasible. This emphasises that it is important that the continuous element should be capable of generating the defined dynamical characteristics as closely as possible. The proposed design methodology cannot rely upon intuitively derived continuous elements as they are highly unlikely to exhibit the desired dynamical characteristics. The previous work has highlighted the importance of the continuous element and it is, therefore, essential that a systematic design synthesis technique is used to derive the parameters of the continuous element.

If two distinct systems are to be coupled to obtain dynamic similarity then the anti-resonances of each system must be the same as those of the original structure (the carrier body). The work reported in Chapter 5 shows that during the coupling of systems the anti-resonances are dominate and always appear in the resultant system. If a dissimilarity exists between the anti-resonances a spurious resonance is generated. The resonant frequencies of the individual systems will move when the two systems are coupled.

The class of problem of designing the continuous element

can be categorised as a Distributed Parameter Optimum design problem. A design methodology is required that is capable of taking a poor estimate of dynamic similarity and systematically examining possible design improvements such that an acceptable design is achieved.

A generalised gradient projection method for distributed parameter optimal design is examined to establish a basis from which a suitable design methodology for the present problem can be developed.

8.2 THE DISTRIBUTED PARAMETER OPTIMAL DESIGN PROBLEM

Researchers in the field of vibrations have examined the problem of establishing a systematic approach to selecting the optimum structural elements to modify when a structure does not reproduce specified vibration levels. The models considered were lumped parameter models where physical structures were reduced to linear spring/mass systems. Vincent [34] examined the effects of single structral parameter changes on the response of a structure. He achieved this by plotting the locus of a response at a point when a simple mass or stiffness was changed as a circle or an arc of a circle in the complex plane.

Done and Huges [35] extended this work to consider the effects upon the structural response of the system when changing multiple system parameters. They demonstrated that when two parameters were altered simultaneously the

response was found to lie in a prescribed "feasible response" region outside of which the response could never be altered with that particular choice of parameters.

In 1976, Done et al [36] developed this work further in an attempt to use the technique to identify changes or extensions to a model so that it could achieve prescribed dynamical characteristics. The technique was used to enhance a simplified finite element model of a structure so that it was capable of reproducing the measured frequency response characteristics of a physical body. Having obtained a simple, yet realistic model it was then possible to perform a design study to optimise the performance of the physical body. This work was not extended to examining the effects of changing distributed parameter elements within the physical structure or the finite element model.

This technique is only suitable for design cases where the physical structure is reduced into a simplified or discretised model and single linear springs or concentrated masses are used to achieve prescribed dynamical characteristics. A different approach is necessary so that the dynamic effects of distributed parameter systems can be manipulated to synthesise structures which have prescribed dynamical characteristcis.

A finite dimensional optimal design methodology was used, in Chaper 4, to establish the parameters of the discrete system which was dynamically similar to a point coordinate

on a continuous structure. It was possible to use this technique because the resultant design (the discrete system) had only a finite number of degrees of freedom. However, the same design methodology cannot be used to identify the characteristics of the continuous element although the objective is extensively the same. This is because the dynamical characteristics of the continuous element are derived from the topology and mass distribution of the continuous element. This means that the designer must work in an infinite dimensional design space of functions, rather than in the finite dimensional space of design parameter vectors.

A particular case of distributed parameter optimal design is used in the calculus of variations. (Appendix 6). This class of problem is for when the design function is dependent only on the spatial distribution of material to optimise sectional areas, route trajetory, weight etc. The theory developed is suitable for design problems that reduce to closed form solutions of nonlinear differential equations which can be explicitly solved. However, the theory does introduce useful concepts such as functional analysis techniques, boundary conditions and the use of small pertubations to obtain optimal designs. The handling of discontinuities is also discussed.

The problem of designing the continuous element involves both design and state variables as was the case for the finite dimensional optimal design problem. Since the

continuous element must exhibit specific characteristics or functions, these impose constraints on the state and design functions. In Appendix 7, a problem associated with such conditions is examined, it is normally referred to as the problem of Bolza [37]. The Bolza problem is of almost the generality required for the distributed optimal design problem. It´s principal shortcoming is the lack of generality in the constraints on equations (A703) and (A704). This is resolved by making the equations inequalities and then solving, as linear programming problems, by introducing slack variables. As a general rule distributed parameter optimal design problems are not linear. It is, therefore, impossible to solve the complete genaralised problem by linear programming techniques. One approach to solving such problems is to expand functions involved in the design problem through the use of Taylor´s formula. Providing that the design changes are small the first order term of the expansion will allow the selection of an optimum direction. Normally the largest values are taken and a new optimum design is specified which is then suitable for reanalysis. This technique is known as the gradient projection method for optimal design and a more complete discussion of the technique can be found in References 38 - 45.

Consider a mechanical structure capable of being described by a linear set of differential equations; statically

$$[K(b)] \quad \{z\} = \{Q\} \qquad \{z\} \in [D] \tag{801}$$

where the operator K depends upon the design variable (b), the vector function $\{Q\}$ is the applied load. The set $[D]$ is a linear subspace of functions satisfying differentiability properties and homogeneous boundary conditions.

dynamically

$$[K(b)]\ [\bar{\Phi}\ ] = [\lambda]\ [M(b)]\ [\bar{\Phi}] \qquad [\bar{\Phi}\ ] \in [D] \tag{802}$$

which is the general eigenvalue problem.
The performance requirements or constraints can be expressed in the form of "pointwise constraints"

$$\theta_\beta\ (b) \leq \emptyset \quad \beta = 1, \ldots\ldots\ldots q \tag{803}$$

and "functional constraints".

$$\psi_\alpha\ (b, z, \lambda) = g_\alpha(\lambda) + \int_\Omega F_\alpha(x, z, b)\, dx \begin{cases} = \emptyset, \alpha = 1 \ldots r' \\ \leq \emptyset, \alpha = r'+1 \ldots r \end{cases} \tag{804}$$

The conditions of equation (803) express explicit bounds on the design variables, which must be satisfied at all points over the domain Ω of the distribution of the independent variable. The functional constraints of equation (804) are used to replace any pointwise constraints over the domain Ω that are of the form

$$\eta(b,z) \leq \phi \qquad x \in \Omega$$

by the equivalent functional constraint

$$\Psi_\alpha = \int_\Omega \langle n \rangle dx = \phi \tag{805}$$

The final element of the optimal design problem is the cost functional that is to be minimised

$$\Psi_o(b,z,\lambda) = g_o(\lambda) + \int_\Omega F_o(x,z,b)\,dx \tag{806}$$

The cost functional can represent weight, displacement, natural frequency and other pertinent costs associated with the design problem.

The gradient projection method that is fully developed in Appendix 8 is based upon the same ideas as used in the finite dimensional gradient projection method described in Chapter 4 and Appendix 3. It requires that first order approximates are made to various functions involved in the optimisation problem and an optimum design improvement computed.

The expression (A813) is well suited to modern numerical analysis methods such as finite element analysis where a discretised spatial model of the structure under examination is generated. This means that the mass and stiffness matrices [M] and [K] are normally available. If the shape functions used to generate the mass and stiffness

matrices are known then it is possible to determine changes δm, δK due to sectional changes δb. The design changes that violate the constraint equations (803) and (804) are then retained to generate a matrix of sensitivity coefficients. Unfortunately this design procedure can be used only for a limiting design case of optimising the dimensions of a known structure. It does not give any suggestion as to a method for altering or extending the structures topology.

8.3 PROPOSED DESIGN METHODOLGY

8.3.1 SELECTED APPROACH

If it is accepted that the only data available to the design engineer is a set of frequency response functions and the coordinates where the measurements are taken, it is unlikely that the initial tentative design will generate the correct state space functions. The designer will be left with three possible approaches for design alterations

(a) Extend or modify the topology of the structure. Care has to be exercised to ensure that the original coordinates of interest are retained

(b) Alter the end restraints of the structure.

(c) Alter the sectional areas of the individual structure elements (conventional sensitivity analysis).

The design methodology for sensitivity analysis is suitable

for option (c). However, the other two options cannot be handled in the same way as they are fundamentally different in their design formulation. The options (a) and (b) imply a procedure of "looking out" or extrapolating from the present design state to another state such that the changes to the present state $\mathbb{Z}^{o}$ move the design in a feasible direction towards the required design state $\mathbb{Z}^{o'}$.

A design synthesis methodology is required so that the designer or an automated design procedure can select additions or modifications to the structures topology which will reduce the difference between the specified state space $\mathbb{Z}^{r}$ and the actual design state space $\mathbb{Z}^{o}$.

The original data obtained from the carrier body are normally supplied as frequency response curves. These can be analysed using system identification techniques to identify the natural resonant frequencies, mass normalised mode shapes and the damping within the structure. It is then only a simple step to obtain mass and stiffness matrices which represent spatial models of the structure at the coordinates of interest.

These mass and stiffness matrices will be fully populated due to truncation effects of the out of range frequencies. However, they are very useful as they provide the mass and stiffness distribution that the tentative design must achieve. It is important to note that although the mapping from the mode vectors to the mass matrix is unique it is

not possible to uniquely perform the inverse of the process (ie the mapping is non-injective,non-surjective). The mass and stiffness matrices, therefore, have no unique physical meaning. The initial tentative design is derived by intuitive reasoning of the design engineer based on descriptions of the original carrier body and the coordinates of interest. If a finite element analysis model is generated for this design it can be analysed to obtain the resonant frequencies and mode shapes.

$$[\bar{\Phi}]^T [M][\bar{\Phi}] = [I] \qquad (31)$$

$$[\bar{\Phi}]^T [K][\bar{\Phi}] = [\lambda] \qquad (32)$$

Using equations (31 & 32) it is possible to determine the mass and stiffness matrices for the tentative design.

The difference between the matrices for the original carrier body and the tentative design represent the changes that have to be effected upon the tentative design to achieve dynamic similarity.

ie $$[M_{orig}] = [M_{t.d}] + [M_{diff}] \qquad (807)$$

$$[K_{orig}] = [K_{t.d}] + [K_{diff}]$$

To achieve the difference matrices $[M_{diff}]$ and $[K_{diff}]$ it might entail large scale changes to the intial design estimate. It is, therefore, not realistic to attempt arbitrary or multiple design changes during each design iteration.

It is proposed to adopt the following design synthesis

algorithm when selecting the additions or modifications to the initial design estimate.

1. Examine the distribution of $[M_{diff}]$ to establish an area where the most significant values exist.
2. Relate this area to the corresponding coordinates on the tentative design estimate.
3. Add to or modify the local topology.
4. Analyse resultant design estimate to obtain new mass and stiffness matrices.
5. Remove the initial design estimate matrices from the new matrices.
6. Check that the residual matrices do in fact produce the desired effect.

The residual mass and stiffness matrices show globally the effect of making a localised change to the design topology.

It is then possible to examine sectional changes to the new element within the design. The sensitivity analysis (equation A813) is performed in relation to the difference matrices $[M_{diff}]$ and $[K_{diff}]$ so that the optimal contribution of the additional element can be established.

Once an optimum condition has been achieved for a single element addition then changes to the end restraints are examined.

The following algorithm is used to obtain optimum end restraints.

1. Restrain the free end of the addition element in one of the six degrees of freedom of motion.
2. Analyse the resultant design estimate to obtain new mass and stiffness matrices.
3. Remove the initial design estimate matrices from the new matrices.
4. Repeat this procedure for all six degrees of freedom of motion.

Using the results from the six iterations and the unrestrained element it is possible to establish the optimum end restraints for the additional element.

Rather than optimising this design change and then incorporating the change within the design estimate it is proposed to repeat the algorithm to build a library of single element and end restraint changes to the initial design element. This is because the effect of a single change on the $[M_{diff}]$ and $[K_{diff}]$ matrices might be a mixture of benifical and detremental additions to the individual matrix elements. Once a sufficiently large library of the effects of selected changes has been made the final stage of the optimisation process can then be performed.

A sorting algorithm (based on a linear programming approach) is used to sweep the library data base to find the optimum changes to the topology. These changes are then made to the tentative design and the analysis is repeated until an acceptable level of similarity is

achieved.

This methodology is a blend of intuitive reasoning and numerical analysis techniques. It is particularly suited to an expert system (or artificial intelligence) application. As the number of design changes increase the expert system would be generating a data base from which it could establish a set of selection rules. This technique is known as the induction method. Based upon these rules it should then be possible for the system to extrapolate new design changes that would be dynamically effective. It is not proposed to employ expert systems, or artificial intelligence, within the present design study study but the observation is made for future possible work.

The characteristics that are required of a suitable expert system are;

i) The induction method is used as the basis for decision making.

ii) It is capable of being integrated with numerical analysis software such as finite element analysis, modal analysis and optimisation software packages.

An expert system builder such as TIMM [46] has these characteristics and may be suitable for future consideration.

8.3.2 DESIGN METHODOLOGY ALGORITHM

1) Obtain data from original structure and using the same number of coordinates of interest as degrees of freedom of interest generate the spatial models $[M_{orig}]$, $[K_{orig}]$ and $[C_{orig}]$.

2) By connecting the coordinates of interest with a continuous element derive the tentative design estimate $\{b^{\circ}\}$.

3) Analyse the design by finite element analysis to obtain resonant frequencies and mass normalised mode shapes. From these values derive the matrices $[M_{t.d.}]$ and $[K_{t.d.}]$.

4) Remove the matrices $[M_{t.d.}]$ and $[K_{t.d.}]$ from the corresponding matrices $[M_{orig}]$ and $[K_{orig}]$ to obtain $[M_{diff}]$ and $[K_{diff}]$.

5) Compare the performance of the tentative design against the original structure. If the similarity is within acceptable limits then end.

6) At this point the design engineer can select one of three possible design optimisation routines. This step is repeated until sufficient data has been generated that a design improvement can be made to the tentative design.

   6a) Element addition

   A selection process is used based on choosing the most likely element addition by examination of the $[M_{diff}]$ and $[K_{diff}]$ matrices.

6b) End restraints

The effects of varying the end restraints of the tentative design are examined to find the optimum end conditions.

6c) Sectional area change

A perturbation analysis of the tentative design (with the additional elements) is performed to find optimum design change.

7) Perform a sorting algorithm to ascertain the optimum design changes.

8) Specify topology of new tentative design which incorporates the optimum design changes. Repeat from step (3).

8.4 THEORETICAL STUDY

8.4.1 ORIGINAL STRUCTURE

A two dimensional space frame was selected as the original structure (Figure 77a). The left end of the structure was fully constrained and the beam number 1 was of a greater section than the others. The structure was inclined and tapered so that a strong twisting moment would be generated. A finite element model was created (Figure 77b) and the coordinates of interest correspond to the nodes 4, 10, 12, and 13. It was assumed that the equipment was attached to nodes 10 and 11. The reason why node 11 was not included within the coordinates of interest was so that a point not directly manipulated within the design procedure could be used as a control within the evaluation

of the dynamic similarity. It was also assumed that the experimental test engineer would have also recorded response data at nodes 7, 9, and 15 in case of encountering a frequency node and to also ensure that sufficient response data were available.

Normally, this data would be in the form of frequency response curves which could be processed using a system identification algorithm to obtain the resonance frequencies and mode shapes. A system identification for the four coordinates of interest and the first four modes of vibration of the structure yielded a spatial model for the original structure. This spatial model $[M_{orig}]$ and $[K_{orig}]$ was then used throughout the subsequent analysis as the design state .

8.4.2 INITIAL TENTATIVE DESIGN

The data available to the designer was assumed to be the spatial coordinates where the dynamic data were recorded and the frequency response data. After the data have been processed, by a system identification algorithm, it was possible for the designer to plot the modes of vibration. The first mode, Figure 78 showed that the structure exhibited three major degrees of motion, ie vertical translation, vertical rotation and a twisting motion. The motion at nodes 4, 7, 10 and 13 was less than the other mode shape values. This suggested that this beam was stiffer or more constrained than the other elements. The amplitute at 4 was much lower then at 13 which suggested

that the major restraint was in a line projected back through node 4. From these observations it is possible to derive the first tentative design (Figure 79). The design was intentially simple so that it bore little resemblence to the original structure.

Linear srings were applied at the nodes 4 and 6 of the tentative design so that the structure could be supported. The rate of the linear springs was established by examining the receptance plot for the nodes 12 and 13 of the the original structure. The work in Chapter 4, equation (424) was used to calculate the spring rates. A pinned joint at node 1 of the tentative design was selected.

A finite element model of the tentative design was generated and analysed. The eigenvalue difference technique, Chapter 5, was used to generate a spatial model of $[M_{t.d.}]$ and $[K_{t.d.}]$ for the tentative design. The spatial models for the original structure and the tentative design were consistant and therefore the difference of the two models represents the error that must be reduced by the design methodology.

The differences were;

$$\begin{bmatrix} 26.197 & -23.156 & 1.073 & 4.65 \\ & 23.008 & -1.195 & -6.091 \\ & & 0.519 & 0.598 \\ & & & 3.953 \end{bmatrix}$$

Mass difference

$$\begin{bmatrix} 722088 & -729460 & 9562 & 227440 \\ & 764758 & -9394 & 247216 \\ & & 2395 & 1231 \\ & & & 84202 \end{bmatrix}$$

Stiffness difference

The matrices are symmetrical

The resonant frequencies were;

Original structure	Tentative design
15.68	12.6
85.45	55.5
96.63	135.2
197.67	216.0

The differences between the two structures were too great to consider that an acceptable level of dynamic similarity had been achieved. It was, therefore, necessary to apply step (6) within the design methodology to move the tentative design towards a feasible solution.

8.4.3 DESIGN CHANGES

The finite element software used throughout the analysis was a commercially available package and it was impossible to obtain sufficient details (in the time available) to be able to perform a direct sensitivity analysis as described by equation A8**13** . However, a series of runs were performed where unit changes to the sectional area of each

element were made. It was then possible to generate a sensitivity matrix for dimensional changes to the tentative design. An examination of this matrix showed that it was impossible to achieve dynamic similarity by altering the sectional areas of the tentative design. Changes or additions to the topology of the tentative design were therefore required.

Although the tentative design was totally different to the original structure the resonance frequencies were within 10 - 35% of the required values and the distribution of the frequencies was approximately correct. However, an examination of the mass difference matrix showed that the mode shape amplitutes for the tentative design were unacceptable. The greatest difference was in the region of nodes 2, 3 and 6. It was impossible to just add concentrated springs and masses at these nodes (an approach similar to Ref [36]) because the off diagonal terms were significant. It was, therefore, necessary to identify what the effects of adding elements or restraints to the tentative design had on the mass and stiffness difference matrices. Whenever changes were made to the tentative design the subsequent analysis was always for the whole of the tentative design and the coordinates of interest were retained constant. Once the spatial model $[M_{t.d}]'$ and $[K_{t.d.}]'$ had been derived for the new structure then the contribution of the change could be established. Since the whole structures and spatial models were handled the degree of resolution of the modelling procedure was very high.

The difference between the extended tentative design and the initial tentative design showed the contribution of the change and since it was a quantitative value it was suitable for inclussion within a design synthesis technique.

Over forty design changes were examined for the tentative design. The effects of each design change and the actual parameters changed were recorded within a computer data retrieval system to assist with the final sorting and selecting procdure.

During the first iteration of the design methodology effort was directed towards identifying what changes were necessary to reduce the mass difference matrix at the nodes 1 and 2.

The design analysis was performed using a combination of different computers and software and was therefore highly dependent upon human interaction and decision making. (Ultimately it is envisaged that the whole process will performed with an integrated suite of software running on one computer). Since the process was not automated the number of design changes that could be carried out in a reasonable time scale was restricted. Figure 80 shows eight principal design changes to the topology of the initial tentative design. Each topology design change incurrs subsequent analysis to examine the end restraints, sectional changes and element length changes. Even this

limited set of design changes produced a large amount of data from which the optimum change had to be selected. A sorting algorithm was used, based on the error in anti-resonace frequencies, resonance frequencies and the mass and stiffness distribution, to select the best three cases. These were;

1) Configuration number 3 with a linear spring at the tip of the new element (Figure 81).

2) Configuration number 4 with the new element pinned-jointed (Figure 82).

3) Configuration number 5 with a linear spring at the tip of the new element (Figure 83).

An examination of the mass difference matrix suggusts that extra mass should be applied at nodes 2 and 3. When configurations were examined where the mass was directly applied at node 2 (configurations 1 and 2) small improvements were obtained. These improvements were not significant, even when the tip of the additional beam was fully constrained. The most significant effects were obtained when elements were added to the tentative design that were not in the close proximity of nodes 2 and 3. Nevertheless, due to the distributed nature of the structure the dynamic effects of the new elements generated apparent mass at nodes 2 and 3.

Case 1 ; Figure 81

The new element (Number 6), Figure 81a, was examined for different end restraints at node 7. The length and the sectional area were altered to provide a quick analysis of the sensitivity of the new element to geometry changes. The optimum condition was found when a linear spring was applied at node 7 and the node was in the same plane as node 2. The first and third resonant frequencies of the tentative design are very accurate (within 2%). The second resonant frequency of the tentative design shows only a small improvement with a reduction of error from 35% to 28%. The mass difference matrix shows an improvement to the mass distribution, particularly at nodes 3 and 6. This improvement in the mass difference matrix is reflected by a small reduction in the first anti-resonance value at, node 3, from 59 rad/s to 55 rad/s. This highlights that a comparison of resonance frequencies only is insufficient to assess dynamic similarity. The intention of the design methodology is not to achieve dynamic similarity in one step but to identify a change in the tentative design such that a feasible direction to an acceptable solution is achieved. This design change fulfills this criterion.

Case 2 ; Figure 82

A variation on the third configuration is to add a new element which is parallel to elements 1 and 2. The optimum design change for this case was found when the new element

was projected back to the same plane as node 1 and was pinned-jointed. The error in the resonance frequencies were 11%, 28%, 20% and 23%. Although these errors were greater than the first design case the first anti-resonance for node 3 was at 34 rad/s, an improvement of 25 rad/s. This is a significant improvement when compared to the first design case showing that an improvement to the mass distribution had been achieved.

Case 3 ; Figure 83

An interesting design case is one when the additional element fitted to the tentative design appears to be well removed from the area of interest. In configuration number 5 the element is fixed at node 6 and extends towards the least constrained area of the tentative design. The error in the resonance frequencies were 10%, 40%, 0.8% and 33%. The first anti-resonance at node 3 is at 51 rad/s. Although the change does not represent an optimium when compared to either of the other two cases it does fulfill the design selection criterion.

These three cases highlight that the mass and stiffness difference matrices can be used as first order derivatives within the design optimisation procedure. They cannot though be used directly to assess where additional elements or changes to the end restraints can be applied. There is an unbounded set of possible design changes that can be made to the tentative design and it is therefore important

to quickly isolate areas within the structure which are fundamental or critical areas within the dynamic similarity process. For example, additional elements at node 2 do not have significant effects, whereas elements appended at node 6 do have significant dynamical effects.

The subject of quantitatively qualifying the dynamic similarity between two structures is examined in the next chapter. It is used within the design synthesis procedure to terminate the iterative process when an acceptable degree of similarity has been achieved. In the early iterative loops of the design synthesis procedure the dominate selection criterion must be based upon anti-resonaces. It is important to select a design change which maximises the changes in the anti-resonances (ie steepest gradient approach). By adopting this selection basis the general mass and stiffness distribution will be achieved as the design moves towards the correct anti-resonance values. Once the correct general mass and stiffness distribution has been achieved the selection process should change to ensure that the correct resonance frequencies are achieved. Based upon these observations the design case (2) would be selected as the optimum design change for the first iteration of the design methodology.

Once this design change has been incorporated within the tentative design, the new tentative design is then assumed to be the initial tentative in the iterative procedure and the whole design process is repeated from step 3.

8.5 SUMMARY

1. Reasearchers in the field of vibrations have only examined the use of single linear springs or concentrated masses to systematically alter the dynamical characteristics of a structure. The effects of distributed parameter changes have not been examined.

2. The design of the continuous element can be classified as a distributed parameter optimal design problem.

3. The present distributed parameter optimal design procedures only utilise techniques where a specified structure is optimised to a given set of cost functions.

4. A design methodology is proposed where a poor initial design estimate is extented so as to satisfy a given set of cost functions.

5. The process is based upon a systematic extension of the initial tentative design estimate by identifying a single optimum design change which directs the tentative design towards an acceptable solution.

6. Design changes can be effected by one of three conditions;

a) Additions or modifications to the design topology.

b) Additions or modifications to the end restraints

c) Geometric changes to the sectional areas of the elements within the design.

7. The proposed design methodology is particularly suited to an inductive expert system application.

8. The first design loop within the proposed design methodology has been examined, with reference to a small design problem, to show that the proposed design methodology is feasible and suitable for inclussion within a design synthesis procedure. After the initial design estimate has been intuitively derived it is possible to automate the optimisation of the design.

Two dimensional structure

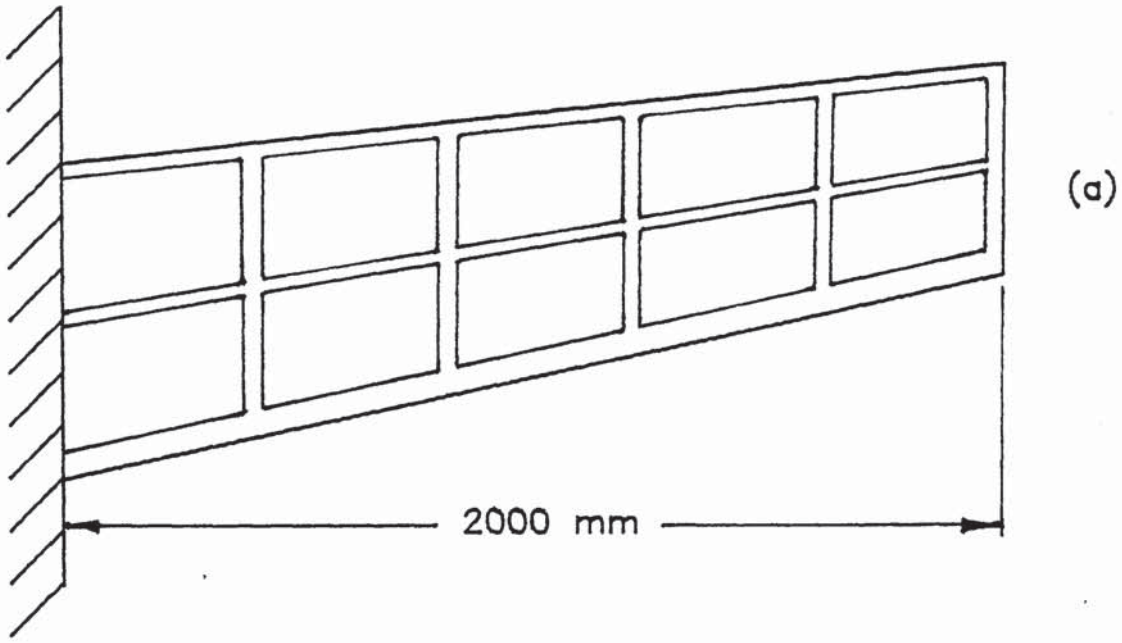

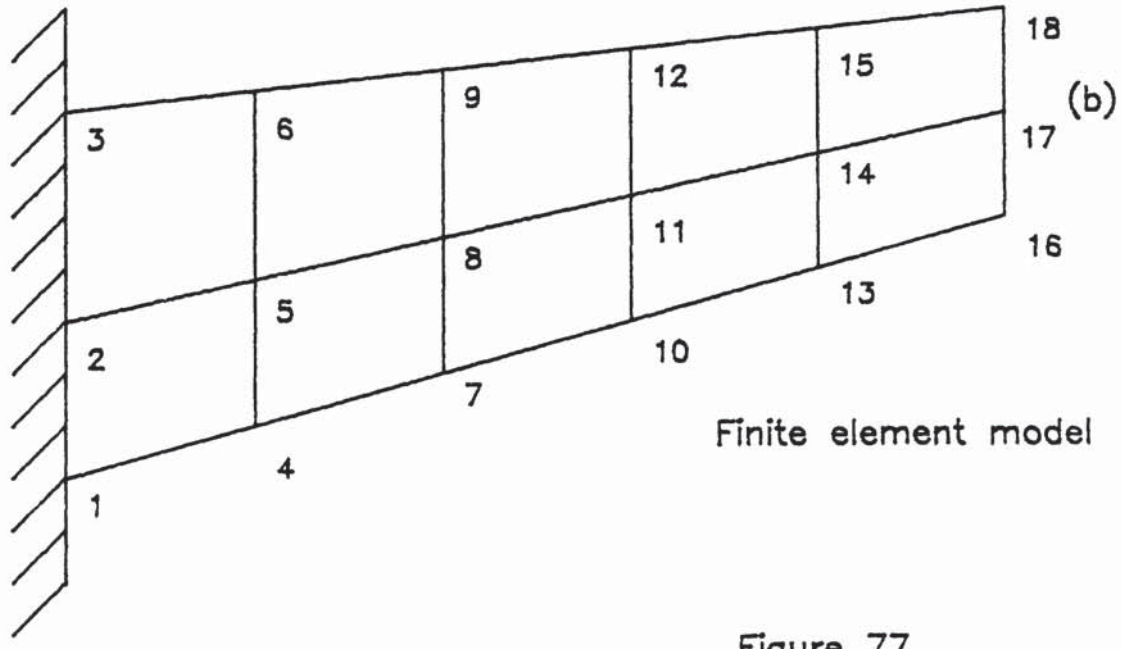

Finite element model

Figure 77

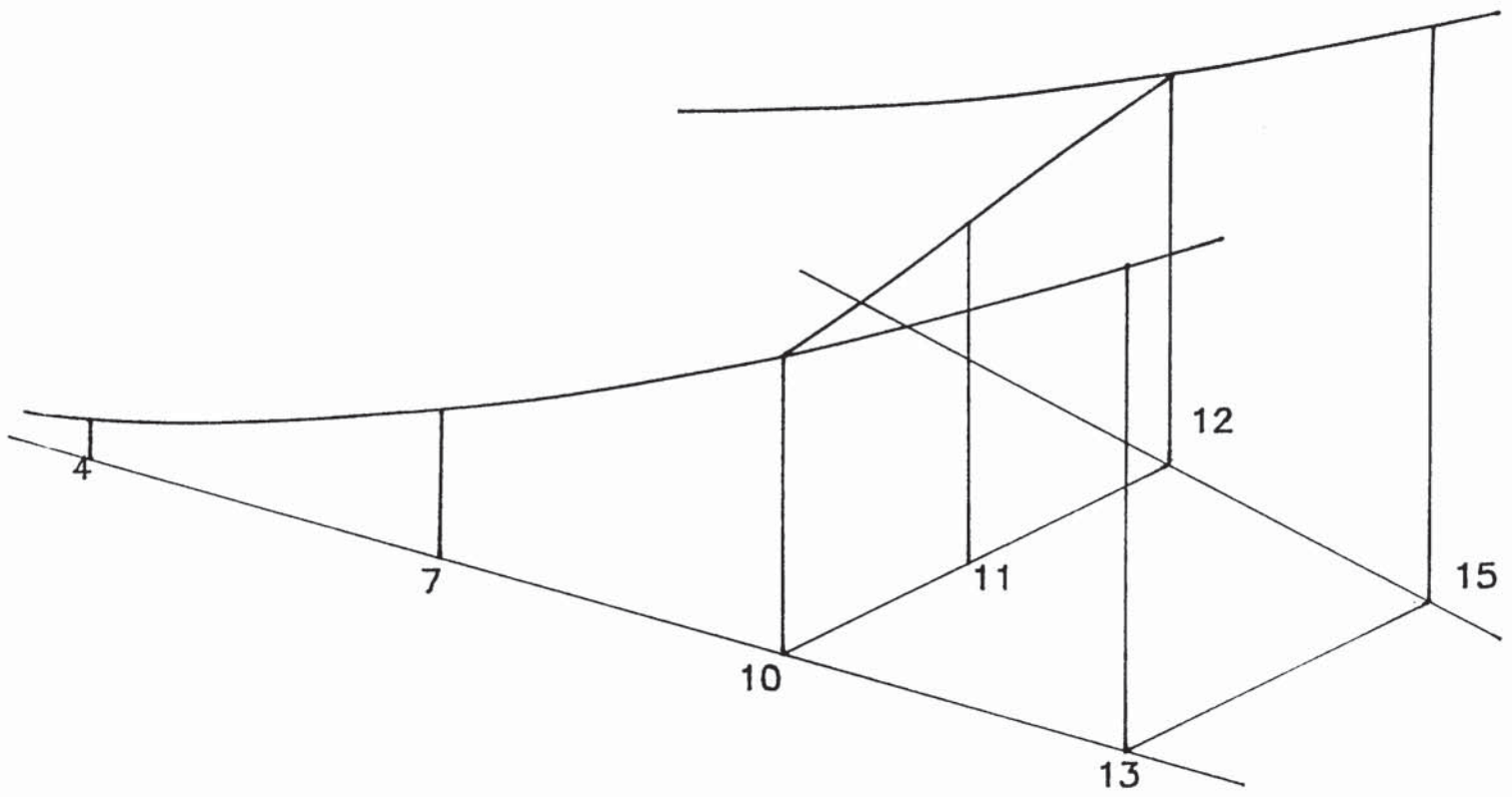

First mode of original structure

Figure 78

First Tentative design

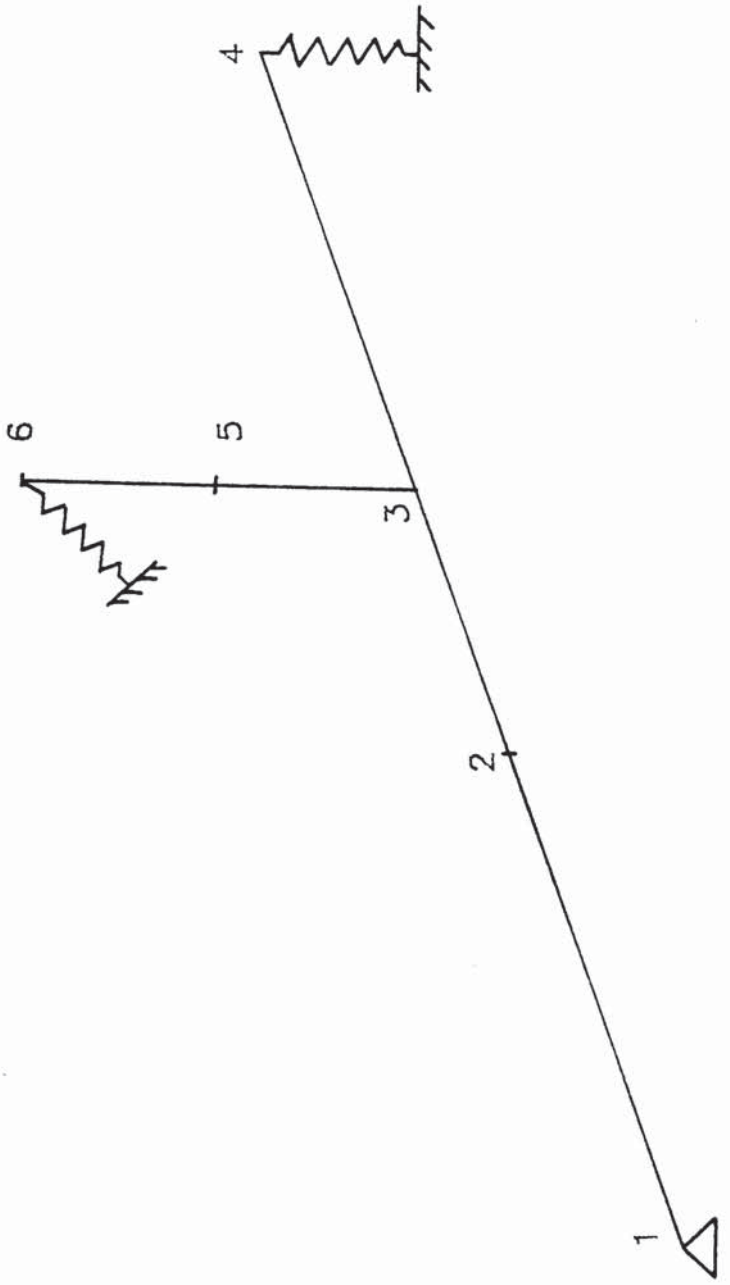

Figure 79

Main design changes

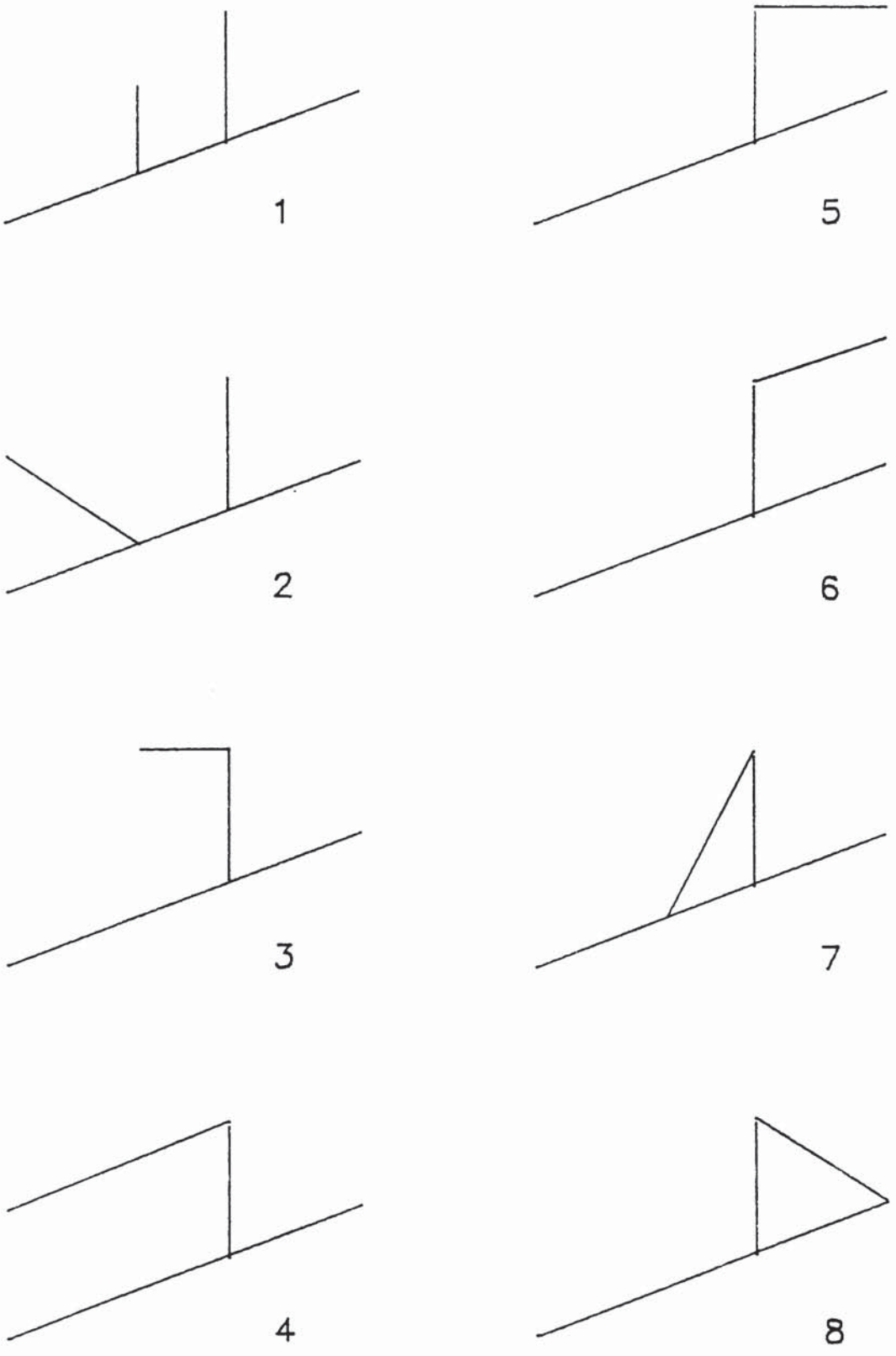

Figure 80

Design change No. 3

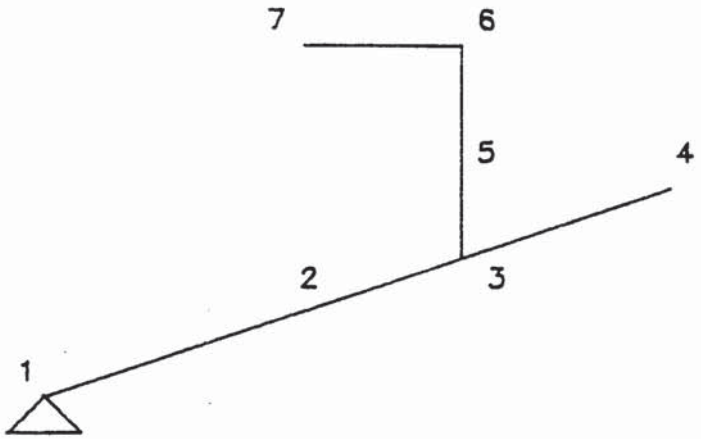

2.64	−5.429	1.634	1.749
	11.156	−3.358	−3.599
		1.011	1.086
			1.181

Mass difference matrix

37170	−77534	24480	21063
	162034	−51203	−43991
		16202	13844
			12087

Stiffness difference matrix

15.63

60.82

94.68

176.4

Resonance frequencies

Figure 81

Design change No. 4

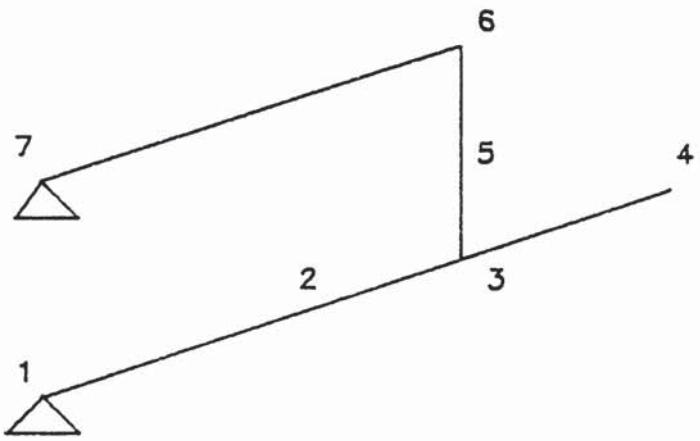

15.27	−30.644	10.053	8.128
	61.48	−20.17	−16.31
		6.618	5.35
			4.37

Mass difference matrix

121300	−245216	82248	56983
	496049	−166427	−115307
		55869	38652
			26887

Stiffness difference matrix

13.9

61.02

76.78

150.8

Resonance frequencies

Figure 82

Design change No. 5

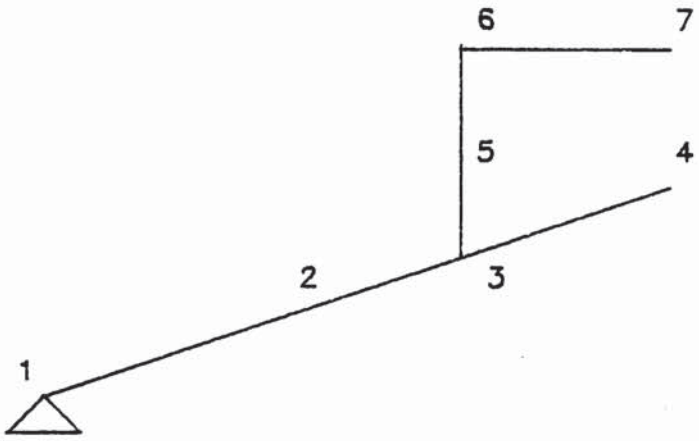

2.69	−5.581	1.956	1.728
	12.309	−4.286	−3.779
		1.54	1.339
			1.252

Mass difference matrix

22771	−46745	15298	11643
	98518	−32078	−25492
		10605	8086
			7180

Stiffness difference matrix

13.98

51.2

95.88

130.8

Resonance frequencies

Figure 83

9. CUMULATIVE DAMAGE

9.1 INTRODUCTION

When the philosophical considerations of the project were examined (Chapter 2) the overall objectives of the project and possible design methodologies were identified. The central objective of the work was to examine the feasibility of designing an environmentally representative test rig upon which transported equipment could be tested. The equipment was to be tested under realistic conditions in controlled laboratory tests until functional failure of the equipment had occurred. These tests would provide a high level of understanding of the equipment as well as confidence of the functional reliability of the equipment.

When equipment failure is observed it is due to an accummulation of cyclic stresses, normally of different levels, that ultimately cause failure of a structure or component. Now, modern transported equipment comprises mechanical, electro-mechanical and electronic systems. The electro-mechanical and electronic system will be encased within the equipment and are normally treated as lumped parameters. They are complex systems in their own right and a failure within these systems constitutes a failure of the whole of the equipment. If vibration tests are performed on the equipment the resultant modal data measured at the case of the equipment will be dominated by the large, high mass components within the equipment. It is, therefore, probable that the resonances and effects of the small intricate sub-systems will not be apparent within

the modal data recorded at the case of the equipment. This introduces a new design constraint to the designer of the test rig as he will require not only the modal characteristics at the attachment points but also knowledge of critical frequencies which are related to the small sub-systems within the equipment. This knowledge of the critical frequencies will be used within the assessment of the quality of dynamic similarity. This constraint reflects upon one of the original design premises, that the same test rig can be used for a range of transported equipment. It is, therefore, imperative that the assessment of the dynamical similarity accounts for not only the accuracy of the resonance frequencies but also the anti-resonance frequencies. If acceptable values are obtained for resonances and anti-resonances the correct mass and stiffness distribution will have been achieved. The correct mass and stiffness distribution will ensure that the correct level of vibration for the frequency range of interest, will be transferred from the rig to the equipment and hence excite the small sub-sysems realistically. Once the test rig exhibits realistic levels of vibration the final variable within the test cycle is the forcing function to the rig. It is important to ensure that this is realistic as incorrect excitation of the rig will produce errors in the performance of the equipment and completely nullify the efforts of obtaining a dynamically similar test rig structure.

It is possible to provide techniques for qualitative

assessment of dynamic similarity by overlaying frequency response plots and by comparing resonance and anti-resonance frequency values.

In addition a quantitative assessment of the dynamic similarity can be achieved by examining the error in the cumulative damage to the equipment at the attachment points.

In the previous chapter it was proposed to use cummulative damage assessment within the design methodology for two functions:

(a) to assist with the selection of the optimum design change to the tentative design.

(b) to provide a quantitative assessment of the quality of the design similarity so that the design loop may be terminated.

In the philosophical consideration (Chapter 2) it was thought that an alternative basis to using modal characteristics for the design methodology was the use of cummulative damage theory and therefore this was borne in mind when cumulative damage was examined.

It is towards these proposals of incorporating cummulative damage assessment within the design methodology that two problem cases are examined.

(i) one degree of freedom system

(ii) multi-degree of freedom system

9.2 CUMULATIVE DAMAGE THEORY

The basic principle of fatigue damage prediction centres around the notion that repeated cycles of stress in a structure or system will ultimately cause a crack to form and then propogate producing a failure. The curve which describes the number of stress cycles required to cause this failure is the well established S-N curve. The simplest rule for the accumulation of fatigue damage is that atributed to Miner. Miner's hypothesis states that the damage D caused to a system is equal to

$$D = \sum_i \frac{n_i}{2N_i} \tag{901}$$

where

N_i is the number of cycles at the at the stress level σ_i required to break the component.

n_i is the number of half cycles of amplitude z_i.

If it is assumed that the stress is proportional to the amplitude then

$$\sigma_i = k z_i \qquad (k \text{ is constant}) \tag{902}$$

The Wohler curve (S-N curve) can be represented as

$$N_i \sigma_i^{\,b} = c \qquad (903)$$

where b and c are constants and a function of the material.

If (902) and (903) are substituted into (901) we obtain an expression for the cumulative damage as

$$D = \frac{k^b}{2c} \sum_i n_i z_i^{\,b} \qquad (904)$$

This expression highlights that the damage is a function of the dynamical properties of the system (z_i) and the material properties (b).

It is normal to lump the constants together so that

$$\frac{2c}{k^b} \cdot D = \sum_i n_i z_i^{\,b}$$

is calculated.

Under realistic operational conditions the system will be exposed to a range of exciting frequencies. If the cumulative damage is plotted against a specified frequency range of the input forcing function, then a plot called the 'fatigue damage spectrum' is obtained. This plot can be used as the basis for quantitatively assessing the damage difference between two structures.

The two systems that are to be compared for dynamic similarity share the same transported equipment. The work on coupling structures has shown that the dynamical

characteristics of the coupled structure is different to the individual component systems and, therefore, if quantitative assessment between the test rig and the original structure is to be made the transported equipment must be coupled to each structure prior to comparison. This imposes a restriction on one of the original design premises of using the 'clean' test rig for a range of transported equipment.

Since the same equipment is used between the two structures the material properties (b) will be constant. This leaves only the dynamical properties of each system to be compared by the use of fatigue damage spectrum plots.

A convenient dynamical property to compare dynamical difference is receptance since it is easy to derive analytically or experimentally. If the receptance (x/F) at each of the attachment points is used, for each coupled system, then the difference between the corresponding receptance curves will provide a measure of the error in the cumulative damage to the equipment. It is assumed that the same input function is applied to each system so that consistant receptance plots are compared. If this error is then multiplied by the number of cycles at each frequency interval a quantitative assessment in the form of a fatigue damage spectrum plot is obtained.

By using receptance curves for the attachment points it is possible to examine the error in:

(a) point cumulative damage

(b) transfer cumulative damage

Since we are considering multi-point attachment equipment the overall motion of the equipment in heave, pitch and roll is important, not the individual motions at each attachment point. This motion is best examined by considering the receptance matrix for the complete structure at the attachment points and hence deriving the fatigue damage spectrum matrix for the same points.

9.3 ONE DEGREE OF FREEDOM SYSTEM

If a one degree of freedom system is considered then there are three possible error conditions.

a) An error in the natural frequency.

b) An error in the damping.

c) An error in the general level of vibration.

a) Natural frequency

A simple one degree of freedom system (Figure 84) was modelled and the conditions of 5, 10, 20, 50 and 100% error in the natural frequency was computed. The nominal correct frequency is 100 Hz.

One degree of freedom system

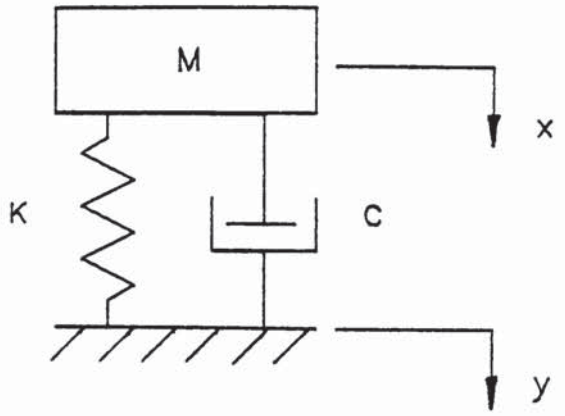

Figure 84

If it is assumed that the the input ( ) is sinusoidal and constant for all the runs then Figure 85 can be obtained which is a plot of the error in displacement ( ) against frequency. A material constant of b=5 has been assumed. The error has been normalised with respect to the 100 % error condition.

The plot has two interesting features ;

i) The negative displacement error is a measure of the damage not being achieved. For each of the error conditions the maximum displacement error is stationary at the frequency of the original system.

ii) The positive displacement error is a measure of the incorrect damage being applied to the system. The peak of each displacement error is a function of the error of the system and is therefore not stationary.

It is possible to plot an envelope of the maximum

displacement errors (Figure 86) which shows that within an error range of ± 30% there is a change of 80% in the displacement. The change in the resonant frequency could cause undesirable vibrations of the individual components within the equipment. The rapid increase in damage (damage normalised displacement) for a small error in resonant frequency emphasises the need for accurate frequencies within the design structure.

b) Damping

The same model (Figure 84) was used, and for this case the damping was changed by the same percentage levels of error (Figure 87). When the envelope of these displacement errors are plotted (Figure 88) it shows that small errors in damping are not critical.

c) General level

Consider the receptance of a single mass with an applied load,

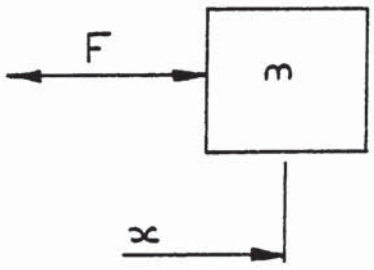

Equation of motion $F = m\ddot{x}$

or $F = -\omega^2 m x$

the receptance is $\alpha_m = \frac{x}{F} = \frac{1}{-\omega^2 m}$

or $\log(|\alpha_m|) = -\log(m) - 2\log(\omega)$

which is a straight line with a slope of -2 on a plot of $\log(|\alpha_m|)$ vs $\log(\omega)$

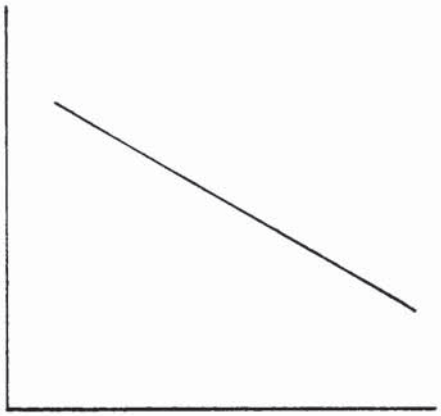

This line will move in the vert. plane depending upon the absolute value of m.

Consider the receptance of a simple spring,

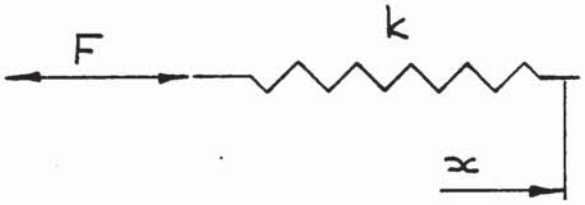

the equation of motion is $F = kx$

the receptance $\alpha_k = \frac{x}{F} = \frac{1}{k}$

or $$\log(|\alpha_k|) = -\log(k)$$

If these characteristics are combined to represent the system in Figure 84, then they can be presented on a logarithmic receptance plot (Figure 89).

One degree of freedom system response

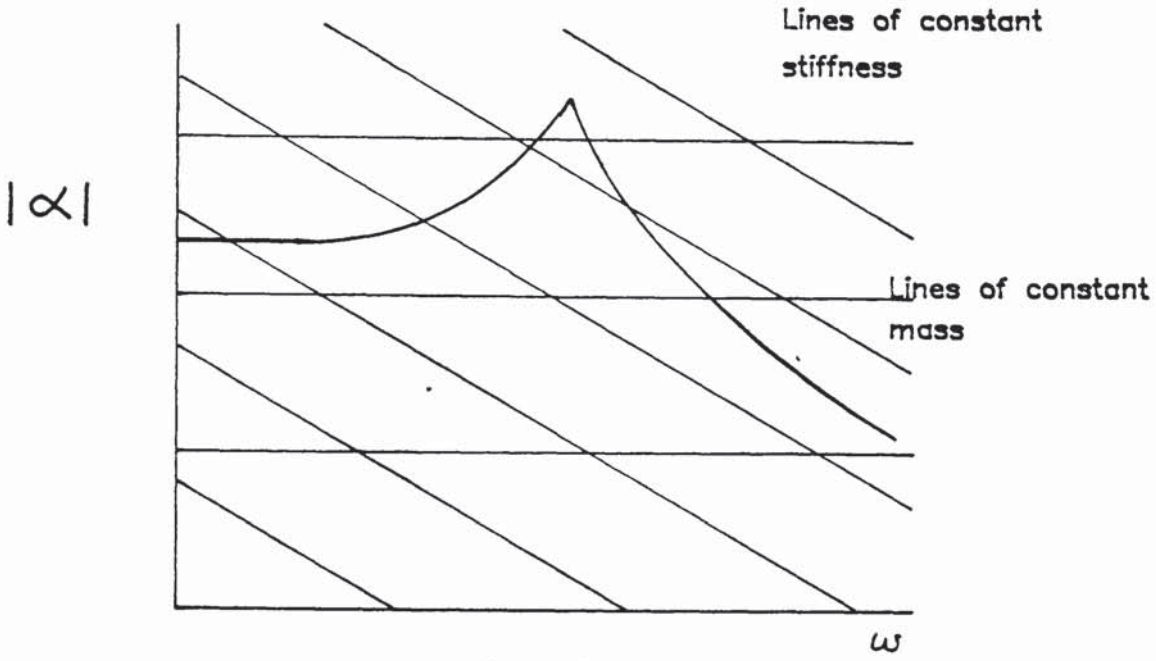

Figure 89

The amplitude of the peak is a function of the damping of the system.

Now, if the value of the stiffness is changed and the corresponding change is made to the mass the resonant frequency of the system will not alter. However, the curve will be displaced in the vertical plane to reflect the changes in the individual elements.

The work in sections (a) and (b) on errors in resonant frequency and damping has shown that the effective contribution to damage is only achieved around the resonant frequency.

Now the generalised expression for receptance is

$$\alpha_{ij} = \sum_{r=1}^{n} \frac{{}_r\phi_i \; {}_r\phi_j}{\omega_n^2 \left(\left(1 - \left(\frac{\omega}{\omega_n}\right)^2 + j 2 \xi_r \frac{\omega}{\omega_n}\right)\right.}$$

where i is response co-ordinate

j is the forcing co-ordinate

If it is assumed that the contribution is constant from other modes at the one selected and that the resonant frequency and damping level are the same between the structures under comparison then

$${}_r\alpha_{ij} \quad \text{proportional} \quad {}_r\phi_i \; {}_r\phi_j$$

Now if the mode shape vectors are mass normalised then

$${}_r\alpha_{ij} \quad \text{proportional} \quad \frac{1}{m_r}$$

where m_r is the modal mass for the r^{th} mode.

Therefore, errors in the general level of frequency response curves have the same form as Figure 88.

Under normal design conditions it is likely that errors will

occur in all three areas. If each error is multiplied by the number of cycles at each frequency interval then the individual damage curves can be added to give the total error to the cumulative damage spectrum.

9.4 MULTI DEGREE OF FREEDOM SYSTEM

The objective of designing a test rig which has defined dynamical characteristics (which are the same as a carrier body) is that when equipment is attached to the rig the dynamical characteristics of the test rig will change in the same fashion as the original carrier body. It is then possible to apply loads to the test rig rather than directly to the equipment.

If a damage assessment is to be made between the test rig and the original structure it must be made with both structures carrying the same equipment. In this way the dynamical changes that occur when two structures are coupled will be included.

Since it is proposed to excite the rig, the equipment will experience heave, roll and pitch in the same order and level as when attached to the original structure, providing dynamic similarity has been achieved. This means that the receptance matrix at the attachment points of the original carrier body and the test rig are the same. It is this feature which will allow a shift away from the present 3-axis testing methods.

To examine point and transfer cumulative damage error two types of multi-degree of freedom systems were examined.

i) Multi-degree of freedom discrete systems.

ii) Continuous and discrete systems.

In both cases the following algorithm was used to identify the cumulative damage error.

a) Specify the characteristics of the equipment.

b) Specify the characteristics of the original carrier body.

c) Specify the characteristics of the tentative design system.

d) Connect (a) and (b) at a defined coordinate.

e) Connect (a) and (c) at a defined coordinate.

f) Using the receptance curves of the coupled systems take (e) away from (d).

g) Plot the resultant error curve (for b=5) for the dynamical difference within the cumulative damage equation (904).

The multi-degree of fredom discrete system was primarily used to examine point coordinate cumulative damage error and the effects on small sub-systems within the transported equipment. The equipment was represented as a four degree of

freedom discrete system (Figure 90)

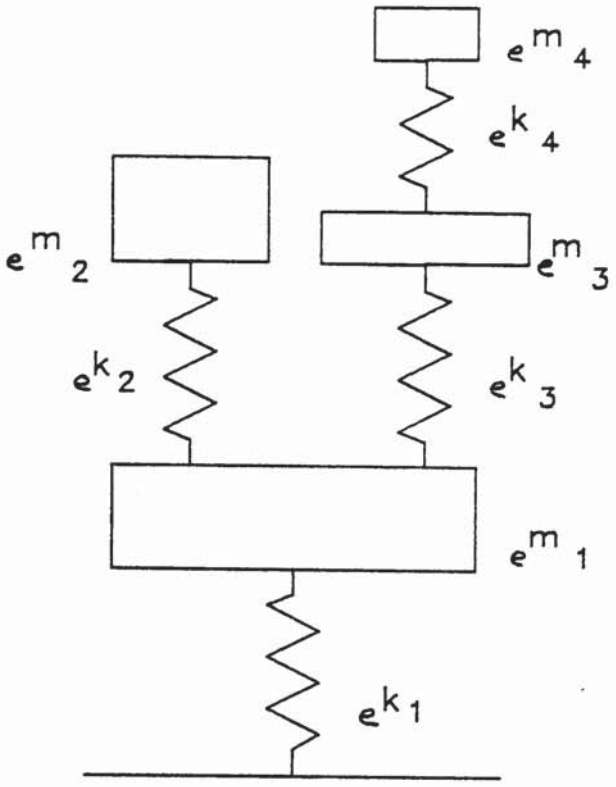

Transported Equipment

$e^{m}_{1} = 3.0$
$e^{m}_{2} = 1.0$
$e^{m}_{3} = 1.0$
$e^{m}_{4} = 0.1$
$e^{k}_{1} = 440$
$e^{k}_{2} = 150$
$e^{k}_{3} = 10$
$e^{k}_{4} = 16$

Figure 90

The mass $_{e}m_{4}$ and the stiffness $_{e}k_{4}$ were selected so that their individual resonance frequency was the same as one of the frequencies generated when the equipment was connected to the carrier body. The characteristics of the tentative design were selected so that an error would occur at this frequency. This was performed so that it was possible to assess the damage error to a small sub-system ($_{e}m_{4}$) within the transported equipment.

The original carrier body and the tentative design were represented by a simple discrete system (Figure 91).

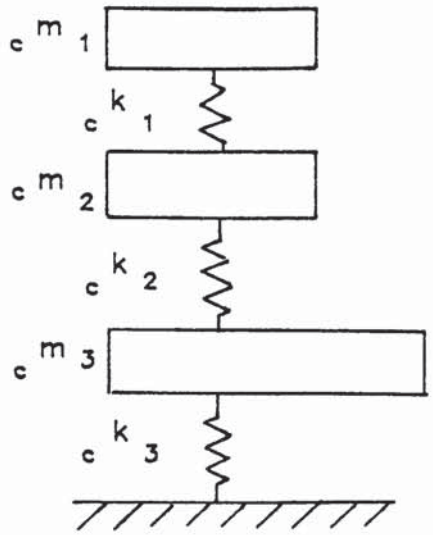

Carrier body

	Orig Structure	Tent Design
$_cm_1$	9.0	8.0
$_cm_2$	6.0	5.4
$_cm_3$	15.0	15.0
$_ck_1$	380	150
$_ck_2$	1750	1000
$_ck_3$	1200	1000

Figure 91

The equipment was coupled to the carrier body by connecting mass $_em_1$ (Eqipment) to mass $_cm_1$ (Carrier body), Figure 92. The effects of coupling the systems are shown in Figures 93 and 94. The resonance frequency of the small sub-system ($_em_4$ and $_ek_4$) within the equipment was set to 13 rad/s which corresponds to the fourth resonance of the coupled system.

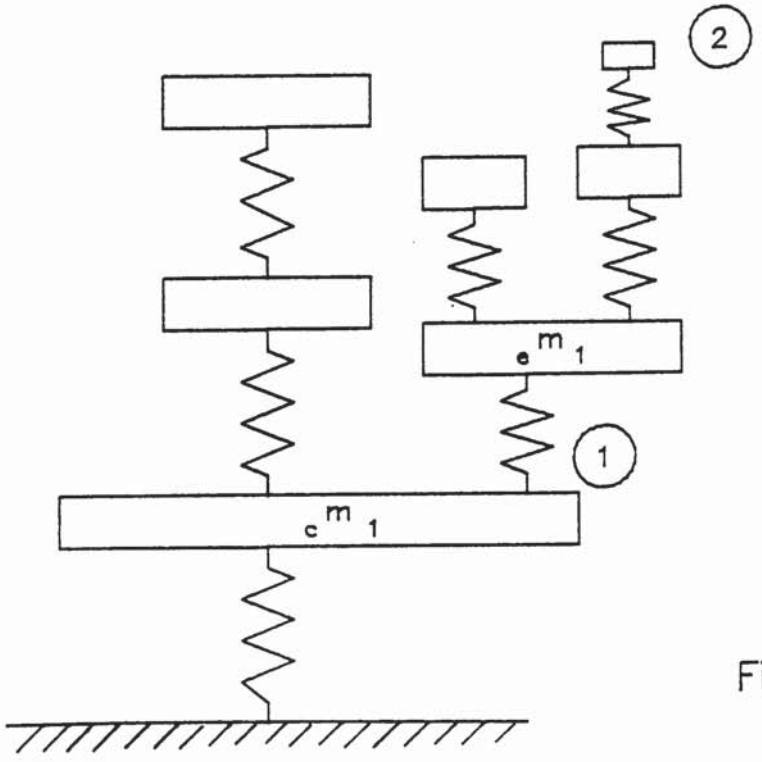

Figure 92

The error in the cumulative damage was initially examined for position 1, Figure 92. The algorithm for obtaining the displacement error was applied to the two coupled structures and a cumulative damage error plot was obtained, Figure 95. The error was conditioned by the material constant, assumed to be 5. The equation (904), states that the cumulative damage is proportional to the amplitude of vibration raised to the power of (b). This results in the narrow, 'spikey' damage error. Values that are negative in Figure 95, represent damage that is not being applied to the equipment and the positive values represent unrepresentative damage. It is interesting to note that for the particular configuration selected, the maximum damage error occurs at 8 rad/s when the two coupled structures are out of phase. The damage error has been plotted against a normalised linear scale to emphasise the two conditions of, (a), additional and, (b), missing cumulative damage. The modulus of the displacement error is shown in Figure 96, where a logarithmic scale is used for the displacement error. Although the two carrier bodies have quite different dynamical characteristics the cumulative damage error at the point of connection is small.

However, if the cumulative damage error is examined for the position 2, Figure 92, which represents the small sub-system within the equipment, the error is large. The modulus of the displacement error (Figure 97) is shown on the same axis scale as the error for position 1. The

general level of error for the small sub-system is at least an order of four greater than the error for position 1. A linear normalised displacement error plot, Figure 98, shows that the significant errors occur at the resonance frequency of the sub-system and at approximately 3 rad/s. A comparison of the eigenvalue analysis of the coupled systems showed that at 2.9 rad/s the two systems are out of phase at position 2.

When the tentative design is coupled to the equipment it does not have the same set of resonance frequencies as the original body. Therefore, the transmissability between positions 1 and 2 are different for each coupled structure. This is highlighted in Figure 98, where the negative peak at 13 rad/s emphasises that the correct level of vibration is not being transferred to the small sub-system at position 2. This observation emphasises the importance of obtaining the correct mass and stiffness distribution for the tentative design to ensure an acceptable level of dynamic similarity. It also emphasises that information relating to any critical sub-system within the equipment must be available to the designer of the test rig so that the quality of the similarity at critical frequencies can be quantified.

Transfer cumulative damage error was examined by using the continuous structures used in Chapter 6, Figures 22a and 22b. When these structures were originally examined it was possible to achieve a visually acceptable level of point

coordinate similarity at the tips of each beam. This was achieved by making a qualitative assessment of the two point coordinate receptance curves. A quantitative assessment of the quality of similarity was obtained by using the error in the cumulative damage between the two structures, Figure 99. The greatest error occurred at the first resonance where there was a 2.4% error in the resonance frequency value between the original structure and the substitute structure. This emphasised the importance of correct resonance frequencies as even a small error resulted in a large error in the cumulative damage spectrum.

If the plot of the displacement error for the transfer receptance between the tip and the 300 mm coordinate (Figure 100) is compared with the error in the point coordinate at the tip then only one extra significant change is observable. An extra error occurs at the first of the intermediate frequencies (1407 rad/s). The amplitude of this error is an order of four lower than the error at the first resonance. If this plot was used in isolation to assess the quality of dynamic similarity it would be easy to mistakenly interept that the transfer dynamic similarity was acceptable. The previous section, examining the effects of dynamical errors on small sub-systems within the equipment, has shown that if one of the intermediate frequencies corresponds with the individual frequency of the sub-system then the cumulative damage is not representative.

When examining the quality of dynamic similarity using the cumualtive damage approach the importance of the anti-resonances within the carrier body and equipment are not apparent. It is, therefore, very difficult to visualise a feasible design methodology using only cumulative damage criteria as a design basis.

9.5 SUMMARY

1. It is possible to obtain a quantitative assessment of the quality of dynamic similarity by using cumulative damage theory.
2. A small error in the resonant frequency has a significant effect on the displacement. Since damage is proportional to the displacement raised to a power greater than one it is important to obtain accurate resonant frequency values within the tentative design.
3. A small error in the damping is not critical.
4. A small error in the general level of the frequency response curve is not critical.
5. An error in the resonant frequency has two major effects;
    a) Damage that is not achieved
    b) Damage that is incurred at a different frequency.
6. To obtain a quantitative assessment of the quality of similarity it is necessary to consider the whole

coupled structure (equipment and carrier body).

7. When the equipment is coupled to the carrier body new resonance frequencies are generated. There is also a shift in the values of the resonaces of the individual systems. These new resonaces mean that the designer of the test rig must be aware of any critical sub-systems within the equipment.
8. Cumulative damage theory cannot be used in isolation as a design basis for representative test rigs, since the importance of anti-resonance values are not apparent.
9. It is desirable to use a combination of modal characteristics and cumulative damage to derive a feasible design methodology that assesses the quality of dynamic similarity.

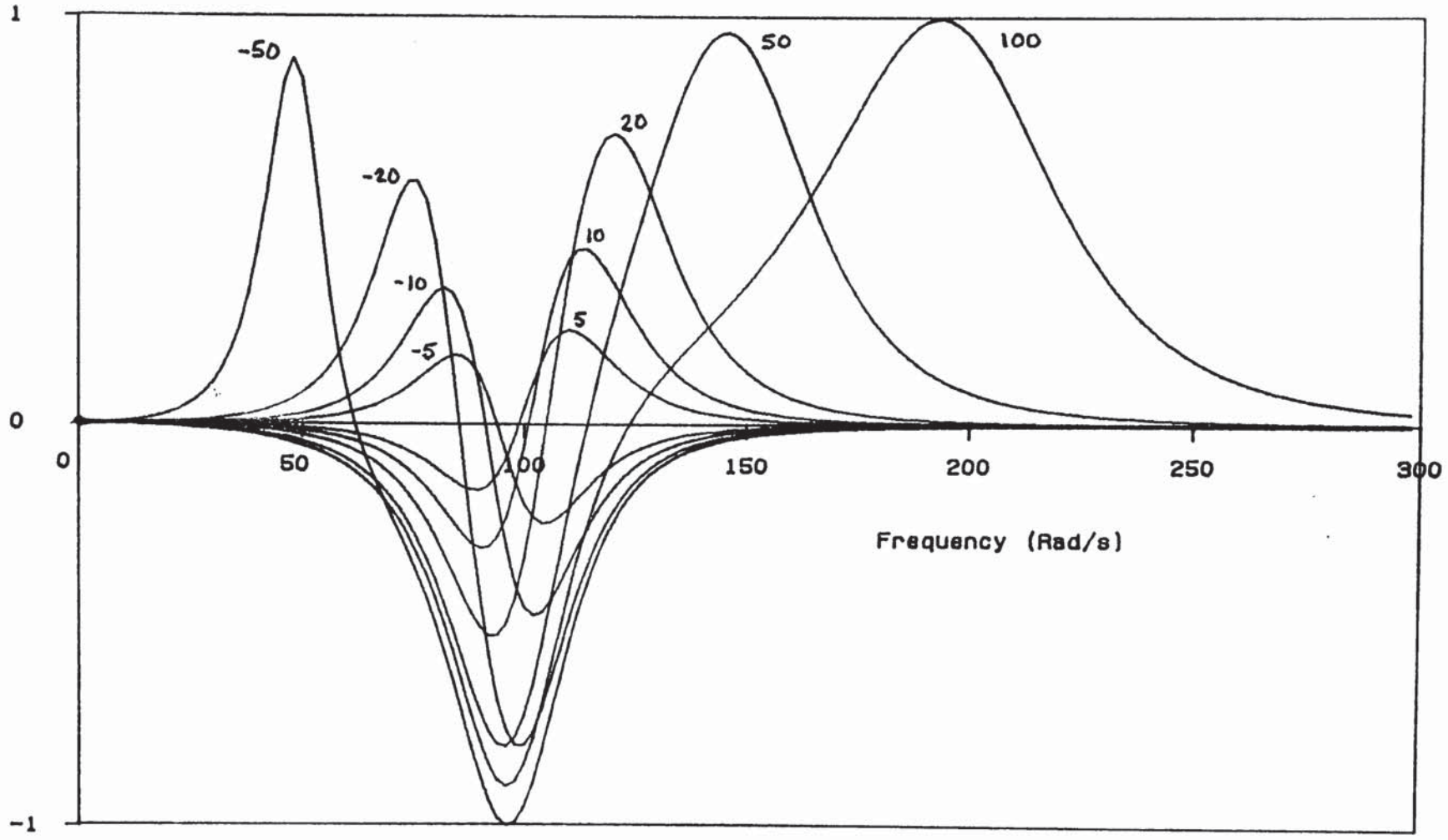

Frequency error for One degree of freedom

Figure 85

Frequency error

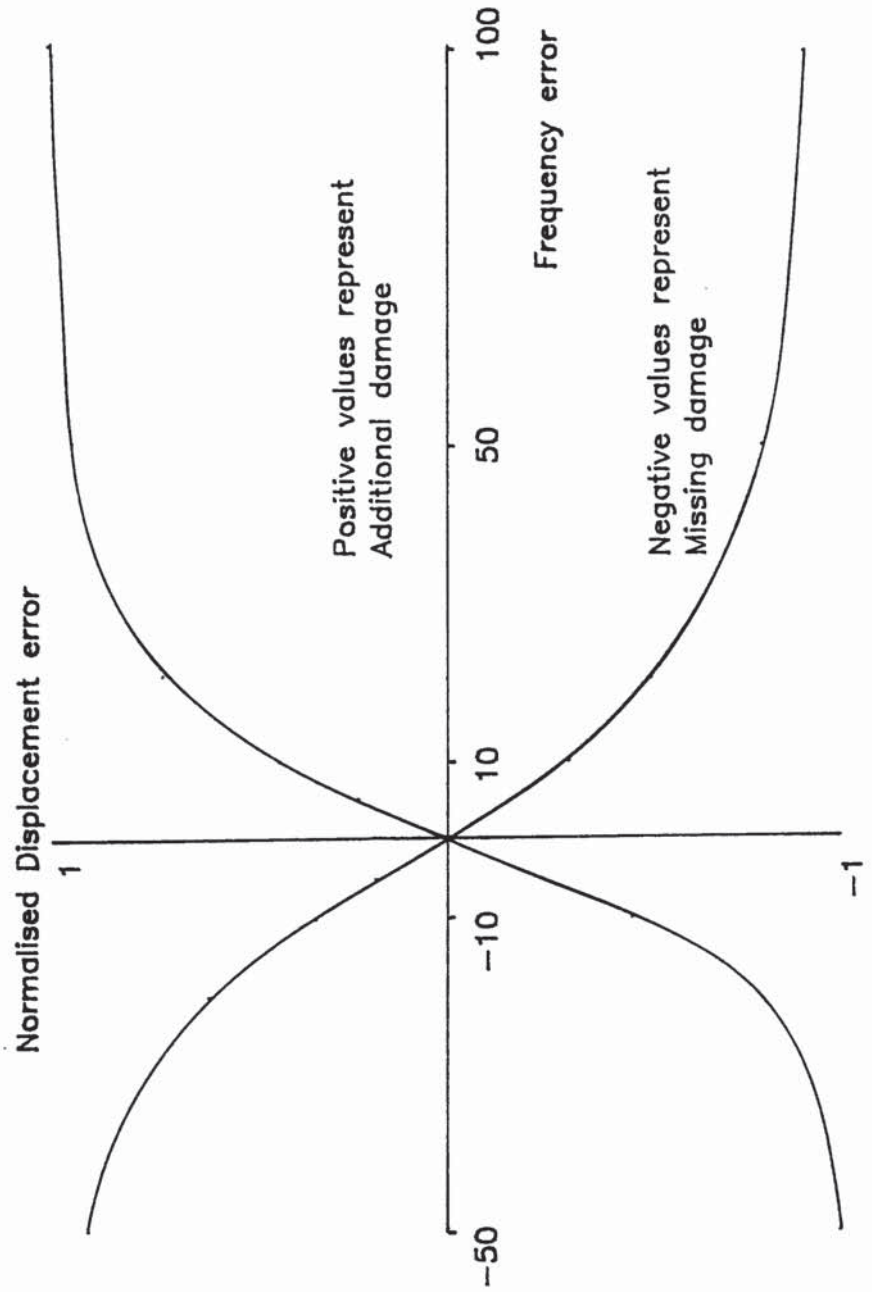

Figure 86

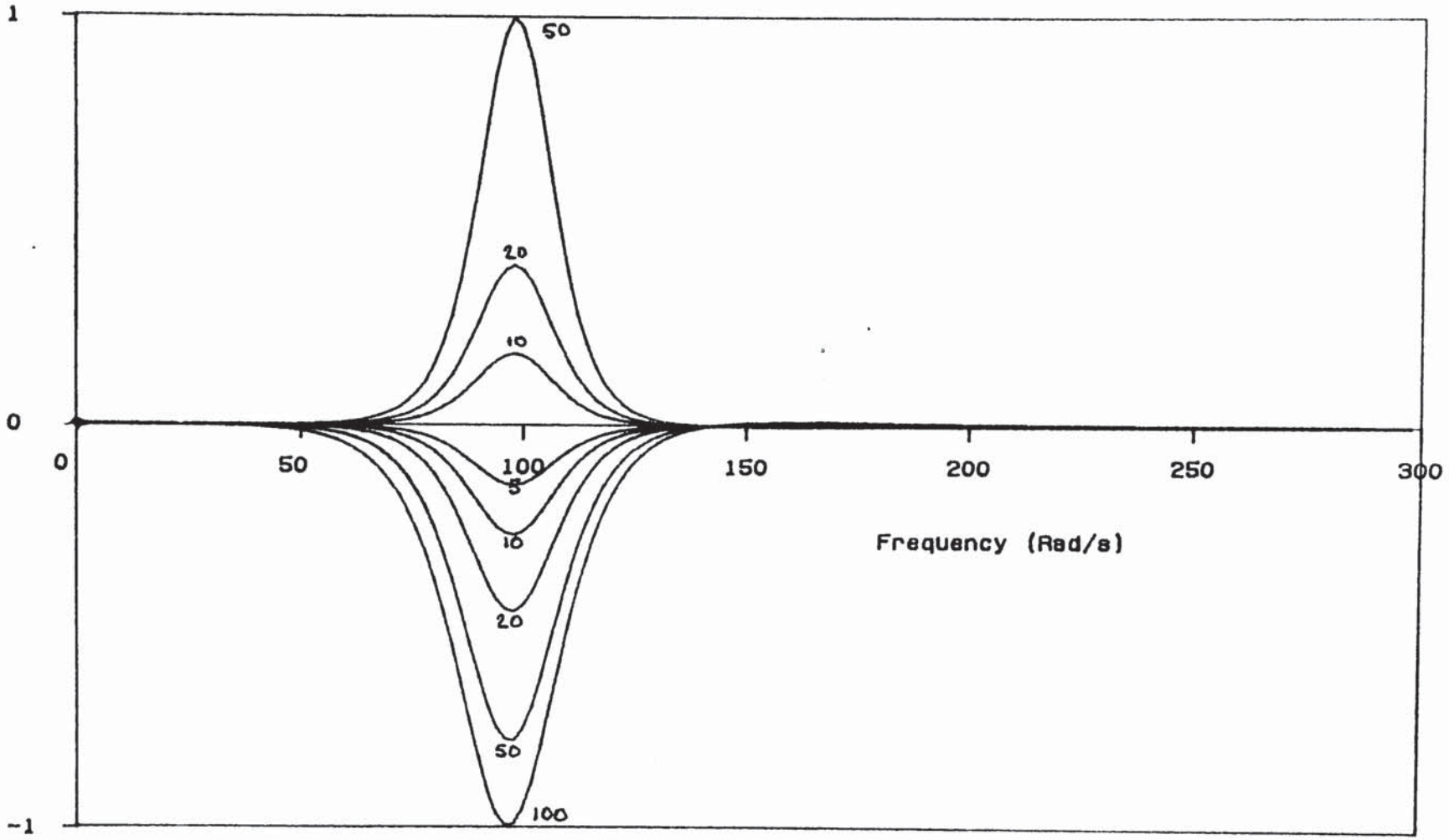

Damping error for One degree of freedom

Figure 87

Damping error

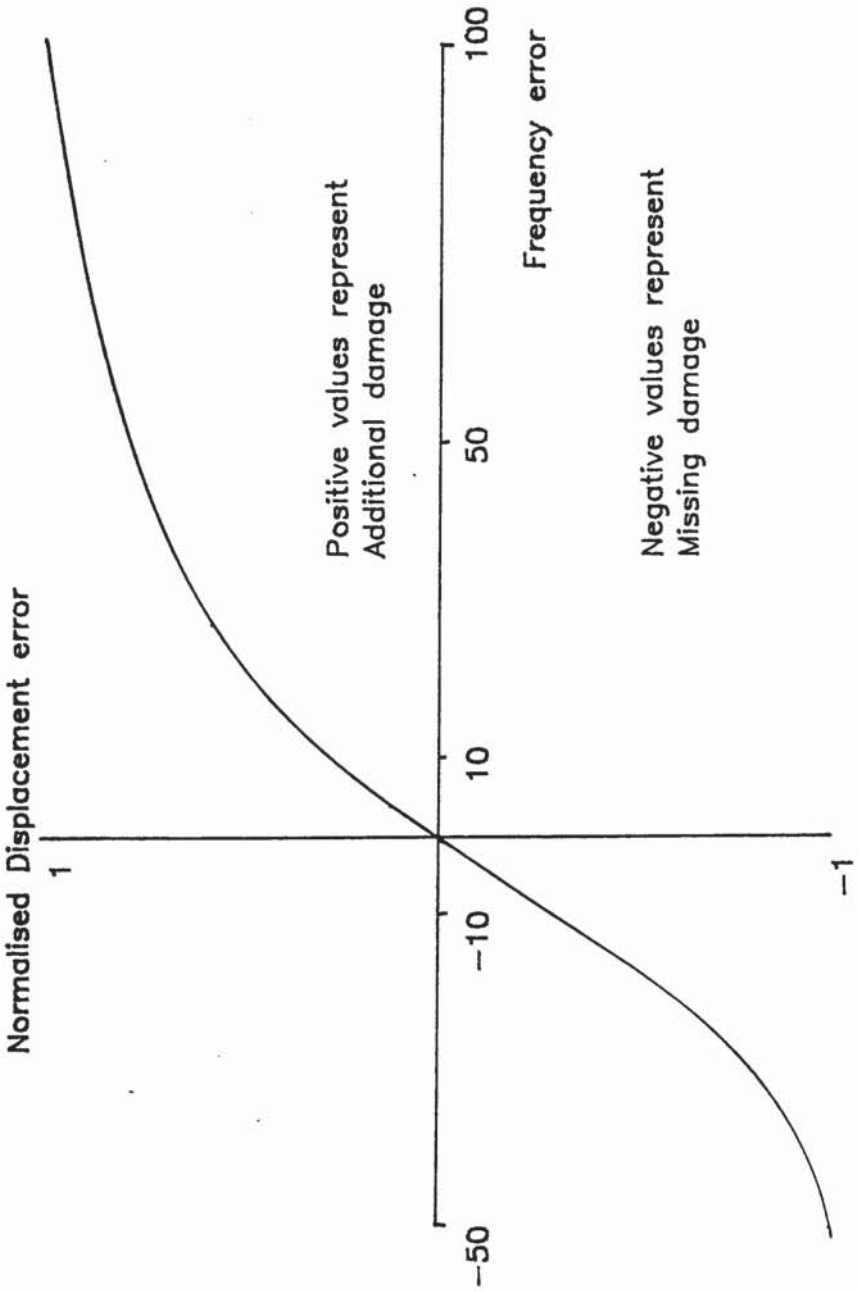

Figure 88

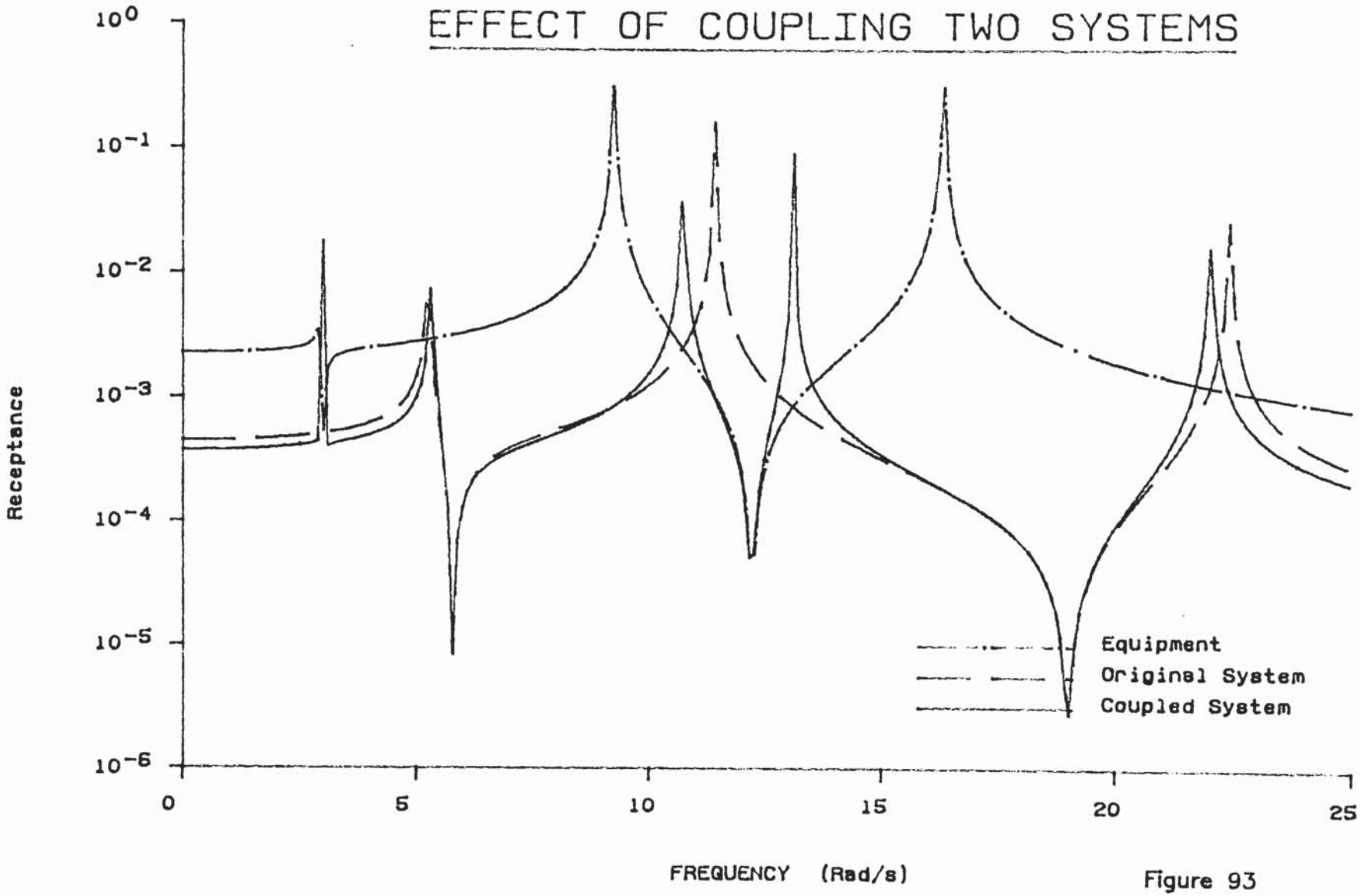
EFFECT OF COUPLING TWO SYSTEMS
Receptance
10^{0}
10^{-1}
10^{-2}
10^{-3}
10^{-4}
10^{-5}
10^{-6}
0
5
10
15
20
25
FREQUENCY (Rad/s)
Equipment
Original System
Coupled System

Figure 93

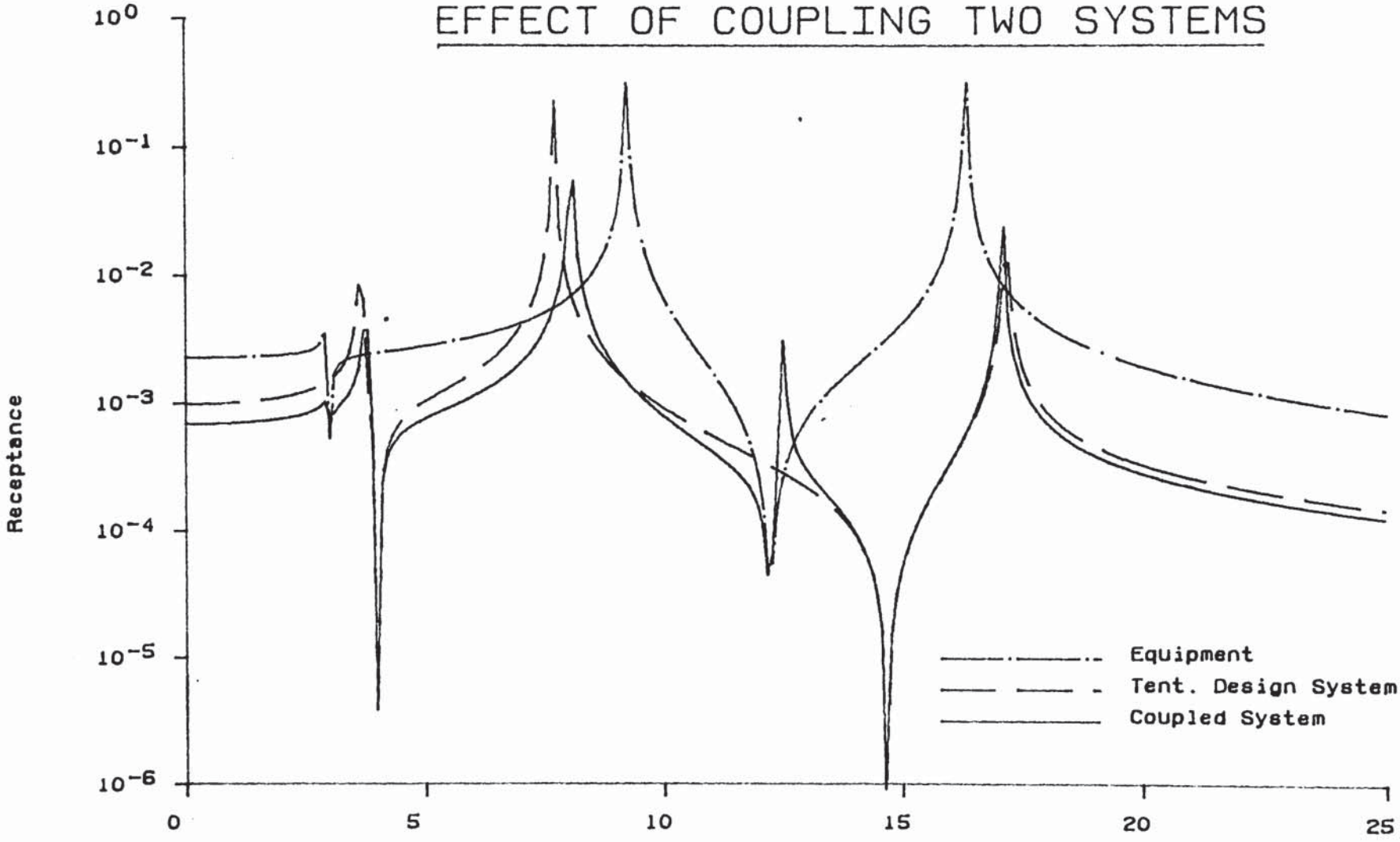
EFFECT OF COUPLING TWO SYSTEMS
Receptance
10^{0}
10^{-1}
10^{-2}
10^{-3}
10^{-4}
10^{-5}
10^{-6}
0
5
10
15
20
25
FREQUENCY (Rad/s)
Equipment
Tent. Design System
Coupled System

Figure 94

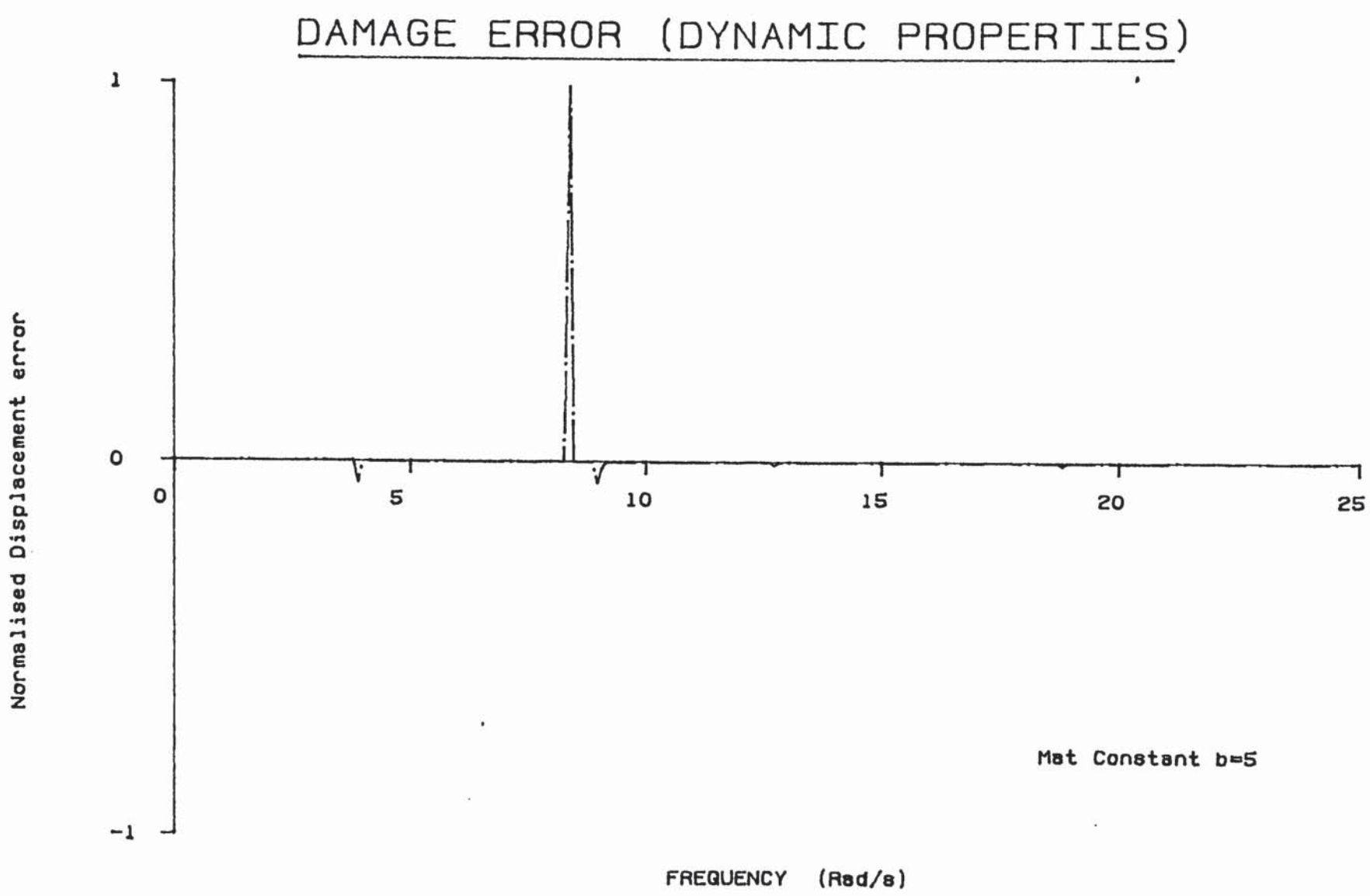
DAMAGE ERROR (DYNAMIC PROPERTIES)
Normalised Displacement error
1
0
-1
0
5
10
15
20
25
Mat Constant b=5
FREQUENCY (Rad/s)

Figure 95

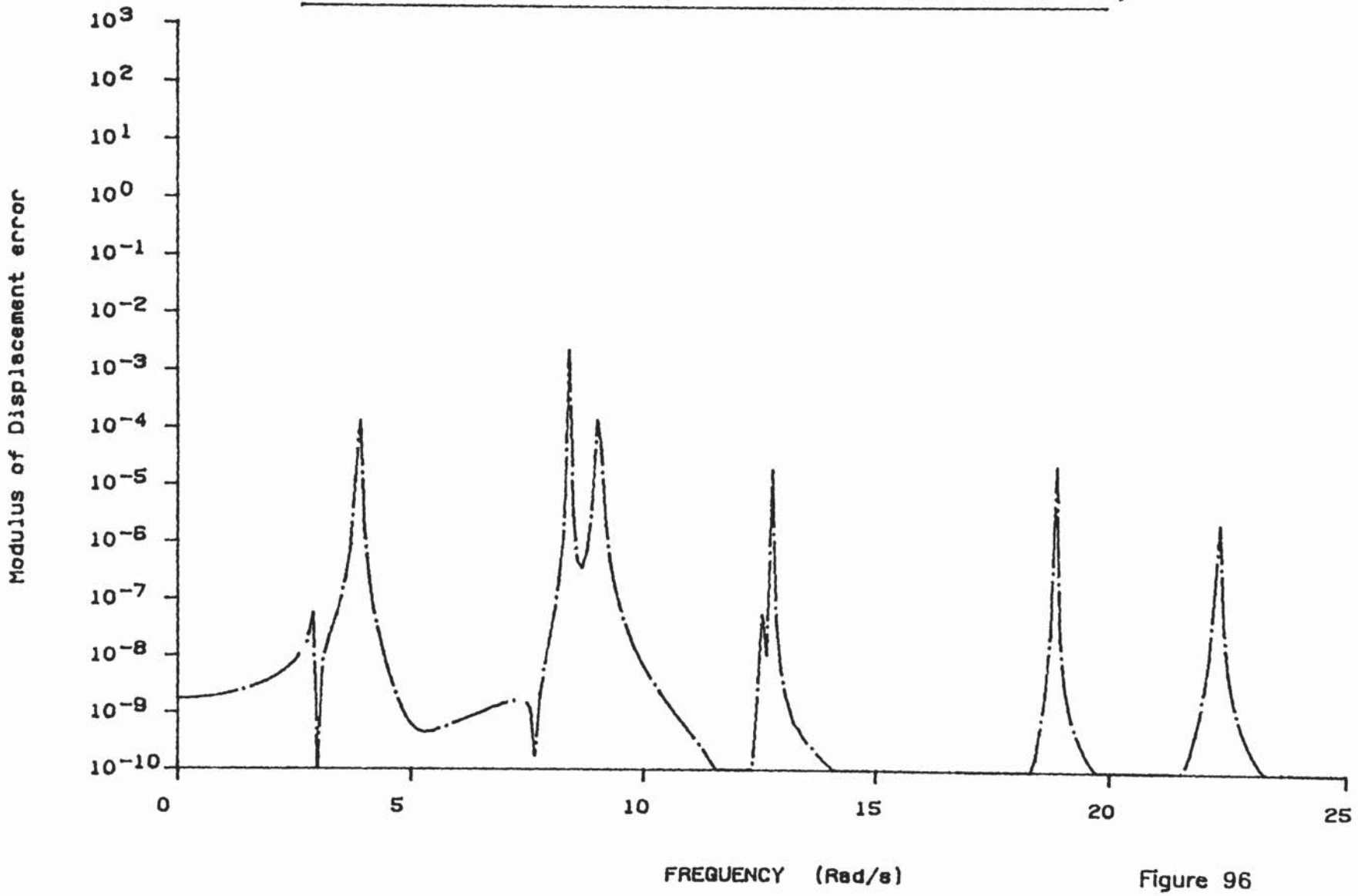
DAMAGE ERROR (Mat Constant b=5)
Modulus of Displacement error
10^{3}
10^{2}
10^{1}
10^{0}
10^{-1}
10^{-2}
10^{-3}
10^{-4}
10^{-5}
10^{-6}
10^{-7}
10^{-8}
10^{-9}
10^{-10}
0
5
10
15
20
25
FREQUENCY (Rad/s)

Figure 96

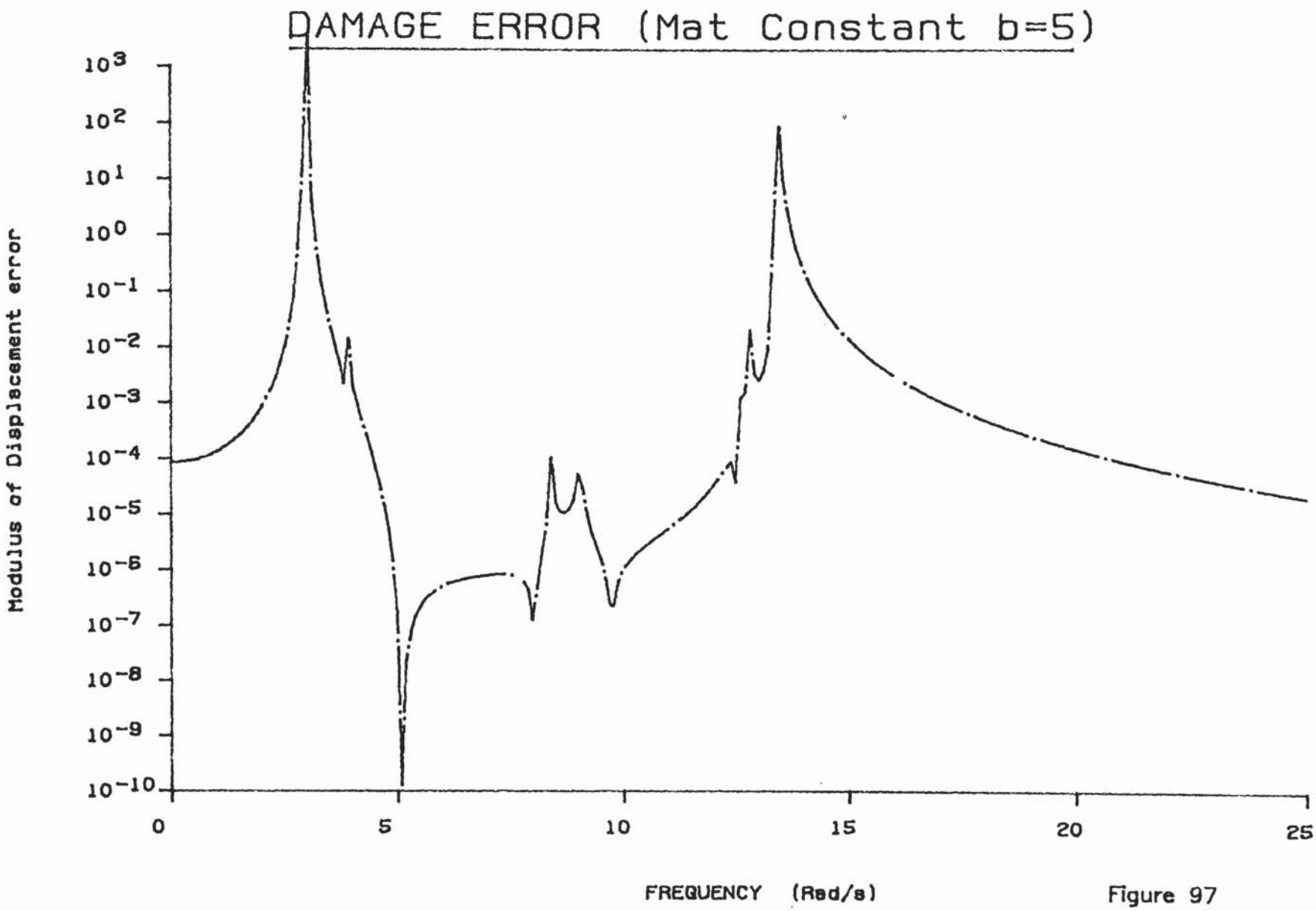
DAMAGE ERROR (Mat Constant b=5)
Modulus of Displacement error
10^3
10^2
10^1
10^0
10^-1
10^-2
10^-3
10^-4
10^-5
10^-6
10^-7
10^-8
10^-9
10^-10
0
5
10
15
20
25
FREQUENCY (Rad/s)

Figure 97

DAMAGE ERROR (DYNAMIC PROPERTIES)

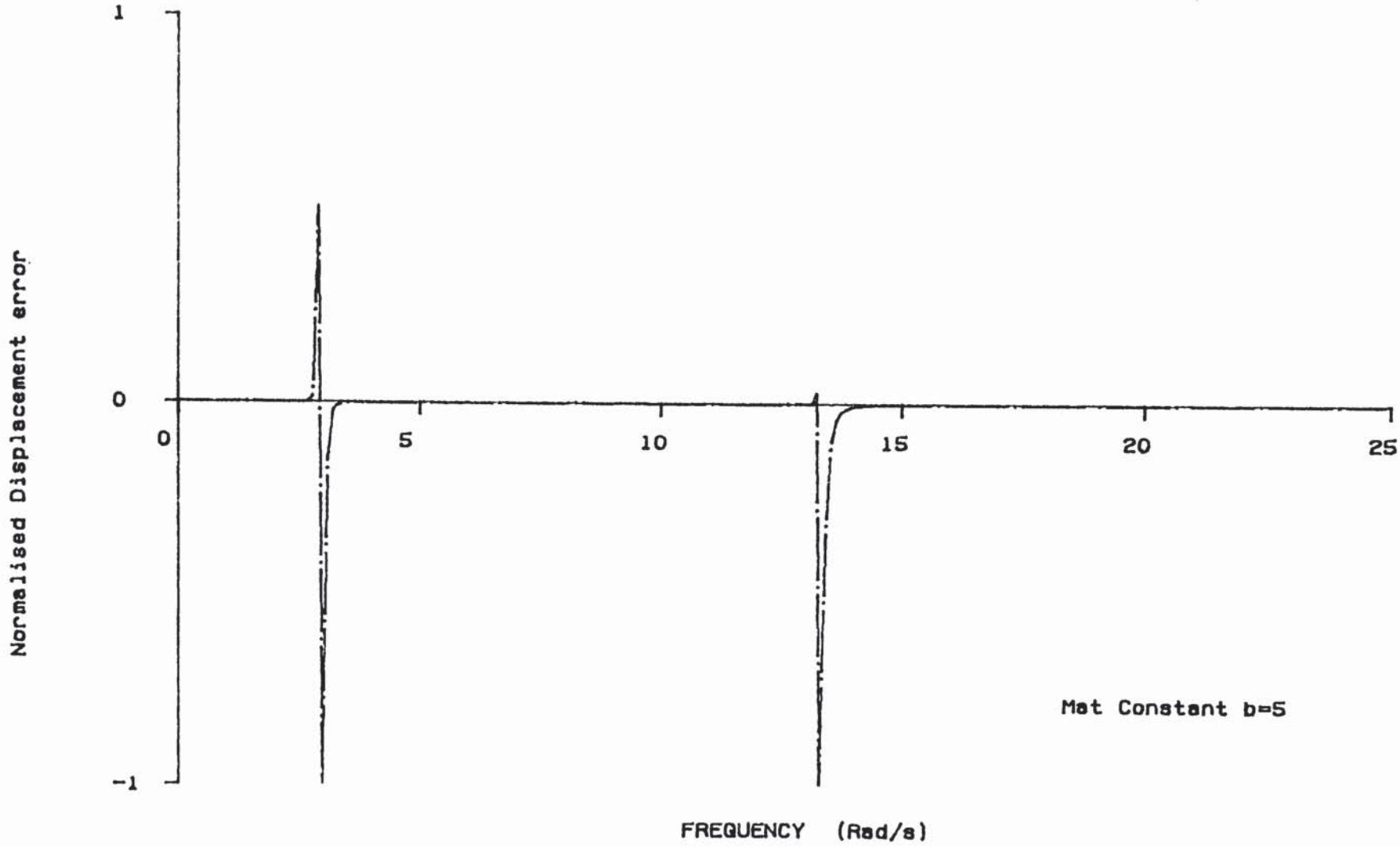

Figure 98

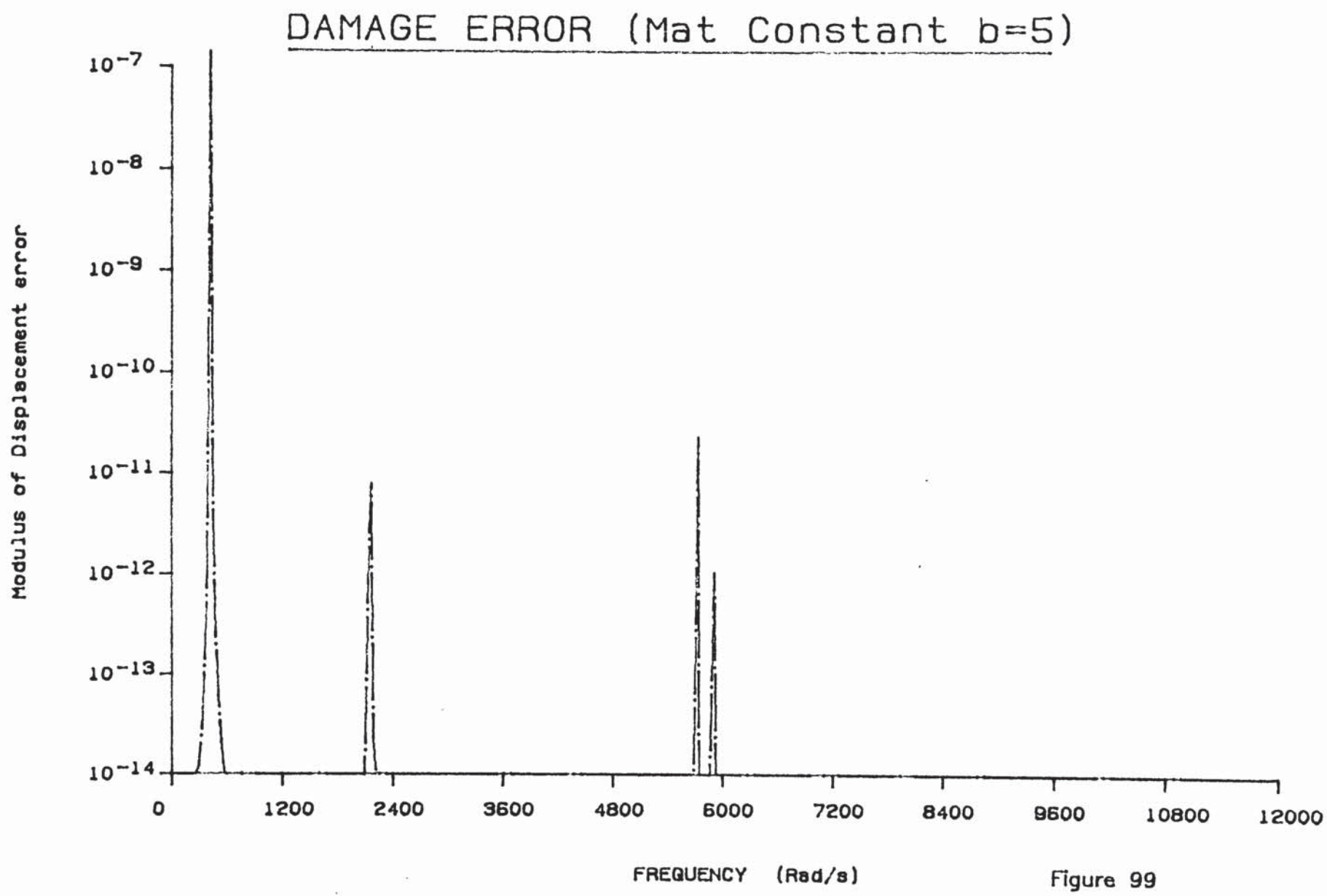
DAMAGE ERROR (Mat Constant b=5)
Modulus of Displacement error
10-7
10-8
10-9
10-10
10-11
10-12
10-13
10-14
0
1200
2400
3600
4800
6000
7200
8400
9600
10800
12000
FREQUENCY (Rad/s)

Figure 99

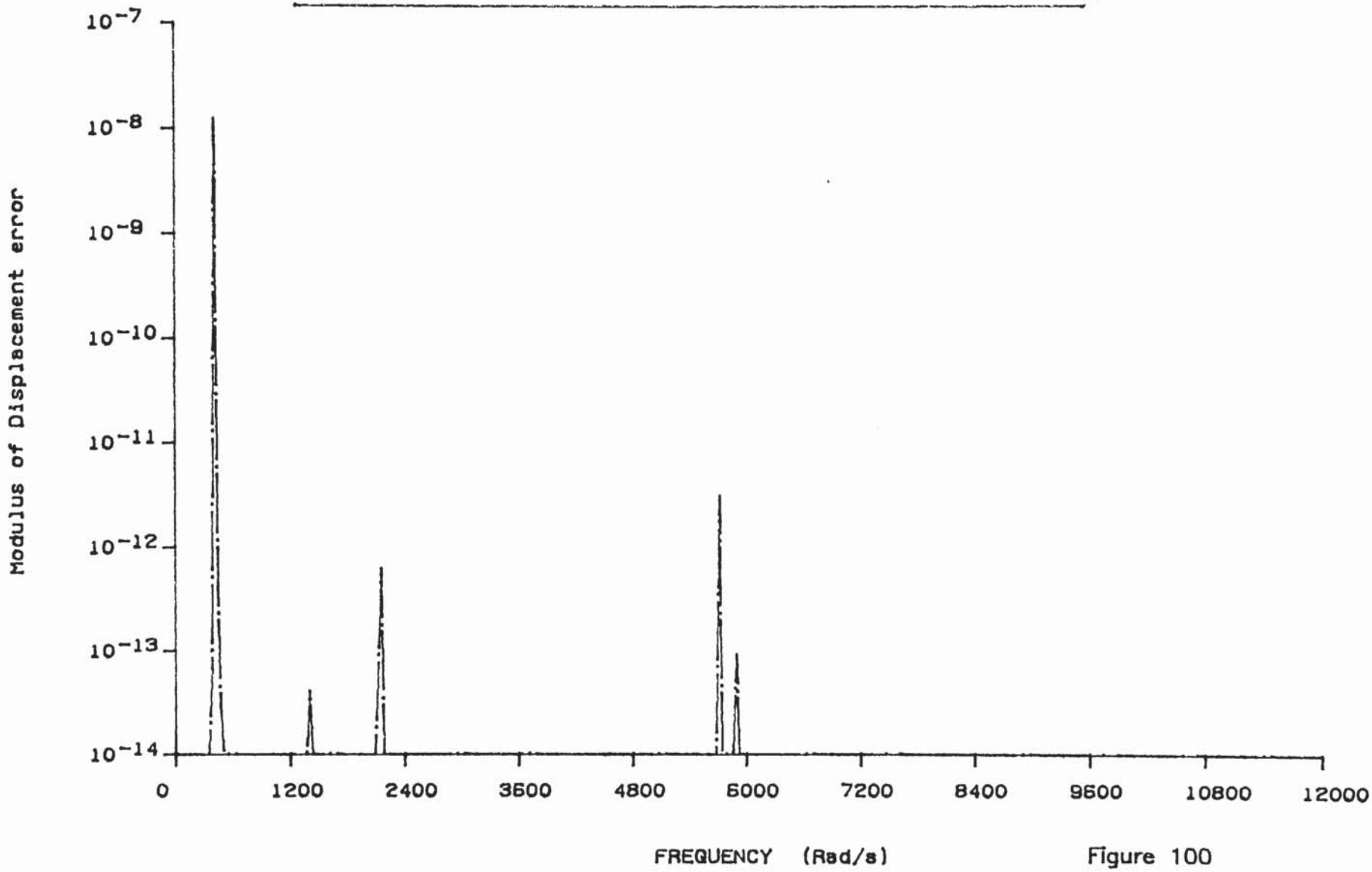
DAMAGE ERROR (Mat Constant b=5)
Modulus of Displacement error
10-7
10-8
10-9
10-10
10-11
10-12
10-13
10-14
0
1200
2400
3600
4800
6000
7200
8400
9600
10800
12000
FREQUENCY (Rad/s)

Figure 100

10 CONCLUSION

1. It is impossible to identify the parameters of a test rig directly from the mass and stiffness matrices derived from the system identification process.

2. The matrices derived by the system identification process are fully populated when the data are recorded from continuous systems. When the data are recorded for translational motion the truncation effects cause negative values for the off-diagonal terms.

3. It has been demonstrated that it is possible to identify a discrete system which is dynamically similar to a point coordinate on a continuous structure, for a translational plane of motion. If equipment is attached to both the continuous structure and the discrete system then a progressive error in dynamic similarity is obtained. This is due to the absense of rotary inertia within the discrete system and the error is particularly evident at the higher modes of vibration. The design methodology is suitable for one plane of motion problems.

4. The design methodology for discrete systems was incorporated within a general design methodology, where a combination of a continuous element and a

discrete system was used to obtain dynamic similarity with another continuous structure. The design methodology was capable of obtaining an acceptable level of dynamic similarity at a point coordinate for both translational and rotational motion.

5. A single discrete system was capable of achieving the correct frequency response level for the whole of the substitute structure. However, at coordinates away from the point of interest (the coordinate where the discrete system was connected) intermediate frequencies were apparent. These frequencies were generated by the interaction of the stationary characteristics of the discrete system and the varying anti-resonance frequencies of the continuous element. It was impossible to achieve an acceptable level of dynamic similarity when two coordinates were considered.

6. The same characteristics were obtained when dynamic similarity was sought between two dimensional structures. Point coordinate similarity was obtained at the coordinate where the discrete system was positioned, but at other coordinates intermediate frequencies were present.

7. When distributed discrete systems were examined it was found to be impossible to obtain even point

coordinate similarity.

8. The design methodology is only feasible when the continuous element is sufficiently dynamically similar to the original body that a single discrete system is used to provide a small ´tuning´ effect.

9. The design of the continuous element cannot be achieved by intuitive reasoning.

10. A design methodology using distributed parameter optimal design techiques has been developed for the systematic synthesis of the continuous element.

11. The distributed parameter design methodology proposes a new technique where a poor initial design estimate is sysmatically refined to move the design in a feasible direction towards an acceptable solution.

12. Cumulative damage assessment provides a basis for quantitatively assessing the quality of dynamic similarity.

13. It is impossible to use cumulative damage techniques in isolation as a design basis for dynamically representative test rigs since the importance of anti-resonances are not evident within cumulative damage theory.

14. A combination of cumulative damage theory and modal analysis techniques provide the basis of a feasible design methodology for dynamically representative test rigs.

11 RECOMMENDATIONS

1. The use of inductive expert systems should be examined as a means of integrating the distributed parameter optimal design methodology into one computer based solution.

2. The finite dimensional optimal design methodology for identifing the parameters of a discrete system should be applied to torsional vibration problems.

3. Analogue modelling techniques to produce representative loading conditions upon the equipment should be examined.

4. Test rigs comprising a continuous element and an active control system which is capable of producing the characteristics of the residual matrices should be examined.

12 APPENDICES

APPENDIX 1

DYNAMICALLY EQUIVALENT BEAMS

The generalised expresion for the resonance frequencies of a simple beam element is

$$\omega = (\beta_r^2)\sqrt{\frac{EI}{\rho A \ell^4}} \qquad \text{(A101)}$$

where (β_r^2) is a function of the end constraints.

If it is assumed that the beams can be of different material then it is possible to allow for the small fluctations that occur between materials in the ratio $\frac{E}{\rho}$

$$\sqrt{\frac{E_a}{\rho_a}} = z_1\sqrt{\frac{E_b}{\rho_b}} \qquad \text{(A102)}$$

where z_1 is a constant of adjustment.

The equation (A101) reduces to

$$\sqrt{\frac{I_a}{A_a \ell_a^4}} = z_1\sqrt{\frac{I_b}{A_b \ell_b^4}} \qquad \text{(A103)}$$

where the suffix **a** is for the first beam

and the suffix **b** is for the second beam

If a rectangular bar section is assumed then

$$\sqrt{\frac{d_a^2}{12\,\ell_a^4}} = z_1\sqrt{\frac{d_b^2}{12\,\ell_b^4}} \qquad \text{(A104)}$$

If the frequency response curves of the two beams are to be the same then the mass of each beam must be the same.

$$\rho_a A_a \ell_a = \rho_b A_b \ell_b \qquad \text{(A105)}$$

from equation A104

$$\frac{d_a}{\ell_a^2} = z_1\frac{d_b}{\ell_b^2} \qquad \text{(A106)}$$

Now, if it assumed that the ratio of the material densities

is z_2 and that the breadth of the beams are kept constant (Case 1), then

from equation (A105)

$$\rho_a d_a b_a \ell_a = \rho_b d_b b_b \ell_b$$

or

$$d_b = \frac{d_a \ell_a}{z_2 \ell_b} \qquad \text{(A107)}$$

substituting equation (A107) into (A106) yields

$$\frac{d_a}{\ell_a^2} = \frac{z_1 d_a \ell_a}{z_2 \ell_b^3}$$

or

$$\ell_b = \sqrt[3]{\frac{\ell_a z_1}{z_2}} \qquad \text{(A108)}$$

substituting equation (A108) into (A107) yields

$$d_b = \frac{d_a}{\sqrt[3]{z_2^2 z_1}} \qquad \text{(A109)}$$

After equation (A106) the assumption was made to keep the breadth constant. This was quite arbitrary, an alternative is to keep the length of the beams the same (Case 2) Since $\ell_a = \ell_b$ then it follows from equation (A106) that

$$d_b = \frac{d_a}{z_1} \qquad \text{(A110)}$$

and using equations (A105) and (A110)

$$b_b = \frac{z_1}{z_2} b_a \qquad \text{(A111)}$$

APPENDIX 2

MATHEMATICAL DEFINITIONS WITHIN DESIGN OPTIMISATION PROCEDURES

Design variables are grouped into a vector such that

$$x = \begin{Bmatrix} x_1 \\ \vdots \\ x_n \end{Bmatrix} = \{x_1, \ldots . x_n\}^T \qquad (A201)$$

A vector of the form of equation (A201) may be interpreted as a point in an n-dimensional real space , R^n

The space R^n is simply the collection of all n-vectors of real numbers

A collection of points D in R^n will be called a set, or a subset of R^n .

A point x in R^n that is in D wil be denoted $x \in D$

In R^n there is a well defined idea of length of a vector, denoted

$$\|x\| \equiv \left[\sum_{i=1}^{n} (x_i)^2 \right]^{1/2} \qquad (A202)$$

and called a norm on R^n .

The scalar product of two vectors x and y of R^n is

$$(x, y) \equiv x^T y = \sum_{i=1}^{n} x_i y_i \qquad (A203)$$

They are orthogonal if their scalar product is zero.

The convergence of a sequence $\{x^i\}$ of vectors in R^n with

the norm of equation (A202) is much like convergence of real numbers. That is

$$\lim_{i \to \infty} x^i = x \quad \text{if for any} \quad \varepsilon > \emptyset$$

there is an $N > \emptyset$ such that $\| x^i - x \| < \varepsilon$ for all $i > N$

An important property of sets in optimisation theory is closeness.

A subset D of R^n is called closed if every sequence in D that converges has a limit in D. A set is called open if its complement (all points in R^n except those in the set) is closed.

A vector function can be defined in the same manner

$$g(x) = [\, g_1(x), \ldots\ldots g_m(x) \,]^T$$

where $g(x)$ is within $x \in R^n$

Such a function is called continuous at $\bar{x}$ if for any $\varepsilon > \emptyset$ there is a $\delta > \emptyset$ such that

$$\| g(x) - g(\bar{x}) \|_m < \varepsilon \qquad \text{if} \qquad \| x - \bar{x} \|_n < \delta$$

The subscripts m and n on the norms denote the dimensions of the space on which the norm is defined.

It is often desirable to deal with a set of functions which satisfy inequalities such that

$$g_i(x) \leqslant \emptyset, \quad i = 1, \ldots\ldots\ldots m \qquad \text{(A204)}$$

or just as $g(x) \leqslant 0$

A useful concept used within optimisation theory is the

idea of the derivative of a vector function with respect to its vector variable

This notation is

$$\frac{\partial g(x)}{\partial x} \equiv \left[\frac{\partial g_i(x)}{\partial x_j}\right]_{m \times n}$$

where i is a row index and j is a column index.

If $f(x)$ is a real valued function of $x \in R^n$ this notation is

$$\frac{\partial f(x)}{\partial x} \equiv \left[\frac{\partial f(x)}{\partial x_1}, \ldots\ldots\ldots \frac{\partial f(x)}{\partial x_n}\right] \qquad \text{(A205)}$$

The derivative of a real valued function is often called the gradient of that function and is denoted by

$$\nabla f(x) \equiv \frac{\partial f(x)}{\partial x} \qquad \text{(A206)}$$

An important theorem in the analysis of functions appearing in optimal design problems is Taylor's theorem

Let the real valued function $f(x)$ have two continuous derivatives in R^n. Then for $x \in R^n$ there is a point $\xi = \alpha x + (1-\alpha)y$ with $0 < \alpha < 1$ such that

$$f(y) = f(x) + \sum_{i=1}^{n} \frac{\partial f(x)}{\partial x_i}(y - x) + \frac{1}{2}\sum_{i=1}^{n}\sum_{j=1}^{n} \frac{\partial^2 f(\xi)}{\partial x_i \partial x_j}(y_j - x_j)(y_i - x_i) \qquad \text{(A207)}$$

In many instances within optimal design problems Taylor's theorem is used to obtain an approximate expression for a function. The most common approximation is the one obtained by deleting secord order terms.

For example, if $\|x - y\|$ is small

$$f(y) - f(x) \doteq \frac{\partial f(x)}{\partial x} (y - x) \qquad \text{(A208)}$$

where by equation (A207) the error in equation (A208) is at most a constant times $\|y - x\|$ if $f(x)$ has bounded secord order derivatives.

The left side of equation (A208) is generally denoted by $\delta f(x)$ and $(y-x)$ is denoted by x.

In this notation equation (A208) becomes

$$\delta f(x) = \frac{\partial f}{\partial x} \delta x \qquad \text{(A209)}$$

Equation (A209) may be thought of as a total differential. Even for vector functions $g(x)$, equation (A209) holds for each component.

defining $$\delta g(x) \equiv [\delta g_1(x), \ldots\ldots\ldots \delta g_n(x)]^T$$

yeilds

$$\delta g(x) = \frac{\partial g(x)}{\partial x} \delta x \qquad \text{(A210)}$$

In optimal design problems $g(x)$ is often a function of $x \in R^n$ and $z \in R^p$. In this case equation (A210) is

$$\delta g(x,z) = \frac{\partial g(x,z)}{\partial x} \delta x + \frac{\partial g(x,z)}{\partial z} \delta z \qquad \text{(A211)}$$

where

$$\frac{\partial g(x,z)}{\partial x} = \left[\frac{\partial g_i(x,z)}{\partial x_j} \right]_{m \times n}$$

and

$$\frac{\partial g(x,z)}{\partial z} = \left[\frac{\partial g_i(x,z)}{\partial z_j} \right]_{m \times p}$$

APPENDIX 3

DESIGN SENSITIVITY ANALYSIS

The finite dimensional optimal design technique can be applied to the solution of the eigenvalue problem.

Given that

$$\{b\} \in R^k$$
$$\{z\} \in R^n$$
$$\{\phi\} \in R^n$$
$$\{\lambda\} \in R^1$$

the task is to minimise

$$\Psi_o(z, \lambda, b) \tag{A301}$$

subject to the state equations

$$h(z, b) = \phi \tag{A302}$$
$$[K(b)]\,\phi = \lambda\,[M(b)]\,\phi \tag{A303}$$

and constraints

$$\Psi(z, \lambda, b) \leqslant \phi \tag{A304}$$

where

$$h(z, b) = \begin{Bmatrix} h_1(z, b) \\ \vdots \\ h_n(z, b) \end{Bmatrix}$$
$$[K(b)] = [k_{ij}\{b\}]_{n \times n}$$
$$[M(b)] = [m_{ij}\{b\}]_{n \times n}$$
$$\Psi(z, \lambda, b) = \begin{Bmatrix} \Psi_1(z, \lambda, b) \\ \vdots \\ \Psi_m(z, \lambda, b) \end{Bmatrix}$$

The symmetric matrices $[M(b)]$ and $[K(b)]$ represent mass and stiffness values within the system. The scalar λ is the eigenvalues.

The effect of small changes to the design vector $\{b\}$ are required so that sensitivity coefficients can be obtained to minimise the expression in Equation (A301). The results of a sensitivity analysis provide design derivatives that are required for virtually all iterative methods of design optimisation. In this development the effect of design changes are obtained by first approximating the non-linear functions in the problem by linear expressions in the variables involved.

An initial estimate of the design vector is made, $\{b^\circ\}$

The state equations (A302) and (A303) are solved for the corresponding state z°, ϕ° and λ°.

Consider a small change to the design vector such that

$$b' = b^\circ + \delta b \qquad \text{(A305)}$$

If the new design variable b' were substituted into (A302) and (A303) new state variables z', ϕ' and λ' would be obtained.

Now the Implicit Function Theorem [30] states
If at $b = \bar{b}$ there is a solution $\bar{z}$ (ie. $h(\bar{z}, \bar{b}) = \phi$) and if the $n * n$ matrix $\partial h / \partial z (\bar{z}, \bar{b})$ is nonsingular, then there is a continuously differentiable solution $z = \theta(b)$ in a neighbourhood of $\bar{b}$. That is, there is $\delta > \phi$ such that $h(\theta(b), b) = \phi$, for all b such that $\| b - \bar{b} \| < \delta$.

Since the Jacobean matrix $J \equiv \partial h / \partial z (z^\circ, b^\circ)$ is nonsingular, the Implicit Function Theorem guarantees that if $\| \delta b \|$ is small, then $z' - z^\circ$ will be small.

This change in z is donated δz so that

$$z' = z^\circ + \delta z$$

Similarly the change δb in b° will cause small changes $\delta \phi$ and $\delta \lambda$ in the solution of the eigenvalue problem of equation (A303).

If the changes in the nonlinear functions are approximated by considering small changes δb in the design then equation (A304) becomes

$$\delta \Psi_o [z^\circ, \lambda^\circ, b^\circ] = \frac{\partial \Psi_o}{\delta z} [z^\circ, \lambda^\circ, b^\circ] \delta z + \frac{\partial \Psi_o}{\partial \lambda} [z^\circ, \lambda^\circ, b^\circ] \delta \lambda + \frac{\partial \Psi_o}{\delta b} [z^\circ, \lambda^\circ, b^\circ] \delta b \qquad \text{(A306)}$$

for the initail state and

$$\delta \Psi_j [z^\circ, \lambda^\circ, b^\circ] = \frac{\partial \Psi_j}{\partial z} [z^\circ, \lambda^\circ, b^\circ] \delta z + \frac{\partial \Psi_j}{\partial \lambda} [z^\circ, \lambda^\circ, b^\circ] \delta \lambda + \frac{\partial \Psi_j}{\delta b} [z^\circ, \lambda^\circ, b^\circ] \delta b \qquad \text{(A307)}$$

for a new point j

Since $h(z^\circ, b^\circ) = \phi$ and $z^\circ + \delta z$ is used to satisfy the equation

$$h(z^{\circ} + \delta z, b^{\circ} + \delta b) = \phi$$

the linearised version of this condition is

$$J \delta z + \frac{\partial h}{\partial b} \delta b = \phi \qquad \text{(A308)}$$

Equation (A308) may be viewed as determining δz as the function of δb and can be solved for δz since the matrix J is nonsingular. Similarly, first order changes in ϕ and λ may be analysed.

Premultiplying equation (A303) by $[\phi]^T$ yields,

$$[\phi]^T [K(b)] [\phi] = [\lambda] [\phi]^T [M(b)] [\phi] \qquad \text{(A309)}$$

Approximating both sides to first order in the variables ϕ, λ and b,

$$\begin{aligned} &\delta\phi^T[K(b)]\phi + \frac{\partial}{\partial b}(\phi^T[K(b)]\phi)\delta b \\ &\quad + \phi^T[K(b)]\delta\phi \end{aligned} = \begin{aligned} &\lambda\delta\phi^T[M(b)]\phi + \lambda\frac{\partial}{\partial b}(\phi^T[M(b)]\phi)\delta b \\ &\quad + \phi^T[M(b)]\delta\phi + \delta\lambda \end{aligned} \qquad \text{(A310)}$$

Since $[K(b)]$ and $[M(b)]$ are symmetric matrices, the first and third terms on both sides of this equation may be transposed to obtain the identity.

$$\begin{aligned} &2\delta\phi^T([K(b)]\phi - \lambda[M(b)\phi] + \frac{\partial}{\partial b}[\phi^T[K(b)]\phi) - \\ &\lambda\frac{\partial}{\partial b}(\phi^T[M(b)]\phi\lambda)\delta b \end{aligned} = \delta\lambda \qquad \text{(A311)}$$

Using equation (A303) the expression reduces to

$$\begin{aligned} \delta\lambda &= (\frac{\partial}{\partial b}(\phi^T[K(b)]\phi) - \lambda\frac{\partial}{\partial b}(\phi^T[M(b)]\phi\lambda)\delta b \\ &\equiv \ell^{\lambda^T}\delta b \end{aligned} \qquad \text{(A312)}$$

This is an explicit relationship that determines the change

in the eigenvalue $\delta\lambda$ in terms of the change δb in the design variables [30].

If numerical methods are to be used so that the design optimisation methodology is automatic, it is necessary to express the change in the design variables (δb) in terms of the cost equation (A304) and the state equations (A302) and (A303). One method of achieving this is to remove the dependence on δz within the equations (A306) and (A307). The objective therefore is to find $\left(\frac{\partial \psi_0}{\partial z}\right)\delta z$ and $\left(\frac{\partial \psi_i}{\partial z}\right)\delta z$ in terms of δb.

Define the column vectors ξ^i, $0 \leq i \leq m$ as solutions of the adjoint equations.

$$J^T \xi^i = \frac{\partial \psi_i^T}{\partial z}, \quad 0 \leq i \leq m \tag{A313}$$

where $J = \frac{\partial h}{\partial z}(z^\circ, b^\circ)$ and the right side of equation (A313) is evaluated at $z^\circ, \lambda^\circ, b^\circ$

take the transpose of (A313) and multiply by δz

$$\xi^{iT} J \delta z = \frac{\partial \psi_i}{\partial z} \delta z \tag{A314}$$

using equation (A308)

$$-\xi^{iT} \frac{\partial h}{\partial b} \delta b = \frac{\partial \psi_i}{\partial z} \delta z \tag{A315}$$

Note that the right side of equation (A315) is the term that has to be eliminated from equations (A306) and (A307).

Substituting from equation (A312) and (A315) into equation (A306) and (A307) yields

$$\left.\begin{aligned} \delta\psi_{\circ} &= \ell^{\circ T}\,\delta b \\ \delta\psi &= \ell^{T}\,\delta b \end{aligned}\right\} \qquad \text{(A316)}$$

where the vector $\{\ell^{\circ}\}$ and the column $\{\ell^{i}\}$ of the matrix $[\ell]$ are evaluated at $z^{\circ}, \lambda^{\circ}, b^{\circ}$ from

$$\ell^{i} = \frac{\partial \psi_i^{T}}{\partial b} - \frac{\partial h^{T}}{\partial b}\xi^{i} \quad \frac{\partial \psi}{\partial \lambda}\ell^{\lambda} \qquad \text{(A317)}$$

The components of $\{\ell^{i}\}$ are called sensitivity coefficients of ψ_i with respect to the corresponding design variables. These vectors yield the explicit derivatives of the cost and constraint functions with respect to the design variables. During the optimisation process it is usual to select the derivatives with the greatest magnitude since they have the most significant effect on the design. This approach is called the steepest descent where the vectors which direct the design to an optimum at the fastest rate are selected.

APPENDIX 4

MATRIX INVERSION

Consider the process of calculating the inverse of a matrix $[B]$.

If $[B]$ is a square matrix then its adjoint $[adj\ B]$ is defined as the transpose of the matrix of its cofactors [47].

If the product $[B][adj\ B]$ is considered this reduces to $|B|[I]$

where $|B|$ is the determinant of

$[I]$ is the unit matrix.

It follows that the matrix $[B]$ can be defined by

$$[B]^{-1} = \frac{[adj\ B]}{|B|} \qquad \text{(A401)}$$

The elements of the $[adj\ B]$ matrix are found by

$$B_{ik} = (-1)^{i+k} \beta_{ik} \qquad \text{(A402)}$$

where i is the row

k is the column

β_{ik} is the minor of element B_{ik}

If a column or row is multiplied by -1 then the columns or rows of the [adj B] matrix will change sign, except the original column or row. The determinate will also change sign, although the modulus remains constant. It therefore follows that when the inverse matrix is found (A401) the change in signs are cancelled except for the original row or column (which has been transposed). During this process the modulus of the matrix elements do not change.

Once a matric has been inverted it is possible to examine the changes in sign to any row or column of the original matrix by changing the sign of the corresponding transposed row or column of the inverted matrix.

APPENDIX 5

IMPEDANCE COUPLING

Consider the connection or coupling of two systems (A and B) to obtain a system C having prescribed characteristics. At the point of connection the displacements will be the same.

ie. $$\{x_A\} = \{x_B\} = \{x_c\} \qquad \text{(A501)}$$

considering equilibrium at point of conection

$$\{F_A\} + \{F_B\} = \{F_x\} \qquad \text{(A502)}$$

where F_x is the externally applied force.

The receptance for a system can be expressed as

$$[\alpha]\ \{F\} = \{x\} \qquad \text{(A503)}$$

Combining equations (A501) and (A502) leads to an expression for the receptance of the combined structure at the point of connection

$$[\alpha_c] = ([\alpha_A]^{-1} + [\alpha_B]^{-1})^{-1} \qquad \text{(A504)}$$

Expression (A504) shows that when structures are coupled the inverse receptance (dynamic stiffness) is required.

If truncated receptance plots are considered and damping is ignored, then the receptance can be expressed as ;

$$\alpha_{jk} = \frac{x_k}{F_j} = \sum_{r=1}^{n} \frac{{}_r\phi_j \, {}_r\phi_k}{(\omega_r^2 - \omega^2)} \qquad \text{(A505)}$$

where r is the mode number

j is the coordinate at which force is applied.

k is the coordinate at which response is measured.

A point coordinate dynamic stiffness plot has the typical form shown in Figure 101

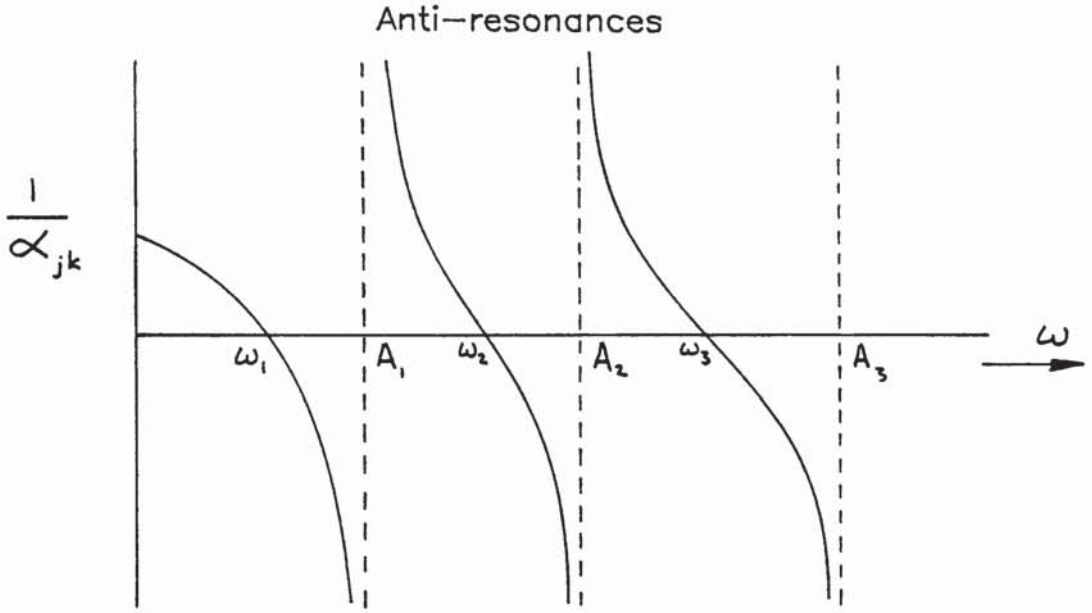

Figure 101

It is indeterminate at positions $A_1, A_2, \ldots A_n$ which are known as the anti-resonance values.

At resonant frequencies the value of $1/\alpha_{jk}$ is zero.
If two structures are coupled (ie dynamic stiffness values added) then it is obvious that the points $A_{1_A}, A_{2_A}, \ldots A_{n_A}$ and $A_{1_B}, A_{2_B}, \ldots A_{3_B}$ of each structure will be dominate within the coupled structure $[\alpha_c]$.

APPENDIX 6

CALCULUS OF VARIATIONS

When considering the design of simple continuous structures it is often the case that the structure has to be an optimum shape of thickness to fulfil specific design functions. These design functions are often functions of another function and are called functionals.

The design problem can, therefore, be stated as:

> Find the function $z(x)$, $x^{\circ} \leqslant x \leqslant x'$ in a class of functions with square integrable derivatives and satisfying end conditions that minimise the functional $\Psi_{\circ}(z)$.

In connection with function spaces, it is often necessary to reqire that a function be small of near zero function so that optimisation theory can be applied [48].

If the norm of a functional is defined as $\|z\|$ then the most commonly used norm is

$$\|z\| = \left[\int_{x^{\circ}}^{x'} z^{2}(x)\, dx \right]^{1/2} \qquad \text{(A601)}$$

for square integrable functions

Relative minima of functionals can now be used. The

functional $\Psi_o(z)$ has a relative minimum at $\hat{z}$ if there is a $\delta > 0$ such that

$$\Psi_o(\hat{z}) \leq \Psi_o(z) \qquad \text{(A602)}$$

for all admissible z with

$$\| \hat{z} - z \| < \delta$$

Let the variable $z(x)$ be a vector valued function of the real variable x, that is

$$z(x) = \begin{Bmatrix} z_1(x) \\ \vdots \\ z_n(x) \end{Bmatrix}$$

where $z_i(x)$ are real valued functions of x.

The fundamental problem of the calculus of variations can be defined as;

Find a function $z(x)$ that has two continuous derivatives in $x^o \leq x \leq x'$ and satisfies the boundary conditions

$z_i(x^o) = z_i^o$ for some indices $1 \leq i \leq n$

$z_j(x') = z_j'$ for some indices $1 \leq j \leq n$ (A603)

and that minimises

$$\Psi_o(z) = \int_{x^o}^{x'} F(x, z, z')\, dx \qquad \text{(A604)}$$

where F is a twice continuous differentiable real valued function of all its arguments and

$$z' = \left\{ \frac{dz_1}{dx}, \ldots \frac{dz_n}{dx} \right\}^T$$

The method of obtaining necessary conditions on the solution $\hat{z}(x)$ of the fundamental problem is to allow small changes in $\hat{z}(x)$ and examine the behaviour of $\Psi_0(z)$. An admissible, small perturbation is shown graphically in Figure 102. The equation for this curve is $\hat{z}(x) + \varepsilon \eta(x)$,

where ε is a small real number.

$\eta(x)$ is a twice continuously differential function that satisfies the conditions

$$\left.\begin{aligned} \eta_i(x^0) = \phi \quad &\text{for each } i \text{ with } z_i(x^0) = z_i^0 \\ \eta_j(x') = \phi \quad &\text{for each } j \text{ with } z_j(x') = z_j' \end{aligned}\right\} \quad \text{(A605)}$$

Perturbation from optimum

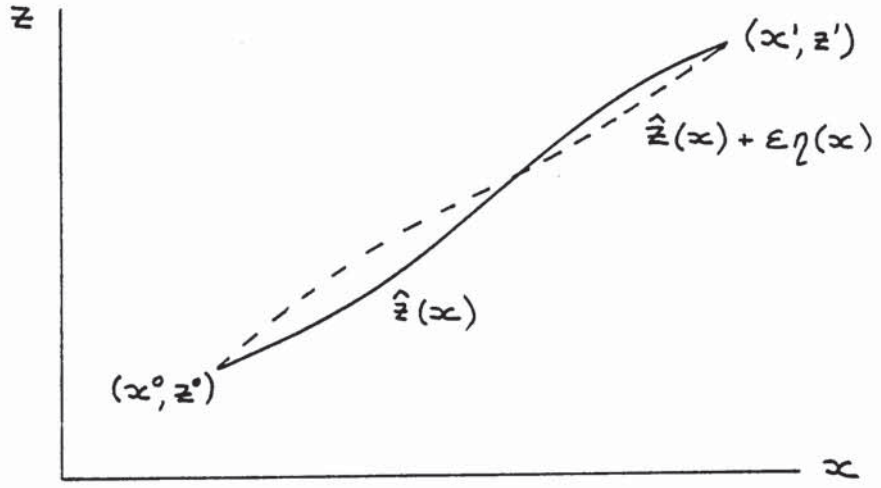

Figure 102

To examine the effect of this perturbation of $\Psi_o(z)$ substitute $\hat{z}+\varepsilon\eta$ into equation (A604)

$$\Psi_o(\hat{z}+\varepsilon\eta) = \int_{x_o}^{x'} F(x, \hat{z}+\varepsilon\eta, \hat{z}'+\varepsilon\eta')\,dx$$

Now $\hat{z}(x)$ is a local minimum of $\Psi_o(z)$ subject to equation (A605). This is any small change in $\hat{z}(x)$ increases $\Psi_o(z)$.

For a given function $\eta(x)$ which satisfies equation (A605), $\hat{z}(x)+\varepsilon\eta(x)$ satisfies equation (A603) for all ε. Therefore, $\eta(x)$, $\Psi_o(\hat{z}+\varepsilon\eta)$ is a real valued function of the real variable . Most importantly, for $\varepsilon = \phi$, $\Psi_o(\hat{z}+\varepsilon\eta)$ has a relative minimum. It is assumed that $F(x,z,z')$ is twice continuously differentiable in z and z' so $\Psi_o(\hat{z}+\varepsilon\eta)$ is a twice continuously differentiable function of ε.

It is required that

$$\delta\Psi_o \equiv \frac{\partial}{\partial\varepsilon}\,\Psi_o(\hat{z}+\varepsilon\eta)_{|\varepsilon=\phi} = \phi \qquad \text{(A606)}$$

The objective now is to transform the condition of equation (A606) into conditions of $\hat{z}(x)$. Performing the differentiation indicated in equation (A606)

$$\frac{\partial}{\partial\varepsilon}\,\Psi_o(\hat{z}+\varepsilon\eta)_{|\varepsilon=\phi} = \int_{x_o}^{x'}\left(\frac{\partial F}{\partial z}\eta + \frac{\partial F}{\partial z'}\eta'\right)dz = \phi \qquad \text{(A607)}$$

where the arguments in the partial derivatives of F in

equation (A607) are $\hat{z}(x)$ and $\hat{z}'(x)$.

Integrating the second term in the integrand of equation (A607) by parts

$$\int_{x^\circ}^{x'} \left[\frac{\partial F}{\partial z} - \frac{d}{dx}\left(\frac{\partial F}{\partial z'}\right)\right] \eta \, dx + \frac{\partial F}{\partial z'}\left[x', \hat{z}(x'), \hat{z}'(x')\right] \eta(x') - \frac{\partial F}{\partial z'}\left[x^\circ, \hat{z}(x^\circ), \hat{z}'(x^\circ)\right] \eta(x^\circ) = \phi \qquad \text{(A608)}$$

Since one may take $\eta(x^\circ) = \eta(x') = \phi$, [30], equation (A608) reduces to

$$\int_{x^\circ}^{x'} \left[\frac{\partial F}{\partial z} - \frac{d}{dx}\left(\frac{\partial F}{\partial z'}\right)\right] \eta \, dx = \phi \qquad \text{(A609)}$$

In any subinterval of $x^\circ \leqslant x \leqslant x'$ where $\hat{z}(x)$ is continuously differentiable, the quantity

$$\frac{\partial F}{\partial z} - \frac{d}{dx}\left(\frac{\partial F}{\partial z'}\right)$$

is continuous, therefore;

$$\frac{\partial F}{\partial z} - \frac{d}{dx}\left(\frac{\partial F}{\partial z'}\right) = \phi \qquad \text{(A610)}$$

However, if $\hat{z}(x)$ has a discontinuity at some point $\tilde{x}$ then equation (A609) need not be continuous at $\tilde{x}$. Since equation (A610) must hold in the subintervals on both sides of $\tilde{x}$ then this equation may be integrated from $\tilde{x} - \delta, (\delta > \phi)$ to x to obtain

$$\frac{\partial F}{\partial z'} = \int_{\tilde{x}-\delta}^{x} \frac{\partial F}{\partial z}\, dx + C \qquad \text{(A611)}$$

The vector $\partial F/\partial z$ is piecewise continuous so that the right side of equation (A611) is continuous. Therefore, $\partial F/\partial z'$ is continuous even at $\tilde{x}$.

Finally, these results may be stated as

$$\frac{\partial F}{\partial z}\left[x, \hat{z}(x), \hat{z}'(x)\right] - \frac{d}{dx}\left\{\frac{\partial F}{\partial z'}\left[x, \hat{z}(x), \hat{z}'(x)\right]\right\} = \phi \qquad \text{(A612)}$$

at points of continuity of $\hat{z}(x)$.

This equation is normally referred to as the Euler-Langrange equation.

$$\frac{\partial F}{\partial z'}\left[x', \hat{z}(x'), \hat{z}'(x')\right]\eta(x') - \frac{\partial F}{\partial z'}\left[x^{\circ}, \hat{z}(x^{\circ}), \hat{z}'(x^{\circ})\right]\eta(x^{\circ}) = \phi \qquad \text{(A613)}$$

for all $\eta(x^{\circ})$ and $\eta(x')$ satisfying equation (A605)

This equation is normally referred to as transversality condition.

$$\frac{\partial F}{\partial z'}\left[\tilde{x}-\phi, \hat{z}(\tilde{x}-\phi), \hat{z}'(\tilde{x}-\phi)\right] = \frac{\partial F}{\partial z'}\left[\tilde{x}+\phi, \hat{z}(\tilde{x}+\phi), \hat{z}'(\tilde{x}+\phi)\right] \qquad \text{(A614)}$$

at each point $\tilde{x}$ of discontinuity of $\hat{z}'(x)$.

This equation is normally referred to as the Weirstrass-Erdmann corner condition.

APPENDIX 7

PROBLEM OF BOLZA

The problem of Bolza is a problem of finding $b(x)$ and $z(x)$, $x^\circ \leqslant x \leqslant x'$, that minimises

$$\psi_\circ = g_\circ(z^j) + \int_{x^\circ}^{x'} F_\circ [x, z(x), b(x)]\, dx \qquad \text{(A701)}$$

where z_i denotes $z(x^j)$, $j = \circ$ or 1 subject to the differential equation

$$\frac{dz}{dx} = f(x, z, b), \qquad x^\circ \leqslant x \leqslant x' \qquad \text{(A702)}$$

boundary conditions and functional constraints

$$\psi_\alpha = g_\alpha(z^j) + \int_{x^\circ}^{x'} F_\alpha [x, z(x), b(x)]\, dx = \circ \qquad \text{(A703)}$$

$\alpha = 1, \ldots . r$

here $j = \circ$ or 1 and pointwise constraints

$$\phi_\beta(x, z, b) = \circ, \qquad \beta = 1, \ldots . q, \quad x^\circ \leqslant x \leqslant x' \qquad \text{(A704)}$$

where

$$z(x) = \begin{Bmatrix} z_1(x) \\ \vdots \\ z_n(x) \end{Bmatrix} \qquad b(x) = \begin{Bmatrix} b_1(x) \\ \vdots \\ b_s(x) \end{Bmatrix} \qquad f(x, z, b) = \begin{Bmatrix} f_1(x, z, b) \\ \vdots \\ f_n(x, z, b) \end{Bmatrix}$$

For the problem considered here it is required that the conditions of Equation (A704) shall not determine any component of $z(x)$ explicity. This is equivalent to requiring that the rank of the matrix

$$\left[\frac{\partial \phi_\beta}{\partial b_k}(x, z, b)\right]_{q \times s}$$

shall be q for all admissible values of the arguments.

The vector variables $z(x)$ and $b(x)$ are called to state variables and design variable respectively. Equations (A703) are presumed to contain boundary conditions on the state variable at the end points of the interval, x^0 and x^1.

The independant variable x may be a space-type variable or time, depending on the problem being considered. The functions g_0, F_0, f, g_α, F_α and ϕ_β are assumed to be continuously differentiable.

A full treatment of the problem can be seen in Refs 30, 38 & 45.

APPENDIX 8

DISTRIBUTED PARAMETER OPTIMAL DESIGN

Consider a mechanical structure capable of being described by a linear set of differential equations; statically

$$[K(b)]\{z\} = \{Q\} \qquad z \in D \qquad \text{(A801)}$$

where the operator K depends upon the design variable (b), the vector function Q is the applied load. The set D is linear subspace of functions satisfying differentiablity properties and homogeneous boundary conditions.

dynamically

$$[K(b)][\bar{\Phi}] = [\lambda][M(b)][\bar{\Phi}] \quad \bar{\Phi} \in D \qquad \text{(A802)}$$

which is the general eigenvalue problem.

The performance requirements or constraints can be expressed in the form of "pointwise constraints"

$$\phi_\beta(b) \leqslant \phi \quad \beta = 1, \ldots q, \quad x \in \Omega \qquad \text{(A803)}$$

and "functional constraints".

$$\Psi_\alpha(b, z, \lambda) = g_\alpha(\lambda) + \int_\Omega F_\alpha(x, z, b)\, dx \begin{cases} = \phi, \ \alpha = 1, \ldots r' \\ \leqslant \phi, \ \alpha = r'+1, \ldots r \end{cases} \qquad \text{(A804)}$$

The conditions of equation (A803) express explicit bounds on the design variables, which must be satisfied at all points over the domain of the distribution of the independent variable. The functional constraints of equation (A804) are used to replace any pointwise constraints over the domain Ω that are of the form

$$\eta(b,z) \leqslant \phi \qquad x \in \Omega$$

by the equivalent functional constraint

$$\Psi_\alpha = \int_\Omega [\eta]\, dx = \phi \qquad \text{(A805)}$$

The final element of the optimal design problem is the cost functional that is to be minimised

$$\Psi_0(b,z,\lambda) = g_0(\lambda) + \int_\Omega F_0(x,z,b)\, dx \qquad \text{(A806)}$$

The cost functional can represent weight, displacement, natural frequency and other pertinent costs associated with the design problem.

The gradient projection method that follows is based upon the same ideas as used in the finite dimensional gradient projection method described in Appendix 3. It requires that first order approximates are made to various functions involved in the optimisation problem and an optimum design improvement computed.

The method is initiated by making an estimate $b^0(x)$ for the

optimum design variable and the state equations (A801) and (A802) are solved for $z^{\circ}(x)$, $y^{\circ}(x)$ and λ° . The inequality constraints of equations (A803) and (A804) are used to isolate the constraints that are violated, (that is, $\phi_{\beta}(b) \geq \varepsilon$ or $\Psi_{\alpha} \geq -\varepsilon$). These are then accounted for in the subsequent design improvement analysis. This technique will converge (if it is at all possible) onto an optimum solution with the minimum of computational effort.

Apply Taylor's formula to the functions and constraints of equations (A803) and (A804)

$$\delta \tilde{\phi} = \frac{\partial \tilde{\phi}}{\partial b} \leqslant \Delta \tilde{\phi} , \qquad x \in \Omega \qquad \text{(A807)}$$

and

$$\delta \tilde{\Psi} = \left[\int_{\Omega} \frac{\partial F_{\alpha}}{\partial b} \delta b \, dx + \int_{\Omega} \frac{\partial F_{\alpha}}{\partial z} \delta z \, dx + \frac{\partial g_{\alpha}}{\partial \lambda} \delta \lambda \right] \qquad \text{(A808)}$$

where the vectors $\tilde{\phi}$ and $\tilde{\Psi}$ denote reduced constraint vectors that contain only those constraints that are violated or critical. The terms $\Delta \tilde{\phi}$ and $\Delta \tilde{\Psi}$ are constraint error corrections.

The gradient projection technique is based upon the idea of seeking a design improvement δb to achieve the constraint error corrections of equations (A807) and (A808) to satisfy a linearised form of equations (A801) and (A802) and to decrease the linearised cost function $\delta \Psi_{o}$ as much as possible.

The first step is to elimate explicit dependence of the

functional in equation (A808) on δz and $\delta\lambda$. The following equations are solved for an adjoint variable ξ^α corresponding to each functional Ψ_α in $\tilde{\Psi}$ and to $\Psi_0(\alpha = \phi)$.

$$K\xi^\alpha = -\frac{\partial F_\alpha^T}{\partial z}, \quad \xi^\alpha \in D \tag{A809}$$

Taking the scalar product of both sides of equation (A801) with ξ^α

$$\int_\Omega \left[\xi^{\alpha T} K \delta z + \xi^{\alpha T} \frac{\partial (Kz)}{\partial b}\delta b\right] dx = \phi \tag{A810}$$

using the symmetry of the operator K and employing equation (A809)

$$-\int_\Omega \frac{\partial F_\alpha}{\partial z}\delta z\, dx + \int_\Omega \xi^{\alpha T}\frac{\partial (Kz)}{\partial b}\delta b\, dx = \phi \tag{A811}$$

The first term on the left of eqation (A811) is precisely the term in equation (A808) involving δz.

A perturbation calculation will determine dependence of $\delta\lambda$ on δb. Taking the scalar product of both sides of equation (A802) with a vector ξ and linearising

$$[\xi, K\delta\Phi] + [\xi, \frac{\partial (K\Phi}{\partial b}\delta b] = \delta\lambda[\xi, M\Phi] + \lambda[\xi, M\delta\Phi] + \lambda[\xi, \frac{\partial (M\Phi)}{\partial b}\delta b]$$

substituting $\xi = \bar{\Phi}$ and rearranging

$$[\bar{\Phi}, \left(\frac{\partial (K\bar{\Phi})}{\partial b} - \lambda\frac{\partial (M\bar{\Phi}}{\partial b}\delta b\right] = \delta\lambda[\bar{\Phi}, M\bar{\Phi}] + [\bar{\Phi}, \lambda M\delta\bar{\Phi}] - [\bar{\Phi}, K, \delta\bar{\Phi}]$$

$$= \delta\lambda + [\delta\bar{\Phi}, (\lambda M\bar{\Phi} - K\bar{\Phi})] \tag{A812}$$

$$= \delta\lambda$$

the scalar on the right can be removed by appying equation (A802) and the notation that the eigenvectors are mass normalised such that

$$[\Phi]^T[M(b)][\Phi] = [1]$$

substitute from eqaution (A811) and (A812) into (A808) yields

$$\delta\psi_\alpha = \left[\frac{\partial F_\alpha}{\partial b}, \delta b\right] + \left[\xi^\alpha, \frac{\partial(Kz)}{\partial b}\delta b\right] + \frac{\partial g_\alpha}{\partial \lambda}\left[\Phi, \left(\frac{\partial(K\Phi)}{\partial b} - \lambda\frac{\partial(M\Phi)}{\partial b}\right)\delta b\right]$$

$$= [\Lambda^\alpha, \delta b] \begin{cases} = \Delta\psi_\alpha, & \alpha = 0, \ldots r' \\ \leq \Delta\psi_\alpha, & \alpha \geq r'+1 \;\&\; \psi_\alpha \geq -\epsilon \end{cases} \quad \text{(A813)}$$

where

$$\Lambda^\alpha \equiv \frac{\partial F_\alpha^T}{\partial b} + \frac{\partial(Kz)^T}{\partial b}\xi^\alpha + \frac{\partial g_\alpha}{\partial \lambda}\left[\frac{\partial(K\Phi)}{\partial b} - \lambda\frac{\partial(M\Phi)}{\partial b}\right]^T\Phi \quad \text{(A814)}$$

This expression is analogous to equation (A317) in Appendix 3 where the sensitivity of the gradient for the finite dimensional design problem is computerised.

13 REFERENCES

1. CHECKLAND. 'System Behaviour', Edited by J. Beishon and G. Peters, The Open University Press, 1972.
2. ASHBY. 'Introduction to Cybernetics' Chapman and Hall, 1956.
3. YOUNG and ON. 'Mathematical modelling via direct use of vibration data', SAE paper 690615, October 1969.
4. FLANNELLY and BERMAN. 'The state of the art of system identification of Aerospace Structures.', ASME, Coll. WAM 1972.
5. RANEY, J P. 'Identification of complex structures using near resonance testing.', Shock and Vibration Bulletin No. 38 pt 2, August 1968 pp 23-32
6. POTTER, R and RICHARDSON, M. 'Mass Stiffness and Damping matrices from Measured Modal Parameters', IIAC. New York, October 1974.
7. THOREN, A R. 'Derivation of mass and stiffness matrices from dynamic test data', AIAA/ASME/SAE 13th Structural Dynamics and Materials Conf., San Antonio, Texas, April 1972.
8. EWINS, D J. and GLEESON, P T. 'A Method for modal identification of lightly damped structures', JSV 1982, pp 57-79.
9. KLOSTERMAN, A L. 'On the experimental determination and use of modal representation of dynamic

characteristics', PhD Thesis, University of Cincinnati, 1971.

10. GAUKROGER, SKINGLE and HERON. 'Numerical analysis of vector response loci', JSV 1973, pp 341,353.
11. GOYDER, H. 'Methods and application of structural modelling from measured structural frequency response data', JSV 1980, pp 209-230.
12. COLLINS, HART, HASSELMAN and KENNEDY. 'Statistical Identification of Structures', AIAA Journal, Vol. 12, February 1974, pp 185-190.
13. CHEN, J C and GARBA, J A. 'Analytical Model improvement using modal test results', AIAA Journal, Vol. 18, June 1980, p684.
14. GROSSMAN, D T. 'An automated Technique for Improving Modal test/analysis correlation', AIAA Paper, 82-0640, New Orleans, La., May 1982.
15. DALE, O B and COHEN, R. 'Multi-parameter identification in linear continuous vibrating systems', Trans. ASME Journal of Dynamics, Systems, Measurement and Control. March 1971.
16. BERMAN, A and FLANNELLY, W. 'Theory of incomplete models of dynamic structures', AIAA Journal, Vol. 9, No. 8, 1971.
17. ROSS, R G. 'Synthesis of stiffness and mass matrices from experimental vibration modes', SAE Paper, 710787.
18. BERMAN, A and WEI, F S. 'Automated Dynamic Analytical Model Improvement', NASA CR-3452, July 1981.

19. GUYAN, R J. 'Reduction of Stiffness and Mass Matrices', AIAA Journal Vol. 3, February 1965, p380.

20. KIDDER, R L. 'Reduction of Structural Frequency Equations', AIAA Journal Vol. 11, June 1973, p 892.

21. BARUCH, M and BAR-ITZHACK. 'Optimal Weighted Orthogonalisation of Measured Modes', AIAA Journal, Vol. 16, No. 4, April 1978, pp 346-357.

22. BARUCH, M. 'Optimisation Procedure to correct Stiffness and Flexibility matrices using Vibration Tests', AIAA Journal, Vol 16, No. 11, November 1978, pp 1208-1210.

23. WEI, F S. 'Stiffness Matrix correction from Incomplete Data', AIAA Journal Vol. 18, No. 10, October 1980, pp 1274,1275.

24. IBRAHIM, S R. 'Dynamic Modelling of structures from Measured Complex Modes', AIAA Journal, Vol. 21, No. 6, June 1983, pp 898-901.

25. BARUCH, M. 'Methods of reference basis for identification of Linear Dynamic Structures', Dept. of Aeronautical Eng. Technion - Israel Institute of Technology TAE, No. 458, September 1981.

26. BERMAN, A. 'Mass Matrix Correction Using and Incomplete set of measured Models', AIAA Journal, Vol. 17, October 1979, pp 1147-1148.

27. BERMAN, A and NAGY, E J. 'Improvement of Large Analytical Model using Test Data', AIAA Journal Vol. 21, No. 8, August 1983, pp 1168-1173.

28. BISHOP and JOHNSTON. 'The Mechanics of Vibration', Cambridge Univeristy Press, 1960.

29. SALTER, J P and ROSKILLY, I G. 'The resonance-envelope Random Vibration Test', RARDE Memorandum 18/72, 1972.

30. HAUG, E and ARORA, J S. 'Applied Optimal Design', Wiley, 1979.

31. HADLEY. 'Linear Programming',

32. EWINS, D J and SAINSBURY, M G. 'Mobility measurements for the Vibration Analysis of connected Structures', Sound and Vibration (USA) No. 42, Part 1, January 1972.

33. KLOSTERMAN, A L and LEMON, J R. 'Dynamic design analysis via the building block approach', Shock and Vibration Bulletin No. 42, pp 97-104, 1972.

34. VINCENT, A H. 'A note on the properties of the variation of structural response with respect to a single structural parameter when plotted in the complex plane', Westland Helicopters Ltd. Report GEN/DYN/RES/010R, 1973.

35. DONE, G T and HUGES, A D. 'The response of a vibrating structure as a function of structural parameters', Journal of Sound and Vibration No. 38, pp 255-266, 1975.

36. DONE, G T, HUGHS, A D and WEBBY, J. 'The response of a vibrating structure as a function of structural parameters - Application and Experiment', Journal of Sound and Vibration, No. 49, pp 149-159, 1976.

37. BRYSON, A and HO, Y. 'Applied Optimal Control', Wiley, 1975.

38. FOX, R L. 'Optimisation methods for engineering

design´, Addision-Wesley, 1971.

39. FRIND, E. and WRIGHT, P. ´Gradient methods in optimum structural design´, Journal of the Structural Division Proceedings of ASCE, 1975.

40. ZOUTENDIJK, G. ´Methods of Feasible directions´, American Elsevier, 1960.

41. FOX, R and KAPOOR, M. ´Structural Optimisation in the Dynamics Response regime´, AIAA October 1970, pp 1798-1804.

42. CASSIS, J and SCHMIT , L. ´Optimum structural Design with dynamic constraints´, Journal ofthe Structural Division, Proceedings of ASce, pp 2053-2071 October 1976.

43. VANDERPLAATS, G. ´An efficient Feasible Directions Algorithm for Design Synthesis´, AIAA Journal November 1984.

44. ARORA ,J and GOVIL, K. ´Design sensitivity analysis with substructuring´, Journal of Mechanical Division, Proceedings of ASCE, August 1977.

45. VANDERPLAATS, G. ´Numerical Optimization Techniques for Engineering Design: with appications´, McGrew-Hill,1984.

46. UNKNOWN ´TIMM Expert System Builder (User manual)´, General Research Corporation, McLean, Virginia.

47. STEPHENSON, G. ´Mathematical Methods for Science Students´, Longmans, 1969.

48. AKHIEZER, N. ´The Calculus of Variations´, Blaisdell, 1962.